

**Julius-Maximilians-Universität Würzburg**

**Fakultät für Biologie**



**Effects of stem cell transcription factor-expressing  
vaccinia viruses in oncolytic virotherapy**

**Dissertation**

zur Erlangung des naturwissenschaftlichen Doktorgrades der  
Julius-Maximilians-Universität Würzburg

vorgelegt von Klaas Ehrig  
aus Braunschweig

Würzburg, 2012

Eingereicht am: \_\_\_\_\_

Mitglieder der Promotionskommission:

Vorsitzender: \_\_\_\_\_

Prof. Joerg Schultz

Erstgutachter: \_\_\_\_\_

Prof. Dr. A. A. Szalay

Zweitgutachter: \_\_\_\_\_

Prof. Dr. Georg Krohne

Tag des Promotionskolloquiums: \_\_\_\_\_

Doktorurkunde ausgehändigt am: \_\_\_\_\_

# TABLE OF CONTENTS

## Contents

<b>Zusammenfassung .....</b>	<b>1</b>
<b>Summary .....</b>	<b>4</b>
<b>1 Introduction.....</b>	<b>7</b>
1.1 Cancer occurrence in humans .....	7
1.2 Causes of cancer.....	8
1.3 Classification and morphology of cancer.....	10
1.3.1 Lung cancer.....	10
1.3.2 Colorectal cancer.....	12
1.4 Stem cells.....	17
1.4.1 Stem cell transcription factor Octamer-binding transcription factor (Oct4).....	20
1.4.2 Stem cell transcription factor Nanog.....	22
1.4.3 Stem cell transcription factor Krueppel-like factor 4 (Klf4).....	23
1.5 Cancer stem cells.....	26
1.6 The relation between stem cells and cancer stem cells.....	27
1.7 Novel approaches in cancer therapy.....	29
1.7.1 Oncolytic viruses in cancer therapy and diagnosis.....	30
1.8 Vaccinia virus.....	31
1.8.1 Morphology.....	32
1.8.2 Vaccinia virus replication cycle.....	32
1.8.3 Targeted and armed oncolytic poxviruses.....	33
1.8.4 Recombinant vaccinia virus constructs used in this work.....	35
1.9 Aims of this work.....	35
<b>2 Material.....</b>	<b>38</b>
2.1 Chemicals and enzymes.....	38
2.2 Buffers and solutions.....	41
2.3 Bacterial strains.....	45

## TABLE OF CONTENTS

2.4	Cell lines and cell culture media.....	45
2.4.1	Cell lines.....	45
2.4.2	Cell culture media.....	46
2.5	Kits .....	48
2.6	Antibodies .....	49
2.7	Synthetic Oligonucleotides.....	49
2.8	Recombinant vaccinia virus constructs .....	50
2.9	Laboratory animals .....	53
2.10	Laboratory equipment and other materials.....	53
2.11	Microscopes.....	55
<b>3</b>	<b>Methods.....</b>	<b>56</b>
3.1	Generation of recombinant vaccinia virus .....	56
3.1.1	Cloning of plasmids for homologous recombination with viral DNA.....	56
3.1.2	Co-transfection of plasmid DNA with parental virus GLV-1h68 .....	56
3.1.3	Plaque selection .....	56
3.1.4	Screening for marker gene expression .....	57
3.1.5	Screening for <i>GPT</i> .....	57
3.1.6	DNA isolation for sequencing .....	58
3.1.7	Amplification and purification of recombinant viruses .....	58
3.1.8	Determination of viral titers by standard plaque assay.....	58
3.2	Virological methods.....	59
3.2.1	Infection of cell cultures .....	59
3.2.2	Viral proliferation assay .....	59
3.2.3	Standard plaque assay.....	59
3.3	Cell biological methods .....	59
3.3.1	Culturing of adherent mammalian cells.....	59
3.3.2	Cell viability assay .....	60
3.4	Detection of gene expression of recombinant vaccinia virus .....	60
3.4.1	Analysis of gene expression by reverse transcriptase (RT-) PCR.....	60

## TABLE OF CONTENTS

3.4.1.1	Isolation of RNA from adherent mammalian cells.....	60
3.4.1.2	Synthesis of complementary DNA (cDNA).....	61
3.4.1.3	Polymerase chain reaction (PCR).....	61
3.4.1.4	Agarose gel electrophoresis.....	61
3.4.1.5	Quantitative real-time polymerase chain reaction (qPCR).....	61
3.4.2	Quantification of GFP expression by FACS analysis .....	62
3.4.3	Fluorescence imaging and immunocytochemistry .....	62
3.5	Protein analytical methods .....	62
3.5.1	Preparation of soluble proteins from mammalian cells.....	62
3.5.2	Ultrafiltration of cell supernatants .....	63
3.5.3	Protein Quantification .....	63
3.5.4	SDS-PAGE.....	63
3.5.5	Protein transfer by Western blot .....	64
3.5.6	Immunodetection.....	64
3.5.7	ELISA.....	65
3.6	Mouse experiments.....	65
3.6.1	Subcutaneous xenografts.....	65
3.6.2	Anesthesia .....	65
3.6.3	Vaccinia viral titers in tumor tissues and body organs.....	66
3.6.4	Preparation of tumor lysates for mouse immune-related protein profiling.....	66
3.6.5	Detection of virus-encoded marker gene RUC-GFP expression .....	66
3.6.6	Histological analysis of tumors .....	66
<b>4</b>	<b>Results.....</b>	<b>68</b>
4.1	Characterization of stem cell transcription factor-encoding vaccinia viruses GLV-1h205 (Nanog) and GLV-1h208 (Oct4).....	68
4.1.1	Virus mediated stem cell transcription factor expression .....	68
4.1.1.1	Analysis of viral replication in the cancer cell lines A549 and PC-3.....	68
4.1.1.2	Analysis of vaccinia virus expressed mRNA transcripts of marker genes and stem cell transcription factors Nanog and Oct4 in infected mammalian cells..	70
4.1.1.3	Analysis of recombinant protein expression in infected mammalian cells.....	71

## TABLE OF CONTENTS

4.1.1.3.1	Analysis of beta-galactosidase expression in infected mammalian cells .....	71
4.1.1.3.2	Analysis of Ruc-GFP and stem cell transcription factor expression in infected mammalian cells by immunocytochemistry .....	72
4.1.1.3.3	Analysis of Nanog expression in infected mammalian cells by ELISA quantification.....	74
4.1.1.3.4	Analysis of Oct4 expression in infected mammalian cells by Western blot .....	75
4.1.1.4	Analysis of cell viability of mammalian cell cultures infected with GLV-1h205 and GLV-1h208.....	77
4.1.1.5	Influence of Nanog expression on cell cycle progression in mammalian cell culture .....	78
4.1.1.6	Influence of Nanog and Oct4 expression on expression of genes involved in epithelial-to-mesenchymal transition (EMT) after infection of A549 in culture ....	80
4.1.2	Effects of a single dose of GLV-1h205 or GLV-1h208 in subcutaneous A549 xenografts.....	82
4.1.2.1	Confirmation of viral tumor infiltration, infection and replication by GFP fluorescence and <i>Renilla</i> luciferase low light imaging.....	84
4.1.2.2	Pfu determination in vaccinia virus-injected A549 tumor-bearing mice at various time points .....	86
4.1.2.3	Histochemical analysis of vaccinia virus colonization in A549 mouse xenografts .....	88
4.1.2.4	Immune-related antigen profiling of A549 tumor-bearing mice after administration of a single dose of replication-competent vaccinia virus strains... ..	89
4.1.3	Characterization of a Nanog $\Delta$ NLS mutant virus.....	90
4.1.3.1	Analysis of viral replication rate of GLV-1h321 in the cancer cell line A549....	91
4.1.3.2	Analysis of recombinant protein expression in mammalian cells infected with GLV-1h321 .....	92
4.1.3.2.1	Analysis of beta-galactosidase expression in infected mammalian cells .....	92
4.1.3.2.2	Analysis of Ruc-GFP and Nanog expression in infected mammalian cells by immunocytochemistry .....	92
4.1.3.2.3	Analysis of Nanog expression in infected mammalian cells by Western blot ..	94
4.1.3.3	Analysis of cell viability of mammalian cells infected with GLV-1h321.....	95

## TABLE OF CONTENTS

4.1.3.4	Effects of a single dose of GLV-1h205 or GLV-1h321 in subcutaneous A549 xenografts .....	96
4.1.3.5	Pfu determination in A549 tumor-bearing mice injected with GLV-1h68, GLV-1h205, and GLV-1h321 at various time points .....	97
4.1.3.6	Effects of a single dose of GLV-1h205 or GLV-1h321 in subcutaneous DU-145 xenografts .....	98
4.2	Oncolytic virotherapy as a treatment of colorectal cancer .....	99
4.2.1	Efficacy of GLV-1h68 in colorectal cancer therapy .....	99
4.2.1.1	Replication of GLV-1h68 in different human colorectal cancer lines in culture	99
4.2.1.2	Cytotoxicity of GLV-1h68 in different colorectal cancer lines in culture.....	100
4.2.1.3	Analysis of viral replication and cytotoxicity on infected host cells using virus-mediated marker gene expression .....	101
4.2.1.4	Effects of a single dose of GLV-1h68 in subcutaneous CRC xenografts .....	104
4.2.1.5	Analysis of viral tumor infiltration, infection and replication by fluorescence detection of viral marker gene (Ruc-GFP) expression.....	107
4.2.1.6	Pfu determination in GLV-1h68-injected HCT-116 tumor-bearing mice at various time points .....	108
4.2.1.7	Histochemical analysis of GLV-1h68 injections in HCT-116 mouse xenografts .. ..	109
4.2.1.8	Immune-related antigen profiling of HCT-116 tumor-bearing mice after administration of a single dose of GLV-1h68.....	110
4.3	Improvement of oncolytic virotherapy with a new replication-competent vaccinia virus strain expressing transcription factor Klf4 .....	111
4.3.1	A potential application of transcription factor Klf4 in colorectal cancer .....	111
4.3.1.1	Analysis of viral replication in the CRC lines HCT-116 and HT-29 .....	112
4.3.1.2	Analysis of recombinant protein expression in infected CRC cells .....	114
4.3.1.2.1	Analysis of beta-galactosidase expression in infected CRC cells .....	114
4.3.1.2.2	Analysis of Ruc-GFP and Klf4 expression in infected CRC cells by immunocytochemistry .....	115
4.3.1.2.3	Analysis of Klf4 expression in infected HT-29 cells by Western blot.....	117

## TABLE OF CONTENTS

4.3.1.3	Cell viability of HT-29 cells infected with Klf4-encoding vaccinia virus strains GLV-1h290-292 .....	118
4.3.1.4	Effects of virus-mediated Klf4 expression on mRNA levels of cellular beta-catenin .....	120
4.3.1.5	Effects of virus-mediated Klf4 expression on cellular protein levels of beta-catenin .....	121
4.3.1.6	Construction and characterization of the Klf4-TAT fusion protein-expressing vaccinia virus strain GLV-1h391 .....	122
4.3.1.6.1	Viral replication of GLV-1h391 in colorectal cancer line HT-29.....	122
4.3.1.7	Marker gene expression in colorectal cancer line HT-29 infected with GLV-1h391 .....	123
4.3.1.7.1	Analysis of beta-galactosidase expression in infected HT-29 cells.....	123
4.3.1.7.2	Analysis of Ruc-GFP and Klf4 expression in infected A549 cells by immunocytochemistry .....	124
4.3.1.7.3	Analysis of Klf4 expression in GLV-1h391-infected HT-29 cells by Western Blot .....	125
4.3.1.8	Cell viability of HT-29 cells infected with vaccinia virus strain GLV-1h391..	126
4.3.1.9	Functional analysis of virus-mediated Klf4-TAT expression .....	128
4.3.1.9.1	Effects of Klf4-TAT expression on cellular beta-catenin levels in GLV-1h391 infected HT-29 cells .....	128
4.3.1.9.2	Effects of Klf4-TAT on cell proliferation .....	129
4.3.1.10	Effects of a single dose of GLV-1h205 or GLV-1h321 in subcutaneous A549 xenografts .....	130
4.3.1.11	Pfu determination in HT-29 tumor-bearing mice injected with GLV-1h68, GLV-1h291, and GLV-1h391 at 21 days post injection.....	132
4.3.1.12	Analysis of viral tumor infiltration, infection and replication by imaging of viral marker gene (Ruc-GFP) expression.....	133
4.3.1.13	Histochemical analysis of viral tumor infiltration and gene expression .....	134
<b>5</b>	<b>Discussion.....</b>	<b>136</b>
5.1	Two new stem cell transcription factor-encoding recombinant vaccinia virus strains show oncolytic potential in A549 non-small cell lung carcinoma .....	137
5.2	Therapeutic efficacy of GLV-1h205 and GLV-1h208 in mouse xenografts .....	139



## TABLE OF CONTENTS

5.3	Is the observed enhanced therapeutic efficacy of GLV-1h205 payload- or promoter-mediated? .....	141
5.4	GLV-1h68 as a potential therapeutic agent in treatment of colorectal cancer .....	143
5.5	Improving therapeutic outcome of oncolytic virotherapy of colorectal cancer by specifically armed vaccinia virus strains .....	145
5.6	Conclusion .....	148
<b>6</b>	<b>References .....</b>	<b>150</b>
<b>7</b>	<b>Appendix .....</b>	<b>168</b>
7.1	Abbreviations .....	168
7.2	Acknowledgements .....	171
7.3	Eidstattliche Erklärung .....	172
<b>8</b>	<b>Lebenslauf .....</b>	<b>173</b>
<b>9</b>	<b>Publikationen .....</b>	<b>174</b>
9.1	Im Rahmen dieser Arbeit entstandene Publikationen .....	174

### Zusammenfassung

Mit prognostizierten 1.638.910 Neuerkrankungen und 577.190 Toden allein in den Vereinigten Staaten, bleiben Krebserkrankungen auch im Jahr 2012 die zweithäufigste Todesursache in der industrialisierten Welt. Dies führt nicht nur zu großem Leid bei den Patienten und deren Familien, sondern auch zu einer immensen Belastung der Krankenkassen und des Gesundheitswesens. Zusätzlich hat die Etablierung der Krebsstammzell-Hypothese grundsätzliche Auswirkungen auf die Erfolgsaussichten konventioneller Krebstherapie, wie Chemotherapie oder Strahlentherapie. Deswegen ist es von größter Notwendigkeit, dass neue Ansätze zur Krebstherapie entwickelt werden, die den Ausgang der Behandlung verbessern und zu weniger Nebenwirkungen führen. Diverse vorklinische Studien haben gezeigt, dass die onkolytische Virotherapie mit Vaccinia-Viren ein potentes und gut tolerierbares neues Werkzeug in der Krebstherapie darstellt. Die Effizienz des Vaccinia-Virus als Therapeutikum allein oder in Kombination mit Strahlen- oder Chemotherapie wird aktuell in mehreren klinischen Studien der Phasen I & II getestet.

Krebsstammzellen und Stammzellen teilen eine Vielzahl von Eigenschaften, wie die Fähigkeit zur Selbst-Erneuerung und Pluripotenz, Stilllegung der Zellproliferation, Resistenz gegen Medikamente oder Bestrahlung, die Expression von diversen Zelloberflächenmolekülen, die Aktivierung und Hemmung spezifischer Signaltransduktionswege oder die Expression von Stammzell-spezifischen Genen wie Nanog und Oct4.

In dieser Arbeit wurden zwei neue rekombinante Vaccinia-Viren entwickelt, welche die Stammzell-Transkriptionsfaktoren Nanog (GLV-1h205) und Oct4 (GLV-1h208) exprimieren, um tiefere Einblicke in die Rolle dieser Masterregulatoren in der Entstehung von Krebs und ihrem Einfluss auf die onkolytische Virotherapie zu gewinnen. Das Replikationspotential beider Virusstämme in menschlichen A549-Zellen und PC-3-Zellen wurde anhand von Replikations-Assays bestimmt. Hierbei zeigte sich, dass GLV-1h205 besser replizierte als GLV-1h208 oder der parentale GLV-1h68-Stamm. GLV-1h208 replizierte hingegen nicht so effizient wie das Kontroll-Virus. Die Expression der Virus-spezifischen Markergene Ruc-GFP und beta-Galaktosidase, wie auch die Expression der Transkriptionsfaktoren Nanog und Oct4 wurde mit Hilfe von RT-PCR, SDS-PAGE und Western blotting, sowie immunozytochemischen Experimenten nachgewiesen. Befunde aus Zytotoxizitätsstudien zeigten, dass das GLV-1h205-Virus Krebszellen effizienter tötet als das parentale GLV-1h68. Es zeigte sich, dass die Zytotoxizität direkt proportional zum Replikationspotential der Viren ist. Die Infektion von A549-Zellen mit GLV-1h205 oder GLV-1h208 resultierte weder in der Hoch-Regulation von Genen, die direkt in den EMT-Prozess involviert sind, noch führte sie zur Expression des Krebsstammzell-spezifischen Zelloberflächenmarkers CD133. Des

## ZUSAMMENFASSUNG

Weiteren wurde der Einfluss einer GLV-1h205-Infektion von A549-Zellen auf den Zellzyklus untersucht. Dies führte jedoch zu keinen nachweisbaren Veränderungen. Zudem wurde die Bedeutung der Virus-vermittelten Transkriptionsfaktor-Expression auf die Behandlung von subkutanen A549-Tumoren in einem Xenograft-Modell untersucht. Die Behandlung mit GLV-1h205 zeigte sich als signifikant effizienter als die Behandlung mit GLV-1h208 oder GLV-1h68 und führte zum Rückgang der Tumore. Die effiziente Kolonisierung des Tumors durch das Virus und die dadurch ausgelöste Zerstörung des Tumorgewebes wurde mit Hilfe von immunohistochemischen Verfahrenstechniken analysiert. Bildgebende Verfahren zur Detektion von *Renilla*-Luziferase und GFP sowie Standard Plaque Assays bestätigten die erfolgreiche Invasion der Viren in das Tumorgewebe, und die Analyse der Immunbezogenen Proteinantigen-Profile der behandelten Mäuse weist auf eine Replikationsabhängige Hoch-Regulierung von Immunbezogenen Proteinen hin. Zur Untersuchung, ob die beobachteten Vorteile in der Behandlung von Lungenadenokarzinomen in Mäusen mit GLV-1h205 Promoter- oder Transkriptionsfaktor-abhängig sind, wurde ein Kontroll-Virus (GLV-1h321) hergestellt, das für eine unfunktionale Nanog-Mutante codiert. Mittels SDS-PAGE und Western blotting sowie Immunocytochemie wurde die Transgen-Expression analysiert. Die Replikation und Zytotoxizität des GLV-1h321 stellte sich als vergleichbar mit dem parental Virusstamm GLV-1h68 heraus. Die Behandlung von A549-Tumoren mit GLV-1h321 war jedoch statistisch signifikant schlechter als die Behandlung mit GLV-1h205; ein Hinweis darauf, dass die beobachteten Vorteile in der Behandlung mit GLV-1h205 Nanog-abhängig sind. Zusätzliche Unterstützung dieser Hypothese findet sich in der Tatsache, dass sich die Behandlung von DU-145-Tumoren mit GLV-1h205 als weniger effizient im Vergleich mit GLV-1h68 oder GLV-1h321 herausstellte.

Ein weiterer Aspekt dieser Arbeit war die Fragestellung, ob sich das onkolytische Vaccinia-Virus GLV-1h68 eignet, als neues und weniger invasives Therapeutikum effizient Darmkrebszellen zu infizieren um sich in ihnen zu replizieren und diese anschließend zu lysieren. Ein derartiger Therapieansatz würde besonders im Hinblick auf spät diagnostizierten, metastasierenden Darmkrebs eine interessante Behandlungsalternative darstellen. Es konnte anhand von Replikations-Assays und Zytotoxizitätsstudien gezeigt werden, dass GLV-1h68 eine Anzahl von unterschiedlich fortgeschrittenen Darmkrebszellen infizieren kann und sich anschließend bis zur Zelllyse in ihnen repliziert. Dies geschieht in einer MOI- und Zelltyp-abhängigen Weise. Virale Markergen-expression wurde anhand von Fluoreszenzmikroskopie und FACS-Analyse untersucht und korrelierte gut mit der Virusreplikation und Zytotoxizität. Desweiteren wurde gezeigt, dass die einmalige Administration von GLV-1h68 in mindestens zwei verschiedenen Darmkrebszelllinien zu einer signifikanten Inhibierung des Tumorwachstums *in vivo* und zu signifikant verbessertem Überleben führt. Standard Plaque Assays von Tumor- und Organlysaten und immuno-

## ZUSAMMENFASSUNG

histochemische Analysen zeigten, dass das Vaccinia Virus ausschließlich das primäre Tumorgewebe befällt und sich darin repliziert. Analysen der Immun-bezogenen Proteinantigen-Profile von behandelten und unbehandelten Mäuse weisen auf eine Beteiligung des angeborenen Immunsystems bei der Tumorregression durch Cytokin- und Chemokin-vermittelte Rekrutierung dendritischer Zellen, Makrophagen und natürlicher Killerzellen hin.

Der Transkriptionsfaktor Klf4 wird zwar stark in ruhenden, ausdifferenzierten Zellen des Darmepithels exprimiert, ist hingegen bei Darmkrebs generell dramatisch herabreguliert. Die Expression von Klf4 führt zu einem Stop der Zellproliferation und inhibiert die Aktivität des Wnt-Signalweges, indem es im Zellkern an die Transaktivierungsdomäne von beta-Catenin bindet. Um die Behandlung von Darmkrebs mit Hilfe onkolytischer Virotherapie weiter zu verbessern, wurden verschiedene Vaccinia-Viren (GLV-1h290-292) erzeugt, die durch verschiedene Promoterstärken die Expression unterschiedlicher Mengen an Tumorsuppressor Klf4 vermitteln. Die anfängliche Charakterisierung der drei Virusstämme mittels Replikations-Assay, Zytotoxizitätstudien, SDS-PAGE und Western blotting, Immunocytochemie sowie die Analyse der Proteinfunktion mit Hilfe von qPCR- und ELISA-Analysen zur Bestimmung von zellulärem beta-Catenin, zeigten eine Promoter-abhängige Expression und Wirkung von Klf4. Für weitere Analysen wurde das Virus GLV-1h291 gewählt, welches nach Infektion die größte Menge an Klf4 produziert und zusätzlich durch die C-terminale Fusion einer TAT Transduktionsdomäne Membran-gängig gemacht (GLV-1h391). GLV-1h391 weist ein identisches Replikationsverhalten wie GLV-1h291 auf, ist jedoch 10-fach weniger zytotoxisch. Weiterhin führte eine Inkubation mit konditioniertem Medium, von GLV-1h391-infizierten Zellen, zu einer deutlichen Inhibition der Zellproliferation. Die Behandlung von HT-29-Non-Responder Tumoren *in vivo* mit GLV-1h291 oder GLV-1h391 führte zu einer signifikanten Inhibition des Tumorwachstums und verlängerte die Überlebenszeit. Es zeigte sich zudem, dass eine Injektion mit GLV-1h391 das Tumorwachstum effizienter verhinderte als eine Injektion mit GLV-1h291. Immunohistochemische Versuche zeigten die exklusive Expression von Klf4 in Tumoren von Mäusen, die zuvor mit GLV-1h291 oder GLV-1h391 injiziert wurden, wo hingegen Standard Plaque Assays von Tumorlysaten zeigten, dass alle Behandlungsgruppen gleiche Mengen an Virus im Tumor aufwiesen. Dies weist auf die Rolle von Virus-vermittelter Klf4-Expression in der Inhibition von HT-29-Tumorwachstum hin. Die Befunde machen das Klf4-TAT-kodierende Vaccinia-Virus GLV-1h391 zu einem vielversprechenden Kandidaten für eine Behandlung von Darmkrebs beim Menschen.

## Summary

Cancer remains the second leading cause of death in the industrialized world with an estimate of 1,638,910 newly diagnosed cases and 577,190 deaths in 2012 in the United States alone, resulting in not only suffering of both, cancer patients and their families but also having a big impact on the health care system. In addition, the data from many different studies investigating the nature of cancer-initiating cells coined the description 'cancer stem cells' and has major implications on conventional cancer therapy. Thus, to improve the outcome of cancer treatment and to lower negative side effects, the development of novel therapeutic regimens is indispensable. It has been demonstrated in many preclinical studies that oncolytic virotherapy using vaccinia virus may provide a powerful and well-tolerable new tool in cancer therapy which is currently investigated in several clinical trials (Phase I & II) as stand-alone treatment or in combination with conventional cancer therapy.

Cancer-initiating cells and stem cells share a variety of characteristics like the ability to self-renew, differentiation potential, quiescence, drug and radiation resistance, activation and inhibition of similar signaling pathways as well as expression of cell surface markers and stem cell-related genes like Nanog and Oct4.

In this work, two new recombinant vaccinia viruses expressing the transcription factors Nanog (GLV-1h205) and Oct4 (GLV-1h208) were engineered to provide deeper insight of these stem cell master regulators in their significance of cancer-initiation and their impact on oncolytic virotherapy. Both viruses were analyzed for their replication potential in A549 and PC-3 human cancer cells. GLV-1h205 showed more efficient viral replication compared to its parental strain GLV-1h68 while GLV-1h208 showed impaired replication potential. Marker gene expression was assessed by RT-PCR, SDS-PAGE and Western blotting, ELISA or immunocytochemistry and comparable to their parental strain GLV-1h68 as well as expression of the respective transcription factor. Analysis of cytotoxicity revealed that GLV-1h205 showed the strongest cytotoxic effect compared to GLV-1h68 and GLV-1h208 which is assumed to be directly proportional to replication efficacy. Infection of A549 cells with GLV-1h205 and GLV-1h208 did neither result in detectable expression of genes involved in EMT nor in expression of cancer stem cell-related cell surface marker CD133. Furthermore, the effect of GLV-1h205 infection on the cell cycle in A549 cells was analyzed, but no changes in cell cycle progression was observed. Next, the effects of virus-mediated expression of stem cell transcription factors on therapeutic efficacy and survival rates in A549 xenograft mouse models was analyzed. Treatment with GLV-1h205 was significantly more efficient compared to treatment with GLV-1h68 or GLV-1h208 and led to efficient colonization of the tumor correlated with cell death, which was assessed by

## SUMMARY

immunohistochemistry. *Renilla* luciferase and GFP imaging and standard plaque assays showed efficient tumor colonization and marker gene expression of GLV-1h205 and GLV-1h208. Mouse immune-related antigen profiling revealed a replication-dependent upregulation of immune-related antigens. A non-functional Nanog mutant-expressing virus strain (GLV-1h321) was engineered to analyze whether the observed therapeutic benefits were promoter- or payload-driven. GLV-1h321 was characterized for foreign transgene expression by SDS-PAGE and Western blotting as well as immunocytochemistry. Replication assay and cell viability assay and showed similar replication behavior and cytotoxicity in A549 cells compared to GLV-1h68. Treatment of A549 tumor-bearing mice with GLV-1h321 led to impaired therapeutic efficacy compared to GLV-1h205, whereas treatment of DU-145 tumors was more efficient and comparable to the parental GLV-1h68, indicating that the observed effects are rather payload- than promoter-driven. Therefore, the virus-mediated expression of stem cell transcription factor Nanog seems to enhance oncolytic virotherapy in A549 lung adenocarcinomas.

Furthermore, this study analyzed the potential of GLV-1h68 to infect, replicate in, and lyse colorectal cancer cell lines to study whether oncolytic vaccinia viruses can be potential new and less invasive treatment regimens for late stage colorectal cancer. It was shown by replication assay and cell viability assay that GLV-1h68 efficiently infects and kills a variety of colorectal cancer lines in a cell line- and MOI-dependent manner. Marker gene expression was assessed by fluorescence microscopy and FACS and correlated well with virus replication and cell killing. Furthermore, GLV-1h68 significantly inhibited the tumor growth in at least two different colorectal cancer lines *in vivo* and led to a significantly better overall survival. Standard plaque assay of tumors and body organs as well as immunohistochemistry demonstrated that the virus exclusively colonized and replicated in the primary tumor. Mouse immune-related antigen profiling revealed the upregulation of a variety of immune-related genes upon virus infection, which is likely to result in an innate immune response at the tumor site by recruiting macrophages, dendritic cells and natural killer cells to the tumor site.

The transcription factor Klf4 is highly expressed in quiescent, terminally differentiated cells in the colonic epithelium whereas it is dramatically downregulated in colon cancers. Klf4 expression leads to cell growth arrest and inhibits Wnt signaling by binding to beta-catenin. To further improve the treatment of colorectal cancers, new recombinant vaccinia viruses (GLV-1h290-292) mediating the expression of differing amounts of the tumor suppressor Klf4 by using different promoter strengths were engineered. Initial characterization of recombinant vaccinia viruses expressing Klf4 by replication assay, cell viability assay, SDS-PAGE and Western blotting, immunocytochemistry and analysis of protein functionality by qPCR and ELISA analysis for cellular beta-catenin expression, demonstrated promoter

## SUMMARY

strength-dependent expression of and impact of Klf4. For further analysis, the vaccinia virus strain with the strongest Klf4 expression (GLV-1h291) was picked for further *in vivo* analysis. To further boost the effects of tumor suppressor Klf4, a vaccinia virus strain expressing Klf4 with a C-terminal fusion of the TAT transduction domain (GLV-1h391) was engineered. GLV-1h391 showed identical replication behavior but a 10-fold decrease in cytotoxicity compared to GLV-1h291. Cell proliferation assay of HT-29 cells incubated with conditioned media from GLV-1h391 led to slower cell proliferation compared to conditioned media from uninfected controls, or GLV-1h68/291-infected cells. Treatment of HT-29 non-responder tumors *in vivo* with GLV-1h291 and GLV-1h391 led to significant tumor growth inhibition and improved overall survival compared to GLV-1h68. It was furthermore shown that GLV-1h391 was more efficient than GLV-1h291 inhibiting HT-29 tumor growth. Immunohistochemistry demonstrated Klf4 expression in virus-patches of HT-29 tumors infected with GLV-1h291 and GLV-1h391 exclusively whereas standard plaque assay confirmed similar viral titers in all tested viruses, suggesting that differences in tumor growth are directly linked to virus-mediated Klf4 expression. This makes the Klf4-TAT expressing GLV-1h391 a promising candidate for the treatment of colorectal cancer in man.

# 1 Introduction

Despite a tremendous medical and scientific effort, according to the World Health Organization (WHO), cancer remains the second leading cause of death in the industrialized world. The International Agency for Research on Cancer (IARC) estimated 12.7 million new cancer cases worldwide in 2008 and a corresponding number of 7.6 million cancer deaths<sup>1</sup>. The American Cancer Society (ACS) estimates 1,638,910 new cases that will be diagnosed and reported in 2012, causing an estimate of 577,190 deaths in the United States alone<sup>2</sup>. In Germany, the Robert-Koch-Institute (RKI) in collaboration with the “Zentrum für Krebsregisterdaten” (ZfKD) estimates 486,000 new cancer cases.<sup>3</sup> With growth and aging of the world’s population, as well as further industrialization of economically transitioning countries, leading to reductions in childhood mortality and deaths from infectious diseases, the global cancer burden in 2030 is estimated to grow to 21.4 million new cancer cases and 13.2 million cancer deaths<sup>1</sup>. Alongside with the suffering and decline in quality of life for both patients and their families, diagnosis and treatment of cancer also created an immense economic impact of \$895 billion, even surpassing the costs created by heart diseases (\$753 billion) in 2008.<sup>4</sup>

## 1.1 Cancer occurrence in humans

Cancer is used as a general term for a group of diseases characterized by abnormal and uncontrolled cell growth and spread in living organisms leading to the formation of neoplasms. Neoplasms, or tumors, can be benign or malignant and reside as non-life threatening tumors in the original tissue they arose from. If the neoplastic growth is uncontrolled and it is characterized as malignant, it is referred to as cancer. Cancer possesses the ability to become anaplastic, invasive and metastatic. Malignant cancers are generally linked with a progressively worsening health status of the patient and can potentially lead to death. Most cancers form a solid tumor, with the exception of leukemia. Most cancer types develop independent of the sex, making cancer occurrence rates in male and female humans comparable. Cancer of the colon and rectum (9% of all cases in both genders), Non-Hodgkin lymphoma (4%), melanoma of the skin (5% in men, 4% in women), pancreatic cancer (3%), and cancer of the kidneys and pelvis (5% in men, 3% in women) all develop in a similar manner in both genders. However, certain cancer types like breast cancer, which develops predominantly in women (29% of all cases), or prostate cancer in men (29% of all cases) are gender-specific. For the longest time, it was assumed that men had a pre-disposition to develop lung cancer, but new studies indicate increasing cases of lung cancer in women, which is correlated with increased numbers of smokers in women.



## INTRODUCTION

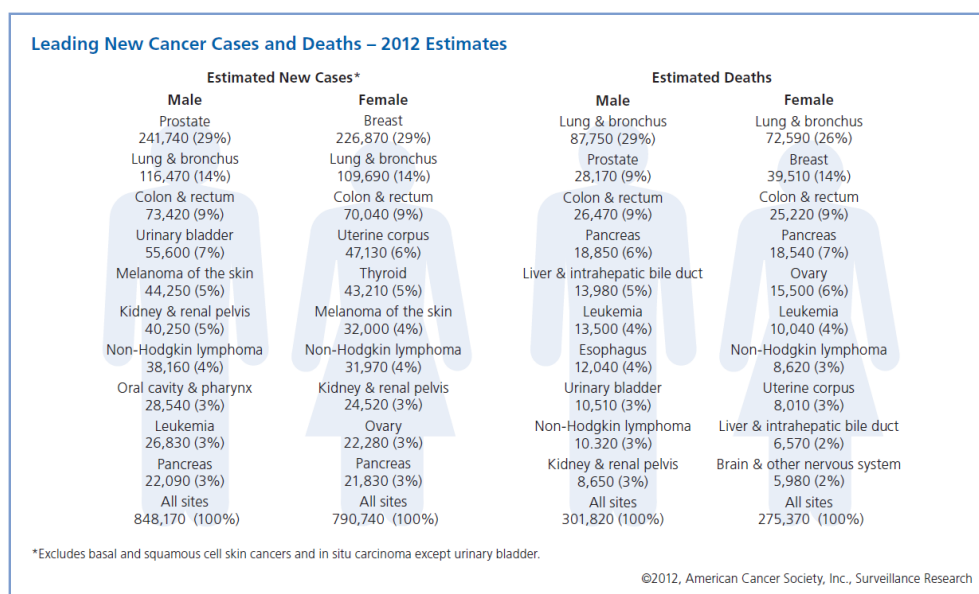


**Fig. 1.1 - Estimates for new cancer cases and deaths in 2012 (from Cancer Facts & Figures 2012)**

### 1.2 Causes of cancer

Today, it is an established fact that cancer is a disease involving dynamic changes and mutations in the genome of the transformed cell. The cause for these genetic changes can originate from external factors like tobacco smoke in lung cancer, infectious agents like the human papillomavirus (HPV) in cervical cancer, chemicals or radiation. Dietary habits and lack of physical exercise further contribute to the risk of developing cancer<sup>5</sup>.

Unlike external factors increasing the risk to develop cancer, which can be avoided to reduce or prevent the development of cancer, there are internal factors and pre-depositions that can increase the risk to develop cancer. These internal factors include inherited genetic mutations in breast cancer, hormones, immune conditions and mutations that occur from dysfunctional metabolic pathways<sup>6</sup>. It is important to note that oftentimes external and internal triggers do not work exclusively by themselves but rather act together or in sequence to initiate or promote cancer development<sup>2</sup>.

The development of cancer or tumorigenesis appears to be a multistep process, reflecting genetic alterations. Each genetic change confers one or another type of growth advantage, that drives the progressive transformation of normal human cells into highly malignant derivatives<sup>7</sup>. The disease shows a high complexity, ranging from genetic changes as little as point mutations in a gene, turning it into an oncogene, or as obvious as chromosomal aberrations. It can be assumed that this complexity translates into the diversity of the disease, represented in the more than 100 different types of cancers that exist today.

In 2000, Hanahan and Weinberg suggested, that the diversity of different cancer types is a manifestation of six essential alterations in cell physiology that collectively dictate malignant

## INTRODUCTION

cell growth, calling it “the hallmarks of cancer”<sup>7-8</sup>. The six alterations that will ultimately initiate the progression from normal cell to tumorigenic cell comprise self-sufficiency in growth signals, insensitivity to growth-inhibitory signals, evasion of apoptosis, limitless replicative potential, sustained angiogenesis, and tissue invasion and metastasis<sup>7</sup>. On a cellular level, cancer cells acquire some of these hallmarks by cancer-promoting oncogene activation, another class of genes (tumor suppressor genes) cause loss of function in DNA replication, cell cycle progression, interaction with the host immune system or tissue adhesion<sup>9</sup>. Furthermore, epigenetic changes are also considered to be involved in cancer development<sup>10</sup>. However, it is noteworthy that cancer development is not exclusively restricted to cell-autonomous processes but is also depending on the interactions between transformed cell and the normal cells in the tumor microenvironment (stroma, inflammatory cells and recruited vasculature). Moreover, virtually all types of human tumors, including their metastatic outgrowths, consist of complex mixtures of several cell types that create the malignancy of cancer<sup>7</sup>.

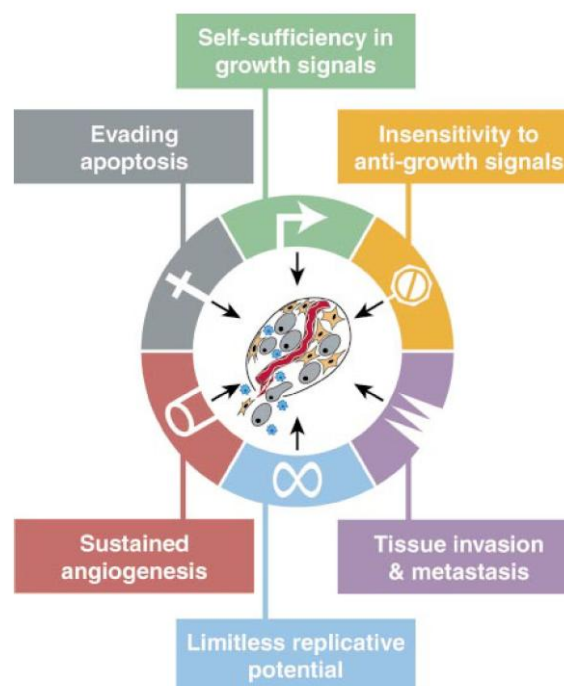


**Fig 1.2 – The six hallmarks of cancer (from Hanahan & Weinberg, 2000)**

The six alterations that will ultimately initiate cancer progression comprise self-sufficiency in growth signals, insensitivity to growth-inhibitory signals, evasion of apoptosis, limitless replication potential, sustained angiogenesis, and tissue invasion and metastasis.

## INTRODUCTION

### 1.3 Classification and morphology of cancer

Cancer is classified by two major characteristics: cell type and the tissue of origin. Location and histological analysis oftentimes help in identification of the tumor.

The majority of human tumors derives from putative epithelial tissues and account for more than 80% of the most common cancer-related deaths in humans in the Western world. These tumors are classified as carcinomas. Carcinomas include cancers developing from the epithelial cell layers of the entire gastro-intestinal tract as well as cancers developing on the outer surface of the body. Carcinomas can be further distinguished by their histological features into adenocarcinomas (originates in the glandular tissues), squamous cell carcinoma (originates in the epidermis of the skin), adenosquamous (a mixture of adenocarcinoma and squamous cell carcinoma), anaplastic carcinoma (dedifferentiated tumors), large and small cell carcinomas. Sarcomas are a second class of cancers that derive from mesenchymal tissues. Thus, sarcomas develop in bone (osteosarcoma), cartilage (chondrosarcoma), fat (liposarcoma) or muscle tissues (myosarcoma). A third group of non-epithelial cancers arises from hematopoietic cells and cells of the immune system. Leukemia (blood or bone marrow cancer) is a cancer of hematopoietic cells that circulate in the blood stream while lymphomas are comprised of tumors of the lymphoid lineages, e.g. B and T lymphocytes that aggregate and form solid tumors. These tumors are mostly found in the lymph nodes<sup>9</sup>. Another considerable group of cancers derives from cells of the central and peripheral nervous system (neuroectodermal tumors). This group of cancers includes gliomas, glioblastomas, neuroblastomas, schwannomas, and medullablastomas<sup>9</sup>. Melanomas arise from melanocytes while germinomas derive from the germinal tissue of the gonads, mediastinum or pineal region.

Despite their very various tissue of origin, most tumors seem to keep some of the distinctive characteristics of their original tissue from which they developed<sup>9</sup>.

#### 1.3.1 Lung cancer

Lung cancer can be divided into two different kinds of cancer – small cell lung cancer (SCLC) and non-small cell lung cancer (NSCLC) which make up 85-90% of all diagnosed lung cancers. Non-small cell lung cancers are generally classified as carcinomas and can be grouped in three different histopathological classes: adenocarcinomas (40%), squamous cell carcinomas (25-30%) and large cell carcinomas (10%).

The major risk factors for lung cancer are exposure to tobacco smoke, radon or asbestos. It is estimated that about 80% of all lung cancer deaths can be related to tobacco smoke, and the risk to develop lung cancer among smokers is many times higher than in non-smokers. It has also been shown that a genetic pre-disposition exists that facilitates the development of lung cancer<sup>11</sup>.

## INTRODUCTION

Symptoms of lung cancer usually do not appear early on but when the disease is already in an advanced, non-curable stage. Another problem is that symptoms are oftentimes misinterpreted for a different problem, eventually delaying the correct diagnosis by a physician. However, diagnosis of lung cancer can be performed by imaging tests like chest X-ray or chest CT scan, bronchoscopy or sputum exam<sup>12</sup>. Non-small cell lung cancer growth and spread are described by the International Union Against Cancer (UICC) TNM staging system. The TNM system is based on three key pieces of information: T indicates the size of the primary tumor and whether it was grown into nearby areas. N describes the spread to the (regional) lymph nodes and M describes whether the cancer has metastasized to other body organs (brain, adrenal glands, liver, kidney or the other lung). The 5-year survival rate at the time of diagnosis for stage IA lung cancer is estimated to be 49% while the 5-year survival rate for stage IV is only 1%. Generally, a diagnosis with lung cancer gives a relatively poor prognosis.

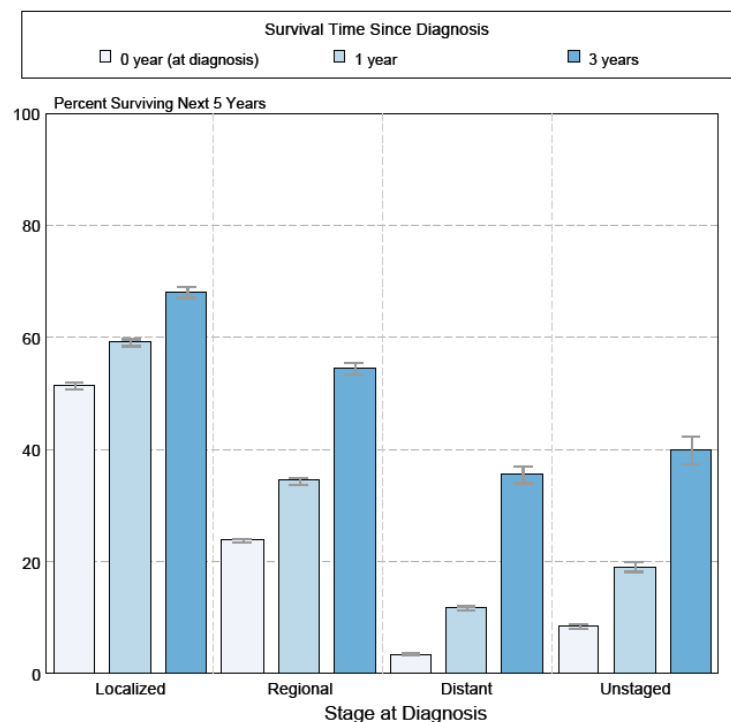


**Fig.1.3 – 5-year survival rates for lung cancer patients (from the NCI’s Surveillance, Epidemiology, and End Results (SEER) data base)**

Depending on the staging of the lung cancer, treatment options include surgery, radiation therapy, chemotherapy (cisplatin, carboplatin), targeted therapy (Avastin®, Tarceva®), photodynamic therapy (PDT) or a combination of more than one treatment.

It is becoming evident now that lung cancers have accumulated numerous clonal genetic and epigenetic alterations, including the classical genetic abnormalities of tumor suppressor

## INTRODUCTION

gene (TSG) inactivation, overactivity of growth promoting oncogenes or promoter hypermethylation as a multistep process<sup>13</sup>. Involved in self-sufficiency of growth signals are the epidermal growth factor receptor (EGFR) and HER2/neu, which are both part of the ERBB family, a group of transmembrane receptor tyrosine kinases. EGFR regulates epithelial proliferation and differentiation and can be overexpressed in lung cancers, which also have a tendency to express EGFR ligands like epidermal growth factor (EGF) and transforming growth factor alpha (TGF-alpha). This creates one potential stimulating autocrine tumor growth loop<sup>14</sup>. Another group of proteins involved in lung cancer development is the RAS proto-oncogene family, of which especially KRAS can be activated by point mutations in the gene, leading to inappropriate signaling for cell proliferation<sup>13</sup>. Gene amplification or transcriptional dysregulation of c-MYC protein expression, a member of the MYC proto-oncogene family, can also cause development of lung cancer. Members of the MYC proto-oncogene family are the ultimate target of RAS signal transduction<sup>15</sup>. Lung cancer cells oftentimes find ways to evade the normal physiological response caused by cellular and DNA damage. Key players in lung cancer include the inactivation of *p53* tumor suppressor gene (TSG) and activation of the *bc12* proto-oncogene. The *p53* protein helps to maintain genomic integrity of DNA from radiation and carcinogens. DNA damage or hypoxia up-regulates *p53* which acts as a transcription factor regulating downstream genes like *p21*, *mdm2*, *gadd45* and *bax*, thereby helping to regulate G1/S cell cycle transition, G2/M DNA damage checkpoint, and apoptosis<sup>15</sup>. Recently, another important mechanism involved in lung cancer development emerged. Promoter methylation in tumors is increasingly recognized as a mechanism to gene inactivation. Several genes have been found to carry aberrant promoter methylation<sup>16</sup>. Another early step in lung cancer pathogenesis is the re-activation of telomerase which helps the indefinite proliferation of cells because the enzyme protects the telomeres of the chromosomes from loss of genetic material by DNA replication.

### 1.3.2 Colorectal cancer

Colorectal cancer develops either in the colon or the rectum, and both organs are part of the gastrointestinal tract. Colorectal cancers develop very slowly over a period of 10 to 15 years<sup>17</sup>. The disease usually begins as a so-called polyp which is non-cancerous and develops at the lining of the colon or rectum. The development of adenomas as a monoclonal derivative of a mutated epithelial stem cell is common, an estimate of one-third to one-half of all individuals will eventually develop one or more adenomas<sup>18</sup>. However, less than 10% of a certain kind of polyp called adenomatous polyp or adenoma actually progresses to cancer. Generally, about 96% of all colorectal cancers arise from adenocarcinomas, which evolve from glandular tissue<sup>19</sup>.

## INTRODUCTION

Development of colorectal cancer is mostly related to lifestyle and age. Modifiable risk factors that have been associated with an increased risk of colorectal cancer in epidemiologic studies include physical inactivity, obesity, consumption of red or processed meats, smoking and moderate-to-heavy alcohol consumption<sup>20</sup>. However, a personal or family history of colorectal cancer or adenomatous polyps increases the relative risk to develop colorectal cancer<sup>21</sup>. Hereditary colorectal cancer exists in two major forms, familial adenomatous polyposis and hereditary nonpolyposis colorectal cancer. Familial adenomatous polyposis and most sporadic cancers are usually found in the distal part of the colon and behave more aggressively while hereditary nonpolyposis colorectal cancers are commonly found in the proximal parts of the colon and behave less aggressively<sup>22</sup>. However, hereditary colorectal cancer makes up for 8-15% of all cases, while sporadic colorectal cancer accounts for 80-85% of all cases.

The most common tests for adenomatous polyps and colorectal cancer detection are flexible sigmoidoscopy, colonoscopy, double-contrast barium enema and fecal occult blood tests and stool DNA tests. These tests are recommended for both sexes from 50 years of age on and should be performed routinely.

Once cancer starts forming in the intestine, it can grow through the lining and into the wall of the colon or rectum. At that stage, the cancer can penetrate blood or lymphatic vessels. Usually, as the colorectal cancer begins to evade the tissue of origin, it spreads to the closest lymph nodes first before invading distant body organs traveling through the blood stream. Typical sites of metastasis are the liver, lungs, the abdominal cavity or ovaries. Like non-small cell lung cancer, colorectal cancer is diagnosed and staged using the International Union Against Cancer (UICC) TNM staging system. Local tumor growth within the colon wall is staged either as TNM I or TNM II. As soon as the cancer starts spreading to the regional lymph nodes, the cancer will be staged as TNM III. Late stage colorectal cancer, or TNM IV, is diagnosed when the colorectal cancer already started metastasizing to distant body organs.

## INTRODUCTION

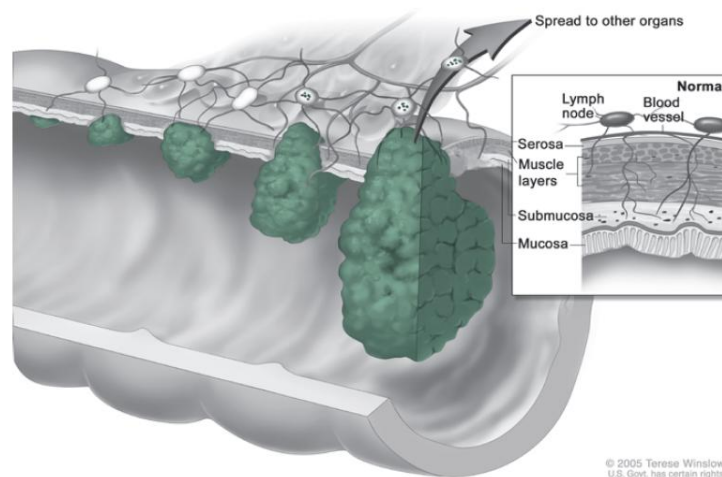


**Fig.1.4 – The different stages of colorectal cancer (from Colorectal Cancer Facts & Figures 2011-2013)**

The overall 5-year survival rate for colorectal cancer in diagnosed cases was 64.3% in 2002-2008. The standard treatment regimen for *in situ* or localized colorectal cancer is surgery and may be the only treatment needed as long as the cancer has not spread to the regional lymph nodes. TNM stage III colorectal cancer (regional) usually requires local surgery of the primary tumor and adjuvant chemotherapy. Commonly used chemotherapeutics are 5-fluorouracil (5-FU), capecitabine, irinotecan or oxaliplatin. Combination therapy increases 5-year survival rates of stage III patients up to 73%, mainly by preventing recurrence of the disease<sup>23</sup>. However, prognosis after diagnosis of stage IV colorectal cancer is generally terminal. Surgery may still be performed for prevention of blockage of the colon or to prevent other complications<sup>20</sup>. Targeted monoclonal antibody therapies have been approved by the US Food and Drug Administration (FDA). Bevacizumab (Avastin®) blocks the blood vessel formation to the tumor and both cetuximab (Erbix®) and panitumumab (Vectibix®) block the effects of hormone-like factors that promote cancer cell growth<sup>20</sup>.

The occurrence of colorectal cancer is described by a well-established accumulation of DNA mutations. It is generally referred to as the adenoma-to-carcinoma sequence. Key features of this model are (1) mutational activation of oncogenes along with mutational inactivation of key tumor suppressor genes; (2) mutations have to occur in at least 4-5 genes; (3) the total accumulation of genetic mutations is more important than their specific order; and (4) mutant tumor suppressor genes exert a biological effect even when present in the heterozygote state<sup>24</sup>.

In familial adenomatous polyposis (FAP), and in a very high proportion of sporadic colorectal tumors, mutations in the adenomatous polyposis coli gene (*apc*) are thought to be the initiating events in tumorigenesis<sup>25</sup>. The somatic mutations that occur in sporadic colorectal tumors are similar in spectrum and location to somatic mutations in FAP polyps, including

## INTRODUCTION

the Wnt/beta-catenin, TGF-beta, Notch and hedgehog (Hh) signaling pathways<sup>24-25</sup>.

The Wnt signaling pathway plays a critical role in embryonic development, as well as in maintenance of homeostasis in mature tissues<sup>26</sup>. The major component of the Wnt/beta-catenin pathway is the beta-catenin destruction complex, which is composed of adenomatous polyposis coli (APC), glycogen synthase kinase 3 $\beta$  (GSK3 $\beta$ ) and Axin. In the absence of ligands binding to the receptors, the destruction complex binds and phosphorylates newly synthesized beta-catenin, which is subsequently degraded by the ubiquitin-proteasome pathway. However, if Wnt ligands bind to the receptors, the beta-catenin destruction complex is inactivated and intracellular beta-catenin levels increase upon protein accumulation. This will allow beta-catenin to be translocated into the nucleus to form a transcriptionally active complex with TCF/LEF, leading to transcriptional activation of specific target genes, including *c-Myc* and *cyclin D*.

In the great majority of cases, *apc* mutations lead to a truncated version of the protein that lacks the C-terminally located serine alanine methionine proline (SAMP) (axin binding) repeat and the first, second and third 20-amino acid repeats (20AARs) involved in beta-catenin binding and degradation<sup>27</sup>. Whereas it is believed that all colorectal cancers are related to the activation of the Wnt signaling pathway, it is not exclusively activated through the mutation of *apc*. The best characterized alternatives to APC mutations are activating mutations of beta-catenin<sup>28</sup>, resulting in deletion of exon 3 or the targeting of individual serine or threonine residues by this exon. These mutations usually involve serines/threonines that are phosphorylated by the destruction complex. Hence, beta-catenin mutations cause the protein to escape proteasomal degradation. Beta-catenin mutations appear to occur mainly in the context of hereditary nonpolyposis colorectal cancer, which is caused by germline mutations in DNA mismatch repair genes *msh2* and *mlh1*<sup>29</sup>. Furthermore, it has been shown that genetic and epigenetic changes in genes that act primarily in other pathways, will influence Wnt activation<sup>25</sup>. For example, mutations in K-ras can induce Wnt signaling *in vitro* by increasing beta-catenin stability<sup>30</sup>. Independently of the Wnt signaling pathway, typical Wnt targets like c-Myc or cyclin D1 can also be amplified.

A second signaling pathway involved in colorectal cancer is the TGF-beta pathway, which is involved in cell proliferation, differentiation, migration and apoptosis<sup>31-32</sup>. Upon ligand binding to the type II TGF-beta receptors (TGFB2), a signaling cascade is initiated by phosphorylation of type I TGF-beta receptors (TGFB1) and subsequent SMAD2 and SMAD3 transcription factor phosphorylation. SMAD2 and SMAD3 will then form a complex with SMAD4 and translocate into the nucleus to interact with key transcription factors like p300/CBP, c-Myc, cyclin D1, p21/27/25 and Rb. Furthermore, TGF-beta signaling can directly stimulate the production of various mitogenic growth factors, like TGF-alpha, fibroblast growth factor (FGF) or epithelial growth factor (EGF), or SMAD-independent



## INTRODUCTION

pathways, such as Ras/Raf/MAPK, JNK, and PI3/Akt<sup>24</sup>. Finally, it has been demonstrated that TGF-beta promotes angiogenesis and regulates cell adhesion, motility and composition of the extracellular matrix (ECM). Frame-shift mutations in the *tgfbr2* gene make up for 30% in patients with sporadic colorectal cancer<sup>33</sup>. Alterations or deletions in SMAD genes further contribute to colorectal cancer development. Together, mutations in SMAD2 and SMAD4 are observed in up to 10-25% of all colorectal cancer cases.

Other pathways that are dysregulated in colorectal cancer are the Notch signaling pathway, which is involved in the proliferation of the intestinal epithelium, the hedgehog signaling pathway, which is involved in proliferation, cell fate decision and embryonic development, as well as RAS signaling (transmission of key extracellular signals into intracellular transduction cascades). Up to 30-40% of colorectal cancer patients carry mutations of the *kras* gene. Furthermore, alterations leading to constitutive activation in PI3K/Akt signaling have been found in colorectal cancer<sup>34</sup>. PI3K/Akt signaling is involved in tumorigenic processes like protein synthesis, glucose metabolism, cell survival and growth, as well as cell proliferation, repair, migration and angiogenesis<sup>35</sup>. Common genetic alterations are activating mutations of *pik3ca*, gain-of-function mutations of oncogenes encoding positive regulators of PI3K (HER2, EGFR, RAS and c-Src), loss-of-function mutations affecting negative regulators of PI3K (PTEN), amplification/overexpression of receptor tyrosine kinases, and mutations of genes that encode for downstream effectors (PDK-1, Akt/PKB)<sup>24</sup>.

Interestingly, in up to 90% of metastatic colorectal cancer cases, an overexpression of epithelial growth factor receptor (EGFR) was detected<sup>36</sup>. Epithelial growth factor receptors bind EGF, transforming growth factor-alpha (TGF-alpha) and a variety of other ligands and are involved in regulation of cell growth, proliferation, survival, invasion, migration and angiogenesis<sup>37</sup>. Also, activation of EGFR signaling leads to development of cellular resistance to chemo- and radiation therapy<sup>24</sup>.

The level of complexity of this signaling network and the various genetic alterations that influence the cellular balance to keep normal epithelial cells in check makes the successful treatment, especially of late stage (TNM stage III & IV) colorectal cancer, very challenging.

## INTRODUCTION

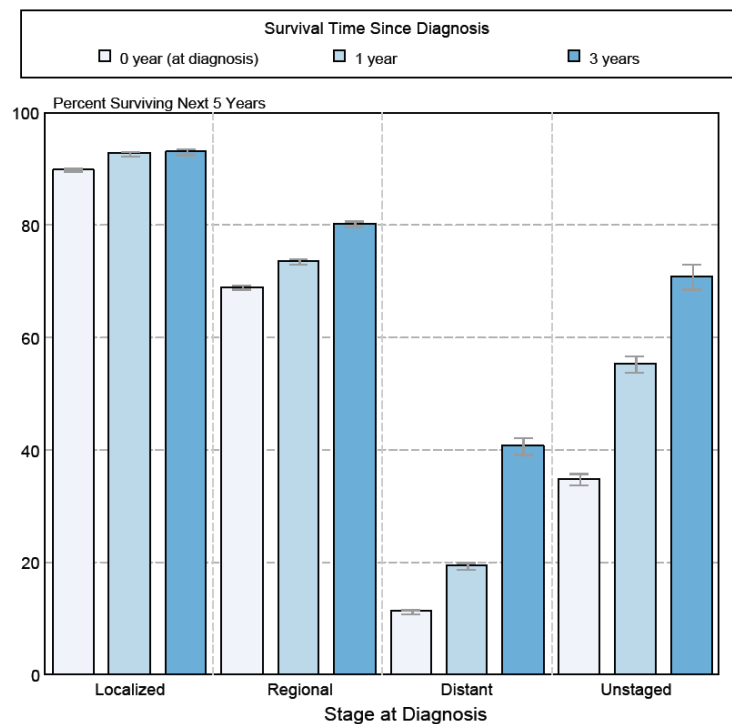


**Fig.1.5 - 5-year survival rates for colorectal cancer patients (from the NCI's Surveillance, Epidemiology, and End Results (SEER) data base)**

### 1.4 Stem cells

Stem cells are defined as cells that have the ability to sustain their population by self-renewal and to generate mature cells of a specific lineage through differentiation. Stem cells maintain tissue homeostasis by replacing terminally differentiated, aged or injured cells<sup>38</sup>. Generally, there are two types of stem cells: embryonic stem cells (ESC), that derive from various embryonic or fetal stages of development totipotent fertilized embryonic stem cells from the fertilized egg to 8 cell stage (pluripotent embryonic stem cells from the inner cell mass of the blastocyst; pluripotent or multipotent fetal stem cells from the fetus or umbilical cord blood) and somatic stem cells (SSC) which reside in their specific tissue that their progeny gives rise to. Embryonic stem cells, first isolated by Thomson *et al.* in 1998<sup>39</sup>, are pluripotent and can give rise to any cell type of the three germ layers (ectoderm, endoderm, mesoderm) of the body. ESC existence in the embryo is generally considered to be transient while it develops and differentiates into an organism. Somatic stem cells are multipotent and give rise to progeny of several distinct cell types of the same germ layer but their identification and isolation proves to be complicated.

The path leading from pluripotent embryonic stem cells to somatic stem cells to terminally differentiated tissue cells can be imagined like a downhill slope with several cell fates deciding crossroads on the way, leading to different end points. As cells move along this cell

## INTRODUCTION

fate downhill slope, they lose their ability to self-renew and to commit to the rest of the cell lineages but become more mitotically active.

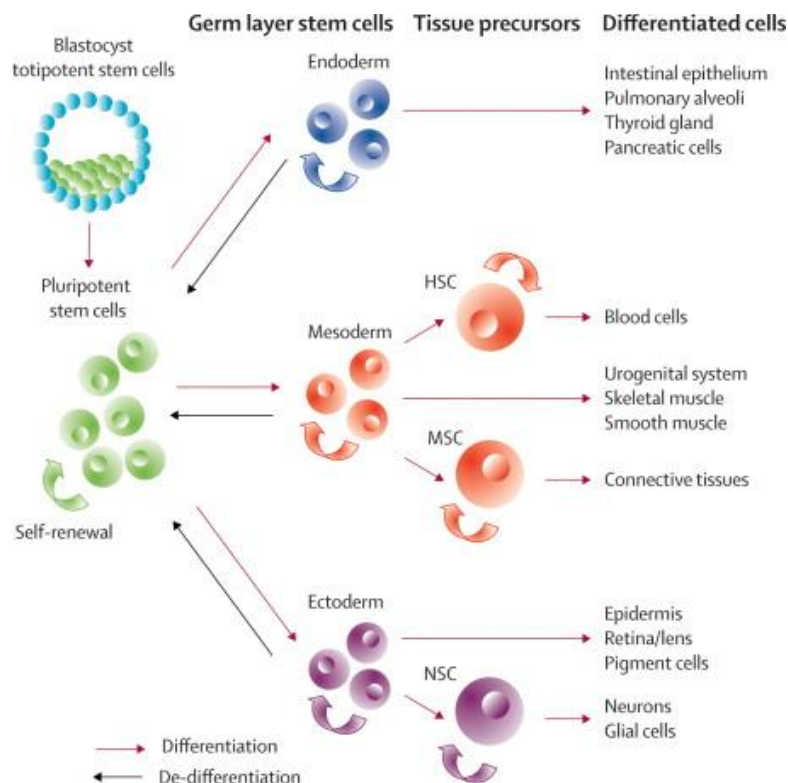


**Fig.1.6 - From pluripotency to terminal differentiation (from Corsten *et al.*, 2008<sup>40</sup>)**

Pluripotent stem cells have the ability to differentiate to all cells of the three germ layers. As they progress to differentiate into subsets of adult tissue precursors and terminally differentiated cells, they lose their ability to determine their cell fate and become lineage restricted.

Self-renewal in somatic stem cells is tightly regulated and can either be achieved through symmetric (*in vitro*) or asymmetric (*in vivo*) cell division<sup>41</sup>. When cells divide asymmetrically, one of the two daughter cells will have the same stem cell fate as the parental cell and retain stem cell characteristics while the second daughter cell is committed to differentiation<sup>42</sup>. This allows the maintenance of a small pool of self-renewing stem cells and the generation of differentiated progeny during the organism lifetime<sup>43</sup>. However, most somatic stem cells are usually retained in the G0 state of the cell cycle, which means that they rest and do not divide or proliferate. The quiescence is tightly regulated and relies on the microenvironment or niche that the stem cells reside in, and which is formed by vascular endothelial cells, pericytes, and stromal cells and low oxygen environment. Hypoxia also shields the stem cells from oxidative damage. Stem cells will only undergo mitosis when exposed to mitogens released from their specific niche<sup>44</sup>. Other somatic stem cells are continuously active, replacing cells as they mature and die off (skin cells for instance).

Sustainment of the human embryonic stem cell state requires external cues like the presence of basic fibroblast growth factor (bFGF), interplay between BMP/TGF-beta

## INTRODUCTION

signaling, as well as internal regulatory pathways that mainly consist of a self-organized transcription factor network and specific cell surface proteins. Signaling pathways involved in stem cell identity are TGF-beta signaling (patterning of mammalian embryogenesis), FGF4 signaling (cell growth and differentiation), wnt signaling (self-renewal), Hh signaling (differentiation), and Notch signaling (cell fate decisions)<sup>45</sup>. Among the cell surface proteins generally involved in embryonic stem cells are E-cadherin, glycolipids stage specific embryonic antigen 3 and 4 (SSEA-3 and SSEA4), and the keratan sulfate proteoglycans Tra-1-60 and Tra-1-81. These proteins can be used as cell surfaces markers defining a stem cell subpopulation. The transcriptional circuitry ensuring the sustainment of the pluripotent state is governed by the transcription factors Octamer-binding transcription factor 4 (Oct4), Nanog and SRY (sex determining region Y)-box 2 (Sox2). These three transcription factors form a core network for the (inter-) regulation of pluripotency by co-occupying target genes which frequently encode other transcription factors involved in development. The transcription factors regulating stemness generally work in unison rather than independently to activate gene expression of genes promoting self-renewal while repressing transcription of genes involved in differentiation. Also, it has been demonstrated recently, that microRNAs play an important role in regulating self-renewal and differentiation by targeting the master regulators Oct4, Sox2 and Nanog<sup>46</sup>. Especially, Oct4 and Sox2 rose to significant scientific recognition in 2006 as part of the 'Yamanaka Factors' with Klf4 and c-Myc. It was demonstrated that introduction of those four transcription factors was sufficient to reprogram terminally differentiated cells back into a pluripotent state (induced pluripotent or iPS cells)<sup>47</sup>. This opened up a new field of research in regenerative medicine and granted Shinya Yamanaka the 2012 Nobel Prize in Physiology or Medicine, only six years after his initial discoveries. Furthermore, it has been reported that embryonic stem cell chromatin is transcriptionally more permissive, and that differentiation is accompanied by a transition to a chromatin that is transcriptionally less active, suggesting the involvement of epigenetic processes in the sustainment of stem cells<sup>48</sup>.

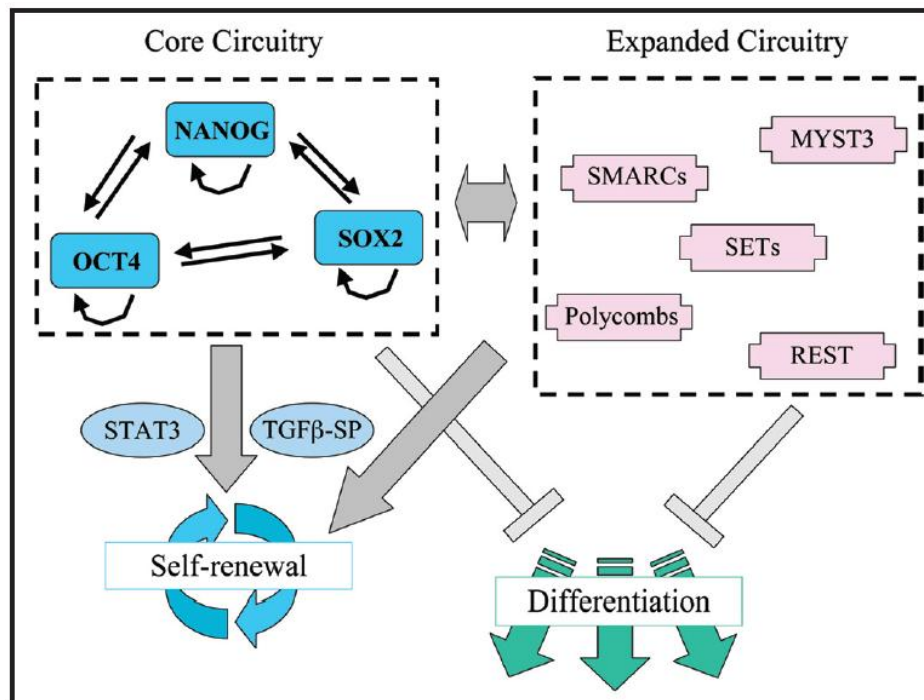


**Fig.1.7 – Regulation of self-renewal and differentiation in ESCs (from Schulz & Hoffmann, 2007<sup>49</sup>)**

The transcription factors constituting the 'core circuitry' activate each other's and their own transcription through positive feedback loops. Furthermore, they promote stem cell self-renewal through STAT3 and TGF $\beta$ -SP signaling proteins and block cell differentiation. All functions are also supported by interactions with chromatin regulators of the so-called 'expanded circuitry'.

#### 1.4.1 Stem cell transcription factor Octamer-binding transcription factor (Oct4)

The POU domain transcription factor Octamer-binding transcription factor 4 (Oct4) was the first discovered in 1990 by Schöler *et al.* as a member of the murine octamer-binding protein family<sup>50</sup>. It is expressed by all pluripotent cells during embryogenesis as well as in ESC cell lines. Furthermore, it was the first identified master regulator of pluripotency<sup>51</sup>. Its molecular mass is 39 kDa and it binds to an octamer motif on the DNA (5'-ATTTGCAT-3'), a transcription regulatory element found in many promoter and enhancer regions. Oct4 has two transactivation domains, of which one has low affinity (POU<sub>S</sub>) and one has higher affinity to DNA (POU<sub>HD</sub>), flanking the DNA-binding domain to exert its transcriptional activities<sup>52-53</sup>. Oct4 regulates cell fate in a dose-dependent manner and <2-fold increase in protein expression leads to differentiation into primitive endoderm and mesoderm, while repression of *oct4* leads to the formation of trophectoderm<sup>54</sup>. Therefore, Oct4 expression in the early embryo is vital for the full development of an organism. Only 'just-right' amounts of Oct4 sustain stemness, which is another indication for the tight regulation of stem cell transcription factors in the regulatory network actively regulating stem cells. This is obtained through a negative autofeedback loop, in which Oct4 represses itself. Oct4 has an interactome of 166 proteins, involving transcriptional activators/coactivators and repressors (e.g. Dax1, Esrrb,

## INTRODUCTION

Klf5, Sall4, Sox2, Tcfcp2l1, Zfp143) and chromatin remodeling complexes (NuRD, SWI/SNF, PRC1)<sup>55-56</sup>. It has been postulated that Oct4, Sox2 and Nanog co-occupy a substantial portion of developmentally important homeodomain proteins, forming a regulatory circuitry consisting of autoregulatory and feed-forward loops that contribute to pluripotency and self-renewal<sup>57</sup>. It has also been demonstrated that Oct4 regulates stem cell identity and cell fate decisions by modulating the Wnt/beta-catenin signaling pathway by binding nuclear beta-catenin and making it available for degradation in the cytoplasm<sup>58</sup>. The role of Oct4 in somatic stem cell self-renewal is still controversially discussed, with reports of Oct4 playing a role in sustainment of self-renewal in somatic stem cells<sup>59</sup>, while other reports demonstrate the contrary<sup>60</sup> or dismiss these findings as artifacts of *in vitro* culture or background noise<sup>61</sup>. Furthermore, it appears that expression of *oct4* pseudogenes can lead to false positive data<sup>62</sup>.

Besides being used as a stemness marker, Oct4 is expressed in the germ line and implicated in germ line-derived tumorigenesis<sup>63</sup>. Clinical studies have shown that Oct4<sup>high</sup> tumors are associated with further disease progression, greater metastasis, and shorter cancer-related survival compared to Oct4<sup>low</sup> tumors<sup>64</sup>. Also, Oct4 is oftentimes used as an intrinsic marker for cancer stem cells in addition to cancer stem cell specific cell surface markers.

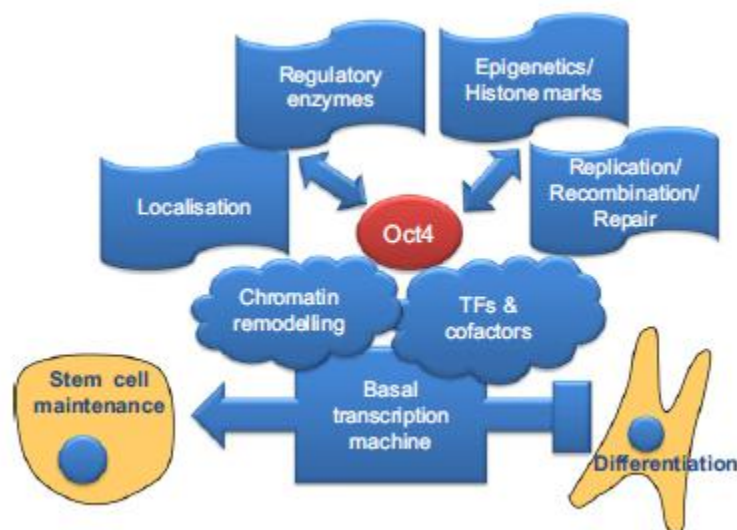


**Fig.1.8 – Schematic model of the Oct4 interactome (from Pardo *et al.*, 2010)**

Different studies shed light on the interactome of stem cell transcription factor Oct4. The Interactome involves 166 proteins, involving transcriptional activators/coactivators and repressors as well as chromatin remodeling complexes and the basal transcription machinery. Oct4 is a master regulator contributing to pluripotency and self-renewal.

## INTRODUCTION

### 1.4.2 Stem cell transcription factor Nanog

Nanog is a divergent homeobox transcription factor expressed in the inner cells of a compacted morula and blastocyst, as well as in early germ cells, embryonic germ cells and embryonic stem cells and disappears after implantation. It has been first described by Chambers *et al.*<sup>65</sup> and Mitsui *et al.*<sup>66</sup> in 2003 and is named after “Tir nan Og”, the mythological Celtic land of the ever-young. Nanog has a molecular mass of 38 kDa and its general structure consists of a serine-rich N-terminus, a DNA-binding homeobox (DNA consensus sequence 5'-TAAT[GT][GT]-3') and a C-terminal domain with tryptophan-rich regions for homodimerization<sup>67</sup>. The homeodomain contains the nuclear localization sequence (NLS) which is necessary for transport into the nucleus after translation of the *nanog* mRNA. In human Nanog, only the C-terminal domain demonstrates transactivation activity<sup>68</sup>.

While Oct4 is crucial for the first embryonic lineage specification from morula to early blastocyst, Nanog expression is crucial for the second specification from early blastocyst to late blastocyst. Both, Oct4/Nanog expression and silencing of the differentiation system are necessary for sustaining stem cell identity<sup>69</sup>. Furthermore, together with Oct4 and activated STAT3, Nanog plays a crucial role in maintenance of self-renewal in embryonic stem cells and can replace leukemia inhibitory factor (LIF)/STAT3 signaling in mouse embryonic stem cells to sustain self-renewal capacity<sup>65-66</sup>. Functionally, Nanog blocks differentiation and deletion triggers differentiation of embryonic stem cells into parietal/visceral endoderm. While Oct4, Sox2 and FoxD3 positively regulate Nanog expression, there is evidence that Tcf3 and p53 repress Nanog promoter activity<sup>70-71</sup>. Nanog acts independently of STAT3, while it does work in concert with Oct4 to support stem cell potency and self-renewal<sup>69</sup>. Oct4 and Sox2, Nanog co-occupy the promoters of a large population of genes (353 genes in human ES cells), that encode for developmentally important homeodomain transcription factors<sup>57,72</sup>. This core transcriptional circuitry involves autofeedback loops, as well as activation of the TGF-beta and Wnt signaling pathways. Nanog is a direct target of TGF-beta/Activin-mediated SMAD signaling, strengthening its role in sustainment of self-renewal<sup>73</sup>. On the other hand, Oct4, Sox2, and Nanog occupy a set of repressed genes that are key to developmental processes<sup>57</sup>. Transcriptional regulators interacting with Nanog include Sall4, Nr0b1, Nacc1, Esrrb, Sp1 or Hdac2 (histone deacetylase 2). Zhang *et al.* demonstrated that Nanog expression significantly increases the proliferation of embryonic stem cells, by increasing the number of cells entering S phase of the cell cycle and shortening the time needed in G1/0 for S phase entry by binding to the regulatory regions and activating gene expression of *cdk6* and *cdc25a*<sup>74</sup>.

Interestingly though, Nanog is not part of the canonical quartet of transcription factors ('Yamanaka factors') employed to reprogram mouse fibroblasts. However, addition to this

## INTRODUCTION

quartet has resulted in increased reprogramming efficiencies in human cells by attaining the pluripotent ground state during the final phase of reprogramming, when other key factors are already present<sup>75-76</sup>.

Like Oct4, Nanog is expressed in some germ line-derived tumors<sup>77</sup> and co-expression of Oct4 and Nanog has been demonstrated to enhance malignancy in lung adenocarcinoma by inducing cancer stem cell-like properties and epithelial-mesenchymal transition (EMT)<sup>78</sup>. In addition, Nanog is overexpressed in early lung cancers, providing a potential diagnostic tool<sup>79</sup>. Nanog overexpression in prostate cancer cells is sufficient to confer cancer stem cell characteristics like promotion of clonogenic survival, drug resistance and tumor development<sup>80</sup>. In 2010, Meng *et al.* demonstrated that Nanog is functionally important in regulating proliferation, invasion and motility of colorectal cancer cells and contributes to epithelial-mesenchymal transition (EMT) by regulating *SLUG* and *SNAIL* gene expression<sup>81</sup>. Furthermore, Nanog expression was also found in human breast cancer<sup>82</sup>, retinoblastoma<sup>83</sup>, ovarian cancer<sup>84</sup> and squamous cell carcinoma<sup>85</sup>.

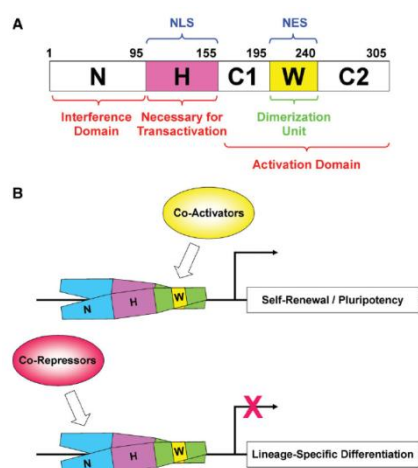


**Fig.1.9 – Molecular structure of human Nanog (from Chang *et al.*, 2009)**

Nanog is a divergent homeobox transcription factor and consists of a serine-rich N-terminus, a DNA-binding homeobox and a C-terminal domain for homodimerization. The homeodomain contains the nuclear localization sequence (NLS) which is necessary for transport into the nucleus. Only the C-terminal domain demonstrates transactivation activity.

### 1.4.3 Stem cell transcription factor Krueppel-like factor 4 (Klf4)

Krueppel-like factor 4 (Klf4), also known as epithelial zinc finger (EZf) was first described as gut-enriched Krueppel-like factor (GKlf) in 1996 by Shields *et al.* and is part of the Krueppel-like family of zinc finger transcription factors<sup>86</sup>. Generally, Krueppel-like factors (Klfs) regulate proliferation, differentiation, development and apoptosis. Klf4 is one of several homologues of the zinc finger transcription factors that resemble the *Drosophila* segmentation gene product Krueppel. In transcription factors with zinc finger motifs, a zinc atom is tetrahedrally coordinated by four amino acid residues, usually cysteine or histidine,



## INTRODUCTION

with a 30-amino acid sequence to form the DNA binding domain. Human Klf4 is a 479 amino acids long polypeptide, containing a N-terminal SH3 domain, a PEST domain, a nuclear localization domain (NLS) and three C<sub>2</sub>H<sub>2</sub> zinc finger motifs in the C-terminus of the protein<sup>86</sup>. A second NLS sequence is located in the zinc finger motif of the protein. The predicted molecular mass of Klf4 is 50 kDa. Klf4 targets GC-rich *cis*-DNA elements, binding to a CACCC consensus sequence and the basic transcription element (BTE). In transcriptional regulation, Klf4 acts as both activator (*klf4*, p21<sup>WAF1/Cip1</sup>, keratine, alkaline phosphatase) and repressor (*cyp1a1*, *cyclin D1*, *cyclin B1*, *cyclin E*) to control proliferation and differentiation.

Interestingly, Klf4 was part of the four reprogramming transcription factors, alongside Oct4, Sox2 and c-Myc, necessary to reprogram differentiated somatic cells back to a pluripotent stem cell-like state. It was demonstrated by Wei *et al.* that Klf4 directly interacts with Oct4 and Sox2 in embryonic and induced pluripotent stem (iPS) cells, indicating that these three transcription factors control activation and repression of downstream gene targets<sup>87</sup>. Changes in *klf4* expression levels upon LIF signaling occur prior to Nanog responses. In embryonic stem cells, Klf4 knockdown leads to differentiation whereas over-expression maintains self-renewal and turns LIF signaling obsolete<sup>88</sup>. It was also demonstrated that Klf4 can bind to the Nanog promoter and regulate Nanog expression, supporting a mechanism in which Klf4 acts as a mediator between LIF-STAT3 and Nanog to regulate ES cell self-renewal and pluripotency<sup>88</sup>. Klf4 expression is developmentally regulated, with higher expression levels at the later stage of fetal development (E15 to E18), when the gut epithelium undergoes major transition.

In the fully developed organism however Klf4 expression is more differentiated. Many Klfs exhibit tissue-selective expression and wide-ranging regulatory functions. Klf4 is most abundant in epithelial tissues like the intestinal tract or the skin, vascular endothelial cells and the thymus<sup>86,89-90</sup>. It is especially highly expressed in terminally differentiated, quiescent post-mitotic cells of the colonic mucosa. Klf4 is exclusively found in the middle to upper regions of the crypt epithelium, while its expression in the proliferating crypt cells is repressed. Expression of Klf4 in cell culture is induced under growth arrest promoting conditions like DNA damage, serum deprivation and contact inhibition. Furthermore, expression of Klf4 leads to inhibition of DNA synthesis. This is accomplished by Klf4 binding to p53, thus allowing p53 to gain access to the p21<sup>WAF1/Cip1</sup> promoter and activate its transcription<sup>91</sup>. Subsequently, p21 expression leads to an arrest in cell cycle progression at the G<sub>1</sub>/S and G<sub>2</sub>/M checkpoints. Additionally, Klf4 directly inhibits *cyclin D1* and *cyclin B1* expression, further enhancing the cell cycle arrest. These findings suggest that Klf4 might play an important role in regulating cell growth of intestinal cells and be involved in terminal differentiation of select epithelial tissues<sup>92</sup>. Down-regulation of Klf4 may result in uninhibited

## INTRODUCTION

cell growth and malignant transformation.

These findings suggest that Klf4 might exert tumor suppressor effects. Indeed, mRNA transcript levels of Klf4 are significantly reduced in patients with familial adenomatous polyposis (FAP) and other colorectal cancers compared to normal tissues of the intestine<sup>93</sup>. Loss of heterozygosity of the *klf4* locus, mutations in open reading frames (ORFs), and hypermethylation of *klf4* promoters have been identified in various human CRCs and cell lines<sup>94</sup>. Findings that Klf4 expression is reduced in intestinal tissues from *Apc*<sup>Min/+</sup> mice, a model of intestinal tumorigenesis, and the inverse correlation between Klf4 levels and size of the intestinal adenoma, further contribute to that notion<sup>92,95</sup>. It has also been demonstrated that Klf4 binds the transcriptional active domain of nuclear beta-catenin and inhibits beta-catenin-mediated transcription, cementing its important role in intestinal homeostasis and colorectal carcinogenesis by inhibiting the Wnt signaling pathway<sup>96</sup>. Re-expression of Klf4 in colorectal cancer cell lines results in diminished tumorigenicity<sup>97</sup>. In colorectal cancer cells (HT-29), gradually increasing Klf4 expression correlates with differentiation stage of HT-29 cells<sup>98</sup>, a fact that was confirmed in colorectal cancer patients<sup>99</sup>. However, adverse expression patterns can be found in squamous cell carcinomas or breast cancers, suggesting a diverse role of Klf4 that is dependent on the tumor type<sup>100-101</sup>.

The role of Klf4 as a potential tumor suppressor in the colonic epithelium and its involvement in regulation of cell proliferation and growth arrest as a make it a promising target in new approaches for the treatment of colorectal cancer.

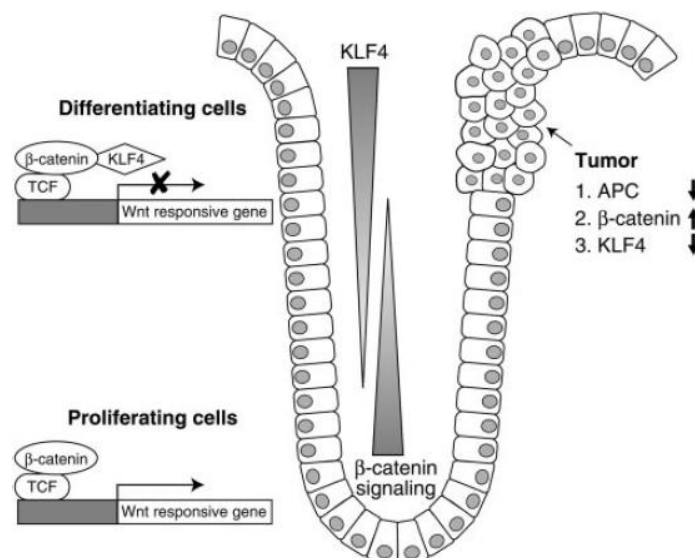


**Fig.1.10 – Model of cross talk between Klf4 and beta-catenin in the intestine (from Zhang et al., 2006)**

In differentiating, quiescent cells, Klf4 binds to beta-catenin and inhibits wnt signaling while wnt signaling is active in proliferating cells. While Klf4 is most abundant in the epithelial cells of the intestinal, its expression gradually decreases towards the proliferating center of the crypt. On the other hand, beta-catenin signaling decreases as cells move out of the crypt and differentiate. In colorectal tumor cells, APC mutations lead to increased beta-catenin signaling and down-regulation of Klf4 expression. This leads to aberrant cell proliferation.

## INTRODUCTION

### 1.5 Cancer stem cells

The clonal evolution model of cancer development proposes that all tumor cells are tumorigenic. In recent years, more and more evidence emerged supporting the hypothesis that within the tumor mass, a small group of cells exist that sustains tumor growth. Like stem cells, this small fraction of cells gives rise, albeit aberrant, to the heterogeneous lineages of the tumor. These cells are referred to as “cancer stem cells” (CSC) and the model was first proposed by Mackillop in 1983.<sup>102</sup> By now, cancer stem cells (or cancer-initiating cells) have been identified in various cancer types like leukemia, breast cancer, glioblastoma, skin cancer, bone cancer, prostate cancer and more recently, also in colorectal cancer<sup>103-109</sup>. However, the frequency of CSCs appears to be highly variable even between tumors of the same type<sup>110</sup>. In recent years, it has been shown that isolation and enrichment of these subpopulations of cells increase the tumor-initiating capacity. A long-living “stem-like” cell subset at the base of the tumor growth would allow progressive growth towards malignancy by accumulation of hallmarks of cancer through mutations and epigenetic changes<sup>111-112</sup>.

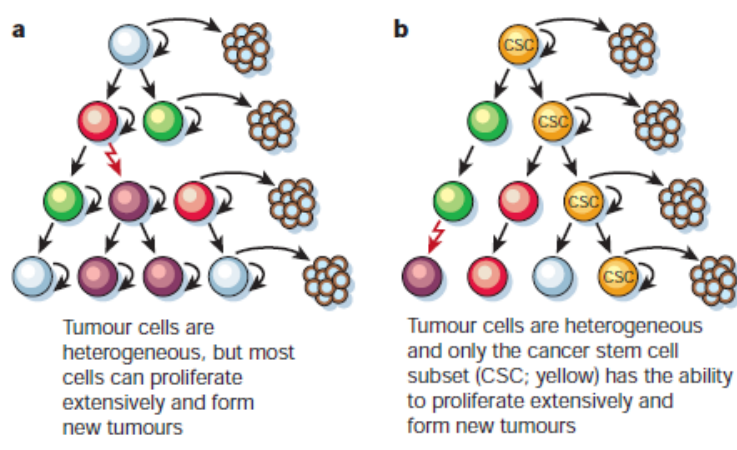


**Fig.1.11 – conventional stochastic and cancer stem cell model for tumor development (from Reya *et al.*, 2001)**

The stochastic model (A) assumes that every single tumor cell can potentially regrow a tumor but does so rarely. The cancer stem cell model (B) assumes that only a subset of cells within a tumor can grow back a heterogeneous tumor.

Per definition, cells have to display distinct characteristics to be considered cancer stem cells. Cancer stem cells have to possess the ability of regenerating the original tumor type when re-injected in a limited number into an orthotopic *in vivo* environment. Therefore, the gold standard for defining cancer stem cells is their capacity to self-renew. This can be observed by serial transplantation of re-isolated cancer stem cells in secondary and tertiary recipients and the regeneration of a phenotypically identical and heterogeneous tumor. This includes differentiation into all cell types of the heterogeneous tumor tissue. Multilineage

## INTRODUCTION

differentiation however, is not required.

Even though the cancer stem cell hypothesis was discussed for a long time, the first identification of a specific cell-surface antigen profile (CD44<sup>pos</sup>/CD24<sup>neg</sup>) that described a cancer stem cell subpopulation successfully re-establishing itself as a tumor xenograft was published in 2003<sup>104</sup>. More recently, aldehyde dehydrogenase (ALDH) has been used as a marker for breast cancer stem cells<sup>113</sup> as well as for acute leukemia<sup>114</sup> and brain tumors<sup>115</sup>. A subpopulation expressing epCAM<sup>high</sup>, CD44<sup>pos</sup>, CD133<sup>pos</sup>, and CD166<sup>pos</sup> has been described as colon-cancer initiating cells in immunodeficient mice<sup>109,116</sup>. For several tumor types, marker sets that are supposed to describe a cancer stem cell subpopulation, have been postulated<sup>117-119</sup>. However, there are lines of evidence that suggest that there is a high degree of variability in the expression of several of the suggested markers for cancer stem cells in different tumor subtypes and histological stages in breast cancer and other cancer types<sup>120-121</sup>.

Furthermore, there is still an ongoing debate over the validity of the cancer stem cells in context with tumor initiation in mouse models. It has been proposed by Kelly *et al.* that the rarity of tumor development of human cancer cells in NOD/scid mice might rather be caused by the lack of a more natural, human microenvironment to support the propagation of human cancer cells. They state that certain malignancies can be maintained by a relatively large proportion of tumor cells rather than exclusively by a small subpopulation<sup>122</sup>. Therefore, xenotransplantations may underestimate the actual percentage of cells that are able to initiate and sustain tumor growth. It has furthermore been demonstrated that modification of xenotransplantation assays dramatically increased the rate of tumorigenic melanoma cells<sup>123</sup>. Thus, the cancer stem cell hypothesis might not fit all human cancers, even though there is evidence that the existence of tumorigenic subpopulations is not an experimental artifact<sup>124</sup>.

The existence of cancer stem cells has enormous implications on cancer therapy. With a treatment-resistant subpopulation fueling tumor growth at the base of a tumor, conventional treatment regimens like surgery, chemotherapy or radiation therapy most likely leave this subpopulation unaffected, resulting in the recurrence of a possibly even more aggressive tumor. If cancer stem cells indeed drive tumor progression, metastasis and recurrence, new treatment approaches, targeting especially the cancer stem cell population will be desperately needed to efficiently treat cancers.

### **1.6 The relation between stem cells and cancer stem cells**

The main reason why tumor-initiating cells are labeled as cancer stem cells is the fact that they possess major features that are also defining somatic stem cells: CSCs are considered

## INTRODUCTION

to be quiescent, able to self-renew, they divide asymmetrically and differentiate into all lineages that comprise a tumor. This basically suggests that cancer stem cells undergo processes that are analogue to somatic stem cells.

In contrast to somatic stem cells which are notable for the vigilance with which their proliferation is controlled and the care with which their genomic integrity is maintained, cancer stem cells are frequently distinguished by their lack of control of such processes<sup>125</sup>. Despite the fact that theoretically any given cell can acquire several genetic mutations that trigger transformation into a cancer cell, somatic stem cells have been proposed to be a formidable origin of cancer development. It is proposed that the long-living somatic stem cells are more prone than short-living terminally differentiated cells to acquire the multiple oncogenic mutations that are required to become cancer cells, as proposed by the multistep model of tumorigenesis. There is also evidence that stem cells require fewer mutations to turn tumorigenic than differentiated cells, which traditionally are believed to need at least six mutations to transform into cancerous cells<sup>7,126</sup>. Furthermore, SSCs already offer their intrinsic machinery to regulate quiescence, DNA repair and drug resistance, making the development of these hallmarks obsolete. On another note, cancer development from somatic stem cells finds further support by the biological characteristics of Wilms tumors, a cancer type which is typically found in young children and arises from embryonic cells of the kidney, neuroblastomas, and teratocarcinomas. All these cancers originate from mutations occurring in embryonic stem cells which disappear during the aging process<sup>43</sup>. Like somatic stem cells, CSC progeny is lineage-restricted to the tumor tissue of origin, giving rise to a phenotypically heterogeneous tumor with various degrees of differentiation. However, it has also been demonstrated, that cancer stem cells can be generated from restricted stem cell progeny<sup>127</sup>.

CSCs and SSCs also share a lot of the factors for the regulation of self-renewal, differentiation and proliferation pathways.<sup>128</sup> Notch (leukemia, mammary tumors), Wnt (colon carcinoma, epidermal tumors) and Sonic hedgehog (medullablastoma, basal cell carcinoma) pathways are involved in regulating stem cell development and associated with cancer<sup>126</sup>. Also, important stem cell master regulators like the transcription factor Oct4, STAT3 and Nanog are expressed in both, human embryonic stem cells and cancer cells<sup>82,129</sup>. *C-MYC* gene reactivation is sufficient to trigger embryonic stem cell programs in normal and cancer cells, demonstrating how easily cancerous cells can convert to expressing embryonic stem cell programs<sup>129</sup>. Based on these findings it is hypothesized that both, ESCs and CSCs are controlled by a few master regulatory genes, of which one is *c-MYC*.

There is more and more scientific evidence that like somatic stem cells, cancer stem cells possess intrinsic survival mechanisms that enable them to resist the cytotoxic effects of chemotherapy and radiation therapy when compared to the non-proliferating population of a

## INTRODUCTION

tumor. In the case of chemotherapy resistance, this is associated with multidrug resistance or ATP-binding cassette (ABC) transporter overexpression, quiescence which avoids triggering intrinsic apoptotic pathways, and constitutive activity of detoxifying enzymes<sup>43</sup>. Preferentially overexpressed ABC transporters in cancer stem cells include P-glycoprotein (Pgp), multi-drug resistance-associated protein 1 (ABCC1) and breast cancer resistance protein-1 (ABCG2), which is also expressed in different stem cells (CD34<sup>pos</sup>/CD38<sup>neg</sup> in hematopoietic stem cells) and reduced or completely lost during cell differentiation<sup>130</sup>. Hypothetically, inhibition of drug transporters in the cancer stem cell subpopulation could sensitize these cells for chemotherapy, although the application is significantly inhibited by *in vivo* toxicity<sup>131</sup>. Additional correlations between stem cells and cancer stem cells can be found in increased telomerase activity and high nuclear to cytoplasmic ratios<sup>132</sup>.

Another characteristic that cancer stem cells share with somatic stem cells is their relatively quiescent state which allows them to evade treatment regimens that are based on drugs that target and kill rapidly proliferating tumor cells. While quiescence in somatic stem cells is regulated by transiently activated signals from the niche they reside in, these signals are in an unregulated, permanent state of activation in the tumor microenvironment. Recently, it has been shown that stem cell niches can undergo changes that promote proliferation and maintenance of cancer cells<sup>133</sup>. There is also evidence that hypoxia in the cancer stem cell niche helps sustaining the CSC population, similar to SSCs<sup>134</sup>. Furthermore, “premetastatic” niches can be generated by cancer cell proliferation or the release of soluble tumor factors (VEGFA, TGF-beta, TNF-alpha) that can support the seeding and proliferation of metastatic tumor cells in secondary and tertiary sites<sup>135</sup>.

The most common strategy today to identify potential markers for cancer stem cell identification is to use markers that are expressed in normal stem cells while oftentimes the functional role of these markers in stem cells is unknown and their role in stem cell biology is unclear<sup>125</sup>. The similarity between cancer stem cells and somatic stem cells can help in a better understanding of the origins of cancer and may open the doors to new approaches to cancer therapy, hopefully leading to more efficient treatment of cancer patients.

### 1.7 Novel approaches in cancer therapy

Despite decent success rates in treatment of cancer with established treatment regimen like surgery, chemotherapy or radiation therapy, not all cancers can be treated successfully. Conventional therapeutic approaches will oftentimes have severe negative side effects. Therefore, it is desirable that new cancer treatments should be as tolerable to the patient as possible, ideally showing little to no severe side effects at all. A promising approach to achieve this goal is to develop drugs that specifically target the malignant cancer cells and avoid damaging the normal surrounding tissues or compromise its proliferation and

## INTRODUCTION

regeneration potential. Furthermore, combination of conventional therapeutic regimens with new cancer drugs in development could further improve success rates in the treatment of cancer patients. In the recent past, different approaches towards safer and more successful treatments are being made, including silver bullets like gene therapy, immunotherapy (vaccines<sup>136-137</sup>, cytokine therapy<sup>138</sup> or monoclonal antibodies<sup>139</sup>) or the use of oncolytic viruses.

### 1.7.1 Oncolytic viruses in cancer therapy and diagnosis

Amongst many new approaches in cancer therapy, a promising novel form is oncolytic virotherapy, a way to elegantly employ nature's own agents to target and kill malignant tumor cells within a living organism. Over the last century, several viruses were reported to display oncolytic effects in cancer patients<sup>140-143</sup>. Generally, oncolytic viruses replicate in and lyse cancer cells upon their release from the host cancer cells. Subsequently, newly formed viral particles will then spread within the tumor and infect surrounding cancer cells, repeating the replication cycle. Virus-mediated mechanisms that induce oncolysis include antivascular effects and the induction of tumor-specific immunity<sup>144</sup>. Another advantage of oncolytic virotherapy is that intravenous administration allows for viral spreading throughout the body via the blood stream, enabling the virus particles to find the primary tumor as well as distant metastases.

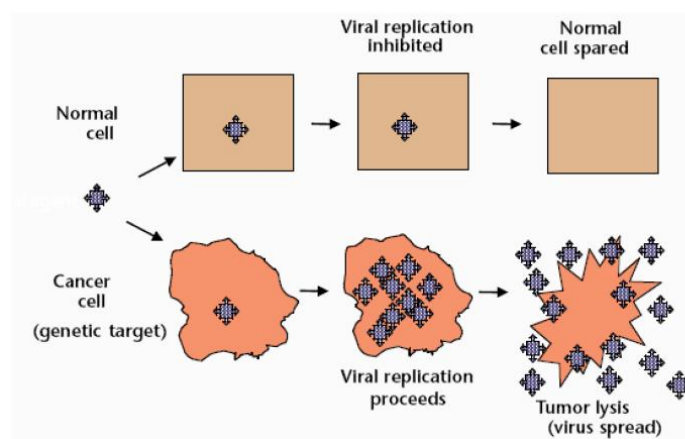


**Fig.1.12 – Schematic of oncolytic virotherapy mechanism of action (from Kirn *et al.*, 2001<sup>145</sup>)**  
Viral replication, cell killing and release are restricted to malignant cancer cells.

Today, oncolytic viruses include attenuated, non-engineered viruses (first-generation), genetically engineered viruses (second-generation) and transgene-armed viruses (third-generation). First attempts in employing viruses in cancer treatment were made with first-generation viruses like West Nile virus<sup>146</sup>, adenovirus<sup>147</sup>, mumps virus<sup>148</sup>, Newcastle disease virus<sup>149</sup> and vaccinia virus<sup>150</sup>. With progression in the field of genetic engineering, research in

## INTRODUCTION

oncolytic virotherapy shifted its focus on engineered viruses. The most notable second-generation virus is adenovirus ONYX-015 which could replicate in tumorigenic cells exclusively due to the deletion of the E1B gene product, a protein which interacts with the tumor suppressor protein p53<sup>151</sup>. Different oncolytic viruses are currently tested in clinical trials either as stand-alone treatment or in combination with standard therapy (<http://www.clinicaltrials.gov>); namely reovirus (REOLYSIN), vesicular stomatitis virus, measles virus (MV-CEA), adenovirus (delta-24-RGD), *Herpes simplex* virus (HF-10, OncoVEX<sub>GM-CSF</sub>) and vaccinia virus (GL-ONC1, JX-594). The first oncolytic virus (adenovirus H101, by Shanghai Sunway Biotech) has been approved in China by the Chinese State Food and Drug Administration (SFDA) for head and neck cancer in 2005<sup>152</sup>.

Another advantage of oncolytic viruses and even bacteria is the potential application in cancer diagnosis. Recent efforts focused on the development of new techniques of visualization. Microorganisms like bacteria and viruses have been genetically engineered to express light-emitting proteins such as bacterial (Lux) or *Renilla* (Ruc) luciferases or green fluorescent proteins and shown to localize and spread in tumor tissues in mouse xenografts<sup>153</sup>. Viral gene expression of the human norepinephrine transporter<sup>154</sup> (hNET) or the human iodide symporter<sup>155</sup> (hNIS) in vaccinia virus have been shown to allow PET imaging of tumors and may prove beneficial in deep tissue imaging of cancers that can not be detected by low light imaging. Optical visualization of tumor tissues and metastases is beneficial in early detection of malignant growing cancers and in post-surgical therapy after excision of the solid tumor. Light emission in virally infected tumor sites may even help in the surgical excision of the tumor tissue itself.

A different approach is the arming of oncolytic viruses with transgenes. It has been shown that recombinant vaccinia virus expressing single-chain antibody GLAF-1 normalizes the aberrant vascularization *in vivo*<sup>156</sup>. New insights in the biology of cancer, the effects of the immune system and progress in genetic engineering together with the inherited biological properties of poxviruses make them a potential candidate for the development as oncolytic agents and diagnostic tools in cancer treatment.

### 1.8 Vaccinia virus

Vaccinia virus is a member of the *poxviridae* family. Viruses of the *poxviridae* are generally divided into *entomopoxvirinae*, which only infects insects and *chordopoxvirinae*, which infect vertebrates. The subfamily of *chordopoxvirinae* is subdivided into eight genera, all of them similar in morphology and host tropism. Like the most famous pox-virus, small-pox causing variola virus, vaccinia virus belongs to the genus of *orthopoxviridae*. While the origins of modern vaccinia virus are unknown due to the lack of record-keeping as the virus was



## INTRODUCTION

repeatedly cultivated and passaged in research facilities, it is still widely used as a model to study poxviruses.

### 1.8.1 Morphology

Poxviruses belong to the group of double-stranded (ds) DNA viruses and are amongst the biggest known viruses. Viral particles are approximately 300 x 240 x 120 nm in size and possess an barrel-shaped structure with a shell of lipoproteins surrounding a complex core structure<sup>157</sup>. The core structure contains the linear dsDNA genome of approximately 192 kilobases (kb), encoding for about 200 non-overlapping genes. The viral DNA is associated with a number of virus-encoded proteins like RNA polymerase and enzymes for RNA capping, methylation and polyadenylation, which are packed within the dumbbell-shaped core to enable early viral protein synthesis upon host cell infection<sup>158</sup>. The core wall consists of a continuous inner layer that is only separated by a few channels and an outer layer in the shape of a palisade structure. The outer layer is made of T-shaped spikes that are anchored in the lower membrane. Three variants of vaccinia virus particles have been shown to be infectious: intracellular mature virus (IMV), cell-associated enveloped virus (CEV) and extracellular enveloped virus (EEV). However, CEVs and EEVs are basically IMVs with an additional envelope of lipoproteins and have a lower buoyant density compared to the intracellular mature virus particles<sup>159</sup>.

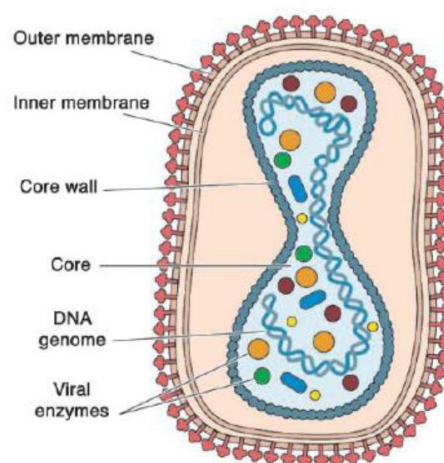


**Fig.1.13 – Virion structure of vaccinia virus (from Harrison *et al.*, 2004<sup>160</sup>)**

The coating of the IMV remains controversial. It is yet unknown if the virion is made up of one or two membranes. The core of the virus contains the dsDNA and proteins necessary for early transcription.

### 1.8.2 Vaccinia virus replication cycle

Unlike other DNA viruses, vaccinia virus remains located in the host cell cytoplasm rather than the nucleus for the duration of its infectious cycle. In the first step of infection, the enveloped virus fuses with the cell membrane or the membrane of an endocytotic vesicle<sup>161</sup>.

## INTRODUCTION

Vaccinia virus mode of entry was described as apoptotic mimicry and pH- and phosphatidylserin-dependent macropinocytosis<sup>162</sup>. After the fusion of viral and cellular membranes, the viral core is released into the cytoplasm and transported further into the cell along microtubules to the cytoplasmic side of the endoplasmic reticulum (ER). The viral core contains all the necessary enzymatic features for early replication and starts synthesis of early viral mRNAs, which resemble host cell mRNAs. Vaccinia virus recruits the cellular translational apparatus to translate mRNAs that encode for proteins involved in subsequent viral DNA synthesis. Other early viral proteins help modifying the host cell to the advantage of the virus and aid virus escape from the host innate immune response<sup>163</sup>. Replication of viral DNA begins in so-called mini-nuclei surrounded by rough ER membranes and immediate and late genes are transcribed.<sup>164</sup> Generally, immediate genes serve for the transcription of late genes which are involved in packaging of the newly synthesized viral particles and for essential proteins that initiate early gene transcription in newly infected cells. After all the necessary proteins have been synthesized, the assembly of the viral progeny particles begins<sup>160</sup>. First, after five hours of infection, crescent-shaped membranes and spherical immature virions (IV) form at the site of DNA replication. These IVs still lack the viral genome and once they take up the DNA, they mature into the barrel-shaped IMV, the first infectious form of the virus<sup>165</sup>. IMVs are either released upon host cell lysis or alternatively move away from the DNA replication sites by binding to microtubules where they can obtain a second double membrane from a trans-Golgi or early endosomal compartment to become an intracellular enveloped virion (IEV)<sup>160</sup>. The IEV particles use cellular microtubules and kinesins to move towards the cell membranes and form CEVs upon fusion. CEVs can then recruit actin from the cytoplasm to be transported to adjacent cells or dissociate from the cell membrane to form EEVs. The majority of EEVs is still associated with the host cell membrane even at late stages of infection<sup>166</sup>.

### **1.8.3 Targeted and armed oncolytic poxviruses**

Since Edward Jenner started testing his vaccination against small pox in 1796, a wealth of clinical experiences with poxviruses, and especially vaccinia virus, is available from its role in the smallpox eradication program during the middle of the 20<sup>th</sup> century. More recently, poxviruses were used in a number of clinical trials for the treatment of cancer, rabies or HIV<sup>158</sup>. Up to this day, vaccinia virus has been shown to be safe for the use in humans. The modified vaccinia virus Ankara (MVA) was initially used as a vaccine against smallpox and is now used as a recombinant vaccine vector for immunization against number infectious diseases and cancers<sup>167</sup>. Interestingly, MVA can efficiently express high levels of foreign genes and is researched in clinical trials as a tool for vaccination against malaria, tuberculosis, HIV/AIDS and cancer<sup>168-170</sup>. The inherited ability to rapidly replicate in and lyse

## INTRODUCTION

human cells in comparison with other viruses makes poxviruses an interesting candidate for cancer therapy<sup>171</sup>. Secondly, poxviruses display a broad tumor tissue tropism because of their membrane fusion entry mechanism which is independent from specific cell surface receptors<sup>162,172</sup>. This makes poxvirus infections easy to study, especially in terms of pre-clinical studies in laboratory animals (mouse xenograft models). Furthermore, vaccinia virus is favorable because it has a large foreign gene-carrying capacity which allows the expression of heterologous genes. Lastly, vaccinia virus replicates exclusively in the cytoplasm of the host cell, with no risk of chromosomal DNA integration. First- and second-generation oncolytic viruses were proven to be safe and still showed a high selectivity for cancer cells but their therapeutic potential was poor. In a subsequent step, genetically armed third-generation oncolytic poxviruses carrying therapeutic transgenes have been engineered to exploit new potentials of this novel approach in cancer therapy. Transgene expression of cytokines, pro-drug converting enzymes as well as immuno-stimulating and anti-angiogenic agents is, due to the preferential expression in cancer cells, highly tumor-specific<sup>156,173-176</sup>. Transgene expression is tried to be applied for imaging purposes by linking reporter gene expression to viral replication<sup>177</sup>. Thus, expression of transgene luciferases, fluorescing proteins or different transporters for accumulation of substrates used in deep tissue imaging (MRI, PET) can be combined with optical imaging techniques.

Cancer cells provide optimal conditions for viral replication like blocks in apoptotic pathways, deregulation of cell cycle control and evasion from the host immune system, which is inherently favored by vaccinia virus<sup>178</sup>. In addition to that, wild-type viruses can efficiently produce a range of gene products that transform normal cells such that they lose the ability to regulate their cell cycles and viral infection can block apoptotic pathways in the host cell. With these conditions already fulfilled in cancer cells, this allows the deletion of genes responsible for host cell transformation. In this process, the virus becomes attenuated and is no longer able to replicate in normal tissues and viral replication is exclusively confined to tumor cells<sup>178</sup>. For example, a deletion of the thymidine kinase gene in vaccinia virus leads to dependence of the virus on cellular thymidin kinase expression which is over-expressed in tumor cells but not in normal cells<sup>179</sup>. The anti-tumoral effect of vaccinia virus can be distinguished into different mechanisms of action. Direct infection of cancer cells with vaccinia virus leads to viral replication and consequently to cell lysis and death by necrosis. In addition, infection can lead to immune-related cell death by a strong inflammatory response triggered by the virus<sup>178</sup>. It has also been shown that attenuated MVA can induce apoptosis in infected melanoma cells, and therefore prime maturation of dendritic cells (DCs) by phagocytosis which ultimately leads to an anti-tumoral T cell response<sup>180</sup>. Furthermore, infection with vaccinia virus can lead to the shutdown of tumor vasculature, cutting off the

## INTRODUCTION

tumor cells from their nutrient supplies. Another major advantage is the ability of vaccinia virus to travel through the blood stream or the lymphatic system and reach distant metastatic sites or lymph nodes<sup>181-182</sup>. Still, the role of neutralizing antibodies, NK and T cells in efficient clearing of the virus from the blood stream needs further investigation.

### 1.8.4 Recombinant vaccinia virus constructs used in this work

The replication-competent recombinant vaccinia viruses used in this work have been constructed and engineered at the Genelux Corporation R&D facility in San Diego, USA. GLV-1h68 is a genetically stable oncolytic virus strain designed to locate, enter, colonize and destroy cancer cells without harming healthy tissues or organs<sup>183</sup>. The GLV-1h68 virus is a derivative of the vaccinia virus Lister strain (LIVP wt), a European vaccine strain. It was constructed by insertion of three expression cassettes [*Renilla* luciferase-*Aequorea* green fluorescent protein (Ruc-GFP), beta-galactosidase and beta-glucuronidase] into the F14.5L, J2R, and A56R loci of the viral genome, respectively<sup>183</sup>. The gene for the Ruc-GFP fusion protein located in the F14.5L locus is under control of a synthetic early/late promoter whereas the marker gene beta-galactosidase (*lacZ*) in the TK/J2R locus is under control of the p7.5 promoter. The transferring receptor gene (*rtrf*) cDNA was inserted in the reverse orientation to vaccinia synthetic early/late promoter to serve as a negative control for a TFR-expressing recombinant virus. The third genetic insertion, beta-glucuronidase (*gusA*) was inserted into the A56R locus and is under control of the p11 promoter. It was recently demonstrated that GLV-1h68 efficiently replicates in and lyses different canine<sup>184-185</sup> as well as human tumor xenograft models like breast cancer<sup>183</sup>, anaplastic thyroid carcinoma<sup>186-187</sup>, malignant pleural mesothelioma<sup>188</sup>, pancreatic tumor<sup>189</sup>, prostate carcinoma<sup>181</sup>, squamous cell carcinoma<sup>190</sup>, sarcomas<sup>191</sup>, or hepatocellular carcinoma<sup>192</sup>. Other viruses used in this work are described in detail in paragraph 2.8 recombinant vaccinia virus constructs.

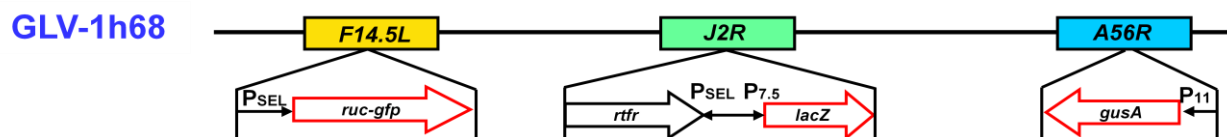


Fig.1.14 – Virus map of the parental GLV-1h68 used in this work

### 1.9 Aims of this work

It has been demonstrated in many preclinical studies (cell culture experiments and *in vivo* studies in small animals) that oncolytic virotherapy using vaccinia virus may provide a powerful new tool in cancer therapy which is currently investigated in several clinical trials

## INTRODUCTION

(Phase I & II). Oncolytic virotherapy may also be used in combination with conventional cancer therapies. Recent findings of small side populations of cancer cells that possess tumor-initiating characteristics lead to the cancer stem cell hypothesis<sup>102</sup>. The data from different studies investigating the nature of these cancer-initiating cells suggest a strong connection with stem cells and therefore coined the description 'cancer stem cells'<sup>126</sup>. Cancer-initiating cells and stem cells share self-renewal, differentiation potential, quiescence, drug and radiation resistance, activation and inhibition of similar signaling pathways, as well as expression of stem cell-related genes like Oct4 and Nanog and cell surface markers<sup>43</sup>. The idea, that only a small subpopulation at the base of the tumor sustains the aberrant tumor-growth and differentiation, has major implications of cancer therapy in terms of successful treatment and recurrence of the tumor<sup>126</sup>.

The aim of this work is to provide deeper insight into (stem cell) transcription factors Klf4, Nanog and Oct4 in oncolytic virotherapy. The study on the overexpression of master regulators in self-renewal and pluripotency Oct4 and Nanog by an oncolytic vaccinia virus could give new insight in the significance of cancer-initiating cells in oncolytic virotherapy. Therefore, recombinant oncolytic vaccinia viruses will be engineered to express the human stem cell transcription factors Klf4, Oct4 and Nanog and characterized for replication, recombinant gene expression and cytotoxicity in cell culture experiments. Furthermore, the effects of expressing stem cell transcription factors Nanog and Oct4, which are potentially involved in cancer stem cell biology, will be studied in different mouse xenograft models in athymic nude mice. The impact of transcription factor expression on therapeutic efficacy and survival rates after the vaccinia virus treatment should be studied in comparison to the parental GLV-1h68 and the functional negative control GLV-1h321. Viral spreading and colonization in the animals should be assessed by standard plaque assay of tumor tissues and body organs and monitoring of marker gene expression. Furthermore, the effects of viral replication on the mouse immune system should be analyzed by mouse immune-related protein antigen profiling.

The second specific aim of this work focuses on the potential of oncolytic vaccinia viruses to treat colorectal cancer and the potential role of transcription factor Klf4 in improving therapy. So far, even though many different tumor types have been shown to be susceptible to treatment with oncolytic recombinant vaccinia virus, no reports exist for colorectal cancer. Despite good prognosis for patients that are treated in the early stages of the disease, metastasis to lymph nodes and distant body organs is still lethal<sup>20</sup>. However, vaccinia virus has been shown to efficiently colonize metastases<sup>181</sup>. Therefore, treatment of colorectal cancer with oncolytic viruses may be beneficial, even in late stage disease. Viral replication and cytotoxicity of GLV-1h68 in different colorectal cancer cell lines will be tested in cell culture and mouse xenograft models. Therapeutic efficacy and overall survival will therefore

## INTRODUCTION

be monitored and viral spreading and colonization will be tested by standard plaque assay of body organs and tumors as well as GFP expression. The effects of vaccinia virus injection on the host immune system should be analyzed by mouse immune-related protein antigen profiling.

Furthermore, the transcription factor Klf4 is dramatically downregulated in colon cancer biopsies compared to normal surrounding tissues<sup>93</sup>. Klf4 directly interacts with beta-catenin and inhibits beta-catenin-mediated transcription<sup>96</sup>. Also, Klf4 is directly involved in cell cycle arrest and therefore, regulation of cell proliferation<sup>95</sup>. Induced expression of Klf4 in colorectal cancer lines led to significantly lower tumorigenicity<sup>97</sup>. Therefore, Klf4 expression in oncolytic virotherapy may further enhance therapeutic benefits. A recombinant vaccinia viruses expressing Klf4 will be engineered and characterized in cell culture for replication behavior, cytotoxicity and transgene expression. Klf4 functionality will be investigated on transcriptional and protein levels to analyze protein functionality. Subsequently, the effects of transcription factors Klf4 expression will be investigated *in vivo*. Therapeutic efficacy and overall survival rates in animals injected with Klf4-expressing viruses in a colorectal non-responder mouse xenograft model will be investigated to analyze a potential benefit in the treatment regimen. Viral colonization of tumors should be assessed and followed during the course of the experiment by standard plaque assay and GFP expression as well as *Renilla* luciferase imaging. Overall survival rates and survival benefits upon treatment with a Klf4 expressing vaccinia virus should be analyzed and compared to control virus treatment.

## 2 Material

### 2.1 Chemicals and enzymes

<u>Chemical</u>	<u>Manufacturer</u>
1 kb DNA Ladder	NEB
1,4-Diazabicyclo[2,2,2]octane (DABCO)	Sigma
2-log DNA Ladder	NEB
3-(4,5-Dimethylthiazol-2-yl)-2,5-diphenyltetrazolium bromide	Sigma
45% Glucose solution	Cellgro
AccuPrime Pfx Supermix	invitrogen
Accutase	Cellgro
Acetic acid (C <sub>2</sub> H <sub>4</sub> O <sub>2</sub> )	Fisher
Agarose	BioRad
Agarose Low Melt	Fisher
Ampicillin	Sigma
Benzonase	Merck
Benzyl-coelenterazine	Nanolight
Bovine serum albumin (BSA)	Sigma
Bovine plasma gamma globuline	BioRad
Buffer 1 10x	NEB
Buffer 2 10x	NEB
Buffer 3 10x	NEB
Carboxymethylcellulose (CMC)	MP
Coomassie brilliant blue G-250	Sigma
Crystal violet	Sigma
Diaminoethanetetraacetic acid (EDTA)	Sigma
Dimethyl sulfoxid (DMSO)	VWR
Dulbecco's modified Eagle's medium (DMEM)	Cellgro
EcoR1	NEB
EDTA-trypsin	Cellgro
Ethanol (p.a.)	Sigma
Ethidium bromide	Sigma
Fetal bovine serum (FBS)	Cellgro
Formaldehyde	Fisher

## MATERIAL

Formalin	Fisher
FuGENE 6 transfection reagent	Roche
G418 sulfate	Cellgro
Gelatine from porcine skin, type A	Sigma
Glycerol	Fisher
Glycine	BioRad
Goat serum	Sigma
Hexadimethrine bromide	Sigma
HEPES buffer	Cellgro
HindIII	NEB
Hoechst	Sigma
HyClone HyPure cell culture water	Fisher
Hydrochloric acid (HCl) 12 M	VWR
Hydrogen peroxide (H <sub>2</sub> O <sub>2</sub> )	Sigma
Hyperladder I	Bioline
Hypoxanthine	Sigma
Isoflorane	Explora
Isopropyl alcohol	EMD
Kanamycin	Sigma
KpnI	NEB
Laemmli sample buffer 4x	BioRad
LB broth	BD
Magic Mark XP Western Standard	invitrogen
Magnesium chloride hexaanhydride (MgCl <sub>2</sub> ·6H <sub>2</sub> O)	Sigma
Methanol	Sigma
Modified Eagle's medium (MEM)	Cellgro
Mowiol 4-88	Sigma
Mycophenolic acid (MPA)	Sigma
<i>N,N</i> -dimethylformamide ((CH <sub>3</sub> ) <sub>2</sub> N(O)H)	Sigma
Non-essential amino acids (NEAA)	Cellgro
Nonidet P-40	Sigma
Nocodazole	Sigma
NuPAGE 10% Bis-Tris Gel	invitrogen
NuPAGE 12% Bis-Tris Gel	invitrogen
NuPAGE LDS sample buffer 4x	invitrogen
NuPAGE MOPS running buffer 20x	invitrogen
NuPAGE sample reducing agent 10x	invitrogen



## MATERIAL

NuPAGE transfer buffer 20x	invitrogen
Pacl	NEB
Paraformaldehyde 16% solution (PFA)	EMS
Phalloidin-TRITC	Sigma
Phenylmethylsulfonyl fluoride (PMSF)	Sigma
Phosphate buffered saline tablets (PBS)	Sigma
Ponceau S solution	Sigma
Potassium chloride (KCl)	Fisher
Potassium ferricyanide ( $K_3Fe(CN)_6$ )	Sigma
Potassium ferrocyanide ( $K_4Fe(CN)_6 \cdot 3H_2O$ )	Sigma
Precision Plus Protein Standards	BioRad
Propidium iodide solution	Sigma
Protease inhibitor cocktail	invitrogen
Quick Ligase	NEB
Quick Ligase buffer 2x	NEB
RNase Zap	Ambion
Roswell Park Memorial Institute medium (RPMI-1640)	Cellgro
Roswell Park Memorial Institute medium w/o phenol red	Cellgro
Sall	NEB
Skim milk powder	BD
Sodium bicarbonate ( $NaHCO_3$ )	Cellgro
Sodium chloride (NaCl)	VWR
Sodium dodecyl sulfate (SDS)	Fisher
Sodium hydroxide (NaOH) 2N solution	Fisher
Sodium pyruvate ( $C_3H_3NaO_3$ ) solution	Cellgro
Sucrose	Sigma
Tris-HCl	Fisher
Triton X-100	Sigma
TRizol reagent	invitrogen
Trypan blue solution	Cellgro
Tween-20	BioRad
X-Gal	Stratagene
X-GlcA	RPI
Xanthine	Merck

## MATERIAL

### 2.2 Buffers and solutions

1 mM Tris-HCl (pH 9.0)	0.158 g	Tris-HCl
	1 L	HyPure Cell Culture dH <sub>2</sub> O
10 mM Tris-HCl (pH 9.0)	1.576 g	Tris-HCl
		HyPure Cell Culture dH <sub>2</sub> O
2x cracking buffer	1 mL	NaOH 2N
	500 µL	SDS (10%)
	2 g	sucrose
24% sucrose solution	1 mM	Tris-HCl (pH 9.0)
	120 g	sucrose
	500 mL	HyPure Cell Culture dH <sub>2</sub> O
28% sucrose solution	1 mM	Tris-HCl (pH 9.0)
	140 g	sucrose
	500 mL	HyPure Cell Culture dH <sub>2</sub> O
32% sucrose solution	1 mM	Tris-HCl (pH 9.0)
	160 g	sucrose
	500 mL	HyPure Cell Culture dH <sub>2</sub> O

## MATERIAL

36% sucrose solution	10 mM	Tris-HCl (pH 9.0)
	180 g	sucrose
	500 mL	HyPure Cell Culture dH <sub>2</sub> O
36% sucrose solution	1 mM	Tris-HCl (pH 9.0)
	180 g	sucrose
	500 mL	HyPure Cell Culture dH <sub>2</sub> O
3.7% PFA	3.7 g	PFA in 37°C H <sub>2</sub> O
	ad NaOH	until solution clears
	10 mL	10x PBS (pH7.4)
	ad 100 mL	dH <sub>2</sub> O
40% sucrose solution	1 mM	Tris-HCl (pH 9.0)
	200 g	sucrose
	500 mL	HyPure Cell Culture dH <sub>2</sub> O
Agarose histology buffer	0.3%	Triton X-100
		1x PBS (pH 7.2)
Agarose histology blocking buffer	0.3%	Triton X-100
	5%	FBS
		1x PBS (pH 7.2)

## MATERIAL

CMC overlay medium	7.5 g	CMC
	50 mL	FBS
	11 mL	penicillin/streptomycin
	500 mL	DMEM
Crystal violet staining solution	1.3 g	crystal violet
	50 mL	ethanol
	300 mL	formaldehyde (37%)
	ad 1 L	dH <sub>2</sub> O
Freezing medium	90%	FBS
	10%	DMSO
Lysis buffer / tumor PFU determination	1 tab	Protease inhibitor comp mini
	10 mL	1x PBS (pH 7.2)
Lysis buffer / tumor lysates	1 tab	Protease inhibitor comp mini
	50 mM	Tris-HCl (pH 7.4)
	2 mM	EDTA (pH 7.4)
	2 mM	PMSF
	10 mL	1x PBS (pH 7.2)
MTT medium	2.5 mg/mL	MTT
		RPMI 1640 w/o phenol red

## MATERIAL

PBS-Tween 20	0.05%	Tween-20
		1x PBS (pH 7.2)
Ponceau staining solution	0.5 g	Ponceau S
	1.0 mL	acetic acid
	ad 100 mL	dH <sub>2</sub> O
Propidium Iodide solution	2 mg	DNase-free RNase
	400 µL	propidium iodide (0.5 mg/mL)
	0.1%	Triton-X
	10 mL	1x PBS (pH 7.2)
RIPA cell lysis buffer	50 mM	Tris-HCl (pH 7.8)
	150 mM	NaCl
	0.1%	SDS
	0.5%	sodium deoxycholate
	1%	NP-40 / Triton X-100
	1 mM	PMSF
	1 tab	Protease inhibitor comp mini
Solution B	2 mM	MgCl <sub>2</sub> ·6H <sub>2</sub> O
	5 mM	K <sub>3</sub> Fe(CN) <sub>6</sub>

## MATERIAL

	5 mM	$\text{K}_4\text{Fe}(\text{CN})_6 \cdot 3\text{H}_2\text{O}$
	ad 100 mL	1x PBS (pH 7.2)
X-Gal staining solution	1.5 mL	Solution B
	0.5 mL	1x PBS (pH 7.2)
	36 $\mu\text{L}$	4% X-Gal in $(\text{CH}_3)_2\text{N}(\text{O})\text{H}$
X-GlcA solution	1.5 mL	Solution B
	0.5 mL	1x PBS (pH 7.2)
	36 $\mu\text{L}$	10% X-GlcA in $(\text{CH}_3)_2\text{N}(\text{O})\text{H}$

### 2.3 Bacterial strains

<i>Escherichia coli</i> DH5 $\alpha$ z-competent	Zymo Research
<i>Escherichia coli</i> TOP10	invitrogen

### 2.4 Cell lines and cell culture media

#### 2.4.1 Cell lines

A549	human non-small cell lung adenocarcinoma (ATCC, catalogue number CCL-185™)
COLO 205	human colorectal adenocarcinoma (NCI-60 collection, NIH)
CV-1	african green monkey kidney fibroblast (ATCC, catalogue number CCL-70™)

## MATERIAL

DU-145	human prostate carcinoma (ATCC, catalogue number HTB-81™)
HCT-15	human colorectal adenocarcinoma (NCI-60 collection, NIH)
HCT-116	human colorectal carcinoma (NCI-60 collection, NIH)
HT-29	human colorectal adenocarcinoma (ATCC, catalogue number HTB-38™)
PC-3	human prostate adenocarcinoma grade IV (ATCC, catalogue number CRL-1435™)
SW-620	human colorectal adenocarcinoma (NCI-60 collection, NIH)

### 2.4.2 Cell culture media

A549	500 mL	RPMI 1640
	50 mL	FBS
	5.5 mL	Penicillin/Streptomycin
COLO 205	500 mL	RPMI 1640
	50 mL	FBS
	5.5 mL	Na Bicarbonate
	5.5 mL	Na Pyruvate
	5.5 mL	HEPES

## MATERIAL

		5.5 mL	Penicillin/Streptomycin
CV-1		500 mL	DMEM High Glucose
		50 mL	FBS
		5.5 mL	Penicillin/Streptomycin
DU-145		500 mL	EMEM
		50 mL	FBS
		5.5 mL	NEAAs
		5.5 mL	Na Pyruvate
		5.5 mL	Penicillin/Streptomycin
HCT-15		500 mL	RPMI 1640
		50 mL	FBS
		5.5 mL	Penicillin/Streptomycin
HCT-116		500 mL	RPMI 1640
		50 mL	FBS
		5.5 mL	Penicillin/Streptomycin
HT-29		500 mL	RPMI 1640
		50 mL	FBS
		5.5 mL	Penicillin/Streptomycin



## MATERIAL

PC-3	500 mL	DMEM
	50 mL	FBS
	5.5 mL	Penicillin/Streptomycin
SW-620	500 mL	RPMI-1640
	50 mL	FBS
	5.5 mL	Penicillin/Streptomycin

## 2.5 Kits

<u>Kit</u>	<u>Manufacturer</u>
Amersham ECL Plus Western Blotting Detection	GE Healthcare
beta-catenin EIA ELISA Kit	Enzo Lifescience
CEA ELISA Kit	abcam
Cell Proliferation Kit II (XTT)	Roche
DC Protein Assay	BioRad
DNA Clean&Concentrator™-5 Kit	Zymo Research
DNase-free™ DNase Treatment & Removal	Ambion
Human Nanog “Super X” ELISA Kit	Antigenix
Mesa Green qPCR™ Mastermix Plus for SYBR® Assay	Eurogentec
Opti-4CN™ Substrate Kit	BioRad
prepGEM™ Tissue DNA Extraction Kit	ZyGEM
PureLink™ PCR Purification Kit	invitrogen
PureLink™ Quick Plasmid Minprep Kit	invitrogen
RNA Extraction Using RNAGEM™ Tissue	ZyGEM
RNEasy Mini Kit	QIAGEN
RT Supermix (M-MuLV) w/ oligo(dT) <sub>18</sub>	BioPioneer
Superscript™ III Reverse Transcriptase	invitrogen
Superscript™ First Strand RT-PCR Kit	invitrogen
Zero Blunt TOPO Cloning Kit	invitrogen
Zymoclean DNA Gel Recovery Kit	Zymo Research

## MATERIAL

### 2.6 Antibodies

<u>Primary antibody</u>	<u>Origin</u>	<u>Manufacturer</u>
anti-A27L (CAKKIDVQTGRRPYE)	rabbit	Genscript
anti-beta-catenin	rabbit	abcam
anti-Histone H3	rabbit	abcam
anti-Klf4	mouse	abcam
anti-Nanog	rabbit	Kamiya Biomedical
anti-Oct4	rabbit	abcam
anti-Vaccinia virus	rabbit	abcam

<u>Secondary antibody</u>	<u>Origin</u>	<u>Manufacturer</u>
anti-rabbit-Alexa Fluor 350	goat	invitrogen
anti-rabbit-DyLight™ 594	donkey	Jackson Immunoresearch
anti-rabbit-HRP	goat	BioRad
anti-rabbit-Rhodamin	goat	abcam

### 2.7 Synthetic Oligonucleotides

<u>Target</u>	<u>Sequence</u>
18s rna fwd	5'-CCTGGTTGATCCTGCCAGTAG-3'
18s rna rvs	5'-CCGTGCGTACTTAGACATGCA-3'
a21l fwd	5'-TCGTTTATCTTGGAACATGG-3'
a21l rvs	5'-AGCCGCATACGTAAACTACA-3'
beta-catenin fwd	5'-GAAACGGCTTTCAGTTGAGC-3'
beta-catenin rvs	5'-CTGGCCATATCCACCAGAGT-3'
beta-galactosidase fwd	5'-TTGTTACTCGCTCACATTTA-3'
beta-galactosidase rvs	5'-ACATATCCTGATCTTCCAGA-3'
human gapdh fwd	5'-ACAAGAGGAAGAGAGAGACC-3'
human gapdh rvs	5'-GCACAGGGTACTTTATTGAT-3'
human klf4 fwd	5'-GGCAAACCTACACAAAGAG-3'
human klf4 rvs	5'-CATATCCACTGTCTGGGATT-3'
human klf4-tat fwd	5'-ACATGTCGACCACCATGGCTGTCAGCGACGCG-3'
human klf4-tat rvs	5'-TCGCCTTACACATGAAGAGGCATTTTGGTCGC AAGAAACGTCGCCGTCCGCCTTAATTAATTAACAT-3'
human nanog fwd	5'-AATCTTCACCTATGCCTGTGA-3'

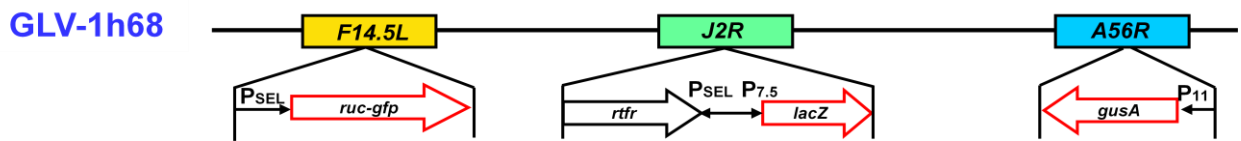
## MATERIAL

human nanog rvs	5'-GCCACCTCTTAGATTTTCATTC-3'
human nanog $\Delta$ nl5 fwd	5'-CTCCCACATGGAGGTTTCGTTCCAGAACCAGAG AATGAAAT-3'
human nanog $\Delta$ nl5 rvs	5'CGAACCTCCATGTGGGAGGCTGAGGTTTCAGG ATGTTGGA-3'
human oct4 fwd	5'-CTATTTGGGAAGGTATTCAG-3'
human oct4 rvs	5'-GTTTCTGCTTTGCATATCTC-3'
ruc-gfp fwd	5'-GAGAGAACCATCTTTTTCAA-3'
ruc-gfp rvs	5'-GTCTGATCTTGAAGTTGACC-3'
slug fwd	5'-TCCGGACCCACACATTACCT-3'
slug rvs	5'-TTGGAGCAGTTTTTGCCTG-3'
snail fwd	5'-CGAGCTGCAGGACTCTAAT-3'
snail rvs	5'-CCACTGTCCTCATCTGACA-3'
nestin fwd	5'-ACCCTTCCAGACTCCACTC-3'
nestin rvs	5'-CACTCCTCTTCTCCCTCCTC-3'
cd133 fwd	5'-CTATTCAGGATATACTCTCAGCATT-3'
cd133 rvs	5'-TTTCTGTGGATGTAACCTTCAGTG-3'

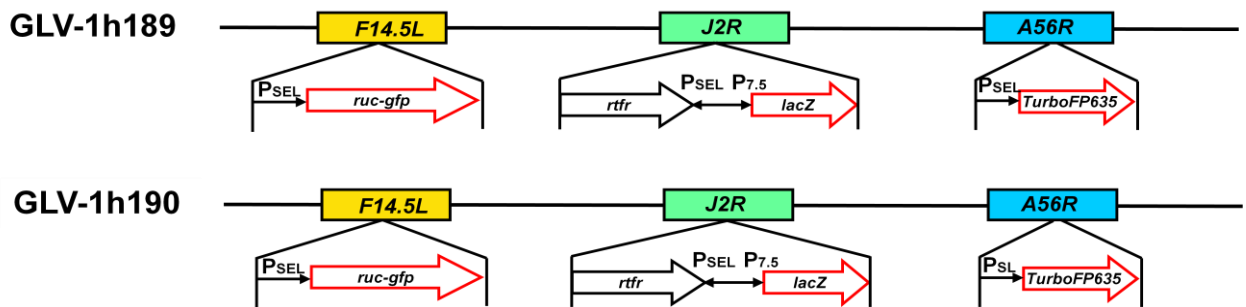
### 2.8 Recombinant vaccinia virus constructs

The replication-competent recombinant vaccinia viruses used in this work have been constructed and engineered at the Genelux Corporation facility in San Diego, USA. GLV-1h68 is a genetically stable oncolytic virus strain designed to locate, enter, colonize and destroy cancer cells without harming healthy tissues or organs<sup>183</sup>. The GLV-1h6 virus is a derivative of the vaccinia virus Lister strain (LIVP wt), a European vaccine strain. It was constructed by insertion of three expression cassettes [*Renilla* luciferase-*Aequorea* green fluorescent protein (Ruc-GFP), beta-galactosidase and beta-glucuronidase] into the *F14.5L*, *J2R*, and *A56R* loci of the viral genome, respectively<sup>183</sup>. The gene for the Ruc-GFP fusion protein located in the *F14.5L* locus is under control of a synthetic early/late promoter whereas the marker gene beta-galactosidase (*lacZ*) in the *TK/J2R* locus is under control of the p7.5 promoter. The transferring receptor gene (*rtfr*) cDNA was inserted in the reverse orientation to vaccinia synthetic early/late promoter to serve as a negative control for a TFR-expressing recombinant virus. The third genetic insertion, beta-glucuronidase (*gusA*) was inserted into the *A56R* locus and is under control of the p11 promoter.

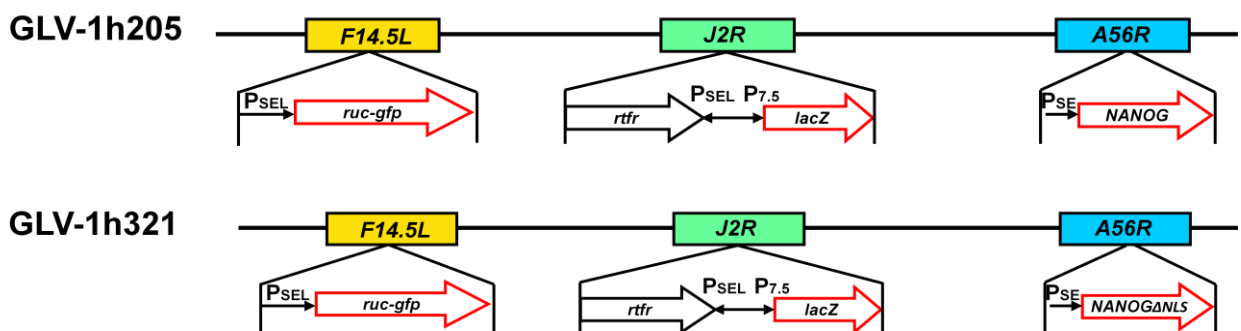
## MATERIAL



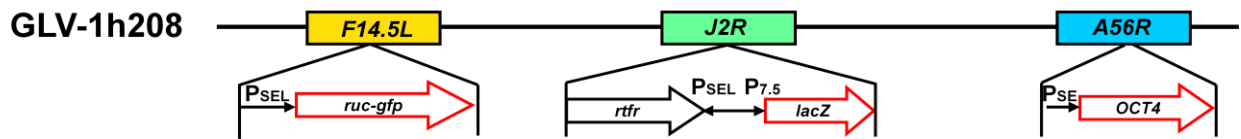
Another virus used in this work is GLV-1h189 which is a direct derivative of the parental GLV-1h68. In the GLV-1h189 and GLV-1h190 genomes, the *gusA* marker gene in the A56R locus was replaced with *turboFP635* by homologous recombination. The *turboFP635* gene is under control of the synthetic early/late or synthetic late promoter.



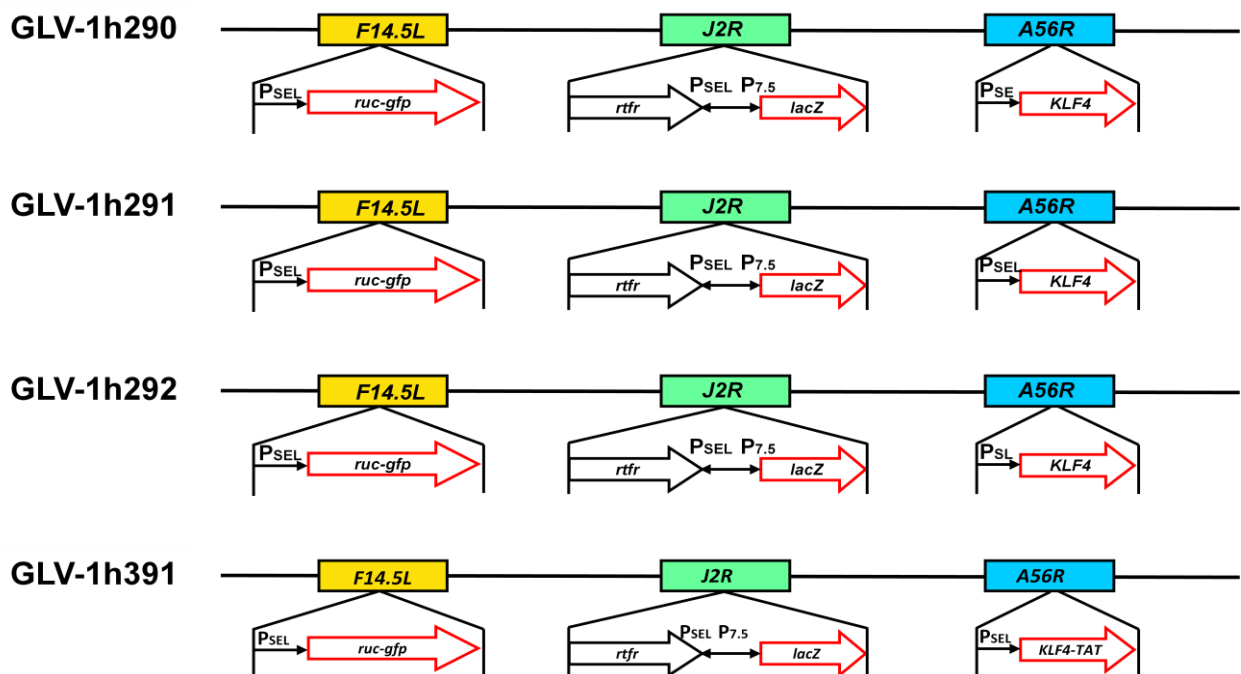
The stem cell transcription factor-encoding vaccinia viruses GLV-1h205 and GLV-1h208 are both derived from the parental GLV-1h68. In the viral genome of GLV-1h205, the beta-glucuronidase gene *gusA* in the A56R was replaced with the human *nanog* gene by homologous recombination. *Nanog* transcription is under the control of the synthetic early promoter. Additionally, a variant of GLV-1h205 was engineered in which the nuclear localization sequence (NLS) of the *nanog* gene product was mutated from an YKQVKT to a LPHGGS amino acid sequence to render the protein incapable to enter the nucleus and exert its function as a transcription factor<sup>67</sup>. Therefore, GLV-1h321 is considered a negative control virus for GLV-1h205 expressing fully functional Nanog. In GLV-1h208, the *gusA* gene was replaced with the human *oct4* gene by homologous recombination. Like Nanog expression in GLV-1h205, gene expression of *oct4* is controlled by the synthetic early promoter.



## MATERIAL



The vaccinia viruses GLV-1h290-292 all carry the human stem cell transcription factor gene *klf4* in the A56R locus, which replaced the *gusA* marker gene by homologous recombination. *Klf4* expression is controlled by the synthetic early, synthetic early/late, and synthetic late promoter, respectively. Lastly, in the GLV-1h391 construct, the *TurboFP635* marker gene from GLV-1h190 was replaced by *klf4-TAT*. The TAT sequence was cloned to the C-terminus of the gene. *Tat* is a gene originally found in HIV and stands for “transactivator of transcription”<sup>193</sup>. The gene product contains a protein transduction domain that allows the Tat protein to enter cells by crossing the cell membrane<sup>194</sup>. The transduction domain also contains a NLS sequence (GRKKR amino acid sequence) which further mediates translocation from the cytosol to the cell nucleus<sup>195</sup>. While the amino acid sequence of the protein transduction domain is known (YGRKKRRQRRR), the mechanism of action still needs further elucidation<sup>196</sup>. The expression of *klf4-TAT* is controlled by the synthetic early/late promoter.



## MATERIAL

### 2.9 Laboratory animals

For *in vivo* experiments, male athymic nude FoxN1 mice were used. The animals were purchased from Harlan. The FoxN1 mouse model is characterized by an autosomal recessive mutation in the *nu* locus on chromosome 11. This leads to a completely hairless phenotype in the mice. Additionally, these animals feature a dysfunctional and rudimentary thymus which manifests in a T cell deficiency. By contrast, B cell function is normal in athymic nude FoxN1 mice. Due to the defects in the immune system of the mouse, athymic nude FoxN1 mice are well suited as adequate laboratory animals in oncology, immunology and additional fields of biomedical research. Another advantage of this mouse model is that xenotransplants will not be rejected by the animal. Antibody production is possible in athymic nude FoxN1 mice as well. Animals were kept in a circadian rhythm of twelve hours of day following twelve hours of night. In addition, light intensity was alleviated to account for the albinism of the mice. All experiments were approved by Explora Biolabs, San Diego.



Fig.2.1 – Phenotype of an athymic nude FoxN1 mouse (from <http://www.harlan.com>)

### 2.10 Laboratory equipment and other materials

<u>Equipment</u>	<u>Manufacturer</u>
Amicon Ultra-15 Centrifugal Filter Unit 10 kDA, 100 kDa NMWL	Millipore
Argus-100 Low Light Imaging System	Hamamatsu
Balance PL1501-S	Mettler-Toledo
Bio Doc-It™ system	UVP
Biosafety cabinet	The Baker Company
Blotting pad, 707	VWR
Carestream Imaging System	Carestream
Cell culture cluster 24-well Costar 3526	Corning
Cell culture cluster 6-well Costar 3516	Corning
Cell culture cluster 96-well Costar 3595	Corning
Cell culture flask T75 cm <sup>2</sup>	Corning
Cell culture flask T225 cm <sup>2</sup>	Corning

## MATERIAL

Cell Lab Quanta SC Flow Cytometer	Beckman Coulter
Cell scraper	Corning
Cell spreader	VWR
Centrifuge Centra CL2	Thermo Scientific
Centrifuge Micro CL 21	Thermo Scientific
Centrifuge Micro 1816	VWR
Centrifuge Sorvall RC 6 Plus	Thermo Scientific
Centrifuge Sorvall Legend RT	Thermo Scientific
Combitips Plus 1 mL, 2.5 mL, 5 mL, 25 mL	Eppendorf
Cryotubes 2 mL	Nalgene
Digital caliper	VWR
Digital dry bath incubator	Boekel Scientific
Dish 100 mm	Fisher Scientific
Falcon 15 mL tubes	BD
Falcon 50 mL tubes	BD
Heater	VWR
Hotplate stirrer 375	VWR
Hybond-P PVDF membrane	Amersham Biosciences
Incubator	Forma Scientific
Incubator HERA Cell 150	Thermo Electron
Incubator Shaker C25	New Brunswick Scientific
Insulin syringe U-100 29G1/2	BD
MagNA Lyser	Roche
MagNA Lyser green beads	Roche
MicroAmp® Fast Optical 96-well reaction plate	Applied Biosystems
Microfuge tubes easy open cap 1.5 mL	Saarstedt
Microplate reader SpectraMax MS	Molecular Devices
Microscope cover glass	Fisher Scientific
Microslides Premium Superfrost®	VWR
Microwave Carousel	Sharp
Mini-Sub® Cell GT	BioRad
Multipipette	Eppendorf
Novex Midi Gel System	life technologies
Parafilm laboratory film	Pechiney Plastic
Packaging	
pH Meter Accumet AR15	Fisher Scientific
Photometer Biomate3	Thermo Spectronic

## MATERIAL

Pipet Aid	Drummond
Pipet Tips 10 µL, 200 µL, 300 µL, 1000 µL	VWR
Pipettes 20 µL, 200 µL, 1000 µL	Rainin
Pipettes 5 mL, 10 mL, 25 mL	Corning
PVDF Membrane Filter Paper Sandwich 0.2 µm	invitrogen
R <sub>2</sub> P roller bottle device	Wheaton
Repeater® stream pipette	Eppendorf
Rocking platform	VWR
Roller bottles, 850 cm <sup>2</sup>	Corning
Sonifier 450	Branson
StepOnePlus Real-Time PCR System	Applied Biosystems
Sterile disposable scalpel	Sklar Instruments
Syringe 1 mL, 30 mL, 60 mL	BD
Syringe 20G	BD
Syringe Driven Filter Unit Millex®-VV PVDF 0.1 µm, 0.2 µm	Millipore
The Panther™ OWL HEP-1 semidry Electroblotter	Thermo Scientific
Thermocycler Mastercycler Personal	Eppendorf
Thermocycler Veriti 96-well Thermal Cycler	Applied Biosystems
Tissue culture dish 60 mm	BD
Titer plate shaker	Thermo Scientific
Illumatool Tunable Lighting System	Lighttools Research
Vibratom VT 1200S	Leica
Vortex VX100	Labnet
Water bath	Boekel Scientific
Water bath Isotemp202	Fisher Scientific
X Cell Sure Lock™	invitrogen

### 2.11 Microscopes

<u>Microscope</u>	<u>Manufacturer</u>
CK30 culture microscope	Olympus
IX71 inverted fluorescence microscope	Olympus
MZ 16 FA stereo fluorescence microscope	Leica



### 3 Methods

#### 3.1 Generation of recombinant vaccinia virus

##### 3.1.1 Cloning of plasmids for homologous recombination with viral DNA

The DNA of the desired gene is amplified by PCR and specific enzymatic restriction sites are attached to the DNA sequence by designing two specific, restriction site-containing primers that are complementary to the 3'-ends of both, sense and anti-sense strand of the DNA target. Restriction sites allow enzymatic cutting of the DNA at the desired position that is needed to ligate the DNA fragment with a plasmid transfer vector that contains the same restriction sites. The gene fragment of choice is amplified by PCR and purified afterwards. The purified PCR product is subcloned into the pCR®-Blunt II-TOPO transfer vector and the transfer vector is taken up by chemically competent bacteria via transformation. Positive clones are grown on LB<sub>Kan</sub> plates and single clones are picked for overnight bacterial cultures in LB medium containing kanamycin. The transfer vector is isolated from the overnight culture and the isolated plasmid DNA is digested with the restriction enzymes and subsequently purified. The gene product can now be ligated with the transfer vector that carries the desired vaccinia virus promoter (synthetic early, synthetic early/late or synthetic late promoter) and flanking regions of the desired target gene locus for homologous recombination.

##### 3.1.2 Co-transfection of plasmid DNA with parental virus GLV-1h68

CV-1 cells are grown in 6-well plates until confluency and are subsequently infected with  $1 \times 10^5$  pfu/mL GLV-1h68. For the co-transfection, 2 µg of plasmid DNA is prepared with non-liposomal transfection reagent and OPTI-MEM medium. After infection, the CV-1 cells are washed twice and cultured in OPTI-MEM. The transfection mix is added to the medium and the CV-1 cells are incubated for 2 days at 37°C until all cells are infected. The cells are harvested and stored at -80°C until further use.

##### 3.1.3 Plaque selection

Cell lysates undergo freeze-thaw cycles and sonication for efficient virus release from the cells and to break up viral aggregates. Prior to infection, CV-1 cells are seeded in 6-well plates and treated with mycophenolic acid (MPA), hypoxanthine and xanthine to block GMP synthesis to interfere with vaccinia virus replication and reduce viral plaque sizes. The addition of xanthine and hypoxanthine and the expression of the *E. coli gpt* gene help to select for positive vaccinia virus plaques that express XGPRT by single-crossover recombination. The *gpt* gene is inserted next to the gene of interest and outside the vaccinia

## METHODS

flanking regions and its expression leads to enrichment of recombinant virus over the parental virus<sup>197</sup>. Pretreated CV-1 cells are infected with different concentrations of virus containing cell lysate. After infection, overlay medium is added to immobilize the virus. Six single plaques are picked and resuspended in DMEM medium. These samples undergo freeze-thaw cycles, sonication for virus release from the cells and another round of infection in pretreated CV-1 cells. After two rounds of plaque selection, MPA, hypoxanthine and xanthine are removed to allow the virus to undergo the desired double cross-over recombination and recombinant virus without the *xgprt* gene can form plaques. The recombinant vaccinia virus undergoes three more rounds of plaque selection without pretreatment of the CV-1 cells. After five rounds of plaque selection, plaque lysates are screened for positive recombination by marker gene expression.

### 3.1.4 Screening for marker gene expression

The new genes of interest were inserted into the A56R locus in which the parental virus GLV-1h68 encodes for the *gusA* gene. Homologous recombination in that locus will replace the former *gusA* gene with the new target gene and therefore, the *gusA* gene product will no longer be expressed by the virus. Testing for beta-glucuronidase activity after five rounds of plaque selection is therefore a feasible and simple way to test for successful recombination of the target gene into the desired locus. Marker gene expression in the F14.5L (*ruc-gfp*) and J2R (*lacZ*) loci is also performed to ensure correct marker gene expression in the respective loci. While GFP expression can easily be assessed by fluorescence microscopy, cells are fixed, washed, and incubated with respective staining solutions to assess expression and activity of beta-galactosidase and beta-glucuronidase. Generally, for the selection of a clone that underwent positive homologous recombination in the A56R locus, marker gene expression will be positive in the F14.5L and J2R locus, while marker gene expression is negative in the A56R locus.

### 3.1.5 Screening for *GPT*

To avoid selection of recombinant viruses that only underwent one cross-over event, selected plaques are also screened for *gpt* expression. MPA-pretreated CV-1 cells are infected with the selected recombinant plaques and viruses that successfully underwent two cross-over events and lost the *gpt* gene will not be able to replicate in the cells anymore. Therefore, virus plaques that are negative for marker gene expression of the target locus and negative for growth in MPA-treated cells can be used for DNA isolation. The selected plaques are then screened for the presence of the target gene by PCR using primers flanking (inside/outside) the target locus.

## METHODS

### 3.1.6 DNA isolation for sequencing

For isolation of viral DNA for sequencing, CV-1 cells in 60 mm dishes are infected with positive round five virus plaque lysates until cytopathic effect (CPE) can be observed. A few infected cells can be picked and used for DNA isolation with a DNA isolation kit while the rest is stored as the P1 stock for further amplification of the virus. After isolation of the DNA, the samples can be prepared for DNA sequencing using primers that bind inside/outside of the target locus. Depending on the size of the target gene, another sequencing step within the target gene has to be added. The obtained sequences can then be blasted against the target gene sequence to confirm correct insertion of the gene into the virus.

### 3.1.7 Amplification and purification of recombinant viruses

After confirmation of the desired DNA sequence in the new recombinant virus, it is propagated in CV-1 cells. After virus infection of the CV-1 cells, they are incubated until CPE can be observed. The CV-1 cells are then harvested and resuspended in the supernatant. The cell pellets are collected after centrifugation and resuspended in a 10 mM Tris-HCl pH 9.0 buffer. The cell suspensions are then mechanically homogenized to release the virus particles from the infected cells. The cell debris is separated by centrifugation and discarded as a pellet. The supernatant now contains the cytoplasmic fractions and virus particles. Equilibrium sucrose gradient centrifugation is used to separate and purify the virus by its size from smaller and bigger particles. After aspiration of the virus band within the gradient, it is washed and resuspended in 1 mM Tris-HCl pH 9.0. The harvested virus is sonicated to separate viral aggregates and will then be used for titer confirmation before storage at -80°C.

### 3.1.8 Determination of viral titers by standard plaque assay

For standard plaque assay, ten-fold serial dilutions of the virus stock are prepared. Confluent CV-1 cells in 24-well plates are infected with 200 µL in duplicates with the respective virus dilution. Overlay medium is added after one hour of infection and the CV-1 cells are incubated for 2 days at 37°C. Cells are then stained with 250 µL of crystal violet per well and incubated for several hours at room temperature. Well plates can then be washed, dried, and virus plaques can be counted. Virus titers are calculated using the following formula:

$$\frac{\text{averaged plaque forming units (pfu)} \times \text{dilution factor}}{\text{infection volume}} = \text{pfu/mL}$$

## METHODS

### 3.2 Virological methods

#### 3.2.1 Infection of cell cultures

Cancer cells were seeded into the desired well plate format. After 24 h in culture, when cells reached a confluence of 95-100%, cells were infected with recombinant vaccinia virus with the desired multiplicities of infection (MOIs). Cells were incubated for 1 h at 37°C, after which the infection medium was removed and cells were cultured in fresh growth medium.

#### 3.2.2 Viral proliferation assay

Cells were infected with recombinant vaccinia virus at an MOI of 0.1 or 0.01, respectively, for 1 h at 37°C and 5% CO<sub>2</sub>. Afterwards, the infection medium was removed and cells were cultured in fresh growth medium. Cells were then harvested in triplicates after 6, 24, 48, 72 and 96 hours post infection (hpi). Following three freeze-thaw cycles and sonication at maximum level constant for 1 min, serial dilutions of the samples were titered in triplicates on confluent layers of CV-1 cells in 24-well plates. Viral titers were determined by standard plaque assay.

#### 3.2.3 Standard plaque assay

For standard plaque assay, ten-fold serial dilutions of the virus stock are prepared. Confluent CV-1 cells in 24-well plates are infected with 200 µL in triplicates with the respective virus dilution. Carboxymethylcellulose (CMC) overlay medium is added after one hour of infection and the CV-1 cells are incubated for 2 days at 37°C. Well plates are then stained with 250 µL of crystal violet per well and incubated for several hours at room temperature. Well plates can then be washed, dried, and virus plaques can be counted. Virus titers are calculated using the following formula:

$$\frac{\text{averaged plaque forming units (pfu)} \times \text{dilution factor}}{\text{infection volume}} = \text{pfu/mL}$$

### 3.3 Cell biological methods

#### 3.3.1 Culturing of adherent mammalian cells

Cells are cultured under sterile conditions in a laminar flow hood. The antibiotics/antimycotics penicillin and streptomycin added to the media prevent bacterial, yeast or fungal contamination of the cells. Used eukaryotic cell lines in this work have been cultured in cell culturing flasks of different sizes in a sensor controlled incubator. The incubator maintains optimal growth conditions through stabilization of exogenous parameters (100% air humidity, 37°C and 5% CO<sub>2</sub>). Fetal bovine serum (FBS) was heat inactivated for

## METHODS

30 min at 56°C prior to addition to the media. Culturing media, washing solutions and EDTA-Trypsin were warmed to 37°C to ensure gentle treatment of the cells. Cells were harvested and passaged before reaching 100% confluence to avoid the generation of bi- or multilayers which slow down or arrest cell growth. Cell culturing media has to be renewed every two to three days to refresh dissipated ingredients. In addition, metabolites and dead cells accumulate in the supernatant. The medium contains a pH tracer that reflects proceeding usage of the medium via a color change from red to yellow. For some experiments, cells were cultured with conditioned medium, containing sterile-filtered and concentrated supernatants of virus-infected cells.

### **3.3.2 Cell viability assay**

The amount of viable cells after virus infection was measured using 3-(4,5-Dimethylthiazol-2-yl)-2,5-diphenyltetrazoliumbromide (MTT). The growth medium was replaced with 0.5 mL sterile MTT solution at a concentration of 2.5 mg/mL in RPMI 1640 without phenol red prior to infection, 24, 48, and 72 hpi. The cells were incubated for 2 h at 37°C in a 5% CO<sub>2</sub> atmosphere. After removal of the MTT solution, the color reaction was stopped by adding 1 N HCl diluted in isopropanol. The optical density was then measured at a wavelength of 570 nm. Uninfected cells were used as a reference and considered 100% viable. Alternatively, the XTT Cell Proliferation kit II (Roche) was used according to manufacturer's instruction to determine cell viability and proliferation. Absorption was measured at 450 and 700 nm.

## **3.4 Detection of gene expression of recombinant vaccinia virus**

### **3.4.1 Analysis of gene expression by reverse transcriptase (RT-) PCR**

For a reverse transcriptase (RT) PCR, complementary DNA (cDNA) is synthesized from isolated mRNA by specific RNA-dependent DNA polymerases (reverse transcriptases). Synthesized cDNA can be used as a template for PCR amplification and is used to analyze and compare gene transcription by PCR with matching primers.

#### **3.4.1.1 Isolation of RNA from adherent mammalian cells**

Cells are grown in 6-well plates to 95% confluence prior to virus infection. Cells are washed with PBS and harvested by scraping. The cell suspension is then centrifuged and the supernatant aspirated. RNA is isolated using the RNEasy® Mini Kit following the manufacturer's instructions. Cells are mechanically homogenized with a 20G syringe. After isolation, the RNA is eluted in RNase-free water. To avoid genomic DNA amplification, samples are treated with DNA-free™ Kit, following the manufacturer's instructions to enzymatically digest genomic DNA.

## METHODS

### **3.4.1.2 Synthesis of complementary DNA (cDNA)**

The isolated mRNA is used as a template to synthesize cDNA using a reverse transcriptase. The commercially available SuperScript™ II & III Reverse Transcriptase Kits were used according to the manufacturer's instructions. A total of 1 µg of mRNA is used as a template and mixed with Oligo(dT) primers and dNTPs. The mixture is heated to 65°C for five minutes and chilled on ice. Then 5x First Strand buffer, DTT, and RNase Out are added and the mixture is incubated at 42°C for 2 min. Subsequently, the reverse transcriptase is added to the mix and incubated for 50 min at 42°C. The reverse transcriptase is heat-inactivated (70°C) and the cDNA is ready to be used as a template in a PCR reaction.

### **3.4.1.3 Polymerase chain reaction (PCR)**

Polymerase chain reaction (PCR) is a very sensitive method for DNA amplification. In a denaturation step the double-stranded (ds) DNA is separated into single strands (ss). During the annealing step, specific primers bind to the ssDNA template. In the following elongation step the DNA polymerase binds to the template and uses abundant dNTPs to extend the primers and to synthesize a complementary strand. PCR reactions were prepared using the AccuPrime™ Pfx Supermix. The DNA denaturing step is executed at 95°C while the annealing temperature is primer-dependent. It is notable that the Pfx DNA polymerase works at 68°C instead of 72°C like the traditional Taq polymerase. Annealing and elongation steps are repeated several (30-40) times to amplify the DNA. The time of elongation is dependent on the size of the DNA fragment that is amplified. After the final elongation step, the DNA is incubated with the polymerase for another 7 min to enable final elongation of unfinished strands.

### **3.4.1.4 Agarose gel electrophoresis**

Horizontal agarose gel electrophoresis is used for DNA fragment separation by size. Agarose concentration of the agarose gel is dependent on the sizes of DNA fragments. Ethidium bromide is added to the agarose containing buffer to intercalate between the DNA bases and enable visualization of DNA bands by UV light. A DNA marker is added to the gel prior to running to identify the size of DNA bands. The size of DNA fragments is measured in base pairs (bp). Negatively charged DNA molecules migrate through the agarose polymer network after impressing a direct current field. Larger DNA molecules need more time to migrate the same distance than smaller molecules, allowing for fractionation of DNA bands.

### **3.4.1.5 Quantitative real-time polymerase chain reaction (qPCR)**

Quantitative real time PCR (qPCR) is a technique based on the PCR method to amplify and simultaneously quantify target DNA or gene transcripts, respectively. The key feature of qPCR is the DNA quantification after each amplification cycle as it accumulates in the

## METHODS

elongation reaction. Real-time PCR results are generally significantly more reliable than the results compared with conventional PCR. For quantification, the fluorescent dye Mesa Green qPCR™ Mastermix Plus for SYBR® Assay kit was used. Relative quantification was used to quantify gene expression levels in all tested samples. Therefore, the housekeeping gene 18S RNA was used as an internal control. The obtained data is presented using the comparative  $C_T$  ( $2^{-\Delta\Delta C_T}$ ) method<sup>198</sup>.

### **3.4.2 Quantification of GFP expression by FACS analysis**

Infected cells were analyzed 24, 48 and 73 hpi. Cells were harvested by Trypsin-EDTA and resuspended in PBS. For discrimination between viable and dead cells, cell were stained using propidium iodide solution for 20 min at 37°C. A total of  $7.5 \times 10^4$  cells per sample were then measured for GFP and propidium iodide signals using a Cell Lab Quanta™ SC flow cytometer and analyzed using Quanta Analyse software.

### **3.4.3 Fluorescence imaging and immunocytochemistry**

Ruc-GFP expression during the course of infection was monitored using a UV filter on an inverse fluorescence microscope. For staining of all cells, Hoechst dye was added to the cells and incubated for 15 min at room temperature (RT). For detection of recombinant transcription factors, cells were infected at the MOI of 0.001. Cells were washed with PBS, fixed with 3.7% PFA and permeabilized with 0.5% Triton X-100 in PBS. Cells were then incubated with 5% BSA in PBS to block antigen epitopes. Next, the fixed cells were incubated with the primary antibody overnight at 4°C. Cells were then washed with PBS to remove residual antibody and incubated at room temperature with a secondary antibody conjugated to a blue or red fluorescent dye. For staining of all cells, either Hoechst dye or propidium iodide was added to the cells and incubated for 15 min at RT. Images were captured using a MicroFire® digital CCD camera and edited using the open-source software GIMP 2.6.

## **3.5 Protein analytical methods**

### **3.5.1 Preparation of soluble proteins from mammalian cells**

Cells were grown in the desired format to 95% confluence prior to virus infection. At the harvesting time point, cells were scraped off the well plate and resuspended in the supernatant. After centrifugation the supernatant is aspirated and the cell pellet resuspended in RIPA buffer and sonicated to break up cell membranes and extract the proteins from the cells. Cells were then treated with benzonase to degrade DNA. After incubation on ice, samples were centrifuged at 4°C and supernatants stored for further analysis.

## METHODS

### 3.5.2 Ultrafiltration of cell supernatants

Cells were grown in the desired well plate to 95% confluence prior to virus infection. At the harvesting time point, cells were scraped off the well plate and resuspended in the supernatant. The cell suspension was sonicated to break up cell membranes and extract the proteins from the cells. For sterile filtration, the suspension was loaded on Amicon Ultra-15 columns with a NMWL of 100 kilo Dalton (kDa). The samples were centrifuged using a rotating swing bucket and the filtered flow-through was transferred to new Amicon Ultra-15 columns with a NMWL of 10 kDa. After another round of centrifugation the concentrated fraction (10 – 100 kDa) was used for further processing while the flow-through was discarded.

### 3.5.3 Protein Quantification

A straight calibration line was established using definite amounts of protein (0, 0.2, 0.4, 0.6, 0.8, 1.0 mg/mL bovine plasma gamma globuline) to analyze the amount of total protein in a sample. The BioRad DC™ Protein Assay kit was used and samples were incubated in the dark for 15 min at room temperature. Absorption at a wavelength of 750 nm was measured using a plate reader. A standard curve was established and exact protein amounts of the samples were calculated by plotting the absorbance against the equation of the trend line of the standard curve.

### 3.5.4 SDS-PAGE

A method of choice for protein analysis is gel electrophoresis. Discontinuous polyacrylamide gel electrophoresis (PAGE) allows for the possibility to eliminate aggregation and precipitation of certain proteins which guarantees a better separation of proteins. SDS-PAGE is used to separate proteins for their molecular weight. Sodium dodecyl sulfate (SDS) is an anionic detergent that is used to denature proteins by wrapping around the protein backbone by binding to positively charged side chains of amino acids. This process charges the proteins homogeneously negative in a constant weight ratio of 1.4 g/g of polypeptide, which makes intrinsic charges of the polypeptides negligible. Thus, polypeptides possess a uniform charge density that is the same negative net charge per unit length. Protein mobility is a linear function of the logarithms of their molecular weights and separation is based on the molecular weight of the proteins<sup>199-200</sup>. Generally, bigger proteins need wide meshed gels to quickly migrate during gel electrophoresis and therefore, smaller proteins migrate faster than bigger proteins. Protein samples were prepared with a total protein concentration of 20 µg and heat inactivation and the reducing agent beta-mercaptoethanol were used to reduce disulfide bonds within the three-dimensional protein structure prior to Bis-Tris gel loading.



## METHODS

### 3.5.5 Protein transfer by Western blot

Proteins within a polyacrylic amide matrix are not accessible for macromolecular ligands like antibodies and have to be transferred to an immobilizing membrane by electrophoresis to make them available for antibody binding<sup>201</sup>. During the electrophoretic migration, the negatively charged proteins bind to the membrane through hydrophobic interaction. The secondary and tertiary structure of the polypeptides is partially restored during this process and allows antibody binding to specific epitopes. For protein transfer, a vertical wet blotting chamber was used. The applied amperage is dependent on the size of the polyacrylamide gel and was calculated using the following equation:

$$\text{Amperage [mA]} = \text{gel size [cm}^2\text{]} \times 0.8$$

To evaluate blotting efficacy, PVDF membranes were stained with Ponceau S staining solution for 5 minutes after blotting. Staining with Ponceau S is reversible and can be washed off by continuous rinsing with ddH<sub>2</sub>O.

### 3.5.6 Immunodetection

For immunodetection, blotted proteins are incubated with primary antibodies that bind to epitopes of the protein of interest. Subsequently, the proteins are incubated with a secondary antibody that was raised against the primary antibody. The secondary antibody binds to species-specific sites and is horseradish peroxidase- (HRP-) labeled. In alkaline conditions HRP acts as a catalyst for the oxidation of luminol to 3-aminophthalic acid. To exhibit its luminescence, luminol must first be activated with an oxidant like hydrogen peroxide (H<sub>2</sub>O<sub>2</sub>). Oxidation of luminol triggers light emission that can be detected using an X-ray film developer. Alternatively, immunodetection can be achieved by colorimetric measures. In colorimetric detection, a soluble substrate (Opti-4CN, a more sensitive version of 4-chloro-1-naphthol) is converted by HRP into an insoluble form of a different color that precipitates next to the enzyme and stains the membrane. Development of the blot can then be stopped at the desired signal intensity by washing away the soluble dye. Prior to immunodetection, blots are blocked to avoid unspecific antibody binding. Tween-20 in intermediate wash steps is used as a detergent that separates unspecific bindings. Blots were incubated with the primary antibodies of according dilutions (1:1,000 – 1:10,000) at 4°C overnight, while accordingly diluted secondary antibodies (1:5,000, 1:10,000) were incubated at room temperature for four hours. For visualization, membranes were either incubated with the ECL detection kit or Opti-4CN colorimetric detection kit.

## METHODS

### 3.5.7 ELISA

Enzyme-linked immunosorbant assay (ELISA) is a biochemical technique used to detect and to quantify the presence of an antibody or antigen in a sample. In a direct ELISA the antigen is coated to a microtiter plate and detected with an antibody. In a sandwich ELISA, the antigen binds to a pre-coated capture antibody in a microtiter plate. Next, a detection antibody binds to the antigen and an enzyme-linked secondary antibody, which binds to the detection antibody, is added. For visualization and quantification, a substrate is added to the microtiter plate which is converted by the enzyme linked to the secondary antibody until the reaction is stopped. The intensity of signal can be measured and converted using a protein standard curve to quantify the amounts of antigen in the sample. Several commercially available sandwich ELISA kits were used for protein quantification.

### 3.6 Mouse experiments

#### 3.6.1 Subcutaneous xenografts

Mice were cared for in accordance with approved protocols by the Institutional Animal Care and Use Committee of Explora Biolabs (San Diego Science Center, protocol number EB11-025). Five- to six-week old male Hsd:athymic Nude-*Foxn1<sup>nu</sup>* mice (Harlan) were implanted subcutaneously (s.c.) with  $5 \times 10^6$  A549, DU-145, HCT-116, HT-29 or SW-620 cells (in 100  $\mu$ L PBS), respectively, into the right hind leg. Treatment started when tumors reached a volume of 200-300  $\text{mm}^3$ . Recombinant vaccinia virus was administered systemically either by retro-orbital (r.o.) or by intravenous (i.v.) injection into the lateral tail vein of  $2 \times 10^6$  or  $5 \times 10^6$  plaque-forming units (pfu), respectively, in 100  $\mu$ L PBS at day 0. Control animals were inoculated with 100  $\mu$ L PBS only. Tumor growth was measured using a digital caliper and tumor volume was calculated as  $0.5 \times (\text{length}-5) \times \text{width} \times \text{height}$  ( $\text{mm}^3$ ). Average tumor volume (ATV) was plotted against at each time point to monitor therapeutic efficacy. Body weight was measured as net body weight (body weight – tumor volume/1000  $\text{mm}^3$ ) to exclude tumor mass. Mice were sacrificed when the body weight dropped one third of their original body weight or the tumor volume exceeded 4000  $\text{mm}^3$ . The experiments were terminated 42 or 49 days post injection (dpi).

#### 3.6.2 Anesthesia

Laboratory mice were solely anesthetized using isoflurane which is a highly volatile anesthetic with hypnotic and muscle-relaxing effects. Mice were put in a knockout box and a mixture of isoflurane and oxygen was administered to the mice. Isoflurane has a very low distribution coefficient and therefore mice react rapidly on increasing or decreasing concentrations.

## METHODS

### 3.6.3 Vaccinia viral titers in tumor tissues and body organs

Tumors and body organs (spleen, kidney, liver, testes, lungs) of virus treated animals were surgically excised at different time points post inoculation and placed in two volumes of homogenization buffer (50 mM Tris-HCl (pH 7.4), 2mM EDTA (pH 7.4)) supplemented with Complete Protease Inhibitor Cocktail. Tumors were homogenized using a MagNA Lyser at a speed of 6,000 for 30 s (three times). After three freeze-thaw cycles, supernatants were collected by centrifugation (6,000 rpm, 5 min, 4°C). Viral titers were measured by standard plaque assay on CV-1 cells.

### 3.6.4 Preparation of tumor lysates for mouse immune-related protein profiling

For the preparation of tumor lysates, at various time points post virus treatment, three mice of each group were sacrificed. Tumors were excised surgically and resuspended in 9 volumes (W/V) lysis buffer [50 mM Tris-HCl (pH 7.4), 2 mM EDTA (pH 7.4), 2 mM PMSF and Complete Mini protease inhibitors] and homogenized using a MagNA Lyser at a speed of 6,000 for 30 s (three times). Supernatants were collected by centrifugation (6,000 rpm, 5 min, 4°C) and analyzed for mouse immune-related protein antigen profiling by Multi-Analyte Profiles (mouse MAPs) using antibody linked beads. Results were normalized based on total protein concentration.

### 3.6.5 Detection of virus-encoded marker gene RUC-GFP expression

GFP expression within tumors upon inoculation of recombinant vaccinia virus was monitored under blue light using a stereo fluorescence macroimaging system. GFP expression was scored using a four point system: 0) no GFP signal, 1) one spot, 2) two or three local spots, 3) diffuse signal from half the tumor, 4) strong signal from whole tumor. *Renilla* luciferase expression was detected by retro-orbital injection of benzyl-coelenterazine (25 µg / 100 µL) and subsequent imaging using the Argus-100 low light imager or the Carestream imaging device. Obtained data was either normalized to photon counts / 30 sec (Argus-100) or average mean intensity (Carestream).

### 3.6.6 Histological analysis of tumors

Tumors were surgically excised and snap-frozen in liquid N<sub>2</sub>, followed by fixation in 4% paraformaldehyde/PBS at pH 7.4 for 16 h at 4°C. Tissues were washed in PBS and embedded in 5% low melt agarose. Tissues were cut using a VT1200S vibratom into 100 µm sections and subsequently permeabilized in 0.2% Triton-X, 5% FBS in PBS. GFP expression was used as an indicator for viral distribution within the tumor tissue. Phalloidin-TRITC was used to label actin. Specific proteins of interest were stained with the respective primary antibodies and fluorescence-labeled secondary antibodies at appropriate dilutions. The fluorescent-labeled preparations were examined using a Leica MZ 16 FA Stereo-

## METHODS

Fluorescence microscope equipped with a FireWire DFC/IC monochrome CCD camera. Digital images were processed with GIMP2 and merged to yield pseudocolored images.

## 4 Results

### 4.1 Characterization of stem cell transcription factor-encoding vaccinia viruses GLV-1h205 (Nanog) and GLV-1h208 (Oct4)

#### 4.1.1 Virus mediated stem cell transcription factor expression

GLV-1h205 carries the gene that encodes for human Nanog, while GLV-1h208 encodes for the gene that encodes for human Oct4. In both viruses, the genes are under the control of the synthetic early promoter. Nanog and Oct4 are both transcription factors that are master key regulators in stem cell self-renewal and pluripotency<sup>57</sup>.

##### 4.1.1.1 Analysis of viral replication in the cancer cell lines A549 and PC-3

After generation of the new recombinant virus strain the replication capability of the viruses in cancer cells was investigated in comparison to the parental virus strain GLV-1h68. Replication was analyzed in the cancer cell lines A549 and PC-3. For analysis of the replication, the respective cell lines were infected with an MOI of 0.1 and viral titers were determined at 6, 24, 48, 72, and 96 hours post infection. The initial infection medium was used as initial virus titer at 0 hours post infection. Viral titers were determined by standard plaque assay. Average data including standard deviation are shown for GLV-1h205 and GLV-1h208 in comparison to GLV-1h68.

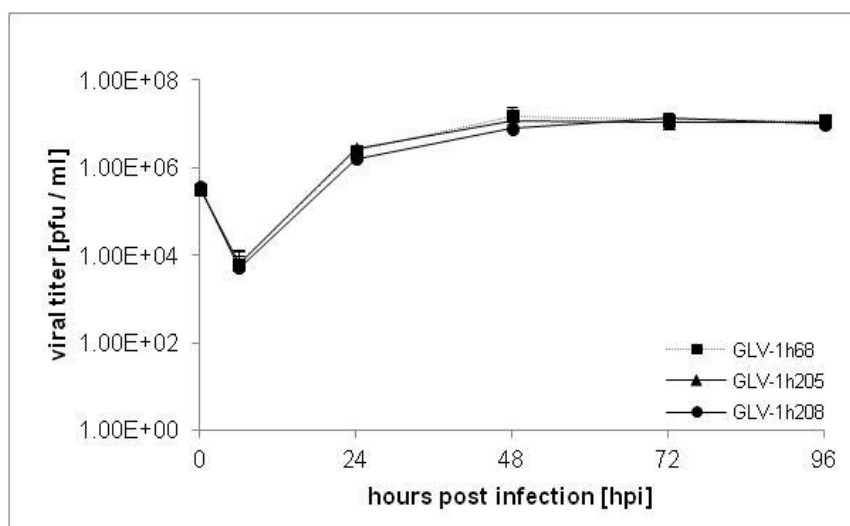
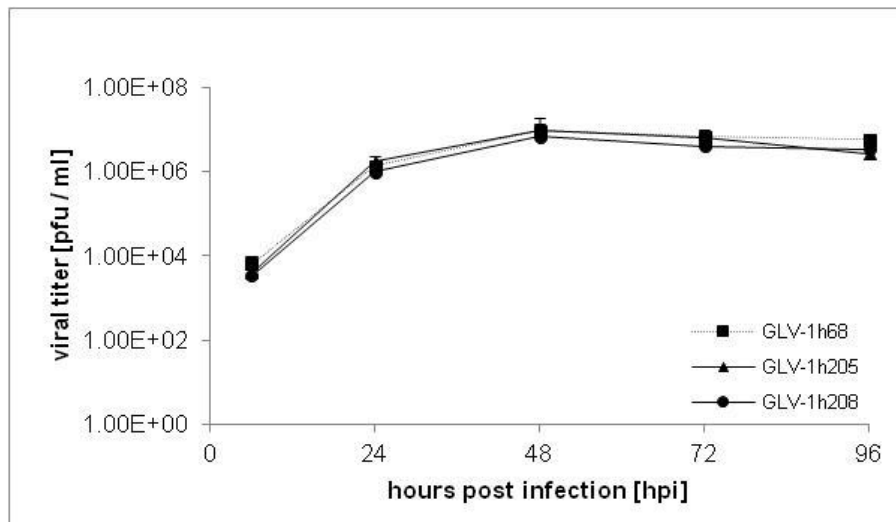


**Fig.4.1 – Analysis of viral titers after infection of A549 cells with GLV-1h68, GLV-1h205 and GLV-1h208**  
Cells were infected at an MOI of 0.1 and samples were collected at various times after infection. Titers were averaged from triplicates and plotted with standard deviations.

Figure 4.1 illustrates the replication efficacy of GLV-1h205 and GLV-1h208 compared to the parental virus GLV-1h68 in A549 cells during the course of the infection. A three-log

## RESULTS

increase in virus titers was observed within the first 48 hours of infection and stayed on a constant level afterwards. Both new virus strains, GLV-1h205 and GLV-1h208, efficiently infected and replicated in A549 cells in comparable levels to the parental virus strain GLV-1h68.



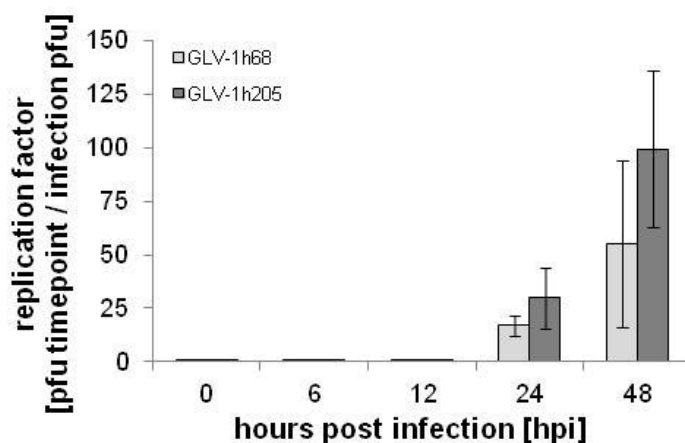
**Fig.4.2 – Analysis of viral titers after infection of PC-3 cells with GLV-1h68, GLV-1h205 and GLV-1h208**  
Cells were infected at an MOI of 0.1 and samples were collected at various times after infection. Titers were averaged from triplicates and plotted with standard deviations.

Figure 4.2 shows the replication efficacy of GLV-1h205 and GLV-1h208 in comparison to the parental GLV-1h68 in PC-3 cells. Similar to the infection of A549 cells, replication of the new virus strains was comparable to the parental GLV-1h68. Again, a three-log increase of viral titers was observed within the first 48 hours of infection before titers stayed on a constant level. To further analyze the replication behavior, A549 cells were infected with GLV-1h205 and GLV-1h68 at an MOI of 0.01 and viral titers were determined at 6, 12, 24, and 48 hpi. The replication factor was determined using the following equation:

$$\frac{\text{virus titer at time point } \left[ \frac{\text{pfu}}{\text{ml}} \right]}{\text{infection pfu } \left[ \frac{\text{pfu}}{\text{ml}} \right]} = \text{replication factor}$$

Viral titers were determined by standard plaque assay. Averaged data from triplicates including standard deviation are shown for GLV-1h205 in comparison to GLV-1h68.

## RESULTS



**Fig.4.3 – Analysis of viral replication rate of GLV-1h205 in comparison with the parental GLV-1h68**  
A549 cells were infected at an MOI of 0.01 and samples were collected at various time points after infection. Titers were averaged from triplicates and the replication factor was plotted with standard deviations.

Figure 4.3 demonstrates the replication factor of the new recombinant virus strain GLV-1h205 in comparison with the parental virus GLV-1h68. Even though a relatively high standard deviation was observed, GLV-1h205 showed a better replication in the 48 hours of infection.

In summary, it was shown that the new virus strains GLV-1h205 and GLV-1h208 efficiently infect and replicate in at least two different human cancer cell lines with a replication behavior that is comparable to the parental virus strain GLV-168. However, GLV-1h205 showed a better replication behavior than the parental GLV-1h68 during the first 48 hours of infection.

### **4.1.1.2 Analysis of vaccinia virus expressed mRNA transcripts of marker genes and stem cell transcription factors Nanog and Oct4 in infected mammalian cells**

To further characterize the new recombinant vaccinia virus strains, A549 cells were infected with GLV-1h205, GLV-1h208 and the parental GLV-1h68 to analyze marker gene expression of *ruc-gfp*, *nanog* and *oct4*, respectively. Cells were mock-infected or infected at an MOI of 5.0 to synchronize the infection and incubated for 2, 4, 6, and 8 hours at 37°C. Cells were harvested at each time point and mRNA was isolated and converted into cDNA for RT-PCR. PCR products were then analyzed by gel electrophoresis for gene expression.

## RESULTS

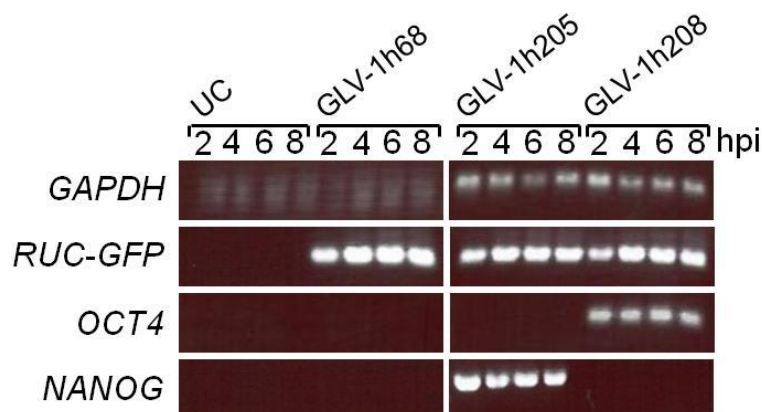


**Fig.4.4 – Analysis of viral (marker) gene transcription**

A549 cells were infected with GLV-1h68, GLV-1h205 and GLV-1h208 at an MOI of 5.0 and harvested at several time points. RNA was isolated and analyzed by RT-PCR. RT-PCR products were visualized by gel electrophoresis.

Figure 4.4 shows the viral (marker) gene expression after infection of A549 cells with GLV-1h205, GLV-1h208 and the parental GLV-1h68. *GAPDH* expression was used as an internal control. All three viruses show expression of *ruc-gfp* mRNA from as early as two hours post infection on. Expression of *oct4* mRNA was only detected in GLV-1h208 while expression of *nanog* mRNA was only detected in GLV-1h205. Both stem cell transcription factor-encoding virus strains expressed their respective transcription factor transcripts from as early as two hours post on while neither expression of *nanog* or *oct4* was detected in GLV-1h68 infected cells or uninfected controls. Both, *nanog* and *oct4* transcripts are therefore exclusively expressed by the respective virus strain.

### 4.1.1.3 Analysis of recombinant protein expression in infected mammalian cells

#### 4.1.1.3.1 Analysis of beta-galactosidase expression in infected mammalian cells

After confirmation of efficient recombinant gene transcription in the new virus strains, efficacy of functional protein expression of marker genes and transcription factors Nanog and Oct4 in infected mammalian cell cultures was analyzed. For beta-galactosidase expression, A549 cells were infected at an MOI of 0.01 for 24 hours to obtain single, isolated plaques. Cells were then treated with a substrate that is converted into a blue dye by beta-galactosidase and observed under the light microscope. Therefore, infected cells that express functional beta-galactosidase protein appear as blue plaques under the microscope.



## RESULTS

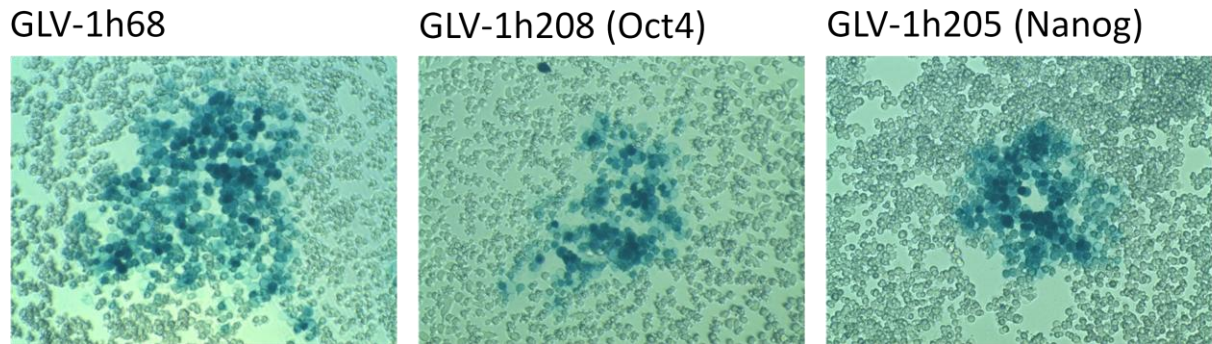


**Fig.4.5 – Expression of beta-galactosidase in infected A549 cells**

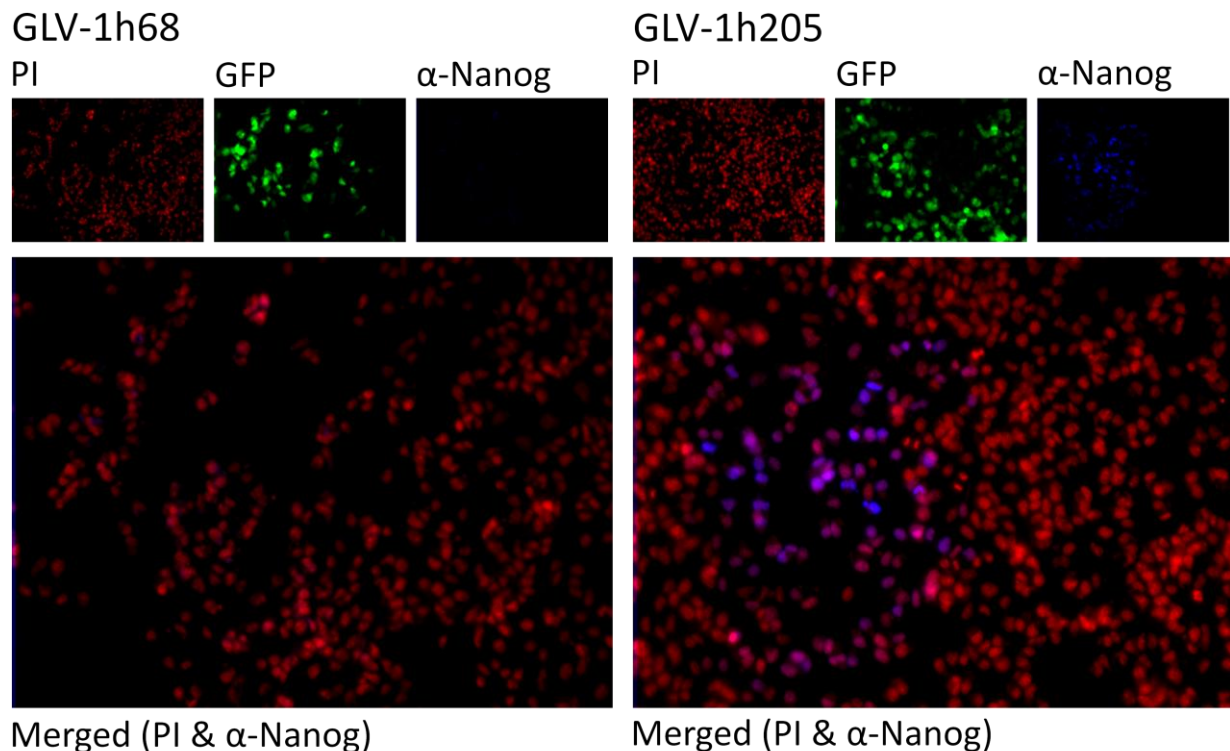
A549 cells were infected at an MOI of 0.01 to obtain single, isolated plaques and stained for beta-galactosidase expression. The two new recombinant virus strains GLV-1h205 and GLV-1h208 as well as the parental GLV-1h68 express functional beta-galactosidase. Pictures were taken at 100x magnification.

Figure 4.5 demonstrates the beta-galactosidase expression in virus-infected A549 cells. Both new recombinant virus strains, as well as the parental strain GLV-1h68, express beta-galactosidase mRNAs that are translated into functional proteins by the host translation machinery. Therefore, beta-galactosidase is a valid marker for efficient infection and replication of GLV-1h205 and GLV-1h208 in infected human cancer cells.

### **4.1.1.3.2 Analysis of Ruc-GFP and stem cell transcription factor expression in infected mammalian cells by immunocytochemistry**

To detect expression of Ruc-GFP fusion protein and the stem cell transcription factors Nanog and Oct4, A549 cells were infected at an MOI of 0.01 to obtain single, isolated plaques. Cells were then fixed and permeabilized to allow antibody binding. For detection of Nanog, cells were incubated with a polyclonal rabbit-anti-Nanog antibody and a AlexaFluor350-labeled secondary anti-rabbit antibody. To analyze the cellular location of Nanog, cell nuclei were stained with propidium iodide. Monochromal images were taken with a digital CCD camera and pseudo-colored using the open-source software GIMP 2.6. Expression of functional *Renilla* luciferase-green fluorescent protein fusion protein was detected by fluorescence microscopy. The parental GLV-1h68 was used as a control virus which is positive for Ruc-GFP expression but negative for Nanog expression.

## RESULTS



**Fig.4.6 – Analysis of Nanog and GFP expression in A549 cells infected with GLV-1h68 and GLV-1h205**

A549 cells were infected at an MOI of 0.01 with GLV-1h205 and the parental GLV-1h68 as a control to obtain single, isolated plaques. Cells were then fixed, permeabilized and incubated with a primary polyclonal rabbit-anti-Nanog antibody (1:500 dilution). Subsequently, cells were stained with an AlexaFluor350-conjugated secondary antibody (1:500) and GFP and Nanog expression was analyzed. Pictures were taken with a digital CCD camera and an inverted fluorescence microscope and pseudo-colored and edited using the open-source software GIMP2.6. Pictures were taken at 200x magnification.

Figure 4.6 shows the expression of viral Ruc-GFP fusion protein in both, GLV-1h68- and GLV-1h205-infected A549 cells in culture. GFP expression was detected in A549 cells infected with either GLV-1h68 or GLV-1h205, indicating efficient infection of the cells. In contrast, Nanog expression was only observed in A549 cells infected with GLV-1h205. Further analysis showed that Nanog is translocated back in the nucleus of the infected cells after translation in the cytoplasm. The translocation to the site of action further indicates protein functionality.

For detection of Oct4, cells were incubated with a polyclonal rabbit-anti-Oct4 antibody and a Rhodamine-labeled secondary anti-rabbit antibody. To analyze the cellular location of Oct4, cell nuclei were stained with Hoechst. Monochromal images were taken with a digital CCD camera and pseudo-colored using the open-source software GIMP 2.6. Expression of functional *Renilla* luciferase-green fluorescent protein fusion protein was detected by fluorescence microscopy. The parental GLV-1h68 was used as a control virus which is positive for Ruc-GFP expression but negative for Oct4 expression.

## RESULTS

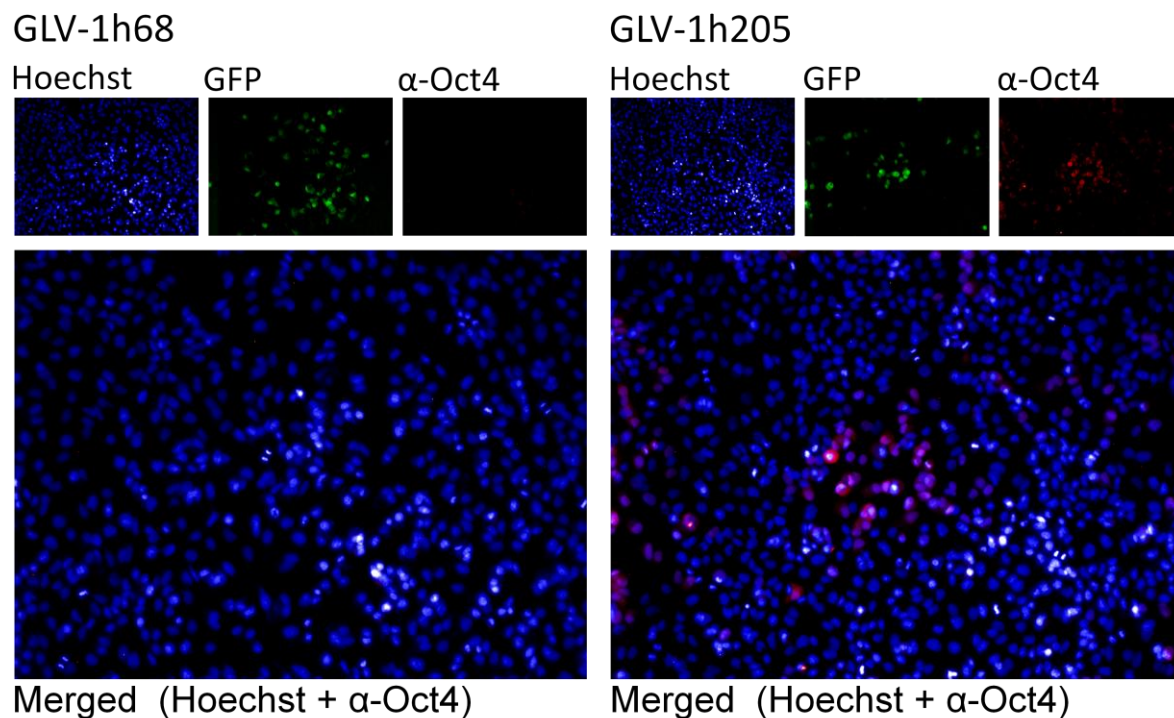


**Fig.4.7 - Analysis of Oct4 and GFP expression in A549 cells infected with GLV-1h68 and GLV-1h208**

A549 cells were infected at an MOI of 0.01 with GLV-1h208 and the parental GLV-1h68 as a control to obtain single, isolated plaques. Cells were then fixed, permeabilized and incubated with a primary polyclonal rabbit-anti-Oct4 antibody (1:500 dilution). Subsequently, cells were stained with an Rhodamine-conjugated secondary antibody (1:500) and GFP and Oct4 expression was analyzed. Pictures were taken with a digital CCD camera and an inverted fluorescence microscope and pseudo-colored and edited using the open-source software GIMP2.6. Pictures were taken at 200x magnification.

Figure 4.7 shows the expression of viral Ruc-GFP fusion protein in both, GLV-1h68- and GLV-1h208-infected A549 cells in culture. GFP expression was detected in A549 cells infected with either GLV-1h68 or GLV-1h208, indicating cell infection and viral protein expression. In contrast, Oct4 expression was observed exclusively in GLV-1h208 infected A549 cells. Further analysis showed a co-localization of Oct4 signal and nucleic staining. Oct4 is therefore transported into the cell nucleus after translation. The translocation to the site of action further indicates protein functionality. Overall, it was demonstrated that mammalian cells infected with both new recombinant virus strains express functional respective transcription factors and marker fusion protein Ruc-GFP. However, neither Nanog nor Oct4 expression was observed upon infection with the parental virus GLV-1h68.

### **4.1.1.3.3 Analysis of Nanog expression in infected mammalian cells by ELISA quantification**

To gather further evidence for the correct expression of human Nanog in mammalian cells infected with the new recombinant virus GLV-1h205, A549 cells were either infected with the parental GLV-1h68 as a negative control or the Nanog-encoding GLV-1h205. Cells were

## RESULTS

infected at an MOI of 5.0 to synchronize the infection and incubated for 6, 24, 48, 72 and 96 hours. Infected cells were harvested and the total protein amount was determined. The samples were prepared for the human Nanog sandwich ELISA and Nanog amounts were quantified following the manufacturer's instructions.

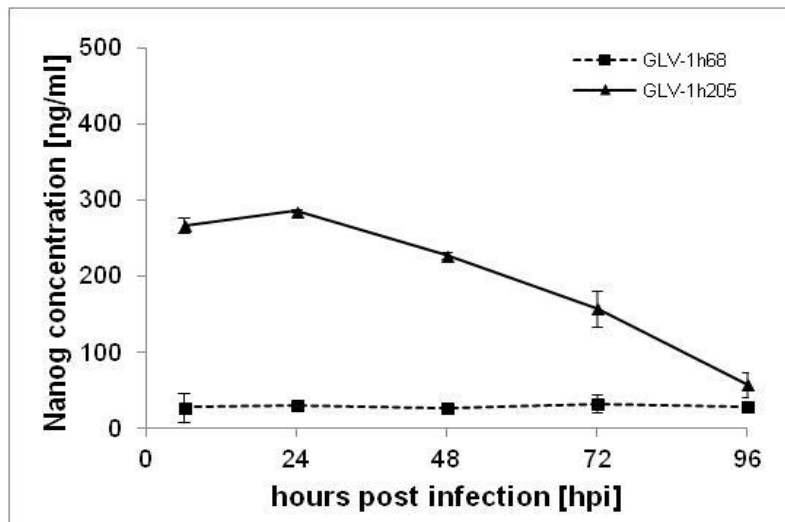


**Fig.4.8 – ELISA for detection of human Nanog in infected A549 cells**

A549 cells were infected with GLV-1h68 and GLV-1h205 at an MOI of 5.0. Samples were harvested at various time points during the course of infection. ELISA was performed according to the manufacturer's instructions and Nanog protein amounts were plotted with standard deviations.

Figure 4.8 demonstrates that A549 cells infected with GLV-1h205 expressed significantly higher levels of Nanog (up to 285.7 ng/mL at 24 hpi) than cells infected with the parental control GLV-1h68. While low baseline levels of Nanog remain constant over the course of the experiment in GLV-1h68-infected cells, Nanog expression in GLV-1h205 was highest within the first 24 hours and decreases constantly during the next 72 hours. The decrease in Nanog amount can be related to A549 cell killing upon viral infection and the half life of the protein itself. Generally, it was shown that only in GLV-1h205-infected cells a significant increase in Nanog expression occurred, further indicating the correct expression of the new insert.

### **4.1.1.3.4 Analysis of Oct4 expression in infected mammalian cells by Western blot**

To further analyze the protein expression of human Oct4 in virus infected cells, Western blot analysis was performed. A549 cells were either mock-infected or infected with GLV-1h68 as a negative control or GLV-1h208 at an MOI of 5.0 to synchronize the infection. Infected cells were incubated for 3, 6, 24, 48, 72 and 96 hours and harvested at the respective time point. Samples were processed to determine total protein amounts. For Western blot analysis, 20 µg total proteins per sample were used. SDS-PAGE and Western blotting was performed

## RESULTS

prior to antibody binding. Histone H3 antibodies were used as a loading control and Oct4 antibodies for detection of the recombinant viral gene product. The blot was developed by colorimetric detection. Histone H3 has a predicted molecular mass of 15 kDa while the band can be detected around 17 kDa. The predicted molecular mass of Oct4 is 39 kDa while the protein band can be detected around 43 kDa.

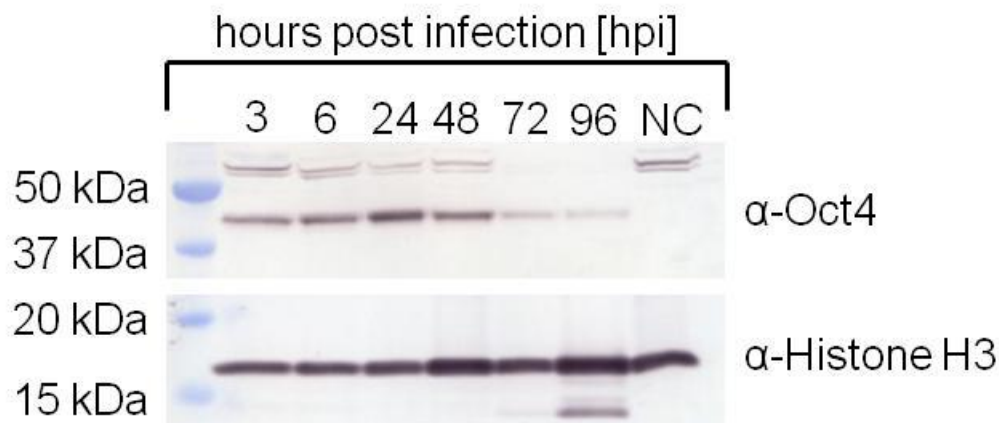


**Fig.4.9 – Western blot analysis of human Oct4 in infected A549 cells**

A549 cells were either mock-infected or infected with the Oct4-expressing GLV-1h208 at an MOI of 5.0. Oct4 expression was followed over the course of 96 hours of infection. Samples were harvested during the course of the experiment and processed for Western blot analysis. The primary Oct4 antibody was used at a concentration of 1 µg/mL while the primary Histone H3 antibody was used at a dilution of 1:5000 due to its high abundance. The blot was visualized by colorimetric detection.

Figure 4.9 clearly demonstrates the expression of human Nanog in infected A549 cell culture. The comparable signal strength in Histone H3 expression suggests that comparable amounts of total protein were loaded prior to SDS-PAGE. Oct4 signal in GLV-1h208 infected cells was detectable from as early as 3 hpi. The maximal signal strength was detected between 6 and 48 hpi. Signal strength decreased from 48 hpi on which can be correlated with cell death by viral replication and Oct4 degradation. It was demonstrated that A549 cells that were infected with the recombinant vaccinia virus express detectable amounts of Oct4, while the amounts were time-dependent. To assure that Oct4 expression is a result of infection with GLV-1h208 and not a general cellular response to vaccinia virus infection, A549 cells were either mock-infected or infected with GLV-1h68 or GLV-1h208 at an MOI of 5.0. Cells were harvested 3, 6 and 24 hpi and total protein amounts were determined. For Western blot analysis, 20 µg total proteins per sample were used. SDS-PAGE and Western blotting was performed prior to antibody binding. The membrane was incubated with a primary antibody against Oct4 and intrinsic unspecific binding of the antibody was used as a loading control. The blot was developed by colorimetric detection.

## RESULTS

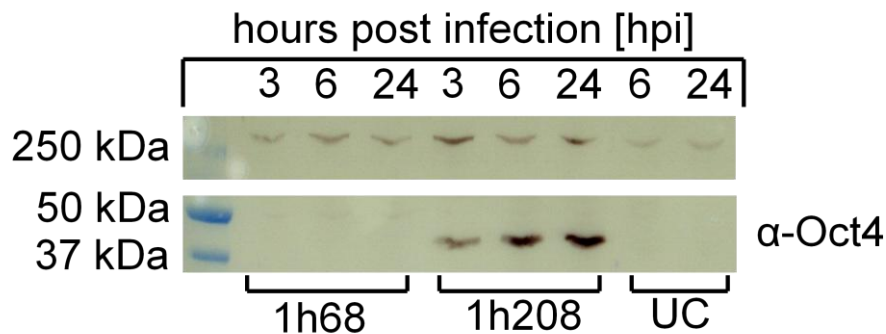


**Fig.4.10 – Western blot analysis of Oct4 expression in GLV-1h208 and GLV-1h68**

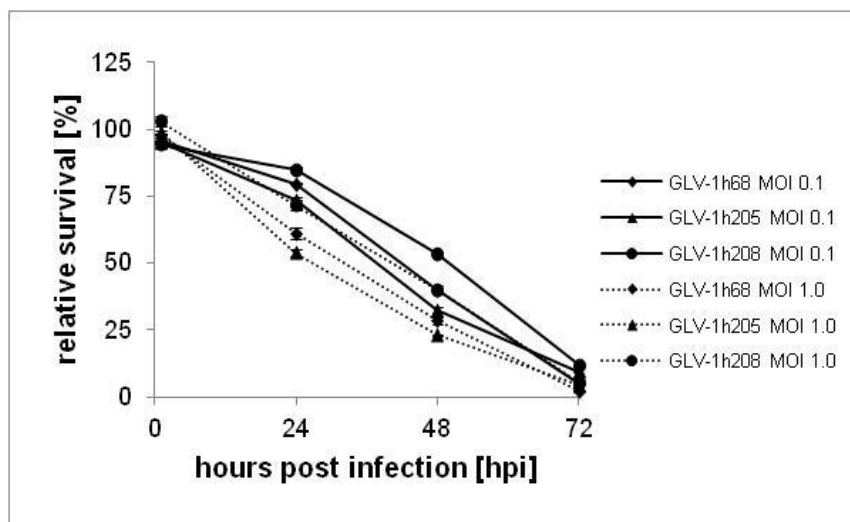
A549 cells were either mock-infected or infected with the Oct4-expressing GLV-1h208 or the parental GLV-1h68 at an MOI of 5.0. Oct4 expression was followed over the course of 24 hours of infection. Samples were harvested at 3, 6, and 24 hpi and processed for Western blot analysis. The primary Oct4 antibody was used at a concentration of 1  $\mu\text{g}/\text{mL}$ . The blot was visualized by colorimetric detection.

Figure 4.10 clearly illustrates that Oct4 expression in infected A549 cells is a result of the infection with the OCT4-encoding recombinant vaccinia virus GLV-1h208. Neither mock-infected A549 cells nor GLV-1h68-infected A549 cells showed detectable levels of Oct4 protein during the course of the experiment while increasing amounts of Oct4 were detected in GLV-1h208-infected cells. Therefore, the existence of cellular Oct4 levels as well as Oct4 expression due to vaccinia virus infection can be ruled out and detected Oct4 is exclusively produced by GLV-1h208.

### **4.1.1.4 Analysis of cell viability of mammalian cell cultures infected with GLV-1h205 and GLV-1h208**

A desirable feature of oncolytic viruses is their ability to efficiently infect, replicate in and lyse human cancer cells. To assess the ability of Nanog- and Oct4-expressing vaccinia viruses GLV-1h205 and GLV-1h208, to kill cancer cells, A549 cells in culture were seeded to a confluence of 95% and either mock-infected or infected with GLV-1h205 or GLV-1h208. As a reference, confluent A549 cells were also infected with the parental strain GLV-1h68. Cells were infected with an MOI of 0.1 and 1.0, respectively to analyze dose-dependency. The infection was followed for 72 hours and samples were analyzed 1, 24, 48, and 72 hours post infection.

## RESULTS



**Fig.4.11 – Viability of A549 cells after infection with GLV-1h68, GLV-1h205, and GLV-1h208**

Analysis of cell viability of A549 cells after infection with replication-competent vaccinia viruses GLV-1h68, GLV-1h205 and GLV-1h208, using MOIs of 0.1 and 1.0, respectively. Viability was monitored over the course of 72 hours and was measured in triplicates and averaged. Plotted averages are normalized against uninfected controls of each time-point which were considered to be 100% viable.

Figure 4.11 shows efficient cell killing of A549 cells by the tested vaccinia viruses. The parental strain GLV-1h68 was used as a reference for the cytotoxic potential of the new recombinant strains GLV-1h205 and GLV-1h208. After 72 hours, only  $4.89 \pm 0.49\%$  (MOI 0.1) and  $2.27 \pm 0.27\%$  (MOI 1.0) of the cells infected with GLV-1h68 were still viable. GLV-1h205 showed higher cytotoxicity at an MOI of 1.0 during the early course of infection ( $53.75 \pm 1.46\%$  viable cells compared to  $61.15 \pm 2.12\%$  in GLV-1h68 after 24 hours of infection) but cytotoxic efficacy is identical after 24 hours of infection. Overall, the Oct4-expressing vaccinia virus GLV-1h208 showed a reduced cytotoxic potential compared to both, GLV-1h205 and the parental strain GLV-1h68. At 24 and 48 hours post infection, the differences in cytotoxicity with GLV-1h68 and GLV-1h205 range between 5-20%. Overall, it was demonstrated that the new recombinant vaccinia viruses GLV-1h205 and GLV-1h208 efficiently infected, replicated in, and ultimately lysed A549 cells in a dose-dependent manner. Compared with the reference strain GLV-1h68, GLV-1h205 showed slightly increased oncolytic potential while the oncolytic potential of GLV-1h208 was reduced.

### **4.1.1.5 Influence of Nanog expression on cell cycle progression in mammalian cell culture**

It has been demonstrated that Nanog overexpression under normal physiological conditions in human embryonic stem cells leads to accelerated transition into the S phase and cell proliferation by directly interacting with CDK6 and CDC25A<sup>74</sup>. To analyze the influence of Nanog expression on cell cycle progression and cell proliferation in human cancer, A549 cells in culture were treated for 18 hours with nocodazole to synchronize cells in the G2/M phase

## RESULTS

of the cell cycle. After Nocodazole release, cells are able to enter the cell cycle again and proliferate. Synchronized cells were then either mock-infected or infected with GLV-1h68 as a negative control and GLV-1h205 at an MOI of 1.0 and 10, respectively, for 6 hours. Mock-infected and infected cells were then harvested and analyzed by FACS analysis for cell cycle progression to determine the distribution of cells at different stages of the cell cycle.

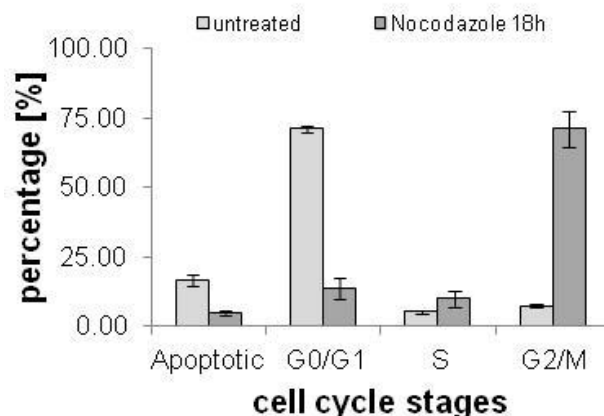


**Fig.4.12 – Cell cycle arrest after Nocodazole treatment**

A549 cells were cultured until 95% confluence and then treated for 18 hours with 200 ng/mL Nocodazole to arrest cells in G2/M. The cells were then prepared for cell cycle analysis by FACS and the distribution of cells in the different stages of the cell cycle was analyzed. Two sets of triplicates were counted ( $1 \times 10^5$  cells), averaged, and plotted with standard deviations.

Figure 4.12 demonstrates the efficient arrest of A549 cells in culture in G2/M by the mitotic inhibitor nocodazole. While untreated cells were mainly to be found in G0/G1 ( $70.92 \pm 1.37\%$ ) and only a low percentage was found to be in G2/M ( $7.28 \pm 0.77\%$ ), after 18 hours of nocodazole treatment, only  $13.65 \pm 3.81\%$  of cells were found to be in G0/G1 while the majority of cells was arrested in G2/M ( $70.97 \pm 6.67\%$ ). Therefore, nocodazole treatment efficiently arrested A549 cells in culture in the G2/M phase of the cell cycle and synchronized the cells for subsequent virus treatment to analyze the effects of Nanog expression on the cell cycle in the early stages of vaccinia virus infection while the host transcription machinery in the infected cells is still active.



## RESULTS

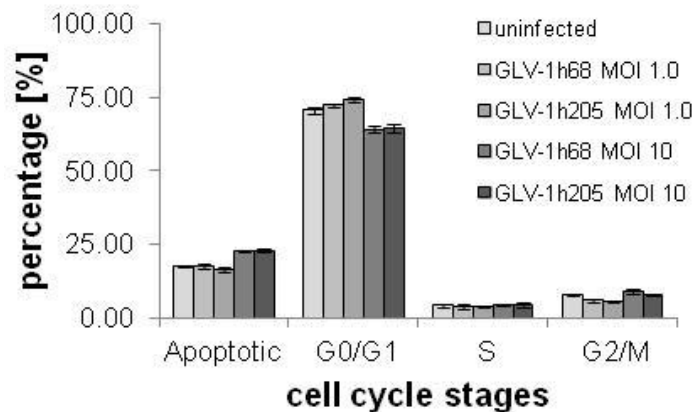


**Fig.4.13 – Cell cycle analysis of infected A549 cells in culture**

Synchronized A549 cells were either mock-infected or infected with the parental GLV-1h68 or GLV-1h205 at an MOI of 1.0 or 10 for 6 hours. Then, cells were prepared for cell cycle analysis by FACS and distribution of cells in the different stages of the cell cycle was analyzed. Sets of triplicates were counted ( $1 \times 10^5$  cells), averaged, and plotted with standard deviations.

Figure 4.13 shows the effect of virus infection with GLV-1h68 and GLV-1h205 on cell cycle progression in the early stages of infection. No significant difference between virus strains was observed. After nocodazole release and 6 hours of virus infection, most cells infected with either GLV-1h68 or GLV-1h205 progressed into the G0/G1 phase ( $72.40 \pm 0.5\%$  or  $74.17 \pm 0.67\%$  at an MOI of 1.0, and  $64.05 \pm 1.06\%$  or  $64.55 \pm 1.33\%$  at an MOI of 10). Distribution of cells entering the S phase was not affected by viral Nanog expression ( $3.57 \pm 0.21\%$  in GLV-1h205 vs.  $3.7 \pm 0.98\%$  in GLV-1h68 at an MOI of 1.0 or  $4.40 \pm 0.78\%$  vs.  $4.33 \pm 0.19\%$  at an MOI of 10). An MOI-dependent increase in dead cells was detected as distributions significantly increased after infection with an MOI of 10 ( $17.55 \pm 0.21\%$  in uninfected cells,  $17.50 \pm 0.92$  or  $16.47 \pm 0.75\%$  in cells infected with GLV-1h68 or GLV-1h205 at an MOI of 1.0 vs.  $22.65 \pm 0.07$  in GLV-1h68 and  $22.93 \pm 0.76$  in GLV-1h205 at an MOI of 10). Therefore, no effect of Nanog expression in cell cycle progression and cell proliferation during the first 6 hours of infection in A549 cell cultures was observed.

### **4.1.1.6 Influence of Nanog and Oct4 expression on expression of genes involved in epithelial-to-mesenchymal transition (EMT) after infection of A549 in culture**

It has been shown that co-expression of Nanog and Oct4 enhances malignancy in lung adenocarcinoma by increasing cancer stem cell-like properties and epithelial-mesenchymal transdifferentiation<sup>78</sup>. To study the effects of virus-mediated Nanog or Oct4 expression on gene expression of factors involved in cancer stem cells or EMT, A549 cells were grown until 95% confluence and either mock-infected or infected with GLV-1h68 as a negative control and GLV-1h205 or GLV-1h208 for 2, 4, 6, or 8 hours. The mock-infected and infected cells

## RESULTS

were then harvested and RNA was isolated from cell lysates. Then, RNAs were converted to cDNAs and RT-PCR was performed to detect mRNA levels of *cd133*, *nestin*, *slug*, and *snail*. Levels of *ruc-gfp*, *nanog* and *oct4* were tested to verify the infection with GLV-1h68, GLV-1h205 or GLV-1h208.

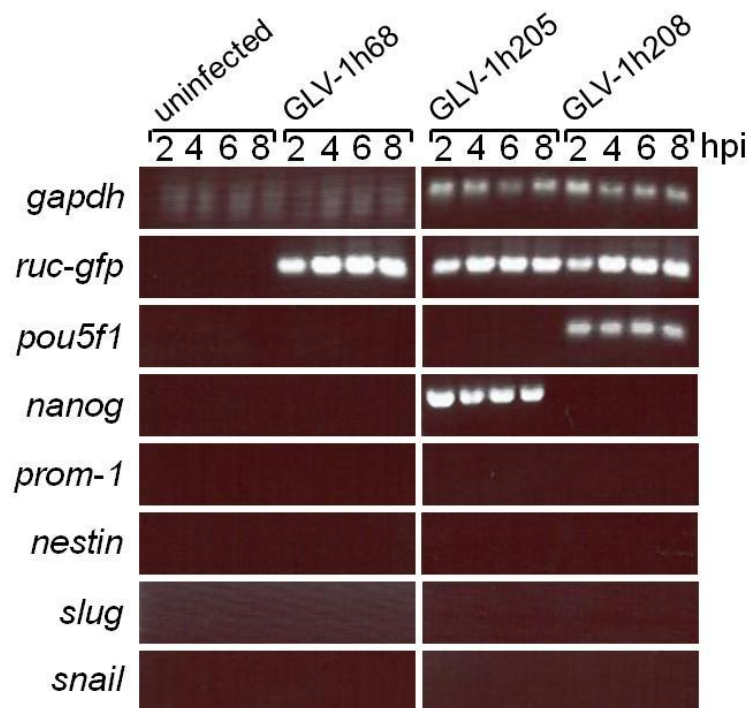


**Fig.4.14 – RT-PCR to analyze expression of genes involved in CSCs and EMT after virus infection**

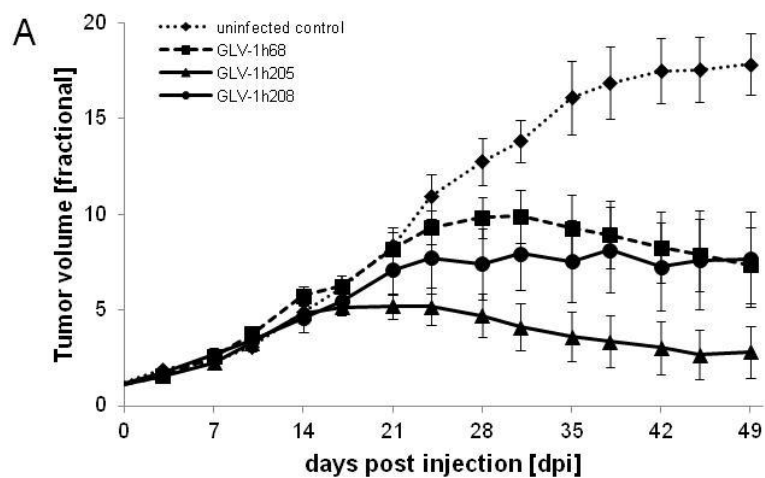
A549 cells were grown until 95% confluence and then either mock-infected or infected with GLV-1h68, GLV-1h205 (Nanog) or GLV-1h208 (Oct4) at an MOI of 5.0 to synchronize the infection. Total RNA was isolated from the infected cells at various time points and mRNA was converted to cDNA for RT-PCR analysis. Expression levels of *cd133*, *nestin*, *slug* and *snail* mRNA upon virus infection were analyzed. *Ruc-gfp*, *nanog* and *oct4* levels were tested to verify virus infection and transcription factor expression.

Figure 4.15 shows that neither the infection with parental vaccinia virus GLV-1h68 nor infection with the Nanog-expressing virus GLV-1h205 or the Oct4-expressing GLV-1h208 increased the mRNA expression levels of CD133, Nestin, Slug or Snail. In no case a signal in RT-PCR analysis was obtained, indicating that vaccinia virus infection and virus-mediated expression of Nanog or Oct4 do not trigger gene expression of factors involved in EMT during the early course of infection before the host transcription machinery is shut down by vaccinia virus replication.

## RESULTS

### 4.1.2 Effects of a single dose of GLV-1h205 or GLV-1h208 in subcutaneous A549 xenografts

To analyze the effects of Nanog-expressing GLV-1h205 and Oct4-expressing GLV-1h208 in A549 mouse xenografts, 32 male athymic nude FoxN1 mice at an age of 4-5 weeks were subcutaneously implanted with  $5 \times 10^6$  A549 cells in 100  $\mu$ L PBS. All animals developed tumors with volumes around 250 to 300 mm<sup>3</sup> after two weeks of implantation. Animals were separated into different treatment groups of eight (n=8) with similar tumor volumes before virus treatment. Animals in the groups were then injected retro-orbitally (r.o.) with 100  $\mu$ L PBS or  $2 \times 10^6$  pfu of either GLV-1h68 as a reference for oncolytic treatment, GLV-1h205 or GLV-1h208. To analyze the effects of Nanog and Oct4 co-expression, animals were grouped (n=5) and then injected retro-orbitally with 100  $\mu$ L PBS or  $3 \times 10^6$  pfu of GLV-1h205 or GLV-1h208, or a combination of  $1.5 \times 10^6$  pfu GLV-1h205 and GLV-1h208. Tumor size was measured with a digital caliper two times a week for all animals until 49 days post injection. Actual tumor volumes were divided by initial tumor volumes to acquire fractional tumor volumes (FTVs). FTVs were averaged and plotted with standard deviations.



## RESULTS

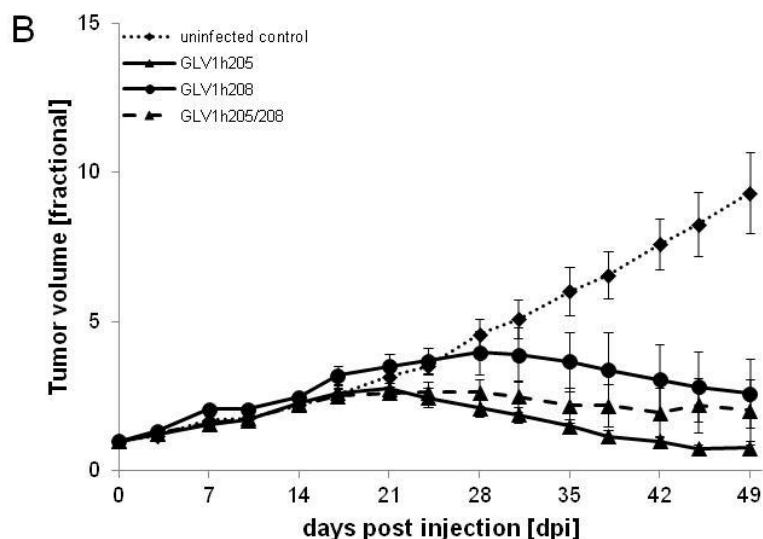


**Fig.4.15 – Effects of recombinant vaccinia viruses GLV-1h68, GLV-1h205 and GLV-1h208 on A549 tumor growth in subcutaneous mouse xenografts**

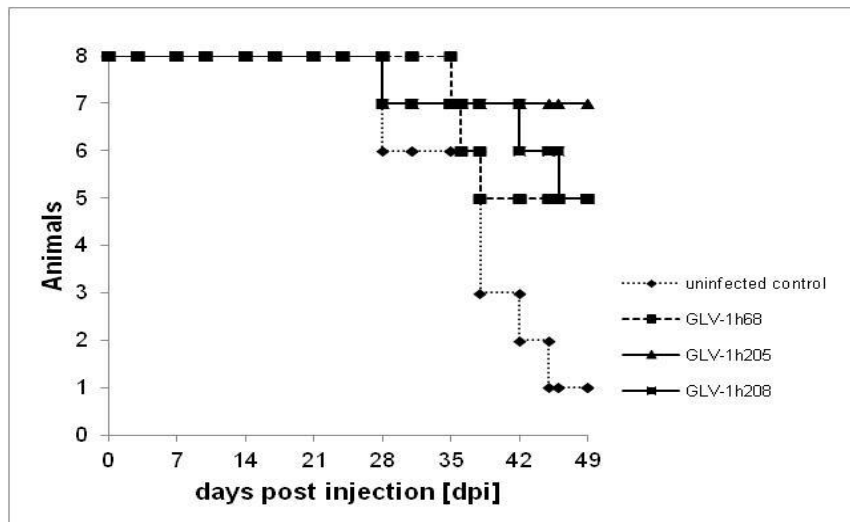
Tumor-bearing mice (n=8) were injected (i.o.) with PBS or  $2 \times 10^6$  pfu of GLV-1h68, GLV-1h205 or GLV-1h208 [A] or  $3 \times 10^6$  pfu GLV1h205 or GLV1h208, or a combination of  $1.5 \times 10^6$  pfu GLV-1h205 and GLV-1h208 [B]. Tumor growth was followed twice a week for 49 days. FTV was plotted with standard deviations as an average of all mice per group. One-way analysis of variance (ANOVA) was used to compare the corresponding data points.  $P \leq 0.05$  was considered statistically significant.

Figure 4.15 illustrates that all three recombinant vaccinia virus strains caused significant growth inhibition after injection in A549 tumor-bearing nude mice. While injection with GLV-1h208 led to tumor inhibition, regression of tumors was observed in tumor-bearing mice that were injected with GLV-1h68 or GLV-1h205. However, treatment with GLV-1h205 was more efficient than treatment with GLV-1h208 or the reference strain GLV-1h68. Tumor volumes became statistically different between untreated mice and GLV-1h205 after 24 days of injection. Statistical significance between untreated mice and GLV-1h208 was observed after 28 days and in GLV-1h68-treated mice after 35 days of injection. While tumor volumes of tumor-bearing mice treated with GLV-1h205 did not exceed a  $5.22 \pm 0.66$ -fold increase, tumor volumes in GLV-1h68- and GLV-1h208-treated mice increased up to  $9.90 \pm 1.39$ -fold (GLV-1h68) or  $8.15 \pm 2.23$ -fold (GLV-1h208). Statistical significance between GLV-1h205-treated and GLV-1h68/GLV-1h208-treated mice was observed 21 dpi. Generally, GLV-1h205 proved to be a more efficient treatment regimen for A549 tumor-bearing mice compared to the parental reference strain GLV-1h68. Treatment with GLV-1h208 caused a faster response in oncolytic efficacy leading to tumor growth inhibition compared to GLV-1h68 but the overall outcome was comparable. Co-expression of Nanog and Oct4 resulted in better therapeutic efficacy compared to GLV-1h208 alone, but impaired efficacy compared to GLV-1h205 alone.

Additionally to tumor growth analysis, overall survival was assessed to further investigate

## RESULTS

cytotoxic side effects of the virus treatment and therapeutic efficacy. Tumor volumes exceeding 4000 mm<sup>3</sup> as well as poor physiological condition (determined by loss of one third of the initial body weight) were used as criteria to sacrifice tumor-bearing nude mice. A Kaplan-Meier diagram was compiled to analyze the survival rates.



**Fig.4.16 – Kaplan-Meier survival diagram of A549 tumor-bearing mice**

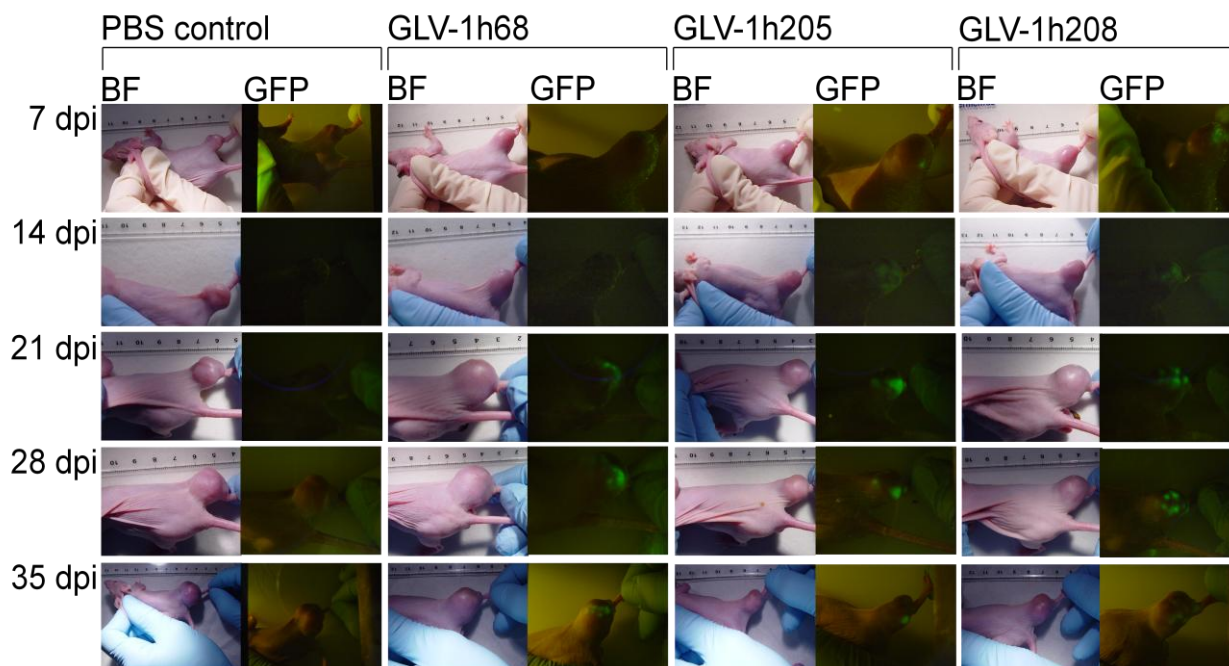
Survival rates of untreated and virus-treated mice were analyzed over the course of 49 days and plotted as a Kaplan-Meier survival diagram. All virus-treated mice showed significant benefits in survival compared to untreated control mice.

Figure 4.16 shows the overall survival of the untreated and virus-treated A549 tumor-bearing mice over the course of 49 days of treatment. Overall, virus-treated animals of all three groups showed significant benefits in survival compared to the untreated controls. All untreated control animals were sacrificed due to high tumor burden whereas animal deaths in virus-treated groups were either due to high tumor burden or poor physiological condition. Generally, the virus treatment was well tolerated by the tumor-bearing mice while giving a significant benefit in survival and tumor burden.

### **4.1.2.1 Confirmation of viral tumor infiltration, infection and replication by GFP fluorescence and *Renilla* luciferase low light imaging**

To confirm the invasion of subcutaneous A549 tumors by the three replication-competent vaccinia virus strains, GFP expression of animals of each group was monitored under blue light using a stereo fluorescence macroimaging system. GFP expression was monitored once a week over the course of five weeks. Bright-field pictures were taken to monitor overall tumor volume.

## RESULTS



**Fig.4.17 – Bright-field and direct fluorescence imaging of untreated and treated A549 tumor-bearing mice**  
Bright-field and fluorescence pictures of one representative animal per treatment group over the course of 35 days post treatment were taken once a week to analyze viral infiltration and infection of the tumor and changes in tumor size.

Figure 4.17 demonstrates the efficient virus colonization of A549 tumors in all three treatment groups. The detected GFP signal was strongest after 21 and 28 days post injection in all three treatment groups and decreased along tumor regression. No GFP signal was detected in untreated control animals. Overall tumor volumes were smallest in GLV-1h205-treated animals, supporting the obtained data from figure 4.15. Unfortunately, deep tissue imaging was not possible and no analysis of infection throughout the whole tumor was performed.

To further analyze viral colonization of the tumors, four mice of each treatment group were imaged for *Renilla* luciferase expression at 14 days post injection by low light imaging. Four mice per group were anesthetized, injected (r.o.) with 5  $\mu$ g / 100  $\mu$ L PBS, and imaged with the Argus-100 low light imager.

## RESULTS

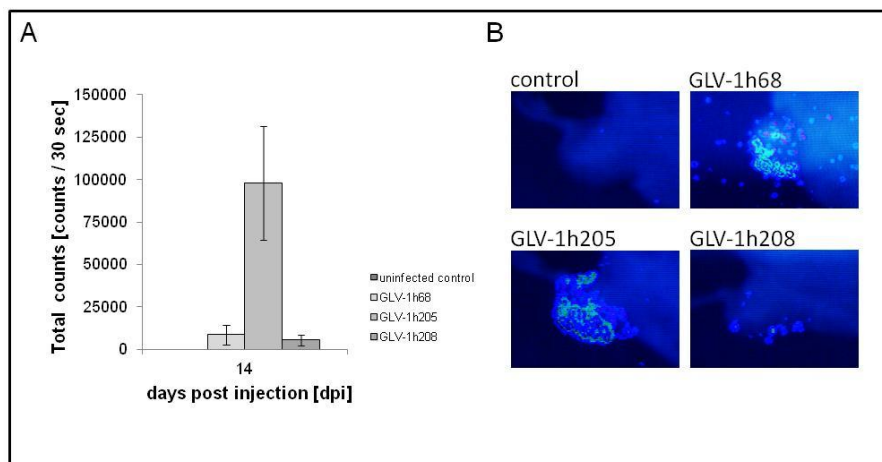


**Fig.4.18 – *Renilla* luciferase low light imaging of untreated and virus-treated A549 tumor-bearing animals 14 dpi**

Four untreated and treated animals of each group were imaged for *Renilla* luciferase expression 14 days post virus treatment. A) Total photon counts of each imaged animal per group were averaged and plotted with standard deviations. B) Representative pictures of photon counts were taken for each treatment group.

Figure 4.18 gives further information about the colonization of A549 tumors by different replication-competent vaccinia virus strains. The significantly strongest signal after 14 days of virus injection was observed in GLV-1h205-injected mice. Photon counts in GLV-1h68- and GLV-1h208-treated mice were comparable. Taken together, GFP and *Renilla* luciferase imaging confirmed that virus replication was confined to the primary tumor site and was not found in different tissues accessible to GFP or luciferase imaging. Overall, the virus treatment groups had good take rates but not all mice were showing virus marker gene expression in the tumors.

### **4.1.2.2 Pfu determination in vaccinia virus-injected A549 tumor-bearing mice at various time points**

The viral distribution within the animals of the different treatment groups was analyzed at various time points after virus treatment. Virus titers were determined by standard plaque assays from tumor lysates or lysates from different body organs (lungs, liver, kidney, spleen, and testes). At five and ten days post virus treatment, five animals per treatment group were sacrificed and virus titers were determined to investigate whether the observed benefit in treatment of GLV-1h205 compared to both other virus groups can be related to virus replication potential during the early course of the infection and to pinpoint the earliest time point where viral titers become different.

## RESULTS

**Tab.4.1 – Virus titers in A549 tumor-bearing mice 5 and 10 dpi**

Treatment	5 dpi		10 dpi	
uninfected control	n.d.	[n=0/3]	n.d.	[n=0/3]
GLV-1h68	$1.19 \times 10^5 \pm 1.49 \times 10^5$	[n=4/5]	$1.53 \times 10^6 \pm 1.06 \times 10^6$	[n=5/5]
GLV-1h205	$5.32 \times 10^3 \pm 9.98 \times 10^3$	[n=2/5]	$1.94 \times 10^6 \pm 2.45 \times 10^6$	[n=5/5]
GLV-1h208	$8.58 \times 10^3$	[n=1/5]	$3.93 \times 10^5 \pm 4.08 \times 10^5$	[n=5/5]

Tumor-bearing mice were sacrificed five or 10 days post virus injection and standard plaque assays from tumor lysates were performed to determine the virus titers in each treatment group. Virus titers are displayed as averaged total pfu / tissue with standard deviations. *n.d.* = not detectable (detection limit < 10 pfu / tumor)

Table 4.1 illustrates the viral replication during the early course of infection. Infection rates after only five days of virus treatment were still very heterogeneous and differed between the treatment groups. Whereas GLV-1h68-treated animals showed very good infection rates (80%), treatment with GLV-1h205 (40%) or GLV-1h208 (20%) was less efficient. However, after ten days of infection, all tested mice had virus take rates of 100% and GLV-1h205-infected mice showed the highest titers while GLV-1h208-treated mice showed significantly lower virus titers than both other recombinant vaccinia viruses. Within day five and ten days of infection, GLV-1h205 started replicating faster than the parental strain GLV-1h68 and GLV-1h208.

To further analyze viral spreading during the late course of the infection, four animals per group were sacrificed at 21 days and 49 days, respectively. Tumor tissues and body organs were surgically removed and viral titers in tumor tissues and body organs were analyzed by performing standard plaque assay.

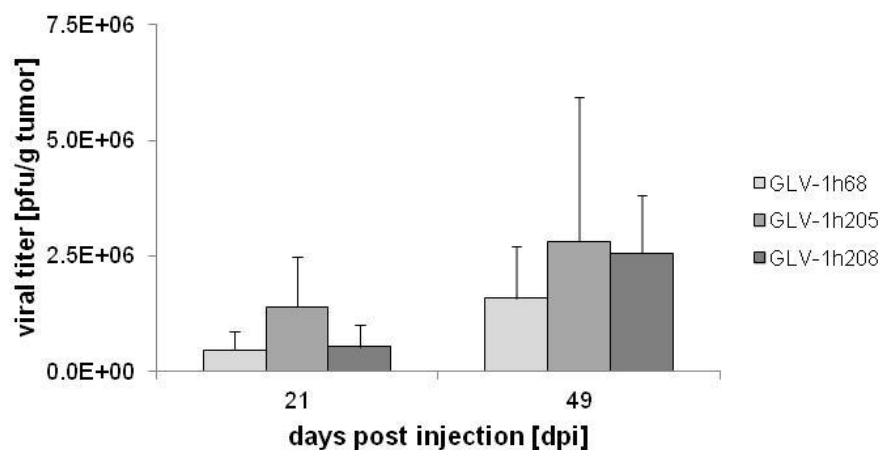


**Fig.4.19 – Viral titers in A549 tumors 21 and 49 dpi**

A549 tumor-bearing mice were sacrificed [n=4] at 21 and 49 days post virus treatment. Standard plaque assays from tumor lysates were performed and viral titers were determined and plotted as pfu / g tumor tissue.



## RESULTS

Figure 4.19 shows the viral distribution in infected A549 tumors in the late stage of the infection at 21 and 49 dpi, respectively. Viral titers at both time points were highest in the GLV-1h205-treated mice. Interestingly, a strong increase in GLV-1h208-treated mice was observed from day 21 to 49 post treatment while the titers of the parental strain GLV-1h68 did not increase to that extent.

**Tab.4.2 – Viral titers in A549 tumors and body organs 21 and 49 dpi**

Body organ (21 dpi)	GLV-1h68 (n=4)	GLV-1h205 (n=4)	GLV-1h208 (n=4)
Testes	n.d.	n.d.	n.d.
Spleen	4.64*10 <sup>1</sup> +/- 6.26*10 <sup>1</sup>	3.02*10 <sup>1</sup> +/- 4.86*10 <sup>1</sup>	1.50*10 <sup>1</sup> +/- 1.93*10 <sup>1</sup>
Liver	n.d.	n.d.	n.d.
Kidneys	n.d.	n.d.	n.d.
Lung	1.63*10 <sup>1</sup> +/- 3.26*10 <sup>1</sup>	4.15 +/- 8.30	n.d.
Tumor	8.73*10 <sup>5</sup> +/- 8.98*10 <sup>5</sup>	3.58*10 <sup>6</sup> +/- 3.66*10 <sup>6</sup>	6.27*10 <sup>5</sup> +/- 6.18*10 <sup>5</sup>

Body organ (49 dpi)	GLV-1h68 (n=4)	GLV-1h205 (n=4)	GLV-1h208 (n=4)
Testes	n.d.	8.08 +/- 1.62*10 <sup>1</sup>	n.d.
Spleen	1.80*10 <sup>1</sup> +/- 3.60*10 <sup>1</sup>	1.36*10 <sup>1</sup> +/- 2.71*10 <sup>1</sup>	3.09*10 <sup>1</sup> +/- 5.19*10 <sup>1</sup>
Liver	n.d.	n.d.	n.d.
Kidneys	n.d.	9.91*10 <sup>1</sup> +/- 1.98*10 <sup>2</sup>	n.d.
Lung	2.89*10 <sup>2</sup> +/- 5.78*10 <sup>2</sup>	1.16*10 <sup>2</sup> +/- 2.33*10 <sup>2</sup>	2.63*10 <sup>1</sup> +/- 5.25*10 <sup>1</sup>
Tumor	4.04*10 <sup>6</sup> +/- 3.58*10 <sup>6</sup>	2.23*10 <sup>6</sup> +/- 2.23*10 <sup>6</sup>	4.40*10 <sup>6</sup> +/- 3.41*10 <sup>6</sup>

Tumor-bearing mice were sacrificed 21 or 49 days post virus injection and standard plaque assays from tumor lysates and body organ lysates were performed to determine the virus titers in each treatment group. Virus titers are displayed as averaged total pfu / tissue with standard deviations. *n.d.* = not detectable (detection limit < 10 pfu / tumor)

Highest viral titers 21 and 49 days post treatment were found in primary tumors. Sporadic virus presence was detected in the testes, kidneys, spleens or lungs. Viral titers in body organs were found to be four- to five-log lower compared to primary tumors. Therefore, virus replication is exclusively confined to the tumor site and detection of viral particles in the body organs may be an indication for metastasis.

### 4.1.2.3 Histochemical analysis of vaccinia virus colonization in A549 mouse xenografts

To analyze the colonization of the primary tumor by oncolytic vaccinia viruses in more detail, animals were sacrificed after 49 days of treatment and the primary tumors were surgically removed. Tissue sectioning was performed as described in section 3.6.6. Sections were incubated with Phalloidin-TRITC as an indicator for live cell staining. Direct fluorescence was used for GFP detection as a tool to localize active virus as the half-life of GFP is 24 hours.

## RESULTS

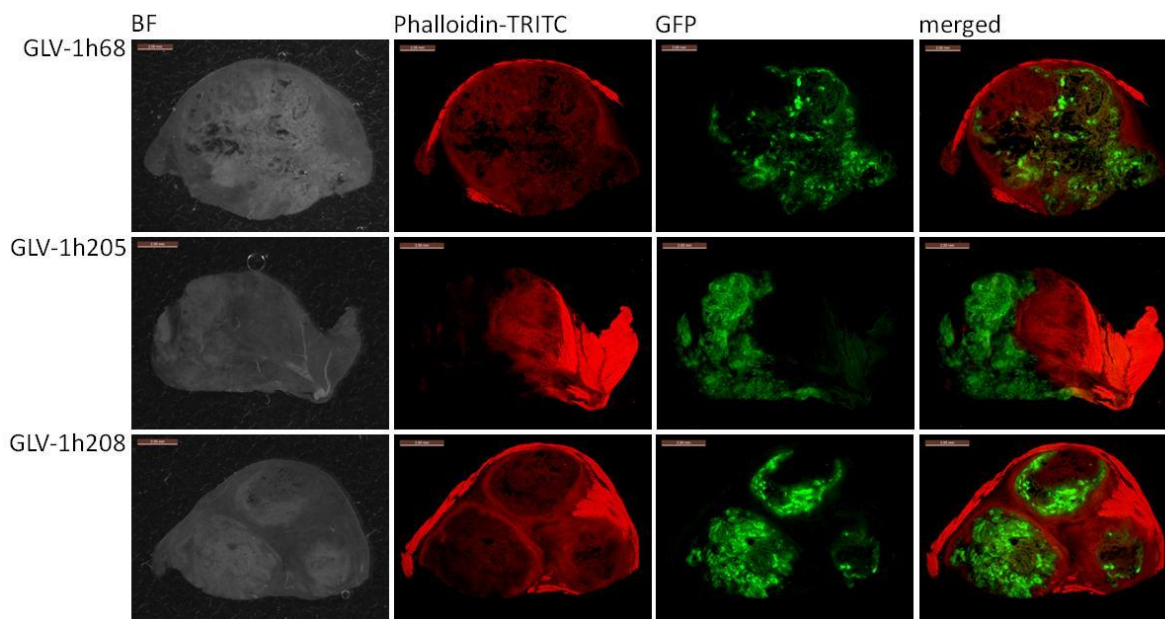


**Fig.4.20 – Immunohistochemical staining of A549 tumor xenografts**

A549 tumor-bearing mice were injected with different replication-competent vaccinia virus strains and sacrificed 49 days post treatment. Tumor sections were labeled with Phalloidin-TRITC for actin staining and then analyzed by fluorescence microscopy for actin filaments of virus-mediated GFP expression. Scale bars represent 2 mm. Large areas lacking actin staining indicate dead tumor tissue caused by oncolytic vaccinia virus.

Immunohistochemical studies of primary tumors dissected from A549 tumor-bearing mice that were treated with different oncolytic vaccinia virus strains 49 days post injection demonstrated that both new vaccinia virus strains GLV-1h205 and GLV-1h208 fully colonized the primary tumor in a similar manner to the parental strain GLV-1h68. Overlays of virus-mediated GFP-expression and Phalloidin-TRITC staining demonstrated the role of oncolytic vaccinia viruses in efficient destruction of tumor tissues.

#### **4.1.2.4 Immune-related antigen profiling of A549 tumor-bearing mice after administration of a single dose of replication-competent vaccinia virus strains**

To analyze the effect of vaccinia virus treatment *in vivo*, immune-related mouse antigen profiling was determined. For this purpose, animals were injected either with PBS alone or GLV-1h68, GLV-1h205 and GLV-1h208. Animals were sacrificed 10 days post injection when the replication potential of GLV-1h205 was stronger compared to GLV-1h208 or the parental control strain GLV-1h68. Tumor lysates were prepared as described in 3.6.4 and samples from three individual mice per group were sent out for analysis. Results were normalized and averaged and then up- and down-regulation against GLV-1h68 was analyzed.

## RESULTS

**Tab.4.3 – Normalized expression levels from immune-related antigen profiling in GLV-1h205/208 corrected against GLV-1h68**

Protein	GLV-1h205		GLV-1h208	
	upregulation	downregulation	upregulation	downregulation
Apolipoprotein A1				1.55
CD40		2.01		4.25
Eotaxin	1.97			
Granulocyte Chemotactic Protein-2				2.38
Interferon gamma Induced Protein 10		2.05		2.36
Interleukin-6	2.28			
Interleukin-11	2.30			
Macrophage Inflammatory Protein-3 beta		2.07		1.90
Macrophage-Derived Chemokine				2.08
Matrix Metalloprotease 9				2.73
Monocyte Chemotactic Protein-1				2.63
Monocyte Chemotactic Protein-3				2.31
Monocyte Chemotactic Protein-5				3.54
Tissue Inhibitor of Metalloproteases 1	2.25			

A549 tumors [n=3 per group] were surgically removed and prepared for antigen profiling. Results were normalized and then corrected against GLV-1h68 expression levels to analyze up- and down-regulation.

The immune-related antigen profiling revealed that infection with oncolytic vaccinia virus strains led to an up-regulation of most of the tested immune-related proteins compared to untreated mice. The majority of the tested proteins were pro-inflammatory cytokines or chemokines, such as IP-10, IL-6, M-CSF, MCP-1, MCP-3, MCP-5 or RANTES. Known players in pro-inflammatory stimulation, antiviral effect and tumor growth control like IFN-gamma or TNF-alpha were also found to be up-regulated. Additionally, as presented in table 4.3, differences in up- and down-regulation of the new recombinant vaccinia viruses in comparison to the parental GLV-1h68 was analyzed. Faster virus replication as observed in GLV-1h205-treated tumors led to a slight up-regulation of eotaxin, IL-6, IL-11 and TIMP-1 compared to the parental GLV-1h68. Slower viral replication as observed in GLV-1h208 was correlated to down-regulation of CD40, GCP-2, IP-10, MMP-9, MCP-1, MCP-3, and MCP-5, among other immune-related antigens.

### 4.1.3 Characterization of a Nanog $\Delta$ NLS mutant virus

The Nanog-expressing vaccinia virus strain GLV-1h205 showed enhanced therapeutic efficacy and superior replication behavior compared to the parental strain GLV-1h68 in A549 non-small cell lung carcinoma tumor-bearing mice. However, while GLV-1h68 expresses *gusA* under the P11 promoter, GLV-1h205 expresses *nanog* under the weaker synthetic early promoter. Therefore, to analyze if improved therapeutic efficacy of GLV-1h68 is

## RESULTS

payload- or promoter-driven, a non-functional Nanog-expressing replication-competent vaccinia virus was constructed (GLV-1h321). A mutation in the NLS sequence from an YKQVKT to a LPHGGS amino acid sequence was cloned into the original *nanog* sequence to render the protein incapable to enter the nucleus and exert its function as a transcription factor. This creates a control virus that expresses a gene product of the same length with the same promoter strength but encodes for a non-functional protein. GLV-1h321 was used to analyze whether enhanced therapeutic effect was payload-driven.

### 4.1.3.1 Analysis of viral replication rate of GLV-1h321 in the cancer cell line A549

After generation of the new recombinant virus GLV-1h321, the replication capability of the virus in cancer cells was investigated in comparison to the parental virus strain GLV-1h68 and GLV-1h205. Replication rate was analyzed in A549 cells in culture. For the analysis of replication rates, cells were infected with an initial MOI of 0.1 and viral titers were determined at 6, 24, and 48 hours post infection. The initial infection medium was used as initial virus titer at 0 hours post infection. The replication factor was determined as described in section 4.1.1.1. Viral titers were determined by standard plaque assay. Averaged data from triplicates including standard deviation are shown for GLV-1h321 in comparison to GLV-1h68 and GLV-1h205.

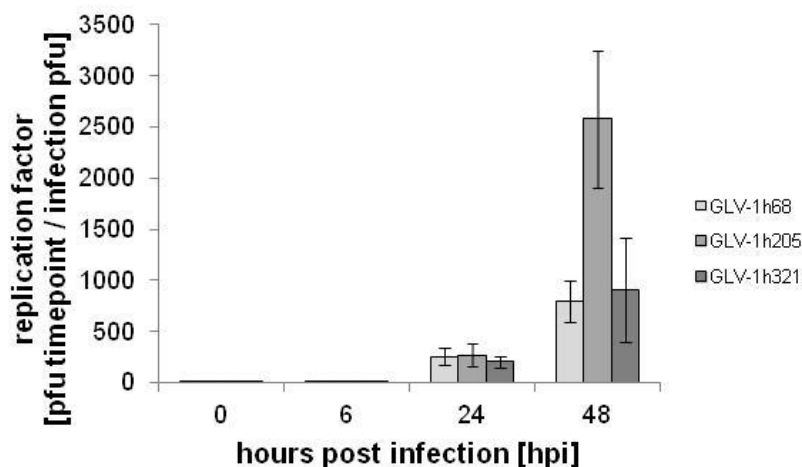


**Fig.4.21 – Viral replication factor of GLV-1h321 compared to GLV-1h68 and GLV-1h205 in A549 cells**

Cells were infected at an MOI of 0.1 and samples were collected at various times after infection. Titers were averaged from triplicates and plotted with standard deviations.

The new recombinant vaccinia virus GLV-1h321 efficiently infects A549 cells and replicated in them. The replication behavior of GLV-1h321 was identical to the parental GLV-1h68 and the replication rate is not as high as observed for GLV-1h205 (Fig.4.3). This suggests that

## RESULTS

the mutation of the *nanog* nuclear localization sequence negatively affects replication behavior of GLV-1h321 compared to GLV-1h205.

### 4.1.3.2 Analysis of recombinant protein expression in mammalian cells infected with GLV-1h321

#### 4.1.3.2.1 Analysis of beta-galactosidase expression in infected mammalian cells

Next, efficacy of functional marker gene expression in GLV-1h321-infected A549 cells was tested. For beta-galactosidase expression, cells were infected at an MOI of 0.01 for 24 hours to obtain single, isolated plaques. Cells were then treated with a substrate that is converted into a blue dye by beta-galactosidase and observed under the light microscope. Therefore, infected cells that express functional beta-galactosidase protein appear as blue plaques under the microscope.

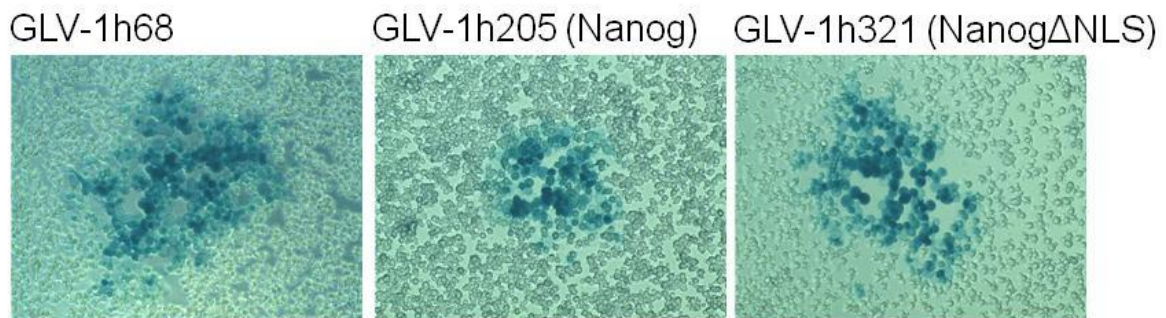


**Fig.4.22 – Expression of beta-galactosidase in infected A549 cells**

A549 cells were infected at an MOI of 0.01 to obtain single, isolated plaques and stained for beta-galactosidase expression. The recombinant virus strains GLV-1h205 and GLV-1h321 both express functional beta-galactosidase. Pictures were taken at a 100x magnification.

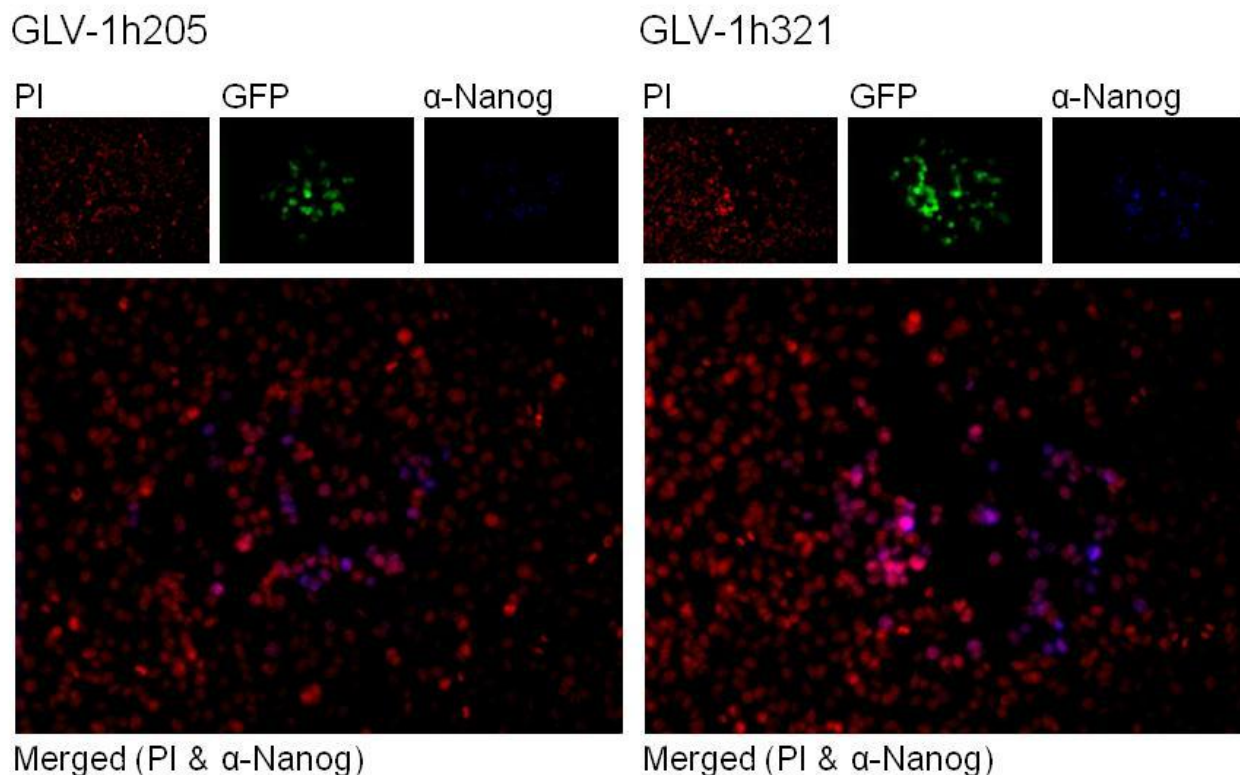
After confirmation of efficient replication of the new virus strain, efficacy of functional protein expression of marker genes and transcription factor Nanog and in infected mammalian cell cultures was analyzed. For beta-galactosidase expression, A549 cells were infected at an MOI of 0.01 for 24 hours to obtain single, isolated plaques. Cells were then treated with a substrate that is converted into a blue dye by beta-galactosidase and observed under the light microscope. Therefore, infected cells that express functional beta-galactosidase protein appear as blue plaques under the microscope.

#### 4.1.3.2.2 Analysis of Ruc-GFP and Nanog expression in infected mammalian cells by immunocytochemistry

For detection of Ruc-GFP fusion protein and Nanog expression, A549 cells were infected at an MOI of 0.01 to obtain single, isolated plaques. Cells were then fixed and permeabilized to allow antibody binding. For detection of Nanog, cells were incubated with a polyclonal rabbit-anti-Nanog antibody and a AlexaFluor350-labeled secondary anti-rabbit antibody. To

## RESULTS

analyze the cellular location of Nanog, cell nuclei were stained with propidium iodide. Monochromal images were taken with a digital CCD camera and pseudo-colored using the open-source software GIMP 2.6. Expression of functional *Renilla* luciferase-green fluorescent protein fusion protein was detected by direct fluorescence microscopy. GLV-1h205 was used as a control virus which is positive for Ruc-GFP and Nanog expression.



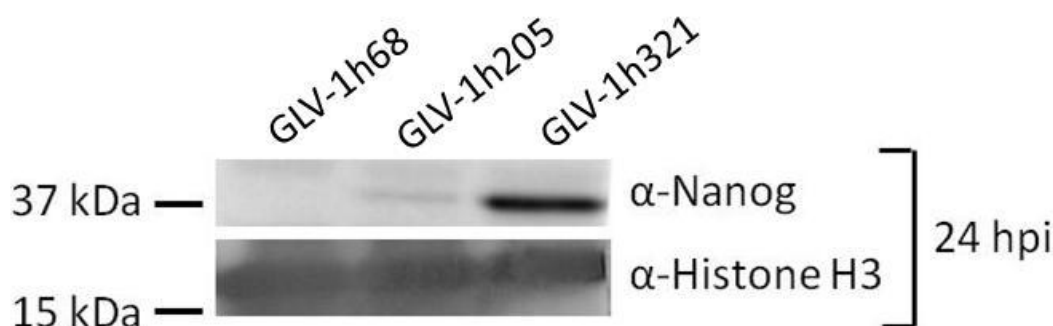
**Fig.4.23 – Analysis of Nanog and GFP expression in A549 cells infected with GLV-1h205 and GLV-1h321** A549 cells were infected at an MOI of 0.01 with GLV-1h205 and GLV-1h321 to obtain single, isolated plaques. Cells were then fixed, permeabilized and incubated with a primary polyclonal rabbit-anti-Nanog antibody (1:500 dilution). Subsequently, cells were stained with an AlexaFluor350-conjugated secondary antibody (1:500) and GFP and Nanog expression was analyzed. Pictures were taken with a digital CCD camera and an inverted fluorescence microscope and pseudo-colored and edited using the open-source software GIMP2.6 Pictures were taken at 200x magnification.

Figure 4.23 shows the expression of viral Ruc-GFP fusion protein in both, GLV-1h205- and GLV-1h321 infected A549 cells in culture. Also, Nanog expression was observed in both, A549 cells infected with GLV-1h205 and GLV-1h321. While Nanog was transported back in the nucleus of the infected cells after translation in the cytoplasm in A549 cells infected with GLV-1h205, the detection of Nanog in GLV-1h321-infected cells was more diffuse. In some cells the Nanog signal overlapped with the GFP signal, indicating primary location of Nanog $\Delta$ NLS in the cytoplasm. However, in some cells the Nanog $\Delta$ NLS overlapped with the nuclear propidium iodide staining. It could not be determined if the Nanog mutant protein was actively transported into the nucleus or held back at the nuclear membranes.

## RESULTS

### 4.1.3.2.3 Analysis of Nanog expression in infected mammalian cells by Western blot

To further analyze the protein expression of human Nanog in virus infected cells, Western blot analysis was performed. A549 cells were infected with GLV-1h68 as a negative control or GLV-1h205 and GLV-1h321 at an MOI of 5.0 to synchronize the infection. Infected cells were incubated for 24 hours and harvested subsequently. Samples were processed and total protein amounts were determined. For Western blot analysis, 20 µg total proteins per sample were used. SDS-PAGE and Western blotting was performed prior to antibody binding. Histone H3 antibodies were used as a loading control and Nanog antibodies for detection of the recombinant viral gene products. The blot was developed by colorimetric detection. Histone H3 has a predicted molecular mass of 15 kDa while the band can be detected around 17 kDa. The predicted molecular mass of Nanog is 38 kDa while the protein band can be detected around 42 kDa.



**Fig.4.24 – Western blot analysis of human Nanog and Nanog $\Delta$ NLS in infected A549 cells**

A549 cells were either infected with GLV-1h68, Nanog-expressing GLV-1h205 or Nanog $\Delta$ NLS-expressing GLV-1h321 at an MOI of 5.0 for 24 hours. Samples were harvested and processed for Western blot analysis. The primary Nanog antibody was used at a dilution of 1:2000 while the primary Histone H3 antibody was used at a dilution of 1:5000 due to its high abundance. The blot was visualized by colorimetric detection.

As seen in Fig.4.24, both, GLV-1h205- and GLV-1h321-infected A549 cells contained detectable levels of human Nanog whereas no Nanog was detectable in GLV-1h68-infected cells. Therefore, Nanog and Nanog $\Delta$ NLS expression was confined to infection with GLV-1h205 and GLV-1h321, respectively. However, detected amounts of Nanog $\Delta$ NLS were much higher compared to normal Nanog in GLV-1h205-infected cells when comparable total protein amounts were loaded. This can be related either to easier release of Nanog $\Delta$ NLS due to its accessibility in the cytoplasm as compared to nuclear located Nanog, protein stability, or to higher protein amounts because more virus-infected cells produce Nanog $\Delta$ NLS because of higher virus purity.

## RESULTS

### 4.1.3.3 Analysis of cell viability of mammalian cells infected with GLV-1h321

To analyze whether the expression of Nanog $\Delta$ NLS affects the cytotoxic potential of GLV-1h321 in comparison to the parental GLV-1h68 and GLV-h205, A549 cells were seeded to confluence of 95% and either mock-infected or infected with GLV-1h205 and GLV-1h321. As a reference, infection with GLV-1h68 was used as a control. Cells were infected at an MOI of 1.0 and the infection was followed for 72 hours. Samples were analyzed 1, 24, 48, and 72 hours post infection.

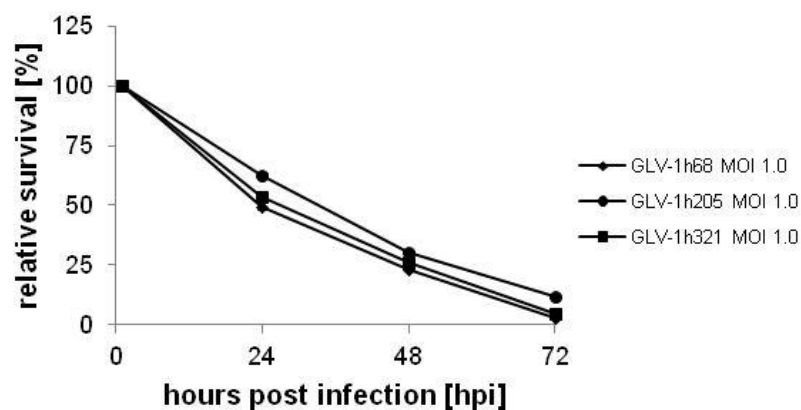


**Fig.4.25 – Viability of A549 cells after infection with GLV-1h68, GLV-1h205, and GLV-1h321**

Analysis of cell viability of A549 cells after infection with replication-competent vaccinia viruses GLV-1h68, GLV-1h205 and GLV-1h321, using an MOI of 1.0. Viability was monitored over the course of 72 hours and was measured in triplicates and averaged. Plotted averages are normalized against uninfected controls of each time-point which were considered to be 100% viable.

Figure 4.25 shows efficient cell killing of A549 cells by all three tested vaccinia viruses. The parental strain GLV-1h68 was used as a reference for the cytotoxic potential of the new recombinant strains GLV-1h205 and GLV-1h321. After 72 hours, only  $2.85 \pm 0.26\%$  of the cells infected with GLV-1h68 were still viable. Both other tested strains also showed efficient cell killing over the course of 72 hours ( $11.58 \pm 0.36\%$  in GLV-1h205-infected cells and  $4.50 \pm 0.27\%$  in GLV-1h321-infected cells). Lower cytotoxic potential of GLV-1h205 can possibly be related to a lower initial infection pfu compared to GLV-1h68 and GLV-1h321 as the oncolytic potential was shown to be higher compared to GLV-1h68 before. Overall, it was demonstrated that the new recombinant vaccinia virus GLV-1h321 efficiently infects, replicates in, and ultimately lyses A549 cells in a similar manner to the parental strain GLV-1h68.



## RESULTS

### 4.1.3.4 Effects of a single dose of GLV-1h205 or GLV-1h321 in subcutaneous A549 xenografts

To analyze if the observed therapeutic benefit in tumor regression of GLV-1h205-treated A549 tumors is payload-driven, 20 male athymic nude FoxN1 mice at an age of 4-5 weeks were subcutaneously implanted with  $5 \times 10^6$  A549 cells in 100  $\mu$ L PBS. All animals developed tumors with volumes around 250 to 300 mm<sup>3</sup> after two weeks of implantation. Animals were separated into different treatment groups of five (n=5) with similar tumor volumes before virus treatment. Animals in the groups were then injected retro-orbitally (r.o.) with 100  $\mu$ L PBS or  $2 \times 10^6$  pfu of either GLV-1h68 as a reference for oncolytic treatment, GLV-1h205 or GLV-1h321. Tumor size was measured with a digital caliper two times a week for all animals until 49 days post injection. Actual tumor volumes were divided by initial tumor volumes to acquire fractional tumor volumes (FTVs). FTVs were averaged and plotted with standard deviations.

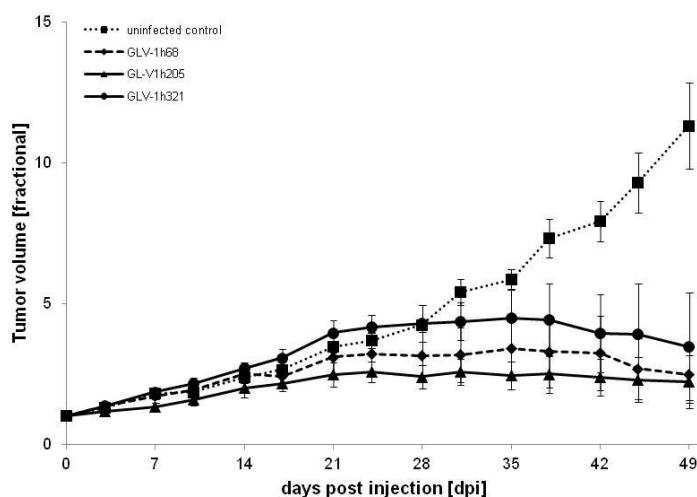


**Fig.4.26 – Effects of recombinant vaccinia viruses GLV-1h68, GLV-1h205 and GLV-1h321 on A549 tumor growth in subcutaneous mouse xenografts**

Tumor-bearing mice (n=5) were injected (r.o.) with PBS or  $2 \times 10^6$  pfu of GLV-1h68, GLV-1h205 or GLV-1h321. Tumor growth was followed twice a week for 49 days. FTV was plotted with standard deviations as an average of all mice per group. One-way analysis of variance (ANOVA) was used to compare the corresponding data points.

The results presented in figure 4.26 confirm the initial finding that GLV-1h205 treatment is more beneficial in A549 tumor-bearing mice than treatment with the parental strain GLV-1h68. Due to the fact that tumors never grew more than  $2.56 \pm 0.45$ -fold bigger than the original tumor volume, tumor growth inhibition rather than regression was observed for GLV-1h205-treated animals. Both control virus strains, GLV-1h68 and GLV-1h321 showed overall bigger tumors and higher variability in treatment efficacy. The differences in tumor volumes

## RESULTS

of GLV-1h205- and GLV-1h321-treated groups became statistically significant after 17 days of treatment. While showing identical replication in cell culture, overall treatment of GLV-1h321 in A549 mouse xenografts showed to be less favorable than treatment with the parental virus strain GLV-1h68. This is a strong indication that the observed increased therapeutic efficacy of GLV-1h205 is rather driven by its Nanog payload than only by faster promoter strength-mediated virus replication.

### 4.1.3.5 Pfu determination in A549 tumor-bearing mice injected with GLV-1h68, GLV-1h205, and GLV-1h321 at various time points

The viral distribution in the A549 tumors of five animals per treatment group was analyzed at 14 days and 49 days post virus injection, respectively. Animals were sacrificed and tumors surgically removed. Virus titers were determined by standard plaque assays from tumor lysates. Viral titers were determined to analyze whether treatment efficacy is correlated to virus replication.

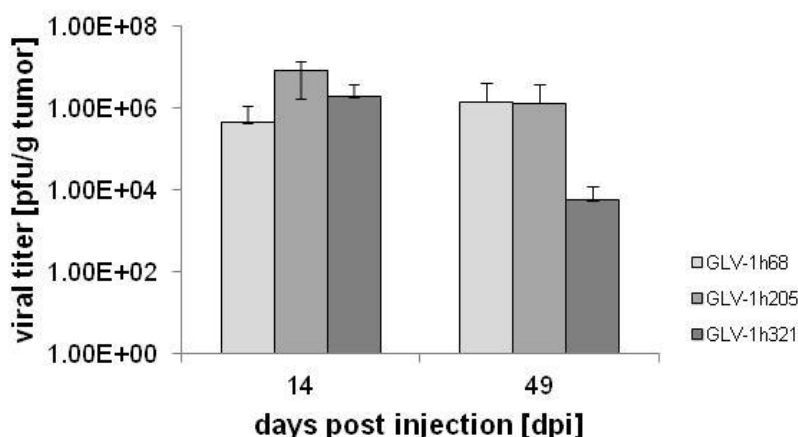


**Fig.4.27 – Viral distribution in A549 tumor-bearing mice injected at 14 and 49 dpi**

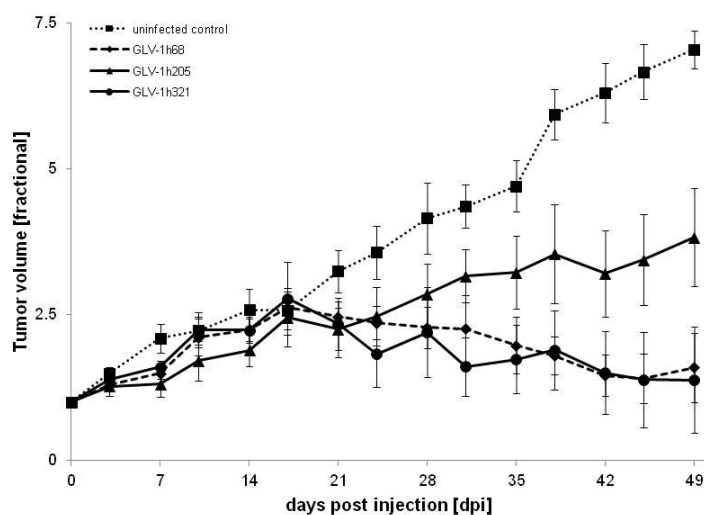
A549 tumor-bearing mice were sacrificed [n=4] at 21 and 49 days post virus treatment. Standard plaque assays from tumor lysates were performed and viral titers were determined and plotted as pfu/g tumor tissue.

Figure 4.27 shows that viral titers were highest in the GLV-1h205 treatment group 14 days post injection when compared to the two control virus strains GLV-1h68 and GLV-1h321. Virus titers in the GLV-1h321 treatment group decreased significantly from 14 to 49 days post injection while titers in GLV-1h205- and GLV-1h68-treated animals remained relatively high. The observed differences of viral replication in the primary tumor site can be correlated to overall treatment efficacy.

## RESULTS

### 4.1.3.6 Effects of a single dose of GLV-1h205 or GLV-1h321 in subcutaneous DU-145 xenografts

To analyze if the observed therapeutic benefit in tumor regression of A549 tumors is a general feature of the virus strain GLV-1h205 or tumor model-dependent, 20 male athymic nude FoxN1 mice at an age of 4-5 weeks were subcutaneously implanted with  $5 \times 10^6$  DU-145 cells in 100  $\mu$ L PBS. All animals developed tumors with volumes around 250 to 300  $\text{mm}^3$  after two weeks of implantation. Animals were separated into different treatment groups of five ( $n=5$ ) with similar tumor volumes before virus treatment. Animals in the groups were then injected retro-orbitally (r.o.) with 100  $\mu$ L PBS or  $2 \times 10^6$  pfu of either GLV-1h68 as a reference for oncolytic treatment, GLV-1h205 or GLV-1h321. Tumor size was measured with a digital caliper two times a week for all animals until 49 days post injection. Actual tumor volumes were divided by initial tumor volumes to acquire fractional tumor volumes (FTVs). FTVs were averaged and plotted with standard deviations.



**Fig.4.28 – Effects of recombinant vaccinia viruses GLV-1h68, GLV-1h205 and GLV-1h321 on DU-145 tumor growth in subcutaneous mouse xenografts**

Tumor-bearing mice ( $n=5$ ) were injected (r.o.) with PBS or  $2 \times 10^6$  pfu of GLV-1h68, GLV-1h205 or GLV-1h321. Tumor growth was followed twice a week for 49 days. FTV was plotted with standard deviations as an average of all mice per group. One-way analysis of variance (ANOVA) was used to compare the corresponding data points.

The data presented in figure 4.28 shows that both control viruses, the parental GLV-1h68 and the NANOG $\Delta$ NLS-encoding GLV-1h321 showed similarly efficient tumor regression from 21 days post virus injection on. Treatment with GLV-1h205 however only lead to significantly slower tumor growth compared to untreated animals. Using the same treatment conditions, both control viruses were significantly more effective in treating DU-145 tumors than GLV-1h205, which is contrary to findings in the A549 mouse xenograft model.

## RESULTS

Differences in tumor volumes between GLV-1h205- and GLV-1h321-treated animals became statistically significant after 31 days of virus injection. This experiment indicates that treatment efficacy of GLV-1h205 is in fact cell line-dependent.

### 4.2 Oncolytic virotherapy as a treatment of colorectal cancer

#### 4.2.1 Efficacy of GLV-1h68 in colorectal cancer therapy

Common treatment regimens for colorectal cancer include surgical excision of primary tumors in the gastrointestinal tract and combination of surgery and chemotherapeutic agents. Overall survival prognoses are good when the cancer is treated during stage I or II. However, stage III colon cancer is still correlated with a poor prognosis and stage IV colorectal cancer is terminal without proper treatment regimens. Lately, the oncolytic vaccinia virus GLV-1h68 was shown to colonize lymph node metastases in a PC3-RFP xenograft mouse model. The virus' ability to specifically target and destroy distant metastatic sites in a living organism might open new treatment possibilities for late stage colorectal cancer.

##### 4.2.1.1 Replication of GLV-1h68 in different human colorectal cancer lines in culture

To test the replication efficacy of recombinant vaccinia virus GLV-1h68 in different human colorectal cancer lines, cells were grown to 95% confluence and then infected at an MOI of 0.1 and viral titers were determined at 6, 24, 48, 72, and 96 hours post infection. The initial infection medium was used as initial virus titer at 0 hours post infection. Viral titers were determined by standard plaque assay. Average data including standard deviation are shown for GLV-1h68 in Colo 205, HCT-15, HCT-116, HT-29 and SW-620.

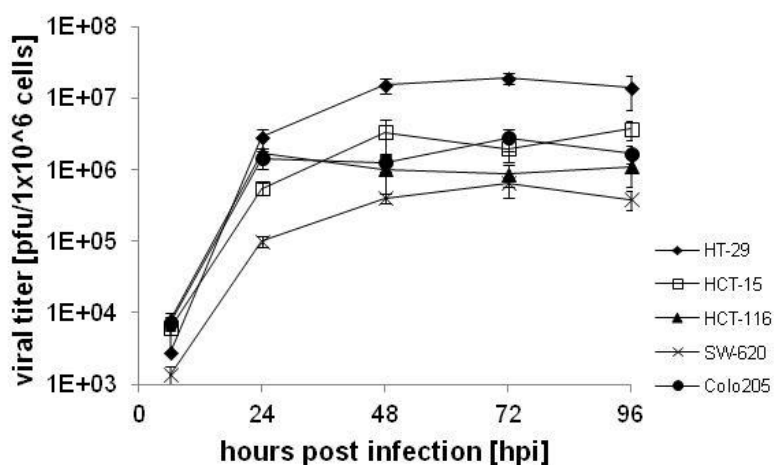


**Fig.4.29 - Analysis of viral titers after infection of five different colorectal cancer lines with GLV-1h68 in culture.**

Cells were infected at an MOI of 0.1 and samples were collected at various times after infection. Titers were averaged from triplicates and normalized to pfu/1x10<sup>6</sup> cells. Averages plus standard deviations were plotted.

## RESULTS

As a result, figure 4.29 shows that GLV-1h68 replicated in all five tested cell lines. Replication efficiency was depending on the infected cell line and high titers after 24 hpi were found in HT-29, HCT-116 and Colo 205 cells while titers were lowest in SW-620. Titers in all tested cell lines peaked after 48 to 72 hours post infection ( $1.91 \times 10^7$  pfu/ $10^6$  cells in infected HT-29 cells and  $6.58 \times 10^5$  pfu/ $10^6$  cells in SW-620), except for HCT-116 and Colo 205, which peaked 24 hours post infection.

### 4.2.1.2 Cytotoxicity of GLV-1h68 in different colorectal cancer lines in culture

To assess whether cell lysis of colorectal cancer cells upon viral infection can be observed and affects viral yields, cell viability assays were performed. All five human colorectal cancer lines were infected in culture with MOIs of 0.1 and 1.0 and the infection was followed for 72 hours. Samples were analyzed 0, 24, 48, and 72 hours post infection.

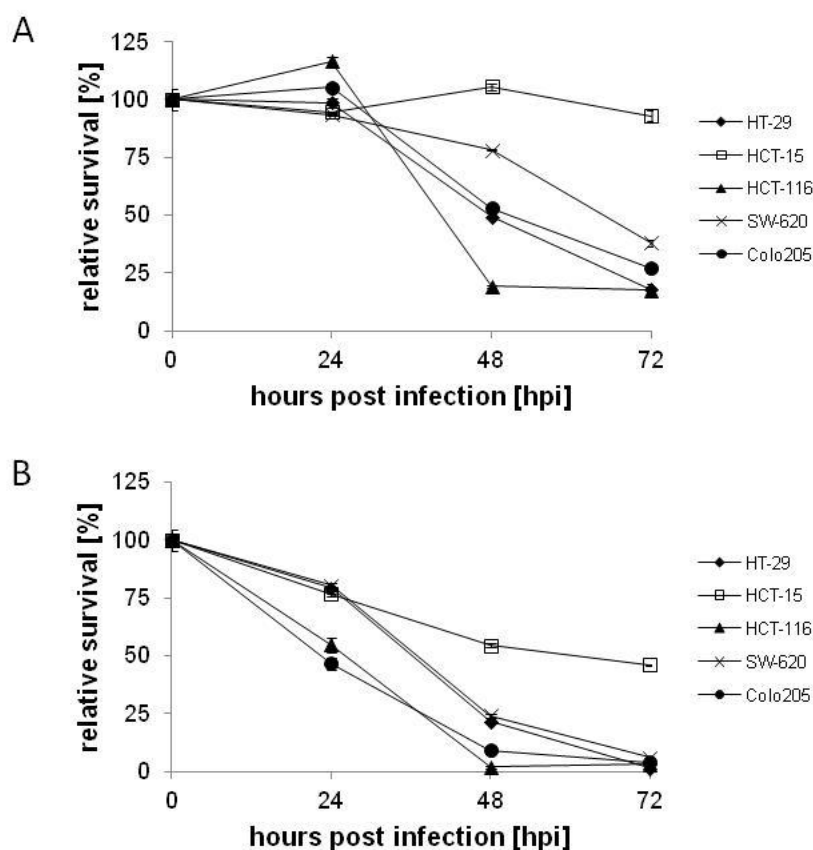


**Fig.4.30 - Cell viability of human colorectal cancer lines after GLV-1h68 infection**

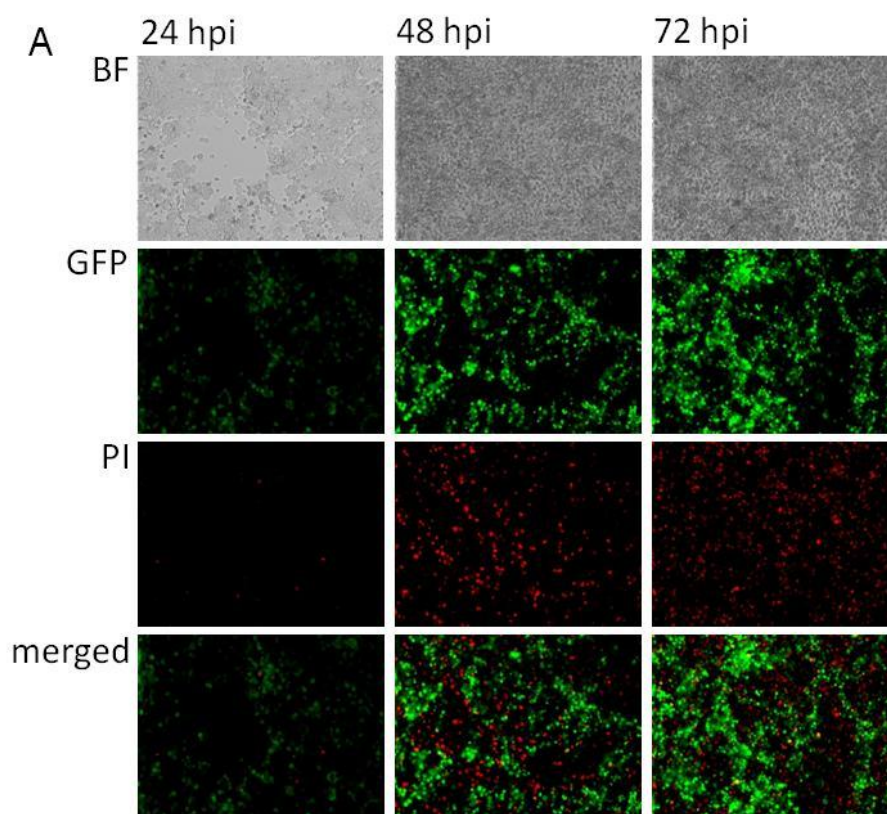
Cells were infected in culture at MOIs of 0.1 (A) and 1.0 (B), respectively, and monitored over a time course of 72 hours. Viability was measured in two sets of triplicates and averaged. Plotted averages are normalized against uninfected controls of each time-point which were considered to be 100% viable.

## RESULTS

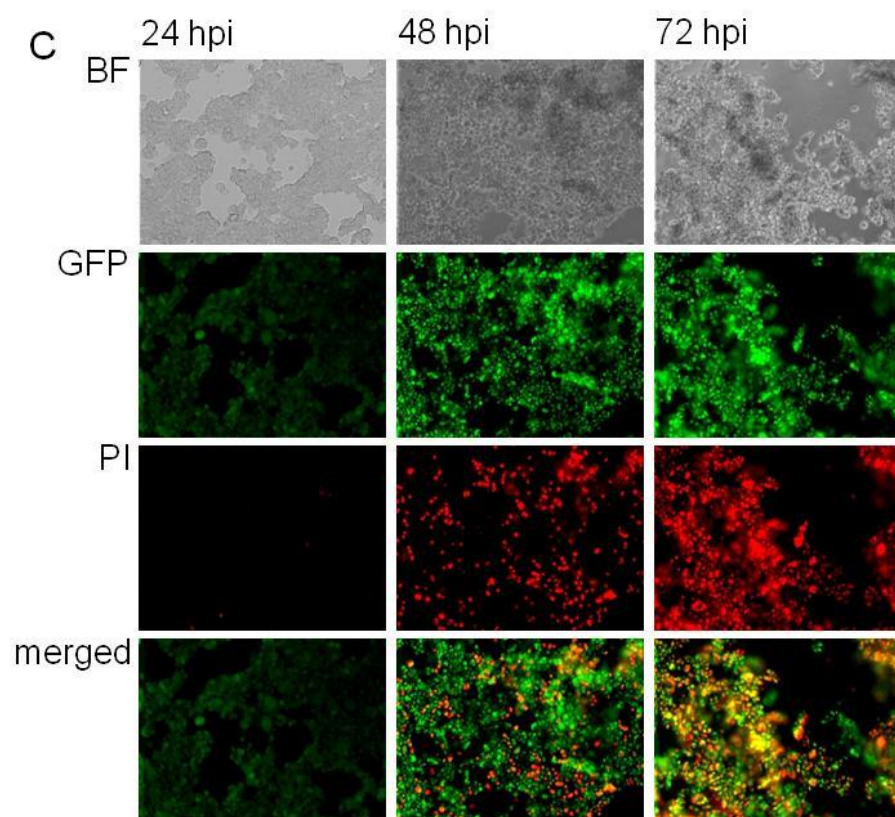
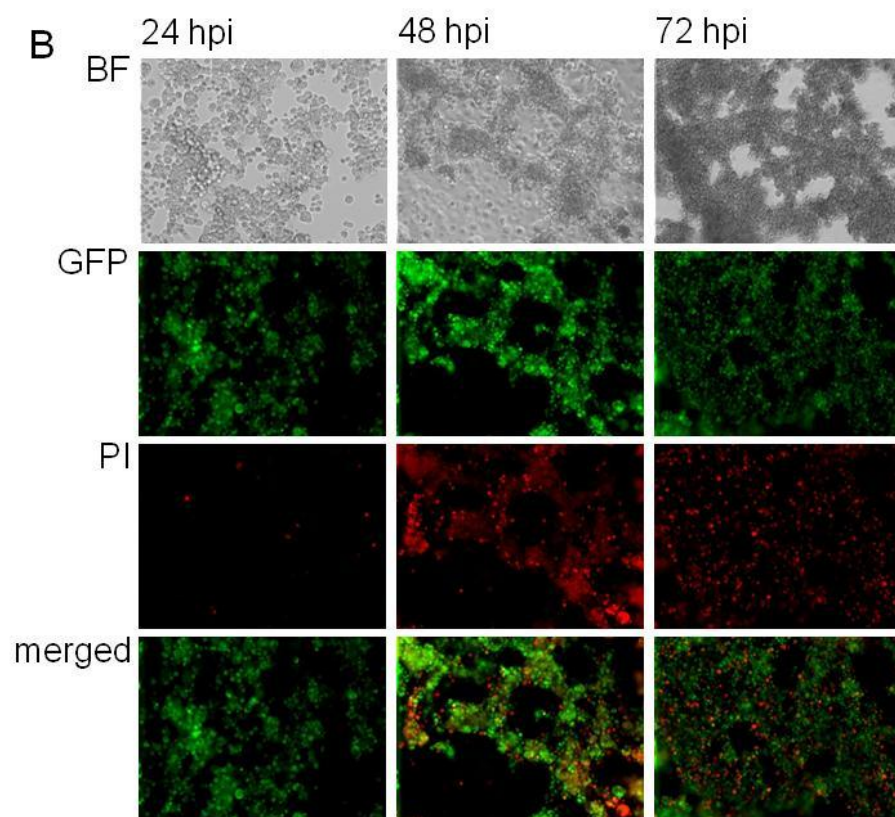
As presented in figure 4.30, in both settings, GLV-1h68 displayed the most efficient cytotoxicity in HCT-116 and was least cytotoxic in HCT-15 cells. After 48 hours of infection only  $19.2 \pm 0.7\%$  (MOI 0.1) and  $1.8 \pm 0.8\%$  (MOI 1.0), respectively, of HCT-116 remained viable. GLV-1h68 showed efficient cytotoxicity in HT-29 and SW-620 cells after 72 hours post infection. A MOI-dependent effect was clearly observable during the course of infection.

### 4.2.1.3 Analysis of viral replication and cytotoxicity on infected host cells using virus-mediated marker gene expression

To confirm that GLV-1h68 infects CRCs and viral replication eventually causes cell death, the expression of viral marker gene *ruc-gfp* in infected CRCs was observed by direct fluorescence microscopy. A count of  $5 \times 10^5$  cells was infected with GLV-1h68 at an MOI of 1.0 and cell morphology changes were followed in bright field pictures over the course of 72 hours (upper row). Ruc-GFP expression (second row) was used as a marker for viral gene expression. Propidium iodide staining (third row) was used to monitor cell death. The colorectal cell lines HCT-15, HCT-116, HT-29 and SW-620 were tested.



## RESULTS



## RESULTS

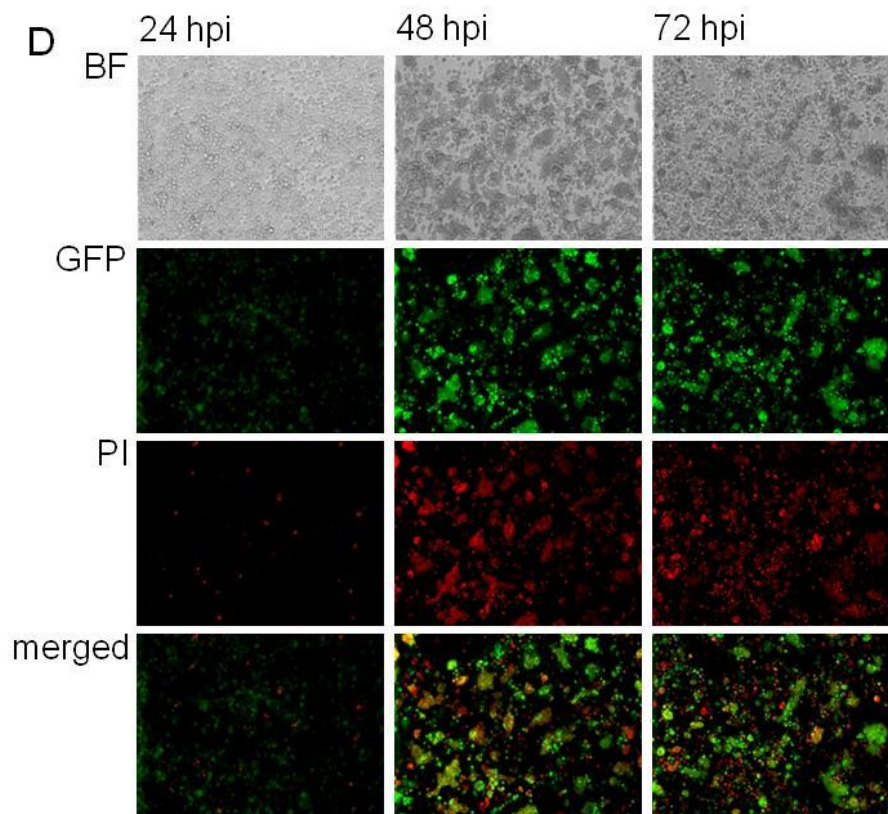


**Fig.4.31 - Fluorescence microscopy of viral marker-gene expression of *Renilla* luciferase-green fluorescent protein in CRC cell lines at an MOI of 1.0 a time-dependent manner.**

The four colorectal cancer lines HCT-15 (A), HCT-116 (B), HT-29 (C), and SW-620 (D) were infected in culture with GLV-1h68. (BF) shows bright field pictures of the morphology of virus-infected cells. (GFP) expression in infected cells was visualized by direct fluorescence; propidium iodide (PI) was used as a marker for dead cells. Colocalization of (GFP) and (PI) signal is shown in the (merged) images. All pictures were taken at 40x magnification.

Efficient infection, replication and gene expression could be observed (Fig.4.31) in a time-dependent manner during the course of infection as cell death upon viral infection increased over time following Ruc-GFP expression. The HCT-116 line was most susceptible to viral replication and cell killing, followed by HT-29 and SW-620. HCT-15 cells proved to be most resistant to viral replication and cell killing. The obtained data confirmed findings from the cell viability assays.

Furthermore, flow cytometry analysis of GLV-1h68 infected cells was performed to quantify the amount of infected (Ruc-GFP expression) and dead cells (propidium iodide staining). For the analysis,  $5 \times 10^5$  cells were infected in triplicates in culture with GLV-1h68 at MOIs of 0.1 and 1.0, respectively. Infection and cell death was monitored at 24, 48, and 72 hpi.



## RESULTS

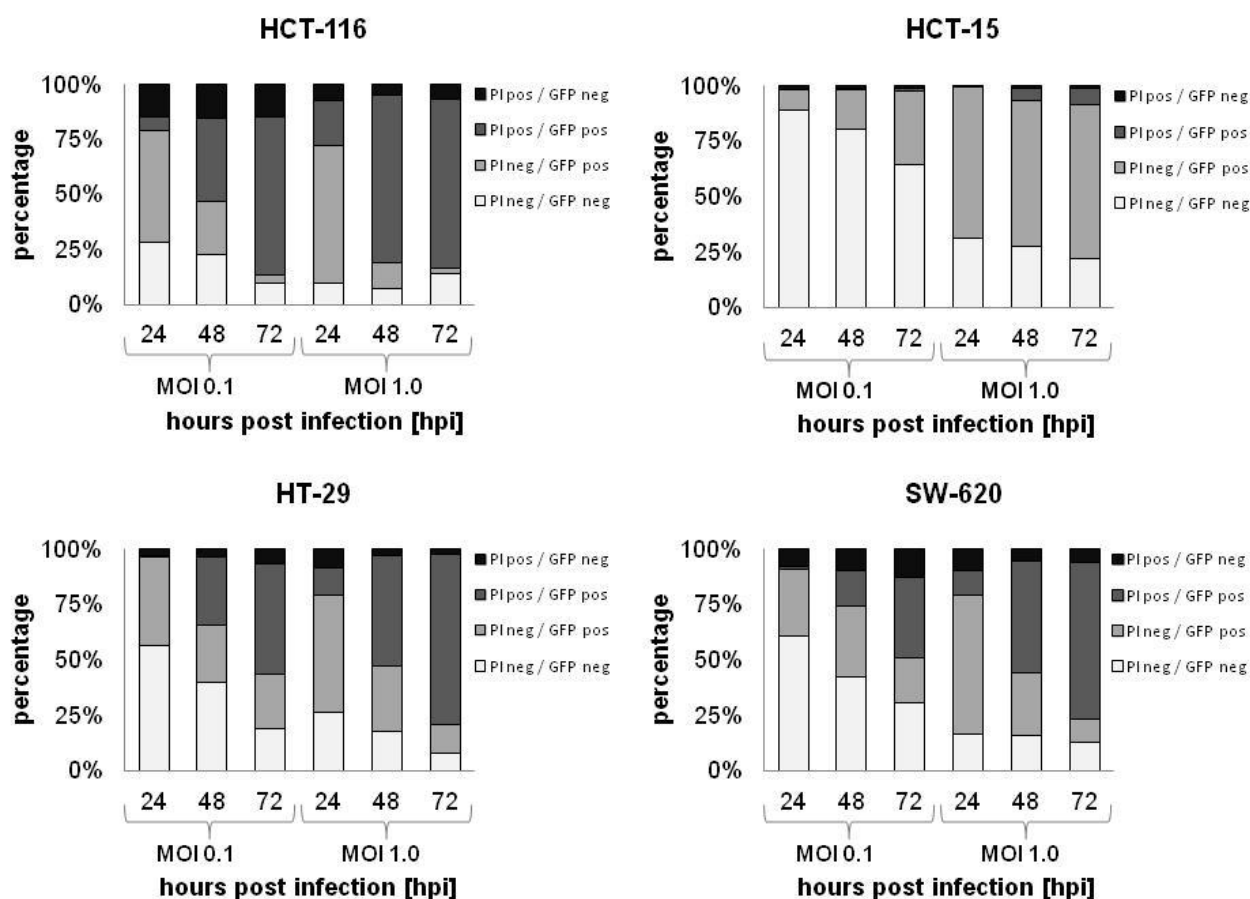


**Fig.4.32 - Flow cytometry analysis of GLV-1h68-infection in various colorectal cancer lines**

CRCs were infected with GLV-1h68 at MOIs of 0.1 and 1.0, respectively. Data represents average distribution of uninfected/infected [GFP neg/pos] and viable/dead [PI neg/pos] cells over the course of 72 hours.

FACS analysis confirmed the efficacy of GLV-1h68 to infect, replicate in and ultimately lyse human colorectal cancer cells in culture (Fig.4.32). GLV-1h68 showed highest efficacy of replication and cytotoxicity in HCT-116, followed by HT-29 and SW-620 and was least effective in HCT-15 cells. A MOI-dependent and cell line-dependent effect of infectivity and viability was observed between different colorectal cancer lines in culture. Taken together, the data obtained from cell culture experiments suggests that GLV-1h68 can be a powerful tool in treatment of colorectal cancers.

### 4.2.1.4 Effects of a single dose of GLV-1h68 in subcutaneous CRC xenografts

After demonstrating the ability of oncolytic vaccinia virus GLV-1h68 to efficiently infect, replicate in, and lyse colon cancer cells in culture, next the efficacy of GLV-1h68 to target colon cancer and its therapeutic effect in a HCT-116 mouse xenograft model was examined. For this purpose, athymic nude mice were subcutaneously implanted with  $5 \times 10^6$  HCT-116 cells. HCT-116 tumor-bearing mice were injected either with  $5 \times 10^6$  pfu of GLV-1h68 (n=10)

## RESULTS

or PBS only (n=5) when the tumor volume reached an average of 250 mm<sup>3</sup>. Tumor volume was measured twice a week with a digital caliper.

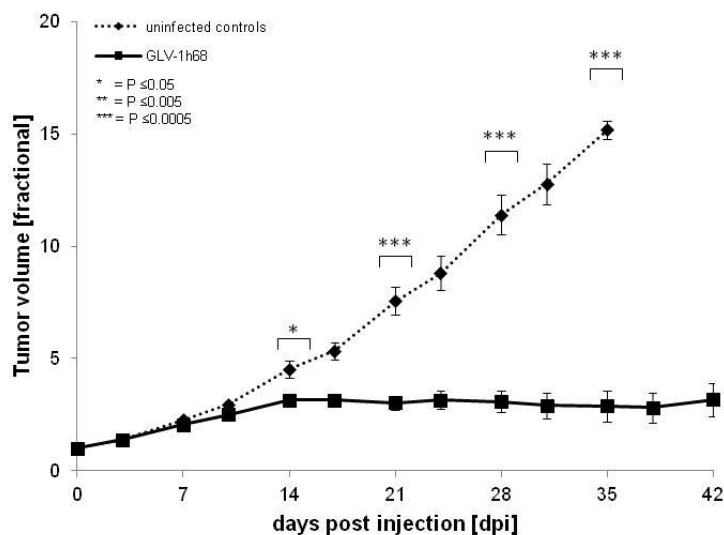


**Fig.4.33 - Effects of a single administration of 5x10<sup>6</sup> pfu/100 µl PBS on tumor development of HCT-116 tumor-bearing mice**

HCT-116 cells were implanted subcutaneously in the right hind leg of athymic nude mice and virus treatment was tested versus PBS treatment. Averaged fractional tumor volume (FTV) of [n=10 for GLV-1h68-treated, n=5 for PBS treated controls] mice is plotted and one-way analysis of variance (ANOVA) was used to compare the corresponding data points. P ≤ 0.05 was considered statistically significant; \* = P ≤ 0.05, \*\*\* P ≤ 0.0005

It was observed that starting 14 days post injection, a single dose of GLV-1h68 could significantly inhibit tumor growth. This tumor growth inhibition became statistically highly significant (P≤0.0005) after 21 days of virus treatment, leading to tumor size stabilization after 28 days of infection (Fig.4.33). The tumors of virus-treated animals did not grow bigger than approximately three times their starting volume whereas tumors of untreated animals grew up to a volume fifteen times bigger than their starting volume. A slight decrease in net body weight could be observed after injection but generally, the virus was well tolerated by the treated animals. Treated animals lived much longer than untreated animals which had to be sacrificed due to high tumor burden (Fig.4.34).

## RESULTS

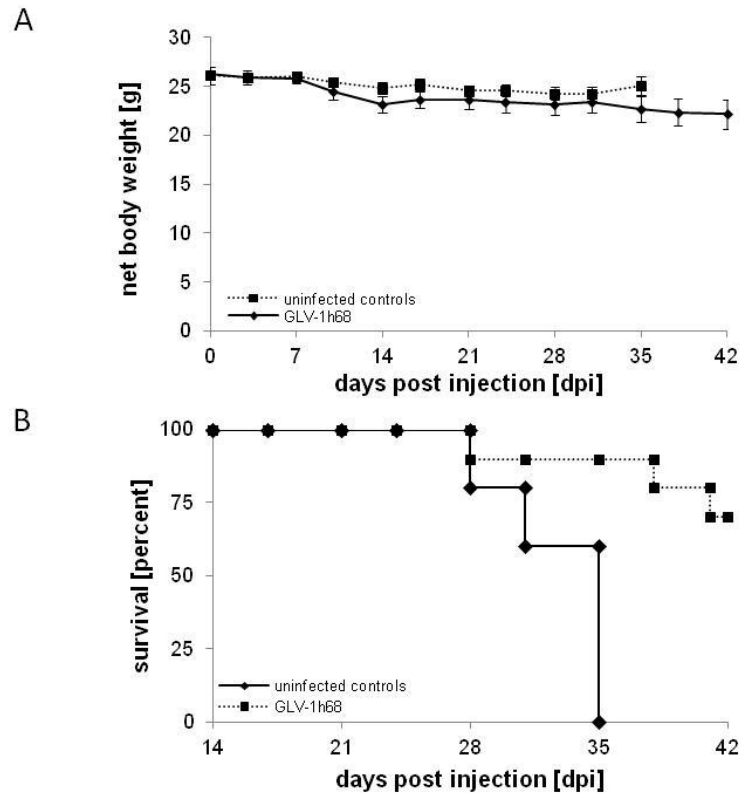


**Fig.4.34 - Changes in net body weight (A) and overall survival (B) of untreated and treated animals.**

A) Net body weight was calculated using the following formula: body weight – (tumor volume/1000 mm<sup>3</sup>). B) Overall survival is plotted as a Kaplan-Meier survival diagram; n=10 for GLV-1h68-treated group, n=5 for PBS-treated group.

To examine if the benefits of a GLV-1h68-treatment are cell line dependent or more widely applicable to CRC, athymic nude mice were subcutaneously implanted with  $5 \times 10^6$  SW620 cells in the right hind flank. SW620 tumor-bearing mice were then injected either with  $5 \times 10^6$  pfu GLV-1h68 (n=10) or PBS when tumor volumes reached an average of 250 – 300 mm<sup>3</sup>. Tumor volume was measured twice a week using a digital caliper.

## RESULTS

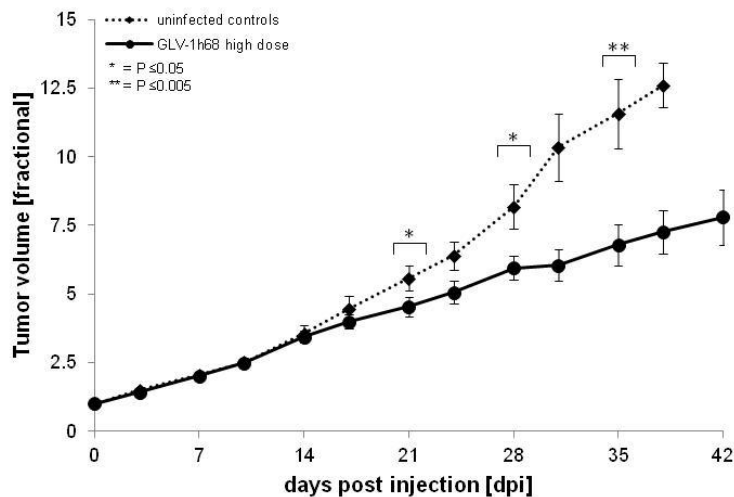


**Fig.4.35 - Effects of a single administration of  $5 \times 10^6$  pfu/100  $\mu$ l PBS on tumor development of SW-620 tumor-bearing mice**

SW-620 cells were implanted subcutaneously in the right hind leg of athymic nude mice. Treatment with GLV-1h68 was tested versus PBS treatment. Average fractional tumor volume of [ $n=10$  for GLV-1h68-treated,  $n=5$  for PBS treated controls] mice is plotted and one-way analysis of variance (ANOVA) was used to compare the corresponding data points.  $P \leq 0.05$  was considered statistically significant; \* =  $P \leq 0.05$ , \*\* =  $P \leq 0.005$

Again, significant inhibition of tumor growth after a single injection of GLV-1h68 was observed (Fig.4.35), becoming statistically significant after 21 days of virus injection. Untreated tumors grew approximately two-fold bigger than virus-treated tumors after 35 days of treatment. Generally, it was shown that GLV-1h68 can inhibit tumor development in at least two different CRC lines *in vivo*.

### 4.2.1.5 Analysis of viral tumor infiltration, infection and replication by fluorescence detection of viral marker gene (Ruc-GFP) expression

To further assess viral spreading and replication in the tumor tissue, viral GFP expression was followed during the course of the experiment by determining the strength of the signal. GFP expression of animals of each group was monitored under blue light using a stereo fluorescence macroimaging system once a week over the course of five weeks. GFP intensity is determined by using a four stage scoring system; 0) no GFP signal, 1) one spot, 2) two or three local spots, 3) diffuse signal from half the tumor, 4) strong signal from whole tumor.

## RESULTS

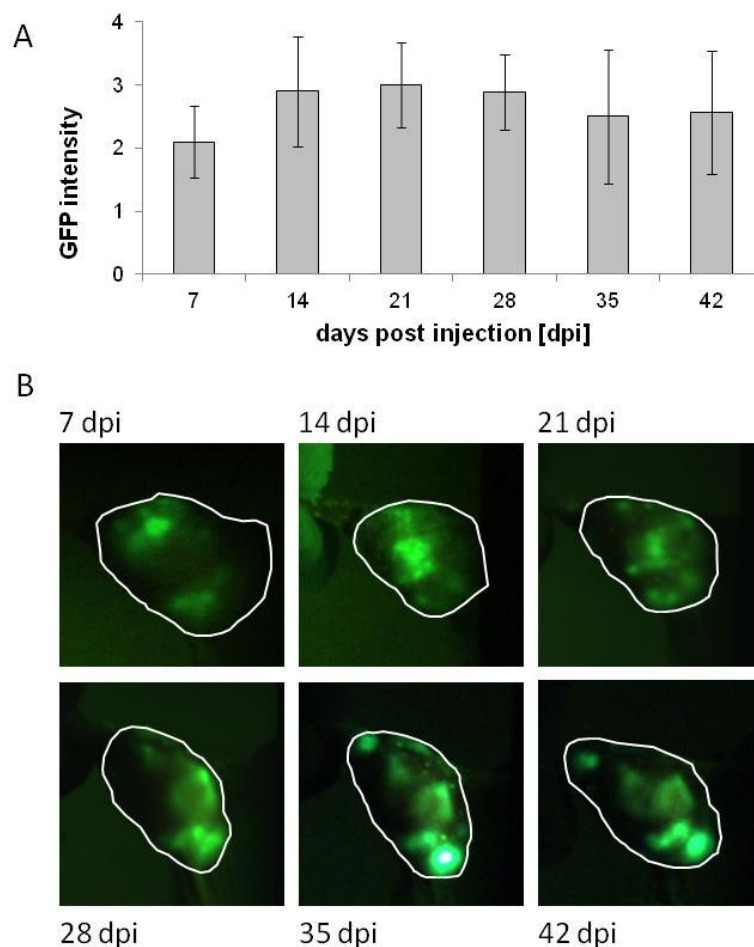


**Fig.4.36 - Expression of viral *Renilla* luciferase-green fluorescent protein at the local tumor site of HCT-116 tumor-bearing mice.**

A) Analysis of GFP signal strength during the course of the experiment. GFP intensity was determined by using a four stage scoring system; 0) no GFP signal, 1) one spot, 2) two or three local spots, 3) diffuse signal from half the tumor, 4) strong signal from whole tumor. B) Fluorescence imaging of GFP expression at the local tumor site.

As presented in figure 4.36, GFP fluorescence was clearly visible from as early as 7 days post injection on and increased until 21 dpi. GFP expression remained relatively stable for the rest of the experiment. It could also be detected that during the course of the experiment GFP expression in the tumor was relatively stable, indicating that GLV-1h68 remained and replicated at the primary tumor site during the course of the experiment.

### **4.2.1.6 Pfu determination in GLV-1h68-injected HCT-116 tumor-bearing mice at various time points**

To analyze the specific tumor-targeting ability of GLV-1h68, 3 and 14 days after virus injection, animals bearing HCT-116 tumors (n=5) were sacrificed. Various body organs (testes, spleen, liver, kidney, lungs) and the primary tumor were dissected and prepared for standard plaque assay to analyze viral spreading in the animals.

## RESULTS

**Tab.4.4 - Viral titers in mouse tissues or tumors**

mouse tissue	viral titers [pfu/g]			
	3 dpi	#	14 dpi	#
tumor	$2.94 \times 10^5 \pm 5.54 \times 10^5$	5/5	$4.21 \times 10^7 \pm 2.48 \times 10^7$	5/5
lungs	$4.21 \pm 6.11$	1/5	$2.62 \pm 3.59$	2/5
liver	n.d.	0/5	$3.88 \pm 8.68$	1/5
spleen	n.d.	0/5	n.d.	0/5
kidney	n.d.	0/5	n.d.	0/5
testes	n.d.	0/5	n.d.	0/5

HCT-116-bearing mice [n=5] were sacrificed 3 days and 14 days [dpi], respectively, after i.v. injection of  $5 \times 10^6$  pfu GLV-1h68. Tissues and tumors were surgically excised, homogenized and viral titers were determined by standard plaque assay. Titters are displayed as means of all animals sacrificed per time point and in the # column the number of positively tested animals of all the tested animals in the group is indicated. n.d. = not detected.

Tab.4.4 shows that after three days of injection,  $2.94 \times 10^5 \pm 5.54 \times 10^5$  viral particles were found in the primary tumor tissues whereas viral particles were not detectable or negligible in the normal organ tissues. Even well-vascularized tissues like the liver or lungs showed no or very low copy numbers of plaque forming vaccinia virus particles, indicating rapid and efficient clearing from the blood stream. Fourteen days post injection, a two-log increase in viral titers in the primary tumor tissue was detected whereas no virus (testes, spleen, kidney) or negligible amounts of virus (liver, lungs) were found in normal tissues.

### **4.2.1.7 Histochemical analysis of GLV-1h68 injections in HCT-116 mouse xenografts**

To analyze the colonization of the primary tumor by oncolytic vaccinia viruses in more detail, animals were sacrificed after 21 or 42 days of treatment and the primary tumors were surgically removed. Tissue sectioning was performed as described in section 3.6.6. Sections were incubated with Phalloidin-TRITC as an indicator for live cell staining. Direct fluorescence was used for GFP detection as a tool to localize active virus as the half-life of GFP is 24 hours.

## RESULTS

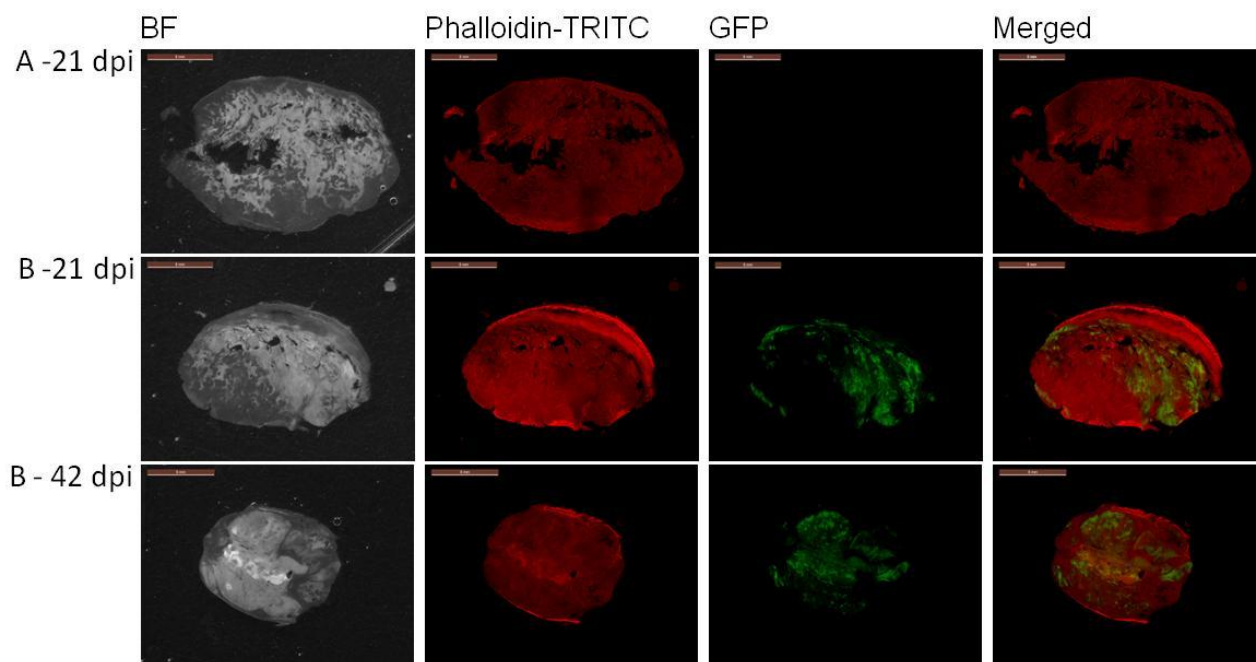


**Fig.4.37 - Histochemical staining of HCT-116 tumor sections**

GLV-1h68-treated mice [B] were sacrificed 21 and 42 days after virus injection [dpi] and untreated mice [A] were sacrificed at 21 dpi as a control. Whole tumor cross-sections (thickness = 100 $\mu$ m) were labeled with Phalloidin-TRITC to detect actin as an indicator for live cells. Large areas lacking actin staining indicates virus-mediated tumor tissue destruction.

Histological analysis (Fig.4.37) showed efficient viral spreading of GLV-1h68 throughout the tumor 21 and 42 days post injection, eventually leading to oncolysis and destruction of the tumor tissue. Tumor sizes in displayed sections are representative for treatment group and time point.

### **4.2.1.8 Immune-related antigen profiling of HCT-116 tumor-bearing mice after administration of a single dose of GLV-1h68**

In order to analyze the effects of GLV-1h68 injection on the host immune system and its potential involvement in tumor growth inhibition and regression, untreated and treated mice [n=3] were sacrificed 21 days post injection, when the differences in tumor volume first became statistically significant ( $P \leq 0.0005$ ). Tumor tissue lysates were prepared as described in Material and Methods.

## RESULTS

**Tab.4.5 - Comparison of mouse immune-related protein antigen profiling in homogenates of untreated/GLV-1h68 treated HCT-116 tumors**

Antigen	GLV-1h68/untreated ratio	Classification
CD40	6.07	TNF receptor
Eotaxin	300.03	Pro-inflammatory cytokine
GCP-2 mouse (CXCL6)	19.25	Pro-inflammatory cytokine
KC/GRO	34.85	Pro-inflammatory cytokine
IFN gamma	4.47	Pro-inflammatory cytokine
IP-10	66.16	Interferon-gamma-induced protein
IL-1 alpha	5.55	Pro-inflammatory cytokine
IL-3	5.49	Pro-inflammatory cytokine
IL-6	12.45	Pro-inflammatory cytokine
IL-10	5.31	Anti-inflammatory cytokine
IL-11	6.92	Pro-inflammatory cytokine
IL-17A	10.19	Pro-inflammatory cytokine
IL-18	5.70	Pro-inflammatory cytokine
Lymphotactin	16.51	Pro-inflammatory chemokine
M-CSF-1	38.51	Pro-inflammatory cytokine
MIP-1 beta	50.07	Pro-inflammatory cytokine
MIP-2 (CXCL2)	55.05	Pro-inflammatory chemokine
MIP-3	5.52	Pro-inflammatory chemokine
MMP-9	9.19	Matrix Metalloprotease-9
MCP-1 (CCL2)	229.11	Pro-inflammatory cytokine
MCP-3 (CCL7)	111.18	Pro-inflammatory cytokine
MCP-5 (CCL12)	56.84	Pro-inflammatory cytokine
RANTES (CCL5)	105.7	Pro-inflammatory chemokine
TIMP-1 mouse	9.36	Tissue inhibitor of metalloprotease type-1
TNF alpha	4.27	Pro-inflammatory cytokine

Antigen	Untreated/GLV-1h68 ratio	Classification
FGF-b	1.55	Fibroblast growth factor
MIP-1 alpha (CCL3)	1.75	Proinflammatory cytokine
MIP-1 gamma (CCL9)	3.14	Proinflammatory cytokine
SGOT (AST)	1.92	Serum glutamic oxaloacetic transaminase

HCT-116 tumors [n=3 per group] were surgically removed 21 days after virus injection and prepared for antigen profiling. Folds of enhancement (A) or suppression (B) are normalized to total protein amounts.

The data obtained from untreated and treated xenografts showed that treatment with GLV-1h68 led to increased levels of many tested pro-inflammatory cytokines and chemokines (GCP-2, KC/GRO alpha, IFN-gamma, IP-10, IL-3, IL-6, Lymphotactin, M-CSF1, MIP-1 beta, MCP-1, MCP3, MCP-5, RANTES) (Tab. 4.5). We found that only a few tested markers were down-regulated upon virus treatment (FGF-beta, MIP-1 alpha, MIP-1 gamma, SGOT).

### **4.3 Improvement of oncolytic virotherapy with a new replication-competent vaccinia virus strain expressing transcription factor Klf4**

#### **4.3.1 A potential application of transcription factor Klf4 in colorectal cancer**

Klf4 is a transcription factor most abundantly expressed in terminally differentiated, quiescent post-mitotic cells of the colonic mucosa<sup>86</sup>. Klf4 expression is induced under growth



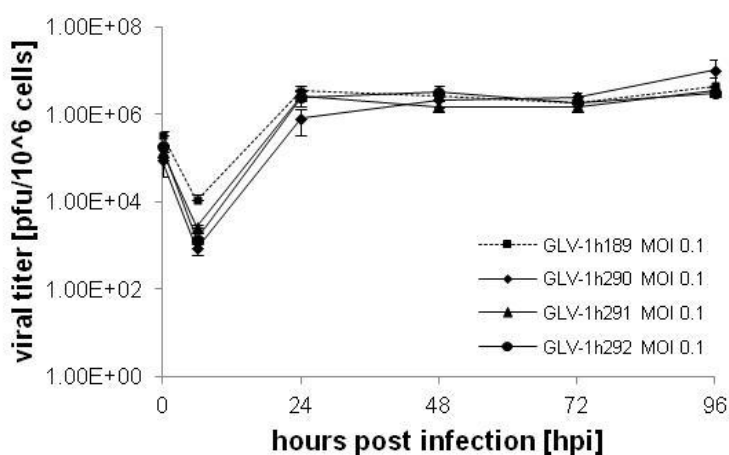
## RESULTS

arrest promoting conditions like DNA damage, serum deprivation and contact inhibition and leads to cell cycle arrest<sup>91</sup>. Furthermore, Klf4 was shown to bind the the transcriptional active domain of nuclear beta-catenin and inhibits beta-catenin-mediated transcription, cementing its important role in intestinal homeostasis and colorectal carcinogenesis by inhibiting the Wnt signaling pathway<sup>96</sup>. Re-expression of Klf4 in colorectal cancer cell lines results in diminished tumorigenicity<sup>97</sup> and therefore, Klf4 can be considered to be a tumor suppressor with a potential application in oncolytic virotherapy of colorectal cancer.

A set of recombinant viruses expressing Klf4 was generated for this work. GLV-1h290-292 encode for the human *klf4* gene under control of the synthetic early, synthetic early/late, and synthetic late promoter. GLV-1h391 encodes for the human *klf4* gene with a TAT sequence for membrane permeability fused to the C-terminus under control of the synthetic early/late promoter. All viruses carry their payload in the HA locus, replacing the marker gene *gusA*.

### 4.3.1.1 Analysis of viral replication in the CRC lines HCT-116 and HT-29

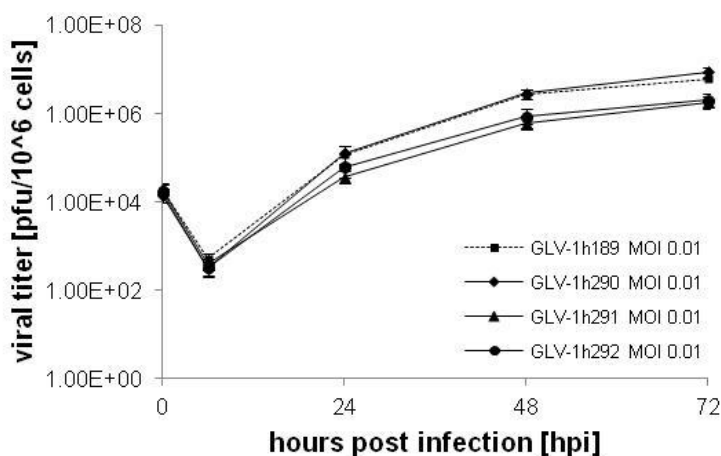
After generation of the new recombinant virus strains the replication capability of the viruses in cancer cells was investigated in comparison to the control virus strain GLV-1h189. Replication was analyzed in the cancer cell lines HCT-116 and HT-29. For analysis of the replication, the HCT-116 cells were infected with an MOI of 0.1 and HT-29 cells with an MOI of 0.01. Viral titers were determined at 6, 24, 48, 72, and 96 hours post infection. The initial infection medium was used as initial virus titer at 0 hours post infection. Viral titers were determined by standard plaque assay. Average data including standard deviation are shown for GLV-1h290-292 in comparison to GLV-1h189.



**Fig.4.38 – Analysis of viral titers after infection of HCT-116 cells with GLV-1h189 and GLV-1h290-292**  
Cells were infected at an MOI of 0.1 and samples were collected at various times after infection. Titers were averaged from triplicates and plotted with standard deviations.

## RESULTS

Figure 4.38 demonstrates the replication efficacy of the new Klf4-encoding virus strains compared to the control virus GLV-1h189 in HCT-116 cells during the course of the infection. A three-log increase in virus titers was observed within the first 24 hours and stayed on a constant level afterwards. All three virus strains efficiently infected and replicated in HCT-116 cells in comparable levels to the control strain GLV-1h189 and the parental strain GLV-1h68 (Fig.4.29). In this susceptible cell line, no difference in replication due to promoter strength was observed. To analyze a potential promoter strength-dependent effect on replication, HT-29 cells were infected at an MOI of 0.01 and viral replication was determined.



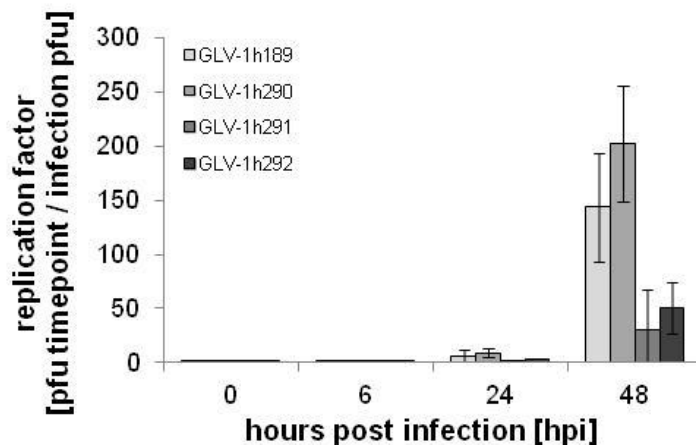
**Fig.4.39 – Analysis of viral titers after infection of HT-29 cells with GLV-1h189 and GLV-1h290-292**  
Cells were infected at an MOI of 0.01 and samples were collected at various times after infection. Titers were averaged from triplicates and plotted with standard deviations.

Figure 4.39 shows the replication efficacy of GLV-1h290-292 in comparison to GLV-1h189 in HT-29 cells. All three viruses replicated well in HT-29 cells and a three- to four-log increase of viral titers was observed within 72 hours of infection. GLV-1h291 (synthetic early/late) and GLV-1h292 (synthetic late) show lower titers compared to GLV-1h189 and GLV-1h290 (synthetic early), indicating a lower replication ability due to higher gene expression burden. To further analyze the replication behavior, HT-29 cells were infected at an MOI of 0.01 and viral titers were determined at 6, 12, 24, and 48 hpi. The replication factor was determined using the following equation:

$$\frac{\text{virus titer at time point } \left[ \frac{\text{pfu}}{\text{ml}} \right]}{\text{infection pfu } \left[ \frac{\text{pfu}}{\text{ml}} \right]} = \text{replication factor}$$

## RESULTS

Viral titers were determined by standard plaque assay. Averaged data from triplicates including standard deviation are shown for GLV-1h290-292 in comparison to GLV-1h189.



**Fig.4.40 – Replication factors of GLV-1h290-292 in comparison with GLV-1h189**

HT-29 cells were infected at an MOI of 0.01 and samples were collected at various time points after infection. Titers were averaged from triplicates and the replication factor was plotted with standard deviations.

The analysis of replication factors in figure 4.40 clearly demonstrates a promoter strength-dependent effect in replication. While GLV-1h290 (synthetic early) showed the highest replication after 48 hours, replication was significantly impaired in GLV-1h291 (synthetic early/late) and GLV-1h292 (synthetic late).

In summary, it was shown that the new KLF4-encoding virus strains efficiently infected and replicated in at least two different human colorectal cancer cell lines. However, the replication behavior is promoter strength-dependent.

### 4.3.1.2 Analysis of recombinant protein expression in infected CRC cells

#### 4.3.1.2.1 Analysis of beta-galactosidase expression in infected CRC cells

After analysis of viral replication behavior, efficacy of functional protein expression of marker genes and Klf4 in infected colorectal cancer cell cultures was analyzed. For beta-galactosidase expression, HT-29 cells were infected at an MOI of 0.01 for 24 hours to obtain single, isolated plaques. Cells were then treated with a substrate that is converted into a blue dye by beta-galactosidase and precipitates in the cells. Therefore, infected cells that express functional beta-galactosidase protein appear as blue plaques under the microscope. Infected plaques were observed under the light microscope.

## RESULTS

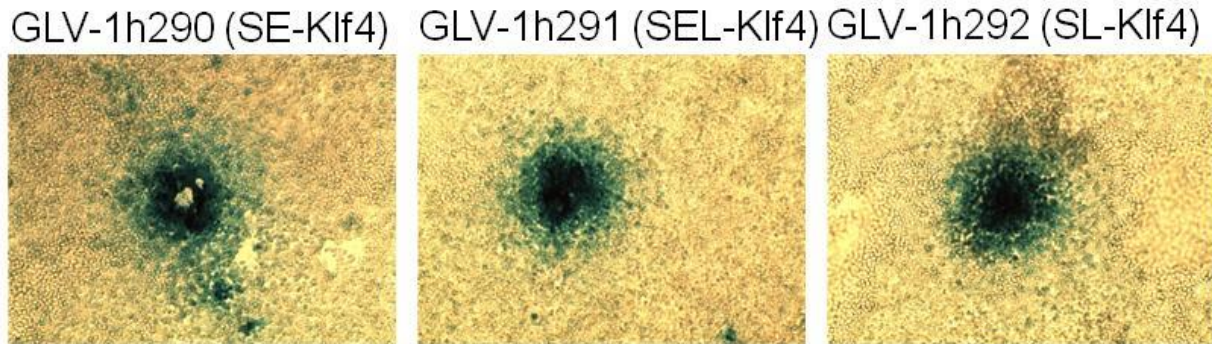


**Fig.4.40 – Expression of beta-galactosidase in infected HT-29 cells**

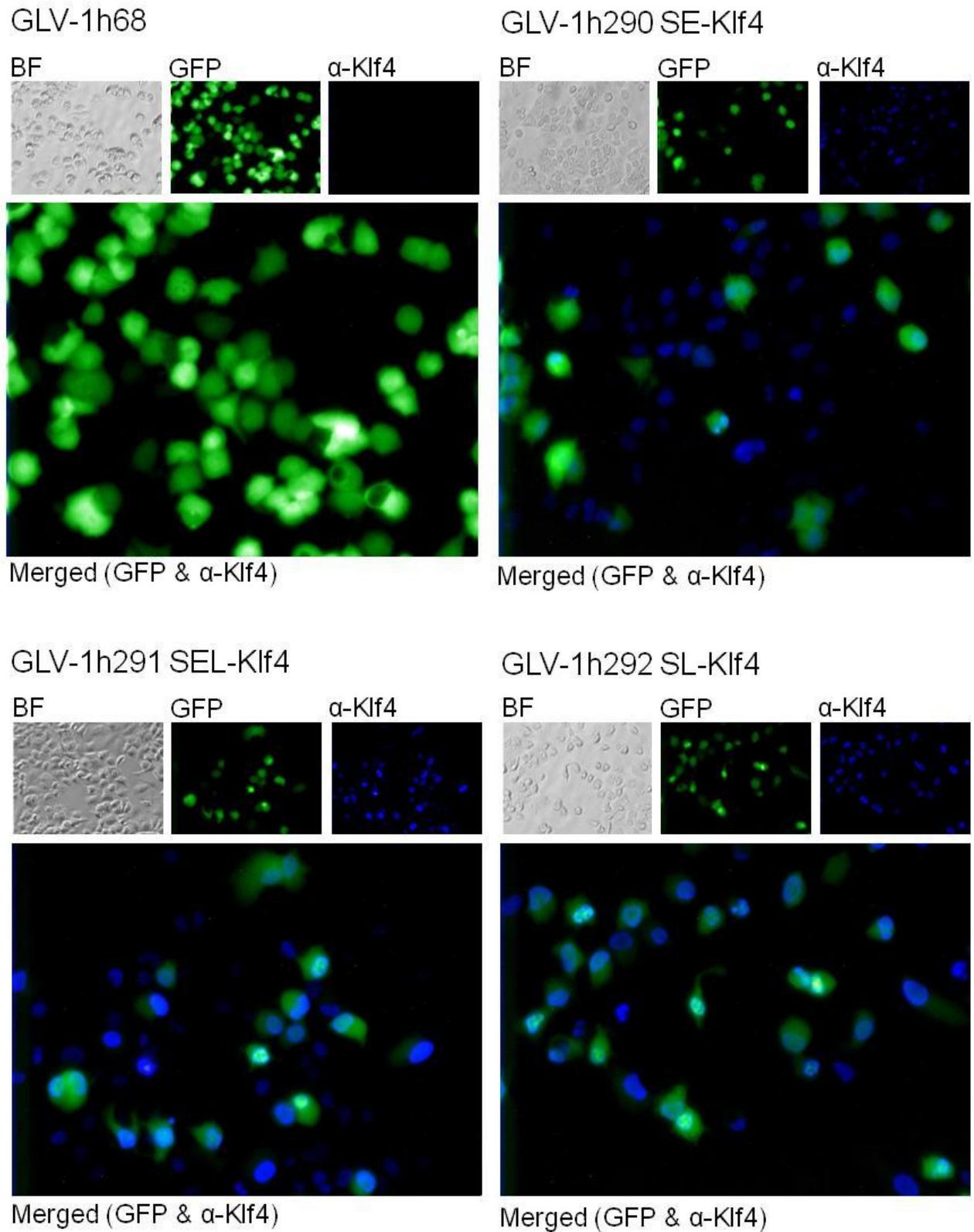
HT-29 cells were infected at an MOI of 0.01 to obtain single, isolated plaques and stained for beta-galactosidase expression. The three new recombinant virus strains GLV-1h290-292 express functional beta-galactosidase. Pictures were taken at 100x magnification.

Figure 4.40 demonstrates that all three new KLF4-encoding vaccinia virus strains express functional beta-galactosidase in infected HT-29 cells. Therefore, beta-galactosidase is a valid marker for efficient infection and replication of GLV-1h290-292 in infected human cancer cells.

### **4.3.1.2.2 Analysis of Ruc-GFP and Klf4 expression in infected CRC cells by immunocytochemistry**

To detect expression of Ruc-GFP fusion protein and Klf4 in all three new constructs, HT-29 cells were infected at an MOI of 0.01 to obtain single, isolated plaques. Cells were then fixed and permeabilized to allow antibody binding. For detection of Klf4, cells were incubated with a monoclonal mouse-anti-Klf4 antibody and a AlexaFluor350-labeled secondary anti-mouse antibody. Monochromal images were taken with a digital CCD camera and pseudo-colored using the open-source software GIMP 2.6. Expression of functional *Renilla* luciferase-green fluorescent protein fusion protein was detected by fluorescence microscopy. The parental GLV-1h68 was used as a control virus (MOI 0.1) which is positive for Ruc-GFP expression but negative for Nanog expression. To analyze the spread pictures of Klf4 and GFP expression were merged.

## RESULTS



**Fig.4.41 - Analysis of Klf4 and GFP expression in A549 cells infected with GLV-1h68 and GLV-1h290-292**  
HT-29 cells were infected at an MOI of 0.01 with GLV-1h290-292 and at an MOI of 0.1 with the parental GLV-1h68 as a control to obtain single, isolated plaques. Cells were then fixed, permeabilized and incubated with a primary monoclonal mouse-anti-Klf4 antibody (1:500 dilution). Subsequently, cells were stained with an AlexaFluor350-conjugated secondary antibody (1:500) and GFP and Klf4 expression was analyzed. Pictures were taken with a digital CCD camera and an inverted fluorescence microscope and pseudo-colored and edited using the open-source software GIMP2.6 Pictures were taken at 400x magnification.

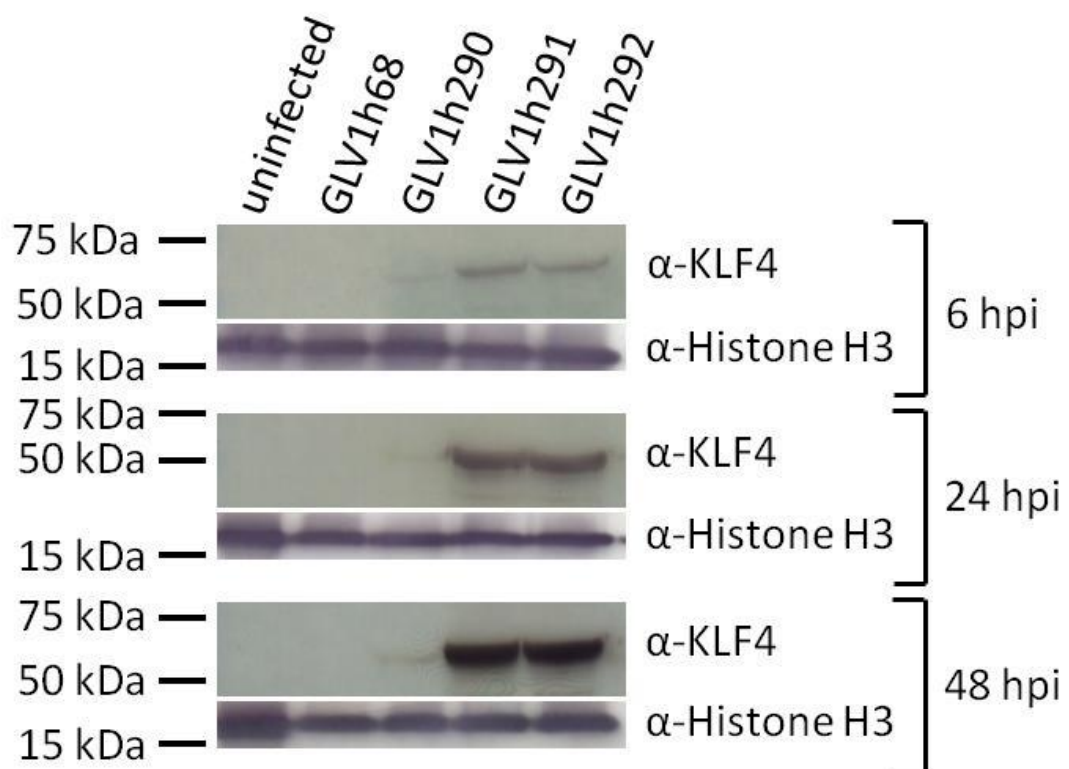
## RESULTS

Figure 4.41 shows the expression of viral Ruc-GFP fusion protein in both, HT-29 cells infected with GLV-1h68 and GLV-1h290-292, in culture. GFP expression indicates efficient cell infection and viral marker protein expression. In contrast, Klf4 expression was observed exclusively in GLV-1h290-292-infected cells. Pictures were taken with identical exposure time, indicating that cells infected with viruses encoding KLF4 under synthetic early/late (GLV-1h291) or late (GLV-1h292) promoter express more functional Klf4 than GLV-1h290, which encodes for KLF4 under control of the synthetic early promoter as signal strengths differ markedly between viruses. Interestingly, Klf4 signal was detected in cells that do not express GFP which indicates that Klf4 staining is likely to be more sensitive than GFP fluorescence. Overall, it was demonstrated that HT-29 cells infected with the new recombinant virus strains expressed functional Klf4 in a promoter strength-dependent manner and marker fusion protein Ruc-GFP. However, no Klf4 expression was observable upon infection with the parental virus GLV-1h68.

### **4.3.1.2.3 Analysis of Klf4 expression in infected HT-29 cells by Western blot**

For analysis of Klf4 expression in virus infected HT-29 cells, Western blot analysis was performed. HT-29 cells were either mock-infected or infected with GLV-1h68 as a negative control or GLV-1h290-292 at an MOI of 5.0 to synchronize the infection. Infected cells were incubated for 6, 24, and 48 hours and harvested at the respective time point. Samples were processed to determine total protein amounts. For Western blot analysis, 20 µg total proteins per sample were used. SDS-PAGE and Western blotting was performed prior to antibody binding. Histone H3 antibodies were used as a loading control and Klf4 antibodies for detection of the recombinant viral gene product. The blot was developed by colorimetric detection. Histone H3 has a predicted molecular mass of 15 kDa while the band can be detected around 17 kDa. The predicted molecular mass of Klf4 is 50 kDa while the protein band can be detected around 60 kDa.

## RESULTS



**Fig.4.42 – Western blot analysis of human Klf4 in infected HT-29 cells**

HT-29 cells were either mock-infected or infected with the Klf4-expressing GLV-1h290-292 at an MOI of 5.0. Klf4 expression was followed over the course of 48 hours of infection. Samples were harvested during the course of the experiment and processed for Western blot analysis. The primary Klf4 antibody was used at a concentration of 1:1000 while the primary Histone H3 antibody was used at a dilution of 1:5000 due to its high abundance. The blots were visualized by colorimetric detection.

Figure 4.42 clearly demonstrates the expression of human Klf4 in infected HT-29 cells. The comparable signal strength in Histone H3 expression suggests that comparable amounts of total protein were loaded prior to SDS-PAGE. Klf4 signal in GLV-1h290-292-infected cells was detectable from as early as 6 hpi. The maximal signal strength was detected at 48 hpi. Klf4 expression levels were highly promoter-dependent as Klf4 band intensity, which can be used in a semi-quantitative manner to determine protein amounts, was much stronger in HT-29 cells infected with virus constructs that carry the *klf4* gene under control of the synthetic early/late (GLV-1h291) or synthetic late (GLV-1h292) promoter. Mock-infected and GLV-1h68-infected cells showed no Klf4 expression.

### **4.3.1.3 Cell viability of HT-29 cells infected with Klf4-encoding vaccinia virus strains GLV-1h290-292**

Next, the oncolytic potential of the three Klf4-encoding vaccinia viruses in HT-29 cell culture was tested. Cells were seeded to a confluence of 95% and either mock-infected or infected

## RESULTS

with GLV-1h290-292. As a reference, confluent HT-29 cells were also infected with the control strain GLV-1h189. Cells were infected with an MOI of 0.1 and 1.0, respectively to analyze dose-dependency. The infection was followed for 72 hours and samples were analyzed 0, 24, 48, and 72 hours post infection.

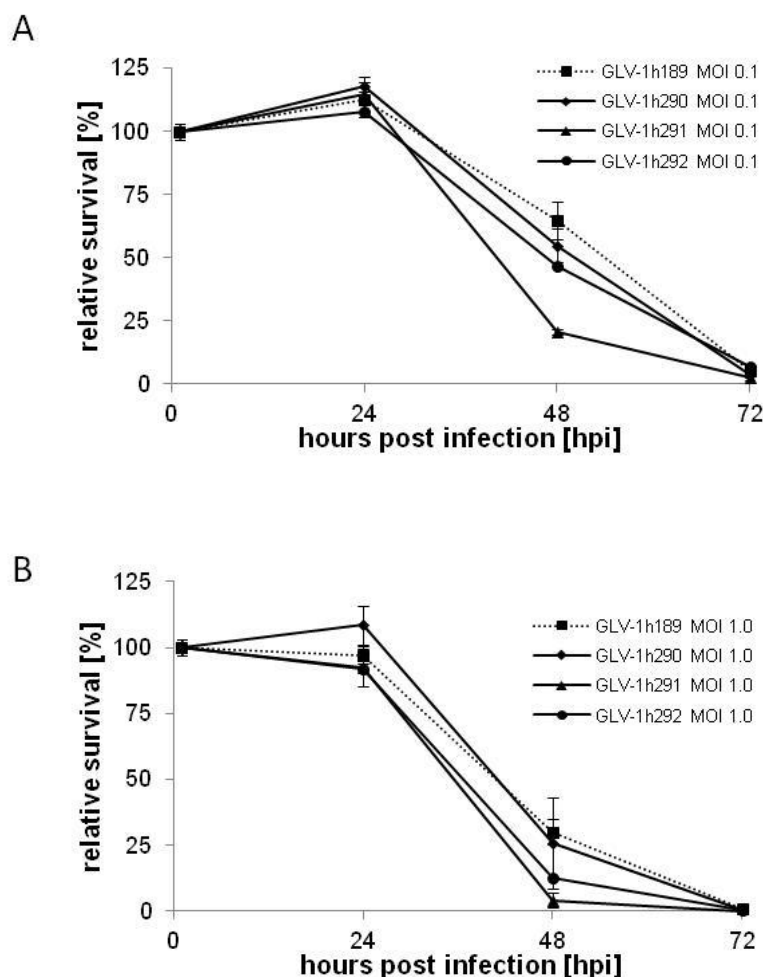


**Fig.4.42 – Viability of HT-29 cells after infection with GLV-1h68, and GLV-1h290-292**

Analysis of cell viability of HT-29 cells after infection with replication-competent vaccinia viruses GLV-1h68, GLV-1h290-292, using MOIs of 0.1 (A) and 1.0 (B), respectively. Viability was monitored over the course of 72 hours and was measured in triplicates and averaged. Plotted averages are normalized against uninfected controls of each time-point which were considered to be 100% viable.

All three new vaccinia virus construct showed efficient cancer cell killing potential in infected HT-29 cells (Fig.4.42). The control GLV-1h189 strain was used as a reference for the cytotoxic potential of the new strains GLV-1h290-292. After 72 hours of infection, only  $5.09 \pm 0.84\%$  (MOI 0.1) and  $0.69 \pm 0.26\%$  (MOI1.0) of the cells infected with GLV-1h189 were still viable. All three Klf4-encoding viruses showed higher cytotoxicity at an MOI of 0.1 ( $54.75 \pm 6.69\%$  for GLV-1h290,  $20.61 \pm 2.53\%$  for GLV-1h291, and  $46.49 \pm 3.49\%$  for GLV-1h292) after 48 hours of infection compared to GLV-1h189 ( $64.81 \pm 7.29\%$ ). The same tendency



## RESULTS

was found at an MOI of 1.0 ( $25.80 \pm 17.51\%$  for GLV-1h290,  $4.16 \pm 2.87\%$  for GLV-1h291, and  $12.42 \pm 2.75\%$  for GLV-1h292 compared to  $30.13 \pm 4.94\%$  for GLV-1h189). Overall, it was demonstrated that the new recombinant vaccinia viruses GLV-1h290-292 efficiently infected, replicated in, and ultimately lysed HT-29 cells in a dose-dependent manner. Compared with the reference strain GLV-1h189, all new constructs showed slightly increased oncolytic potential, with GLV-1h291 standing out as the most cytotoxic strain.

### 4.3.1.4 Effects of virus-mediated Klf4 expression on mRNA levels of cellular beta-catenin

It was published that Klf4 binds to the transcriptional activation domain of beta-catenin<sup>96</sup>. It therefore inhibits beta-catenin-mediated transcription. To test the effects of Klf4 expression on infected colorectal cancer cells, HT-29 cells were mock-infected or infected with GLV-1h189 as a control virus at an MOI of 5.0. Other HT-29 cells were infected with GLV-1h290, GLV-1h291, or GLV-1h292 at an MOI of 5.0. All cells were incubated for 24 hours and subsequently processed for RNA isolation and DNase digestion. All cellular mRNAs were transcribed into cDNA using reverse transcriptase and cellular mRNA levels of beta-catenin were quantified by qPCR as described in 3.4.1.5. The mRNA levels of beta-catenin in GLV-1h290-292-infected cells were normalized against GLV-1h189 (100%).

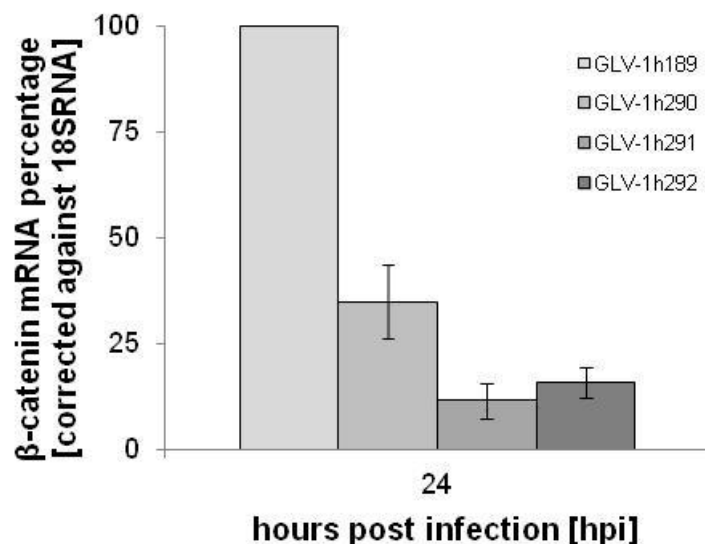


**Fig.4.43 – Cellular levels of beta-catenin mRNA in HT-29 cells after vaccinia virus infection**

Cellular mRNA from infected HT-29 cells was isolated and transcribed to cDNA for quantitative real-time PCR. To analyze a Klf4-dependent effect on cellular beta-catenin mRNA levels, results were normalized and corrected against mRNA levels in GLV-1h189. 18SRNA was chosen due to the high resistance in levels upon virus infection. Three samples per group were analyzed in triplicates and mean values are plotted with standard deviations.

## RESULTS

Virus-mediated Klf4 expression in infected HT-29 directly affected cellular mRNA levels of beta-catenin (Fig.4.43). After 24 hours of infection, only  $34.94 \pm 8.60\%$  compared to beta-catenin mRNA levels in cells infected with GLV-1h189 was detected after HT-29 infection with GLV-1h290. A promoter strength-dependent effect was clearly visible, as beta-catenin mRNA levels decreased to  $11.54 \pm 4.03\%$  in cells infected with GLV-1h291 (synthetic early/late) and  $15.78 \pm 3.54\%$  in cells infected with GLV-1h292 (synthetic late). Therefore, infection of HT-29 cells led to a promoter strength-dependent decrease in beta-catenin transcripts compared to the control virus GLV-189.

### 4.3.1.5 Effects of virus-mediated Klf4 expression on cellular protein levels of beta-catenin

To analyze whether Klf4 expression in infected CRC cells also leads to a decrease in cellular protein amounts of beta-catenin, confluent HT-29 cells were either mock-infected or infected with GLV-1h290-292 at an MOI of 5.0. As a control, HT-29 cells were infected with GLV-1h189 at an MOI of 5.0. Cells were incubated for 48 hours and samples were then processed for quantification by ELISA. Total protein amounts were adjusted to  $50 \mu\text{g}$  per sample. Amounts of cellular beta-catenin were quantified following the manufacturer's instructions.

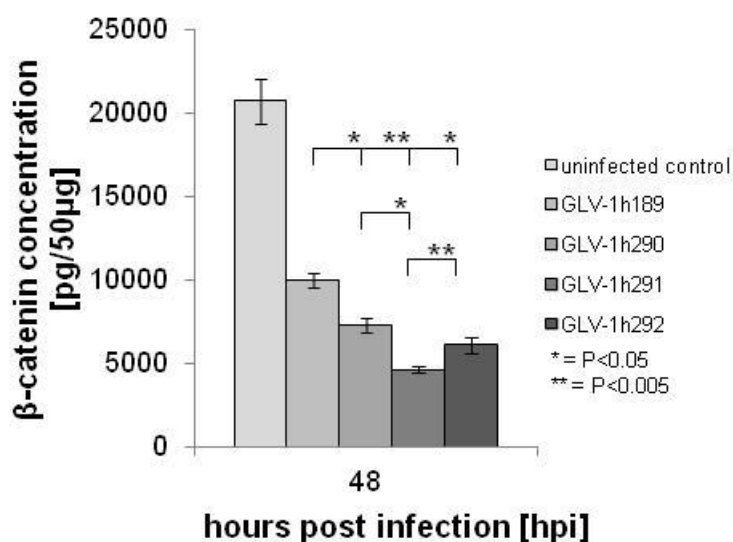


**Fig.4.44 – Cellular beta-catenin protein levels in HT-29 after vaccinia virus infection**

HT-29 cells were either mock-infected or infected with GLV-1h290-292 at an MOI of 5.0. GLV-1h189 was used as a control virus. Infected cells were incubated for 48 hours and total protein was isolated and prepared for ELISA quantification of beta-catenin levels. ELISA was performed according to manufacturer's instructions and beta-catenin levels were plotted with standard deviations.

## RESULTS

Infection of HT-29 cells with vaccinia virus strains led to a significant decrease in cellular beta-catenin protein levels (Fig.4.44). Forty-eight hours post infection, beta-catenin levels decreased at least in half (in GLV-1h189-infected cells) or more (in GLV-1h290-292-infected cells). Furthermore, in a similar manner to beta-catenin mRNA levels, infection with all three *klf4*-encoding virus strains led to a significant decrease in beta-catenin levels compared to the control virus GLV-1h189. Also, as described for cellular mRNA levels of beta-catenin, protein levels decreased in a promoter strength-dependent manner upon viral infection. The strongest decrease in beta-catenin was observed in cells infected with GLV-1h291 (synthetic early/late), followed by GLV-1h292 (synthetic late) and GLV-1h290 (synthetic early).

### **4.3.1.6 Construction and characterization of the Klf4-TAT fusion protein-expressing vaccinia virus strain GLV-1h391**

Cell culture analysis of three recombinant vaccinia virus strains encoding for the human transcription factor Klf4 under different promoter strengths (synthetic early, early/late, and late) identified GLV-1h291 as the most powerful candidate for translation into small animal experiments. However, there is little knowledge about stability, degradation, or half life of transcription factors released from necrotic cells into the tumor environment. It is questionable whether released transcription factors are able to penetrate the extracellular matrix and find their way past the cytoplasmic membranes of neighboring cells to exert a bystander effect in neighboring tumor cells. It is possible that transcription factors are taken up by pinocytosis and will subsequently degraded to a high percentage in the lysosomes. Therefore, a virus strain (GLV-1h391) was designed and constructed that encodes for human Klf4 with a C-terminal TAT sequence, which will enable the transcription factor to penetrate cytoplasmic membranes of surrounding cells once released from the infected cells and slow down tumor progression of surrounding colorectal cancer cells.

#### **4.3.1.6.1 Viral replication of GLV-1h391 in colorectal cancer line HT-29**

After generation of the new recombinant virus strain the replication ability was analyzed in comparison to the control virus strains GLV-1h189 and GLV-1h291. Replication was analyzed in the colorectal cancer cell line HT-29. For analysis of the replication, the respective cell lines were infected with an MOI of 0.1 and viral titers were determined at 6, 24, 48, 72, and 96 hours post infection. The initial infection medium was used as initial virus titer at 0 hours post infection. Viral titers were determined by standard plaque assay. Average data including standard deviation are shown for GLV-1h291 and GLV-1h391 in comparison to GLV-1h189.

## RESULTS

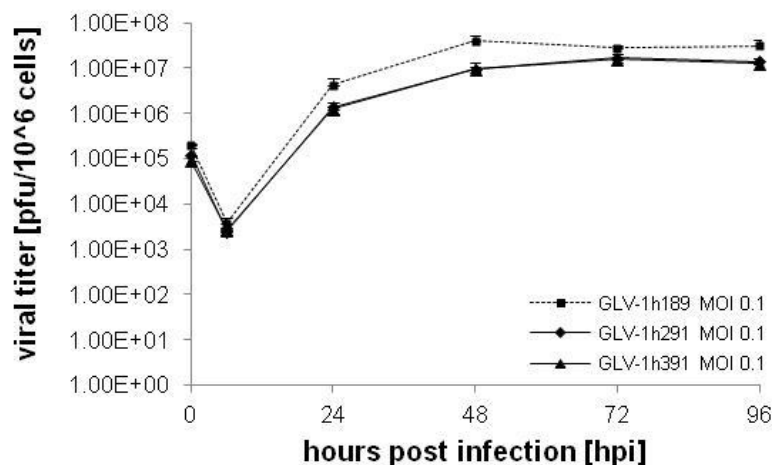


**Fig.4.45 – Analysis of viral titers after infection of HT-29 cells with GLV-1h189, GLV-1h291, and GLV-1h391**

Cells were infected at an MOI of 0.1 and samples were collected at various times after infection. Titers were averaged from triplicates and plotted with standard deviations.

Figure 4.45 demonstrates that GLV-1h391 replicated in an identical manner to GLV-1h291 in HT-29 cells. Both Klf4-encoding viruses show inferior replication to GLV-1h189. A three-log increase in virus titers was observed within the first 24 hours of infection and stayed on a constant level afterwards. The new virus strain GLV-1h391 (Klf4-TAT) efficiently infects and replicates in HT-29 cells in comparable levels to the corresponding strain GLV-1h291 (Klf4).

### **4.3.1.7 Marker gene expression in colorectal cancer line HT-29 infected with GLV-1h391**

#### **4.3.1.7.1 Analysis of beta-galactosidase expression in infected HT-29 cells**

Efficacy of functional protein expression of marker genes in HT-29 cells infected with GLV-1h391 was analyzed. For beta-galactosidase expression, HT-29 cells were infected at an MOI of 0.01 for 24 hours to obtain single, isolated plaques. Cells were then treated with a substrate that is converted into a blue dye by beta-galactosidase and observed under the light microscope. Therefore, infected cells that express functional beta-galactosidase protein appear as blue plaques under the microscope.

## RESULTS

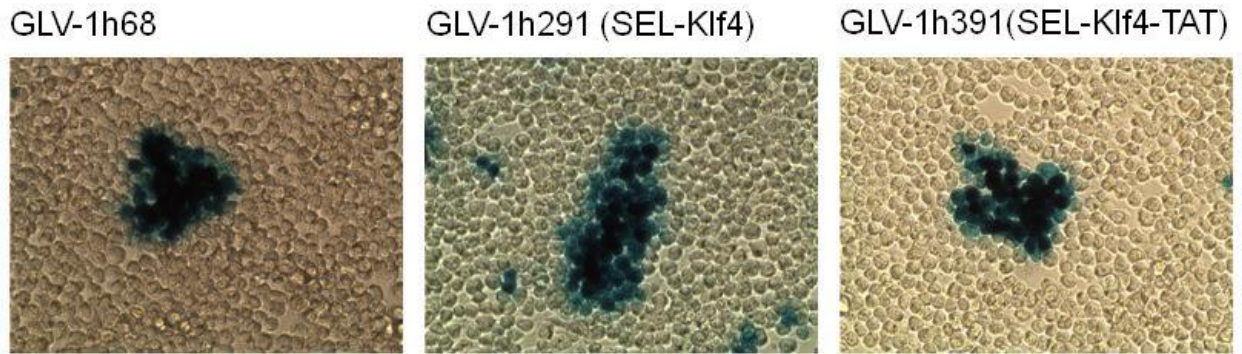


**Fig.4.46 – Expression of beta-galactosidase in infected HT-29 cells**

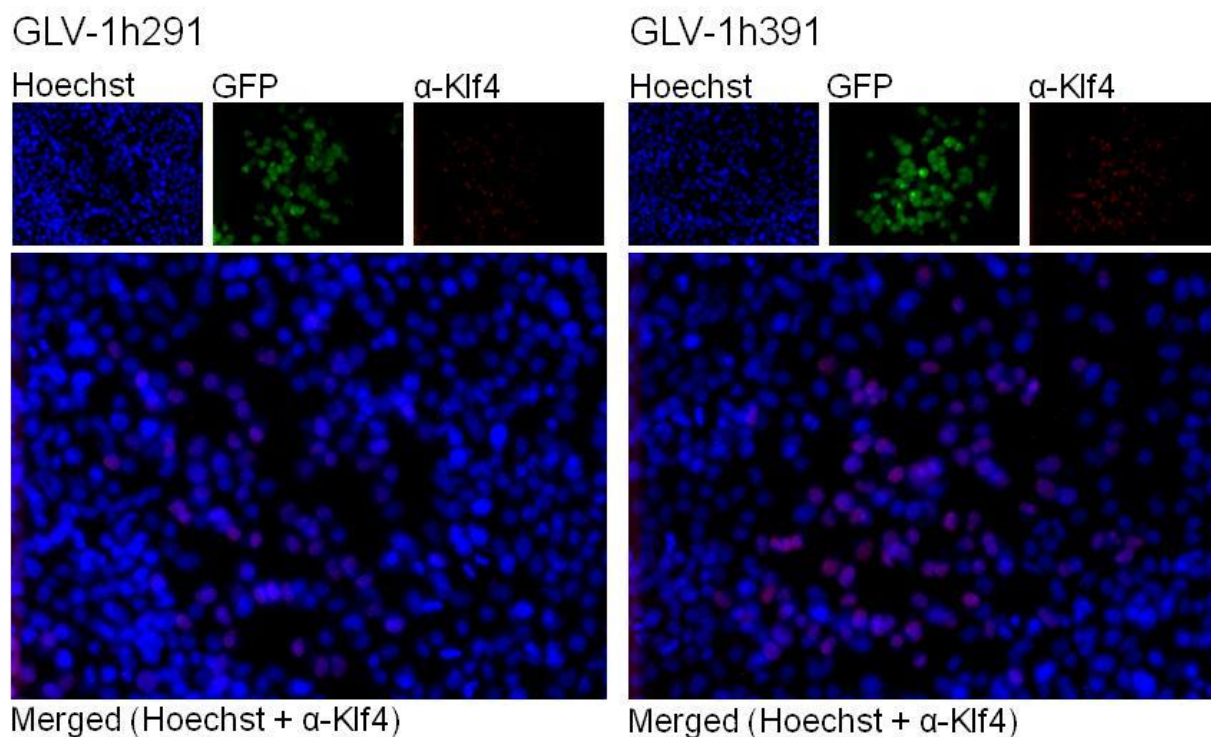
HT-29 cells were infected at an MOI of 0.01 to obtain single, isolated plaques and stained for beta-galactosidase expression. The new recombinant virus strain GLV-1h391, as well as the parental strain GLV-1h68 and GLV-1h291, express functional beta-galactosidase. Pictures were taken at a 100x magnification.

Figure 4.46 shows the beta-galactosidase expression in virus infected A549 cells. The new virus strains GLV-1h391, as well as both control viruses, express functional beta-galactosidase in infected cells.

### **4.3.1.7.2 Analysis of Ruc-GFP and Klf4 expression in infected A549 cells by immunocytochemistry**

For detection of Ruc-GFP fusion protein and Klf4 expression in the new virus construct, A549 cells were infected with GLV-1h391 as well as GLV-1h68 and GLV-1h291 as negative and positive controls at an MOI of 0.01 to obtain single, isolated plaques. Cells were then fixed and permeabilized to allow antibody binding. For detection of Klf4, cells were incubated with a polyclonal rabbit-anti-Klf4 antibody and a Rhodamin-labeled secondary anti-rabbit antibody. To analyze the cellular location of Klf4, cell nuclei were stained with Hoechst. Monochromal images were taken with a digital CCD camera and pseudo-colored using the open-source software GIMP 2.6. Expression of functional *Renilla* luciferase-green fluorescent protein fusion protein was detected by direct fluorescence microscopy.

## RESULTS



**Fig.4.47 – Analysis of Klf4 and GFP expression in A549 cells infected with GLV-1h291 and GLV-1h391**  
A549 cells were infected at an MOI of 0.01 with GLV-1h291 and GLV-1h391 to obtain single, isolated plaques. Cells were then fixed, permeabilized and incubated with a primary polyclonal rabbit-anti-Klf4 antibody (1:250 dilution). Subsequently, cells were stained with an Rhodamin-conjugated secondary antibody (1:500). Cell nuclei were counterstained with Hoechst and GFP and Klf4 expression was analyzed. Pictures were taken with a digital CCD camera with an inverted fluorescence microscope and pseudo-colored and edited using the open-source software GIMP2.6 Pictures were taken at 200x magnification.

Figure 4.47 shows that HT-29 cells infected with GLV-1h391 efficiently expressed detectable levels of Klf4-TAT. Klf4-TAT signal was detected in virus-infected plaques only, in comparable levels to GLV-1h291. Overlays of Klf4 signal and Hoechst staining demonstrated nuclear localization of the protein. This indicates that the fusion of a C-terminal TAT sequence does not affect the transportation of Klf4 through the nuclear pores into the cell nucleus. Overall, Klf4-TAT expression is equally efficient to Klf4 expression of GLV-1h291-infected cells with no signs of reduced functionality.

### **4.3.1.7.3 Analysis of Klf4 expression in GLV-1h391-infected HT-29 cells by Western Blot**

To verify the protein expression of Klf4 in virus infected HT-29 cells, Western blot analysis was performed. Cells were infected with GLV-1h68 as a negative control and GLV-1h291 as a positive control or GLV-1h391 at an MOI of 5.0 to synchronize the infection. Infected cells were incubated for 24 hours and harvested subsequently. Samples were processed and total protein amounts were determined. For Western blot analysis, 20  $\mu$ g total proteins per sample were used. SDS-PAGE and Western blotting was performed prior to antibody

## RESULTS

binding. Histone H3 antibodies were used as a loading control and polyclonal rabbit-anti-Klf4 antibodies for detection of the recombinant viral gene product. The blot was developed by colorimetric detection. Histone H3 has a predicted molecular mass of 15 kDa while the band can be detected around 17 kDa. The predicted molecular mass of Klf4 is 50 kDa while the protein band can be detected around 60 kDa. The predicted molecular mass of Klf4-TAT is slightly higher due to the fusion of twelve additional amino acids at the C-terminus of the protein.

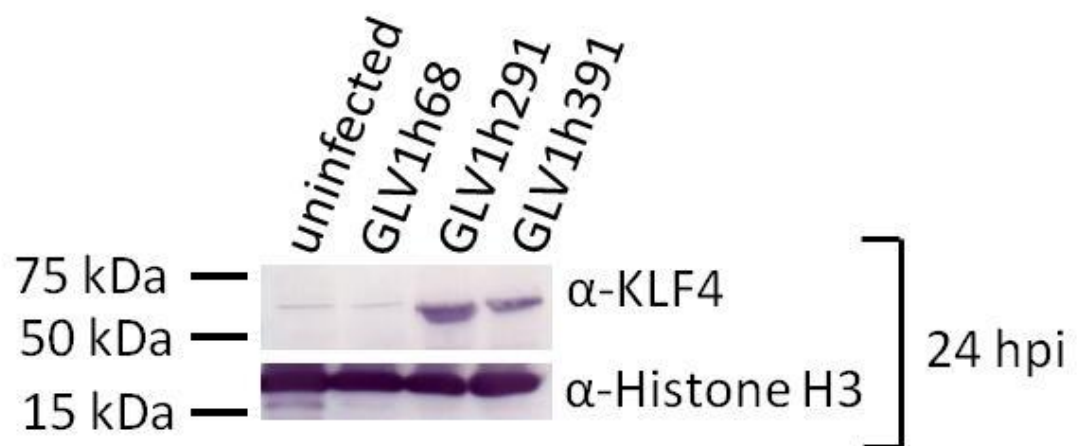


**Fig.4.48 – Western blot analysis Klf4 and Klf4-TAT in infected HT-29 cells**

HT-29 cells were either infected with GLV-1h68, Klf4-expressing GLV-1h291 or Klf4-TAT-expressing GLV-1h391 at an MOI of 5.0 for 24 hours. Samples were harvested and processed for Western blot analysis. The primary Klf4 antibody was used at a dilution of 1 µg/mL while the primary Histone H3 antibody was used at a dilution of 1:5000 due to its high abundance. The blot was visualized by colorimetric detection.

As seen in Fig.4.48, both, GLV-1h291- and GLV-1h391-infected HT-29 cells contained detectable levels of Klf4 whereas only low intrinsic base line levels of Klf4 were detectable in mock-infected and GLV-1h68-infected cells. Therefore, Klf4-TAT expression is positively confirmed in GLV-1h391. As expected, the detected Klf4-TAT protein is slightly bigger than the original untagged Klf4.

### **4.3.1.8 Cell viability of HT-29 cells infected with vaccinia viruse strain GLV-1h391**

The oncolytic potential of *klf4-TAT*-encoding GLV-1h391 in HT-29 cell culture was tested next. Cells were seeded to a confluence of 95% and either mock-infected or infected with GLV-1h391. As a reference, confluent HT-29 cells were also infected with the control strain GLV-1h189. Cells were infected with an MOI of 0.1 and 1.0, respectively to analyze dose-dependency. The infection was followed for 72 hours and samples were analyzed 0, 24, 48, and 72 hours post infection.

## RESULTS

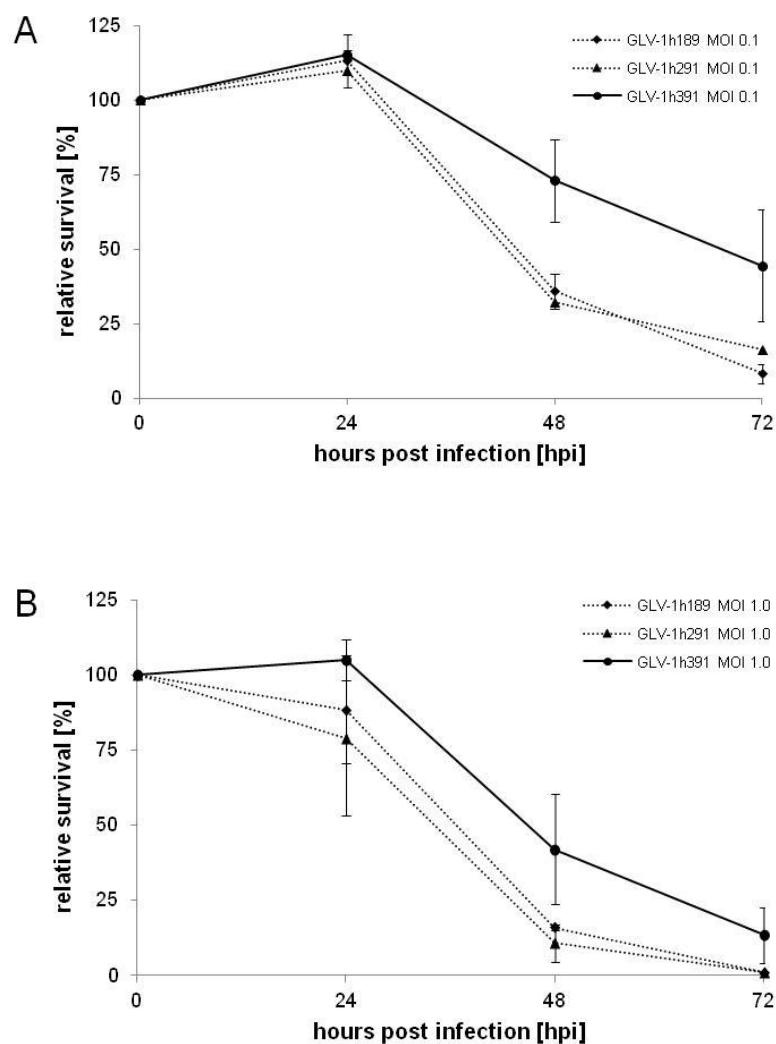


**Fig.4.49 – Viability of HT-29 cells after infection with GLV-1h189, GLV-1h291, and GLV-1h391**

Analysis of cell viability of HT-29 cells after infection with replication-competent vaccinia viruses GLV-1h189, GLV-1h291, and GLV-1h391, using MOIs of 0.1 (A) and 1.0 (B), respectively. Viability was monitored over the course of 72 hours and was measured in triplicates and averaged. Plotted averages are normalized against uninfected controls of each time-point which were considered to be 100% viable and from three independent experiments.

Cell viability assays revealed that the new KLF4-TAT-encoding vaccinia virus strain GLV-1h391 was about 10-fold less cytotoxic compared to the control viruses GLV-1h189 and GLV-1h291. While infection with GLV-1h291 reproduced similar results as shown in before (Fig.4.42), cells infected with GLV-1h391 showed a better overall survival over the course of 72 hours of infection. This effect takes effect after only 24 hours of infection ( $105.11 \pm 11.69\%$  viable in GLV-1h391-infected cells at MOI 1.0 compared to  $88.48 \pm 18.00\%$  in GLV-1h189-infected cells or  $79.02 \pm 25.19\%$  in GLV-1h291-infected cells). After 48 hours of infection, the cytotoxic effect of GLV-1h189 ( $35.96 \pm 5.96\%$  and  $15.86 \pm 0.83\%$  viable for MOI 0.1 and 1.0, respectively) and GLV-1h291 ( $32.35 \pm 18.39\%$  and  $10.71 \pm 6.15\%$  viable)



## RESULTS

impacts cell viability much more than infection with GLV-1h391 ( $73.09 \pm 13.74\%$  and  $41.90 \pm 12.67\%$  viable, respectively). In summary, the Klf4-TAT expressing virus strain GLV-1h391 exerts a cytotoxic effect on HT-29 cells upon infection, which is approximately 10-fold lower compared to GLV-1h189 or the Klf4 expressing GLV-1h291.

### 4.3.1.9 Functional analysis of virus-mediated Klf4-TAT expression

#### 4.3.1.9.1 Effects of Klf4-TAT expression on cellular beta-catenin levels in GLV-1h391 infected HT-29 cells

To analyze whether the addition of a C-terminally located TAT sequence affects the functionality of Klf4, confluent HT-29 cells were either mock-infected or infected with GLV-1h291 or GLV-1h391 at an MOI of 5.0. As a control, HT-29 cells were infected with GLV-1h189 at an MOI of 5.0. Cells were incubated for 48 hours and samples were then processed for quantification by ELISA. Total protein amounts were adjusted to 50  $\mu\text{g}$  per sample. Amounts of cellular beta-catenin were quantified following the manufacturer's instructions.

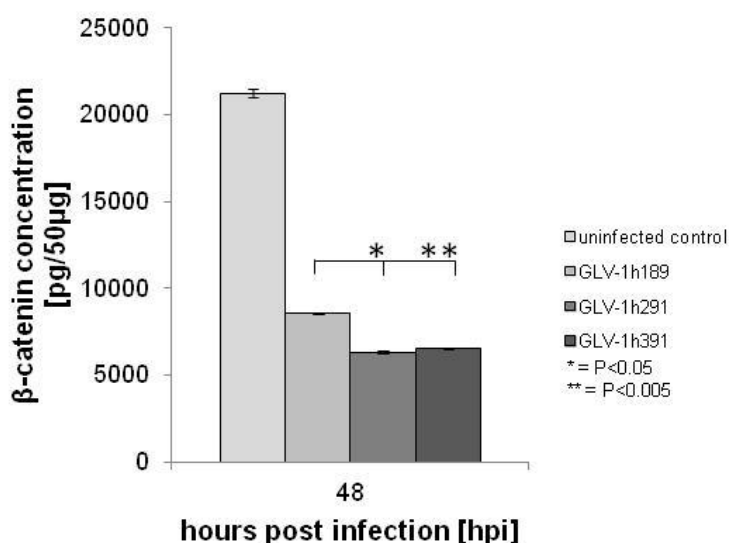


**Fig.4.50 – Cellular beta-catenin protein levels in HT-29 after infection with GLV-1h391**

HT-29 cells were either mock-infected or infected with GLV-1h291 and GLV-1h391, respectively, at an MOI of 5.0. GLV-1h189 was used as a control virus. Infected cells were incubated for 48 hours and total protein was isolated and prepared for ELISA quantification of beta-catenin levels. ELISA was performed according to manufacturer's instructions and beta-catenin levels were plotted with standard deviations.

The fusion of a C-terminal TAT sequence to Klf4 does not affect its potential to decrease cellular beta-catenin levels in infected HT-29 cells in culture (Fig.4.50) Detected levels of beta-catenin in mock-infected, GLV-1h189-infected, and GLV-1h291-infected cells correspond well with previously obtained data (Fig.4.44) Beta-catenin levels in GLV-1h291-

## RESULTS

and GLV-1h391 infected HT-29 cells are identical and significantly lower compared to uninfected cells and control virus. This is an indication for functionality of Klf4-TAT.

### 4.3.1.9.2 Effects of Klf4-TAT on cell proliferation

To analyze the ability of Klf4-TAT to penetrate cytoplasmic membranes, CV-1 cells in confluent T225 flasks were infected with  $1 \times 10^7$  pfu of GLV-1h391 until CPE was observed 48 hours post infection. Cells were then mechanically harvested and pelleted. Cell pellets underwent three freeze-thaw cycles and were subsequently resuspended in 15 mL medium. Cell suspensions were then sonicated to break up cell membranes and treated with benzonase to release Klf4-TAT into the supernatant. The suspension was sterile-filtered using Amicon-15 Ultra tubes with a NMWL of 100 kDa. The flow-through was concentrated using Amicon-15 Ultra tubes with a NMWL of 10 kDa. The concentrated fraction was suspended in fresh HT-29 growth medium. HT-29 cells were seeded as triplicates at a cell number of  $1 \times 10^3$  in 96-well plates and incubated with the conditioned growth medium for 72 hours. Cell numbers were determined at 0, 24, and 48 h post treatment by XTT cell proliferation assay.

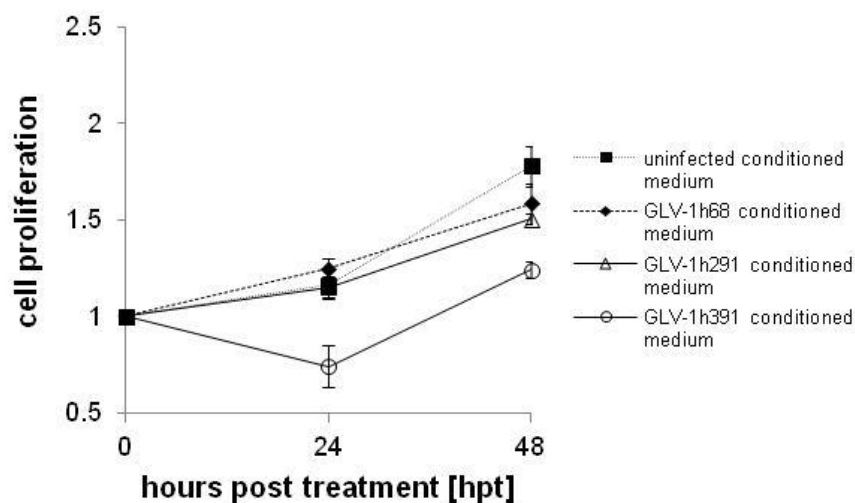


**Fig.4.51 – Cell proliferation of HT-29 cultured in conditioned medium**

A total of  $1 \times 10^3$  HT-29 cells were seeded into 96-wells as quadruplicates and treated for 48 h with conditioned media from sterile-filtered and concentrated suspensions of CV-1 cells which were either mock-infected or infected with GLV-1h68, GLV-1h291, or GLV-1h391. At 0, 24 and 48 hours post treatment, cell proliferation was analyzed by XTT assay.

It was observed that HT-29 cells cultured in conditioned media from GLV-1h68- and GLV-1h291-infected CV-1 cells proliferated at a slightly faster rate than the untreated controls after 24 hours. Cells cultured in conditioned medium from GLV-1h391-infected CV-1 cells grew slower than the untreated controls. This is an indirect indication that Klf4-TAT in the conditioned media (Fig.4.51) is able to penetrate cytoplasmic membranes to slow down cell

## RESULTS

proliferation. Increased proliferation rates seen in cells cultured with GLV-1h68/291-derived conditioned media are likely linked to vaccinia virus growth factor present in the conditioned medium<sup>179</sup>.

### 4.3.1.10 Effects of a single dose of GLV-1h205 or GLV-1h321 in subcutaneous A549 xenografts

It was demonstrated in cell culture experiments, that GLV-1h291 and GLV-1h391 both, efficiently infected, replicated in, and lysed HT-29 colorectal cancer cells in culture. Both viruses trigger expression of functional Klf4 or Klf4-TAT and marker proteins Ruc-GFP and beta-Galactosidase upon infection. To investigate whether Klf4/Klf4-TAT expression in colorectal cancer cells results in beneficial therapeutic treatment, athymic nude mice were subcutaneously implanted with  $5 \times 10^6$  HT-29 cells. This cell line was chosen based on its non-responder behavior in xenograft models<sup>202</sup> and was assumed to give the clearest indication on benefits upon Klf4/Klf4-TAT expression as treatment with GLV-1h68 does not result in significant tumor growth inhibition. Tumor-bearing mice were injected either with  $5 \times 10^6$  pfu of GLV-1h68, GLV-1h291, GLV-1h391 (n=10), or PBS only (n=5) when the tumor volume reached an average of 250 mm<sup>3</sup>. Tumor volume was measured twice a week with a digital caliper.

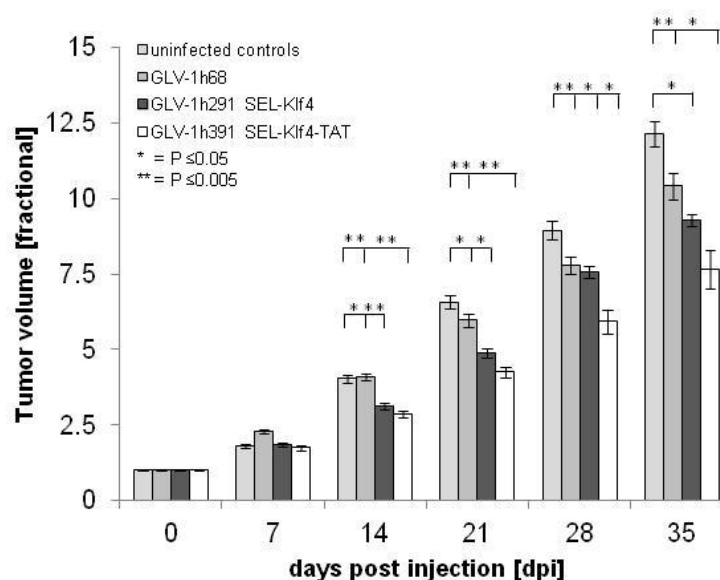


**Fig.4.52 - Effects of a single administration of  $5 \times 10^6$  pfu/100  $\mu$ l PBS of Klf4/Klf4-TAT-encoding vaccinia viruses on tumor development of HT-29 tumor-bearing mice**

HT-29 cells were implanted subcutaneously in the right hind leg of athymic nude mice and Klf4/Klf4-TAT-encoding virus strains were tested against PBS or GLV-1h68 treatment. Averaged fractional tumor volume (FTV) of [n=10 for virus-treated, n=5 for PBS treated controls] mice is plotted and one-way analysis of variance (ANOVA) was used to compare the corresponding data points.  $P \leq 0.05$  was considered statistically significant; \* =  $P \leq 0.05$ , \*\*  $P \leq 0.005$

## RESULTS

Fourteen days post injection, a single dose of either GLV-1h291 or GLV-1h391 significantly inhibited overall tumor growth during the course of the experiment compared to untreated controls and GLV-1h68-treated animals (Fig.4.52). Between GLV-1h291 and GLV-1h391 treatment groups, tumor growth inhibition was more efficient in the Klf4-TAT-encoding GLV-1h391 virus treatment group compared to the GLV-1h291 treatment group, becoming statistically significant after 28 days of treatment. A slight decrease in net body weight could be observed after injection but generally, GLV-1h291 and GLV-1h391 viruses were better tolerated by the treated animals than GLV-1h68. To further quantify the effects of GLV-1h291/391 on HT-29 tumor growth, animals were followed for survival and the mean time to reach 10 times the initial starting volume,  $FTV = 10V(0)$  was calculated for each of the groups.

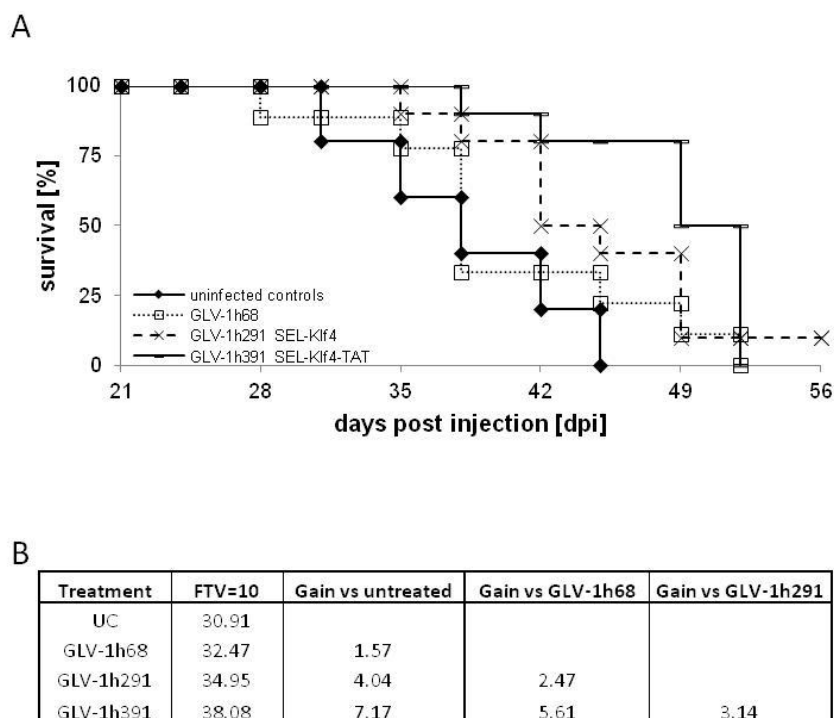


**Fig.4.53 – Kaplan-Meier survival diagram and survival benefits of HT-29 tumor-bearing mice**

Survival rates of untreated and virus-treated mice were analyzed over the course of 56 days and plotted as a Kaplan-Meier survival diagram (A). The mean time to reach  $FTV = 10(0)$  was calculated for each group and gains were plotted in (B).

Supporting the previously obtained data (Fig.4.52), overall survival after 49 days of treatment was higher in the GLV-1h391 treatment group (80%) compared to untreated (0%) and treated control groups (10% in GLV-1h68/291-treated animals) (Fig.4.53). Overall, GLV-1h291-treated animals showed a 4.04-day gain against untreated animals and a 2.47-day gain against GLV-1h68-treated animals. Animals treated with GLV-1h391 showed a 7.17-

## RESULTS

day gain versus untreated, a 5.61-day gain versus GLV-1h68-treated, and a 3.14-day gain versus GLV-1h291-treated animals, making it the most efficient treatment regimen in all tested groups.

### 4.3.1.11 Pfu determination in HT-29 tumor-bearing mice injected with GLV-1h68, GLV-1h291, and GLV-1h391 at 21 days post injection

The viral distribution in the HT-29 tumors of the different treatment groups (n=5) was analyzed at 21 days post virus injection, when tumor growth inhibition in Klf4/Klf4-TAT-encoding virus groups was statistically significant. Viral titers were determined to analyze whether treatment efficacy was correlated to virus replication. Animals were sacrificed and tumors surgically removed. Virus titers were determined by standard plaque assays from tumor lysates.

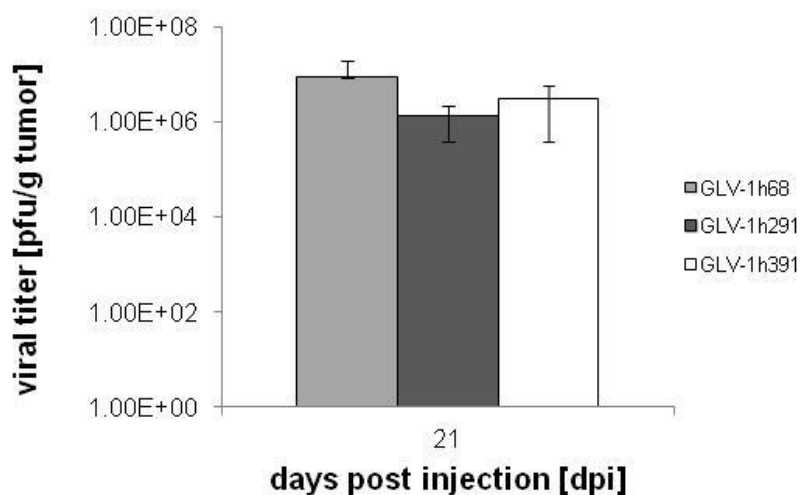


**Fig.4.54 – Viral distribution in HT-29 tumor-bearing mice injected at 21 dpi**

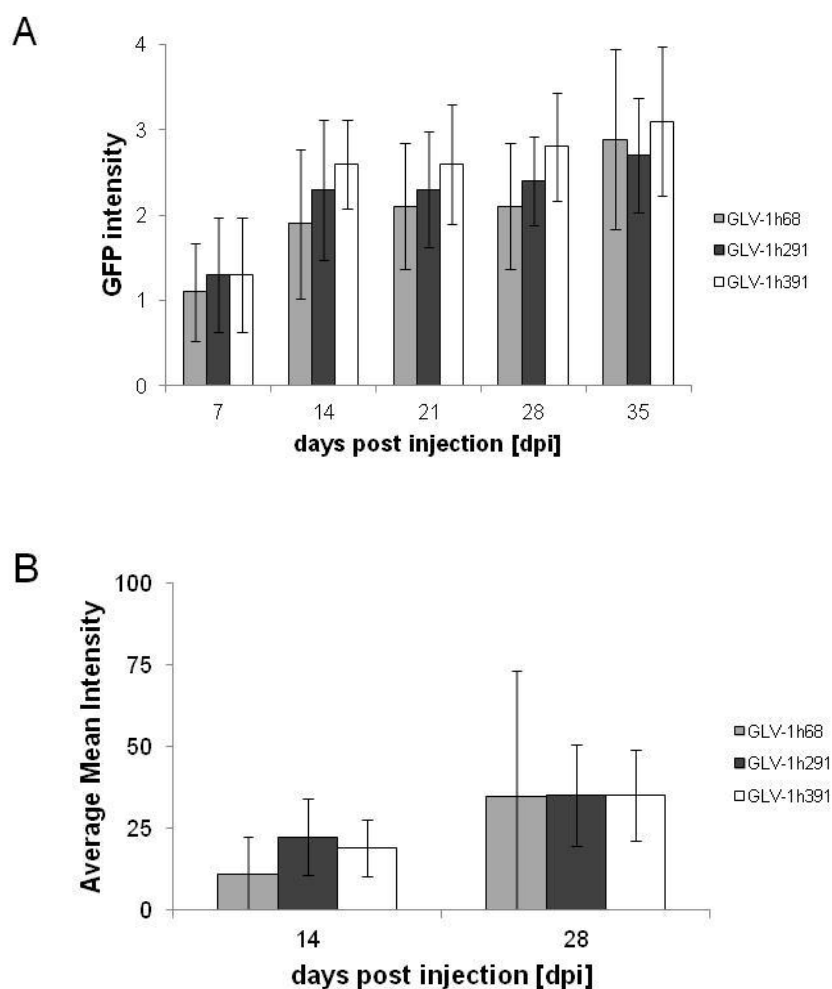
HT-29 tumor-bearing mice were sacrificed [n=5] at 21 days post virus treatment when tumor volumes of GLV-1h291-treated and GLV-1h391-treated animals were significantly smaller than tumors of untreated and GLV-1h68-treated controls. Standard plaque assays from tumor lysates were performed and viral titers were determined and plotted as pfu/g tumor tissue.

Figure 4.54 shows that viral titers after 21 days of treatment are at comparable levels, indicating an efficient tumor colonization of all three recombinant viruses. Averaged titers in the GLV-1h68 treatment group animals were higher compared to GLV-1h291/391 treatment groups, corresponding with the replication efficacy of GLV-1h291/39 compared to control viruses observed in cell culture experiments (Fig.4.45).

## RESULTS

### 4.3.1.12 Analysis of viral tumor infiltration, infection and replication by imaging of viral marker gene (Ruc-GFP) expression

To further assess viral spreading and replication in the tumor tissue, viral GFP expression was followed during the course of the experiment by determining the strength of the signal. GFP expression of animals of each group (n=10) was monitored under blue light using a stereo fluorescence macroimaging system once a week over the course of five weeks. GFP intensity is determined by using a four stage scoring system; 0) no GFP signal, 1) one spot, 2) two or three local spots, 3) diffuse signal from half the tumor, 4) strong signal from whole tumor. Additionally, animals (n=5) were imaged for *Renilla* luciferase expression at day 14 and 28 post virus injection. Results were quantified and averaged for each treatment group.



**Fig.4.55 - Detection of viral *Renilla* luciferase-green fluorescent protein at the local tumor site of HT-29 tumor-bearing mice.**

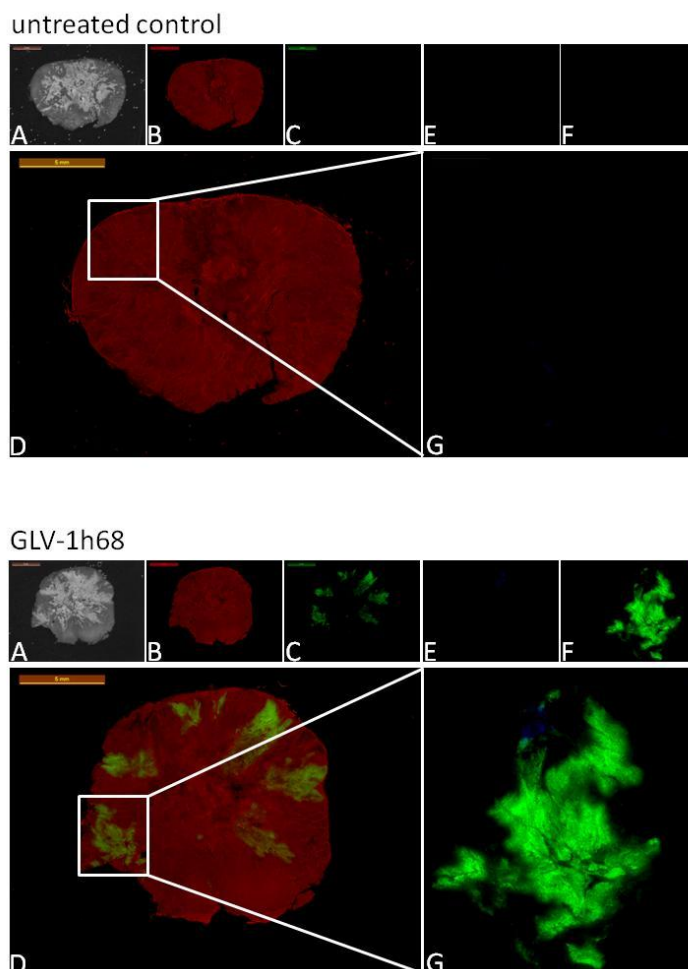
A) Analysis of GFP signal strength during the course of the experiment. GFP intensity was determined by using a four stage scoring system; 0) no GFP signal, 1) one spot, 2) two or three local spots, 3) diffuse signal from half the tumor, 4) strong signal from whole tumor. B) Quantified and averaged luciferase imaging of GFP expression at the local tumor site at 14 and 28 days post injection.

## RESULTS

As presented in figure 4.55, GFP fluorescence was clearly visible from as early as 7 days post injection on and increased over the course of the experiment. No significant differences in treatment groups were observed and all groups showed efficient colonization of the tumor site, infiltration into tumor cells and viral replication indicated by GFP marker gene expression. Luciferase signals corresponded with GFP expression (data not shown), showing an increase in signal from 14 days to 28 days post injection. No significant differences in signal strength were obtained.

### 4.3.1.13 Histochemical analysis of viral tumor infiltration and gene expression

To analyze the colonization of the primary tumor by oncolytic vaccinia viruses in more detail, animals were sacrificed after 21 days of treatment, when differences in tumor volume were statistically significant for seven days. The primary tumors were surgically removed and tissue sectioning was performed as described in section 3.6.6. Sections were incubated with Phalloidin-TRITC as an indicator for live cell staining. The following section was then incubated with a primary polyclonal antibody to Klf4 and a 594-conjugated secondary antibody to allow for Klf4 detection in GFP<sup>+</sup> virus-infected patches. Direct fluorescence was used for GFP detection as a tool to localize active virus as the half-life of GFP is 24 hours.



## RESULTS

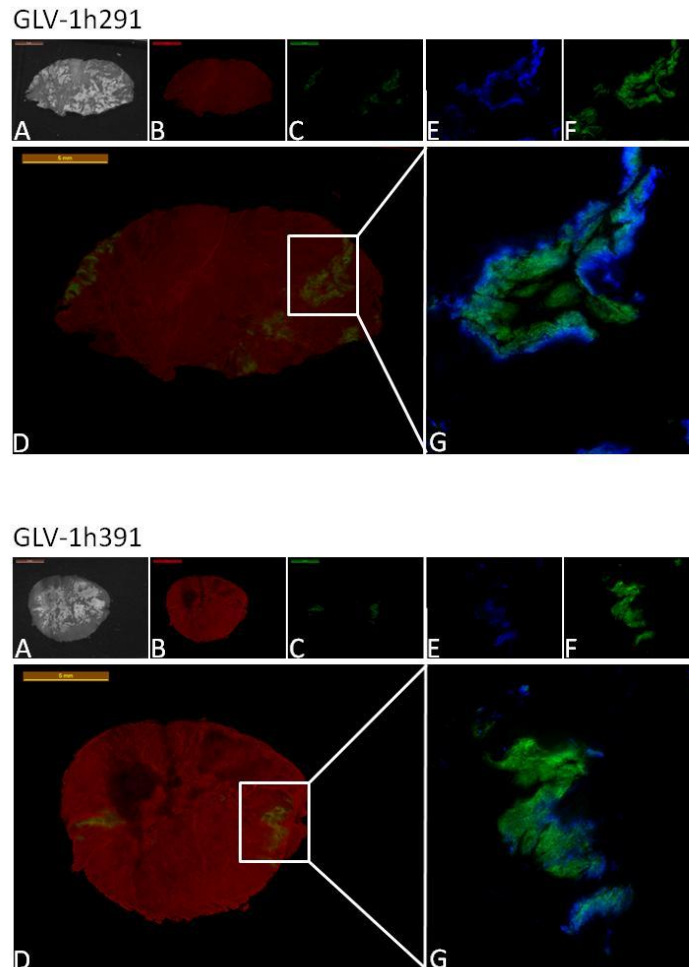


**Fig.4.56 - Histochemical staining of HT-29 tumor sections**

Untreated and treated mice were sacrificed 21 dpi. Whole tumor cross-sections [A] (thickness = 100  $\mu\text{m}$ ) were labeled with Phalloidin-TRITC [B] to detect actin as an indicator for live cells and analyzed for virus colonization by GFP detection [C]. Overlays [D] indicate virus distribution in the tumor. Following sections were labeled with Klf4 antibody [E] to detect Klf4 expression in the tumor tissues. GFP<sup>pos</sup> virus patches [F] were identified in whole tumor cross-sections, magnified and merged to analyze virus-mediated Klf4 expression [G]. Pictures were taken with a digital CCD camera and edited and pseudo-colored using open-source software GIMP 2.6.

Analysis of GFP expression shows that all three tested viruses are capable of efficiently colonizing subcutaneously implanted HT-29 tumors in a xenograft mouse model (Fig.4.56). However, Klf4 expression was only detected in tumors from animals treated with GLV-1h291 or GLV-1h391. Interestingly, Klf4 was mainly detected at the edge of virus patches.



## 5 Discussion

With an estimated 12.7 million new cancer cases worldwide in 2008 and a corresponding number of 7.6 million cancer deaths<sup>1</sup>, it is evident that development of novel therapeutic approaches, as stand-alone treatments or in combination with conventional treatment options, is crucial. In recent years, oncolytic virotherapy has emerged as one of the most promising new fields in cancer therapy, offering high tumor selectivity and little side effects. Results with several different viruses have been so promising that several clinical trials are currently ongoing and the adenovirus H101 was the first oncolytic virus approved for the treatment of head and neck cancer in man in China<sup>152</sup>. Finding novel treatments for gender-independent cancers with poor prognosis like lung cancer and late stage colorectal cancer might be of special interest as they likely offer the opportunity to treat a broad spectrum of patients suffering from the disease.

Along with new cancer treatment regimes being explored and pushing to the market, compelling new research in the biology of cancer is published, with a major focus on cancer stem-like cell biology and its importance in cancer therapy. The shared biological features between stem cells and cancer stem-like cells (self-renewal and pluripotency<sup>126</sup>, survival mechanisms<sup>129</sup>, quiescence and longevity<sup>110</sup>, and cell surface marker expression<sup>124</sup>) and the close biological relation of stem cells and cancer stem-like cells<sup>125</sup> suggest that master key regulators in stem cell biology might also play an important role in cancer biology. Amongst several cell surface markers, cellular levels of stem cell transcription factors Nanog and Oct4, are oftentimes found up-regulated in cancer tissues and are frequently used as intracellular markers for cancer stem-like cells<sup>203</sup>. While Oct4 was part of the original “Yamanaka Factors” that were shown to initiate reprogramming in terminally differentiated cells to a pluripotent ground state<sup>47</sup> and founded the field of induced pluripotent stem (iPS) cells, Nanog was only later shown to be involved in more efficient reprogramming<sup>75</sup>. To date, retro- or lentiviral expression of Oct4 and Nanog served the purpose of reprogramming of somatic cells into iPS cells<sup>204</sup> or the generation of artificial cancer stem-like cell population<sup>205</sup>. Interestingly, Chiou *et al.* demonstrated, that Nanog and Oct4 are upregulated in lung adenocarcinoma patients and might positively regulate tumor metastasis through enhancing EMT<sup>78</sup>. A major part of this study focused on the effects of virus-mediated expression of cancer stem-like cell characteristic Nanog and Oct4 and its effect on therapeutic efficacy and diagnosis.

In the second part of this study, the potential of oncolytic recombinant vaccinia viruses in the treatment of colorectal cancer was investigated. Late-stage colorectal cancer is still correlated with a poor survival prognosis and even though surgery and combination with

## DISCUSSION

chemotherapy only significantly improves survival if the cancer is detected early on. The development of treatment regimens that improve late-stage colorectal cancer is therefore crucial. Furthermore, the role of virus-mediated Klf4 expression, a tumor suppressor in colorectal cancer, on therapeutic outcome was investigated.

### **5.1 Two new stem cell transcription factor-encoding recombinant vaccinia virus strains show oncolytic potential in A549 non-small cell lung carcinoma**

Nanog and Oct4 are two key regulators in stem cells, ensuring self-renewal and pluripotency by controlling an impressive interactome of proteins<sup>57</sup>. However, both transcription factors are also likely to play an important role in aggressiveness of cancer. Two different vaccinia virus strains were engineered to investigate the role of virus-mediated Nanog and Oct4 expression in the context of oncolytic virotherapy. GLV-1h205 carries the gene for human Nanog under the control of the synthetic early promoter while GLV-1h208 carries the gene for human Oct under the control of the same promoter.

In initial experiments, the new virus strains were characterized for their replication potential and marker gene expression in human cancer cells in culture. While both viruses replicated well in at least two different human cancer lines, the Nanog-encoding GLV-1h205 strain showed superior replication when compared to GLV-1h208 and the parental control virus GLV-1h68. Analysis of the replication factors of GLV-1h68 and GLV-1h205 especially in the first 48 hours of infection using a low MOI of 0.01 revealed that GLV-1h205 replicated faster than its parental strain GLV-1h68. This may be caused either by the payload function in the cell or on the differences between promoter strengths as described by Chen *et al*<sup>206</sup>. Virus replication efficiency was found to be inversely proportionate to the added strength of promoters linked to foreign genes inserted into the viral genome<sup>206</sup>. The parental GLV-1h68 encodes for *gusA* in the A56R locus which is under control of the P<sub>11</sub> promoter while this gene is replaced by *nanog* under control of the synthetic early promoter in GLV-1h205 and *oct4* under control of the synthetic early promoter in GLV-1h208. The P<sub>11</sub> promoter strength is comparable to the strong synthetic late promoter while the expression of genes under the control of synthetic early promoters is considerably weaker<sup>207</sup>. Furthermore, mRNAs of genes under control of the early promoter can be detected as early as 20 minutes after infection and peak in their levels around 100 minutes post infection and have a half-time of 30 min after reaching their maximum expression. Late gene mRNAs are not detected until 140 minutes after infection and cellular levels increase during the course of infection<sup>208</sup>. Thus, it is to be expected that viral replication of GLV-1h205 and GLV-1h208 in comparison to the parental GLV-1h68 is more efficient. However, the impaired ability of GLV-1h208 to replicate might hence be payload-driven.

## DISCUSSION

Ruc-GFP mRNA as well as Nanog mRNA or Oct4 mRNA transcripts, respectively, were detected as early as two hours after infection. While Ruc-GFP mRNA was found in the parental strain and the new recombinant virus strains, Nanog mRNA expression was confined to GLV-1h205-infected cells and Oct4 mRNA expression to GLV-1h208-infected cells, proving the correct insertion of the respective gene cassette into the A56R locus. All three tested genes are under the control of either the synthetic early (*nanog*, *oct4*) or synthetic early/late (*ruc-gfp*) promoter, therefore transcript detection as early as two hours of infection was to be expected<sup>208</sup>.

The correct expression and translation of the two remaining marker genes *lacZ* and *ruc-gfp* was tested in the new virus strains. Both new strains express both, functional beta-galactosidase and *Renilla* luciferase-green fluorescent protein (Ruc-GFP) in comparable levels to the parental strain GLV-1h68 and therefore offer different ways of imaging modalities to monitor viral infection. The expression of Nanog was tested by immunocytochemistry experiments and quantified using ELISA. Nanog protein was expressed and transported into the cell nucleus indicating functionality. Translocation of Nanog into the nucleus is mediated by an intrinsic nuclear localization sequence<sup>67</sup>. ELISA quantification showed that highest levels of Nanog protein were detected between 6 and 24 hours of infection during a synchronized infection. Decreasing protein levels are likely to be explained by the downregulation of viral gene expression of genes under the control of early promoters and the relatively short half-life of the mRNA transcripts<sup>208</sup> as well as increasing cell death caused by the viral infection. Also, the protein half-life of 120 min<sup>209</sup> will play an important role in the sustainment of Nanog levels during the course of infection. Similar results were obtained for GLV-1h208-mediated Oct4 expression. Oct4 was detected upon virus infection using immunocytochemistry and located in the nucleus of the infected cells. Like for Nanog upon infection with GLV-1h205, no Oct4 was detected in uninfected cells or cells infected with GLV-1h68, indicating that Oct4 expression is exclusively mediated by GLV-1h208. Oct4 was detected as early as three hours post infection by Western blot and protein levels peaked between 6 and 24 hours of infection after a synchronized infection. As for Nanog, protein levels during the course of infection are likely to be affected by transcription control, protein half-life and cell death. GLV-1h205 and GLV-1h208 both express all three recombinant genes in the expected manner.

Both new virus strains still retained the cytotoxic potential of the parental strain GLV-1h68. However, GLV-1h205 showed slightly higher cytotoxicity in A549 cells compared to GLV-1h68 whereas GLV-1h208 showed impaired cytotoxic potential. Differences in cytotoxicity between GLV-1h68 and GLV-1h205 are likely caused by the faster replication rate in GLV-1h205. However, even though compared to GLV-1h68, the new GLV-1h208 strain theoretically has a lower payload burden by exchanging *gusA* under control of the P<sub>11</sub>

## DISCUSSION

promoter with *oct4* under the control of the synthetic early promoter, replication and cytotoxicity are impaired. It can be speculated that this is an effect triggered by the *oct4* gene product itself.

Nanog overexpression in human embryonic stem cells leads to accelerated transition from G0/G1 into the S phase of the cell cycle and cell proliferation by interacting with CDK6 and CDC25A<sup>74</sup>. Cell proliferation is aberrant and uncontrolled in cancer cells and thus undesirable for any cancer treatment regimen. Therefore, the effect of virus-mediated Nanog expression on cell cycle progression in cultured A549 cells was analyzed. After synchronization of cells in the G2/M phase and subsequent release, treatment with GLV-1h205 for 6 hours did not lead to an observable progression of cells from G0/G1 to S phase. Vaccinia virus infection leads to a block in host transcription and protein synthesis from as early as two hours post infection<sup>210</sup> on and eventually causes cell death. The hostile takeover of the cell and virus-mediated cell death make an impact of Nanog on cell proliferation unlikely. However, vaccinia virus has been shown to actively modulate the expression of cellular regulators of the cell cycle towards a progression from G0/G1 to S phase<sup>211</sup>. Also, vaccinia virus infection leads to the expression of vaccinia growth factor (VGF), a homologue of epidermal growth factor (EGF) which facilitates the spreading of the infection. Nanog mRNA will be transcribed and translated as early as 20 minutes after virus infection, giving the gene product a short window of action in the infected cell. It can be speculated that preparations on transitioning from G1/G0 to S phase mediated by Nanog may be beneficial for virus replication and thus improve the cytotoxicity of recombinant vaccinia viruses, cumulatively adding to the exogenous function of vaccinia virus growth factor.

It has been shown that co-expression of the transcription factors Nanog and Oct4 leads to enhanced malignancy in lung adenocarcinomas by promoting epithelial-mesenchymal-transition (EMT) and thus, facilitation of metastasis<sup>78</sup>. Infection with GLV-1h205 or GLV-1h208 alone did not increase transcription of *nestin*, *slug*, or *snail*, which are involved in EMT. Also, no upregulation of CD133 was observed. It can be concluded that infection with a stem cell transcription factor expressing vaccinia virus strain does not lead to promotion of EMT or cancer stem-like cell properties in infected cells.

### **5.2 Therapeutic efficacy of GLV-1h205 and GLV-1h208 in mouse xenografts**

Both new recombinant virus strains were tested for their therapeutic efficacy and safety in a mouse xenograft model. Therefore, A549 tumor-bearing athymic nude mice were injected with a single dose of the respective virus strains or GLV-1h68 as a control. Treatment of A549 tumors with GLV-1h68 lead to tumor inhibition after 28 days of treatment with subsequent tumor regression. Tumor regression in GLV-1h68-treated A549 tumors did not follow the three phase model postulated by Zhang *et al.* for mammary carcinoma

## DISCUSSION

xenografts<sup>183</sup>. Whereas the tumor inhibition (Phase II) and regression (Phase III) show similar characteristics, alterations in the growth phase (Phase I) were observed. In contrast to mammary carcinoma xenografts, vaccinia virus-treated A549 tumors did not grow larger as their respective untreated controls in the early course of treatment. However, treatment with GLV-1h205 was significantly more efficient compared to animals injected with GLV-1h68 or GLV-1h208. The onset of tumor inhibition was observed about 7 days earlier compared to both other strains and faster, more efficient tumor regression led to an almost complete tumor regression in treated animals. The tumor burden was approximately three times higher in GLV-1h68- or GLV-1h208-treated animals. It can be assumed that the increased replication rate in GLV-1h205 compared to GLV-1h68 will impact the therapeutic efficacy of the new vaccinia virus strain in mouse xenografts<sup>206</sup>. Interestingly, treatment with GLV-1h208, which also carries a weaker promoter in the A56R locus, was not as efficient. Moreover, it led to tumor inhibition after 21 days of treatment but no tumor regression was observed as it was for GLV-1h68 and GLV-1h205. Thus, it can be speculated that virus-mediated Nanog expression enhanced the efficacy of vaccinia virus treatment in mouse xenografts while Oct4 expression did not result in treatment benefits. Overall survival rates are an indication for treatment efficacy. It is noteworthy that treatment with a combination of GLV-1h205 and GLV-1h208 did not result in poor prognosis or enhanced tumor growth but also led to tumor regression. The observed tumor regression in mice treated with the virus combination indicates that either Oct4 expression impairs the efficacy of GLV-1h205 or the decrease of faster replicating GLV-1h205 simply correlates with slower tumor regression. However, virus-mediated co-expression of Nanog and Oct4 did not negatively influence treatment efficacy of oncolytic virotherapy in lung adenocarcinoma as described for co-expression of Nanog and Oct4 in lung adenocarcinoma tumor tissues alone<sup>78</sup>. Treatment with all three virus strains was well tolerated by the animals and virus was mainly detected in the tumor tissues. The presence of viruses in the tumors was generally 10,000 - 100,000-fold higher compared to tested normal body organs which documents the tumor-specific virus replication well. Amongst the three virus groups, viral titers after 21 days of treatment were highest in the GLV-1h205-treated animals, an *in vivo* reflection of GLV-1h205's superior replication rate in culture compared to GLV-1h68. Viral titers of GLV-1h208 indicate that replication catches up during the course of the infection as viral titers are comparable to GLV-1h68 after 21 but are higher after 49 days of injection. Detected virus in healthy organs can hypothetically be caused by metastasis of cancer cells from the primary tumor to distant sites. Tumor colonization of the tested vaccinia virus strains was followed by monitoring GFP marker gene expression and *Renilla* luciferase imaging. Small virus patches in the tumors were identified by GFP expression as early as 7 days post injection with increasing GFP signal over the course of the experiment. This indicates the efficient colonization of the

## DISCUSSION

tumors by vaccinia virus. Quantification of marker gene expression by *Renilla* luciferase imaging after 14 days showed significantly higher levels of photon counts in GLV-1h205-treated animals compared to GLV-1h68 and GLV-1h208. High marker gene expression is correlated to viral replication and therefore another indication for the enhanced replication in GLV-1h205, which ultimately results in a better therapeutic outcome. Quantifying marker gene expression during the early course of treatment might therefore be a useful tool to predict therapeutic outcome. Viral oncolysis was analyzed by immunohistochemistry and it was demonstrated that GLV-1h68 as well as its derivatives GLV-1h205 and GLV-1h208 efficiently colonize tumor tissues. It was shown for all three virus strains that increased GFP signals correlated with decreasing actin signals in A549 tumors, indicating an increase in virus-mediated cell death *in vivo*. Immune-related antigen profiling of tumor-bearing mice was performed 10 days after initial treatment, when viral titers in GLV-1h205-treated animals were higher than in GLV-1h68- or GLV-1h208-treated animals. Upon virus treatment, upregulation of inflammation-related antigens in treated animals was observed as described by Gentshev *et al.*<sup>184</sup>. This leads to the initiation of innate responses and recruitment of immune cells like macrophages, dendritic cells, neutrophils, and B cells, which might be sufficient to ultimately lead to tumor regression in cooperation with oncolytic processes<sup>192,212</sup>. When upregulation of immune-related antigens was normalized against treatment with GLV-1h68, Eotaxin, IL-6, IL-11 and TIMP-1 levels were approximately two-fold higher in GLV-1h205-treated animals. In animals treated with GLV-1h208 however, CD40, GCP-2, IP-10, MIP-3b, MDC, MMP-9, MCP-1, MCP-3 and MCP-5 were two-fold lower. Therefore, it is likely that the strength of the host's immune response is directly proportional to the amount of replicating vaccinia virus in the tumor tissue.

Overall, it appears that replacing the *gusA* gene in the A56R locus of GLV-1h68 under control of the P<sub>11</sub> promoter with *nanog* under control of the synthetic early promoter leads to more efficient viral replication which consequently leads to enhanced tumor regression in A549 tumors *in vivo*. However, the insertion of *oct4* into the viral genome leads to impaired viral replication and therapeutic efficacy in mouse xenograft models compared to the parental GLV-1h68 strain.

### **5.3 Is the observed enhanced therapeutic efficacy of GLV-1h205 payload- or promoter-mediated?**

To analyze whether the enhanced therapeutic efficacy observed in GLV-1h205-treated tumor-bearing mice is payload- or promoter-mediated, a new vaccinia virus strain was engineered. A genetic mutation in the gene sequence of the payload rendering it non-functional would allow for a viral gene knockout in the same locus (A56R), identical promoter strength (synthetic early), and identical gene product size, thus creating a control virus strain

## DISCUSSION

that is identical except for payload function. Therefore, the *nanog* gene sequence was analyzed and a reported NLS sequence (YKQVKT) in the homeodomain which is necessary and critical for nuclear distribution<sup>67</sup> was mutated to render the protein unable to enter the nucleus and exert its function as a transcription factors. Characterization of the new virus strain GLV-1h321 in cell culture demonstrated efficient replication and stable marker gene expression of *lacZ* and *ruc-gfp*. However, the replication factor of GLV-1h321 is similar to GLV-1h68, indicating that overexpressed functional Nanog protein may improve replication behavior of vaccinia viruses. Analysis of Nanog $\Delta$ NLS expression in cell culture was inconclusive. Immunofluorescence experiments with GLV-1h321-infected cells indicated cytoplasmic distribution, but Nanog $\Delta$ NLS was also localized in or at the nucleus. It was not possible to distinguish whether Nanog $\Delta$ NLS was located in the nucleus or only associated with the nuclear membrane. Western blot analysis revealed that protein levels of Nanog $\Delta$ NLS in GLV-1h321-infected cells were much higher compared to Nanog levels in GLV-1h205 cells. This may be attributed to the higher abundance of unbound protein in the cytoplasm. Compared to Nanog levels however, protein analysis showed higher expression levels of Nanog $\Delta$ NLS in cell culture experiments. No differences in cytotoxicity were observed in cell culture, suggesting that higher Nanog $\Delta$ NLS levels do not affect the oncolytic potential of GLV-1h321. In mouse xenograft experiments with A549 tumor-bearing mice, treatment with GLV-1h321 was less efficient as GLV-1h68 and especially GLV-1h205. Like treatment with GLV-1h68 and GLV-1h205, the administration of GLV-1h321 leads to tumor growth inhibition and regression but from 17 days post treatment, GLV-1h321 tumors were significantly bigger than tumors of animals treated with GLV-1h205. Interestingly, while virus titers in GLV-1h205 and GLV-1h321 treatment groups are comparable 14 days after infection, titers in GLV-1h321 decreased during the treatment, further correlating treatment outcome with viral replication.

Furthermore, it was analyzed whether the observed effects are tumor type-dependent by administering a single dose of GLV-1h68, GLV-1h205, and GLV-1h321, respectively, to DU-145 tumor-bearing athymic nude mice. In contrast to A549 xenografts, treatment with GLV-1h205 led to the poorest outcome among tested virus groups while GLV-1h321 and GLV-1h68 efficiently replicated in the primary tumor site and lead to tumor inhibition and regression while GLV-1h205 treatment only slowed down tumor growth.

In conclusion, this work represents the first study that analyzed the effects of virus-mediated stem cell transcription factor expression in oncolytic virotherapy. While expression of Oct4 by vaccinia virus seems to negatively impact the replication potential of the virus and therefore, therapeutic outcome *in vivo*, the expression of Nanog led to enhanced replication and therapeutic efficacy in A549 tumor-bearing animals. Co-expression of both stem cell transcription factors did not result in poorer outcome of the disease. These effects can be

## DISCUSSION

Nanog- or promoter strength-mediated. This work presents data suggesting that the observed enhancements over GLV-1h68 in replication and therapy of A549 tumors are rather payload-mediated or a combination of payload and increased virus replication than promoter strength-mediated only. Virus-mediated expression of stem cell transcription factors and a hypothetical subsequent shift towards cancer stem-likeness could even be beneficial as Wang *et al.* demonstrated the preference of oncolytic vaccinia virus to infect and replicate in cancer stem-like cells<sup>213</sup>. However, unlike reports showing that Nanog and Oct4 co-expression in lung adenocarcinomas is correlated to poor prognosis and outcome<sup>78</sup>, transient virus-mediated expression of Nanog, Oct4 or the combination of both, did not result in impaired therapeutic efficacy or poor prognosis. Thus, the role of stem cell transcription factors in stemness of cancer cells might require consistent expression over longer periods of time, comparable to its role in reprogramming of somatic cells into iPS cells (2-4 weeks)<sup>75,214-215</sup>. It is debatable whether transcription factors released from dying cancer cells are able to sustain in the stroma of the tumor or penetrate cytoplasmic membranes of neighboring cells<sup>216</sup>. Also, it has been argued that multiple factors influence the prevalence of cancer stem-like cells and the expression of stem cell transcription factors in infected and thus dying cancer cells alone is not sufficient to cause a shift in the cancer stem-like subpopulation of the respective cancer.

### **5.4 GLV-1h68 as a potential therapeutic agent in treatment of colorectal cancer**

Colorectal cancer is amongst the most abundant cancers occurring in both sexes. Despite a generally good prognosis after treatment with standard therapy regimens, stage IV diagnosis of colorectal cancer still results in a terminal outcome for the patient. Moreover, surgery and chemotherapy are either invasive or toxic procedures performed on the patient. Therefore, the development of novel treatment regimens of colorectal cancer is still a concern. With the emergence of oncolytic virotherapy, several oncolytic viruses like adenovirus<sup>217</sup>, echovirus<sup>218</sup>, Herpes simplex virus type 1<sup>219</sup>, Newcastle disease virus<sup>220</sup>, reovirus<sup>221</sup>, Sendai virus<sup>222</sup>, or vesicular stomatitis virus<sup>223</sup> are tested at different stages for treating colorectal cancer. However, a major drawback of many oncolytic viruses is the need for regional or local delivery. This work describes for the first time that oncolytic vaccinia virus GLV-1h68 can efficiently infect, replicate in, and lyse a variety of human colorectal cancer lines in culture. In all tested cell lines, viral replication can be correlated well with cell viability and marker gene (GFP) expression. Furthermore, flow cytometry analysis and fluorescence microscopy confirmed that GFP signal was detectable in the majority of the dead cells population. Taken together, we found no evidence that the five tested human colorectal cancer cells are resistant to infection, replication and subsequent lysis by oncolytic vaccinia virus GLV-1h68 in cell culture. However, it appears that viral replication efficacy and



## DISCUSSION

cytotoxicity are not only MOI-dependent but also cell line-dependent, suggesting variable treatment doses and therapeutic success for the different cell lines. Furthermore, this work demonstrates for the first time that systemically administered oncolytic vaccinia virus GLV-1h68 efficiently infiltrates, replicates in and inhibits the growth of human colorectal HCT-116 and SW-620 tumors *in vivo*, making it a potential tool for therapeutic purposes. Tumor growth inhibition correlated well with viral titers in the tumor and *Renilla* luciferase-GFP fusion marker gene expression from as early as 7 days post injection on in HCT-116 tumor-bearing mice. Thus, there is strong evidence that GLV-1h68 invades and replicates in human colorectal cancers in a mouse xenograft model.

It has been demonstrated before that infection of tumor tissues *in vivo* and viral replication leads to a strong upregulation of pro-inflammatory cytokines and chemokines as well as the formation of an inflammation site in the tumor environment which is normally protected from the host immune system<sup>181,192,202</sup>. Upon treatment of HCT-116 tumor-bearing mice with GLV-1h68, we found a strong up-regulation in pro-inflammatory cytokines and chemokines, like GPC-2, KC/GRO, IFN- $\gamma$ , IP-10, IL-6, M-CSF-1, MIP-1 beta, MIP-2 and MIP-3, MCP-1, MCP-3, MCP-5, RANTES and TNF- $\gamma$ . Interferon gamma is crucial for immunity against intracellular pathogens and tumor control and is produced predominantly by natural killer (NK) cells and natural killer T (NKT) cells as part of the innate immune response<sup>224</sup>. It is furthermore involved in clearance of vaccinia virus after infection of a host organism<sup>225</sup>. Alongside with the up-regulation in IFN- $\gamma$ , a 66-fold increase in IP-10 levels was detected, a chemokine attracting T lymphocytes, monocytes and NK cells to the inflammation site<sup>226</sup>. Up-regulation of additional chemokines, like KC/GRO, GPC-2, GM-CSF 1, RANTES and MCP and MIP family members, further contribute to the recruitment of components of the innate immune system to the inflammation site, exhibiting a similar role to IP-10. TNF-alpha has been shown to induce apoptotic cell death, induction of inflammation, and viral replication<sup>227</sup>. Taken together, it is proposed that recruiting components of the innate immune system to the inflamed tumor site helps inhibition and regression of the tumor, as described by Worschech *et al.*<sup>202</sup>.

Interestingly, we found SGOT levels in infected animals to be down-regulated compared to untreated animals. It has been shown that SGOT levels in the blood may be an indicator for liver or heart damage, as well as for cancer. Elevated levels of SGOT in untreated animals may indicate liver metastasis by colorectal tumor cells evading the primary tumor site or more general because of the higher tumor burden in untreated animals 21 days post injection.

For the analysis of treatment efficacy in late stage colorectal cancer, it is crucial to determine whether the oncolytic vaccinia virus GLV-1h68 can also target, invade and destroy distant lymph node, liver and lung metastases in addition to the primary tumor. The ability of GLV-

## DISCUSSION

1h68 to be delivered intravenously and to efficiently target and invade tumors and metastases *in vivo*<sup>181</sup> provides a powerful tool of non-invasive treatment of colorectal cancers, potentially even in late stage progressed colorectal cancers.

### **5.5 Improving therapeutic outcome of oncolytic virotherapy of colorectal cancer by specifically armed vaccinia virus strains**

It has been demonstrated in this work that the recombinant vaccinia virus strain GLV-1h68 can efficiently target, colonize and inhibit the growth of human colorectal tumors *in vivo*. However, it was evident that treatment efficacy of vaccinia virus strain GLV-1h68 of colorectal cancers is not only dose-dependent but also cell line-dependent. An advantage of vaccinia virus in oncolytic virotherapy is the large foreign gene-carrying capacity which allows the expression of heterologous genes. Genetically armed third-generation oncolytic poxviruses carrying therapeutic transgenes have been engineered in the recent past to exploit new potentials of this novel approach in cancer therapy. The transgene expression oftentimes includes cytokines, pro-drug converting enzymes as well as immuno-stimulating and anti-angiogenic agents.

Expression of Krueppel-like transcription factor 4 (Klf4) has been shown to inhibit cell proliferation and cause cell cycle arrest<sup>91</sup> whereas down-regulation of Klf4 may result in uninhibited cell growth and malignant transformation as described in various human colorectal cancers and cell lines<sup>94</sup>. Klf4 inhibits Wnt signaling<sup>96</sup> and its re-expression leads to diminished tumorigenicity in colorectal cancer cell lines<sup>97</sup>, making it an intriguing option for colorectal cancer-targeted arming of vaccinia virus.

For this purpose, oncolytic recombinant vaccinia virus strains of encoding *klf4* under the control of the synthetic early (GLV-1h290), synthetic early/late (GLV-1h291), and synthetic late (GLV-1h292) promoter were engineered to analyze the effects of virus-mediated tumor suppressor Klf4 expression in different amounts on colorectal cancer cells. To get a clearer picture whether virus-mediated Klf4 expression enhances the oncolytic potential of vaccinia virus treatment in colorectal cancer, the established *in vivo* non-responder cell line HT-29 was chosen<sup>202</sup>. GLV-1h68 is able to infect, replicate in, and lyse HT-29 cells in culture and also invades and colonizes subcutaneous tumors but eventually fails to inhibit tumor growth *in vivo*. Therefore, the HT-29 model is formidable to analyze Klf4-mediated effects in colorectal cancer. All three *klf4*-encoding virus strains showed replication potential in both, colorectal responder cell line HCT-116 and non-responder cell line HT-29 in culture. Differences in replication efficacy are due to different promoter strengths, as mentioned before<sup>206</sup>. Furthermore, all three new virus strains positively expressed marker genes *lacZ* and *ruc-gfp*. Klf4 was detected by immunocytochemistry in the cell nucleus, indicating correct protein folding and transport through the nuclear membrane. Western blot analysis

## DISCUSSION

demonstrated promoter strength-dependent protein expression with lowest detected levels in GLV-1h290-infected cells and highest expression in GLV-1h291-infected cells which corresponds well with described marker gene expression using these promoters<sup>207</sup>. High protein levels were still detected after 48 hpi in cells infected with GLV-1h291 or GLV-1h292, which is likely caused by the longer expression of late vaccinia genes. Interestingly, cell viability assays showed that the slow replicating GLV-1h291 (synthetic early/late promoter) and GLV-1h292 (synthetic late promoter) were more cytotoxic than the fast replicating GLV-1h290 (synthetic early promoter) or the control virus. This indicates a payload-mediated cytotoxic effect on the colorectal cancer line HT-29. It was demonstrated by Zhang *et al.* that Klf4 interacts with beta-catenin in the nucleus and inhibits Wnt/beta-catenin-mediated signaling and transcription by binding to the transactivation domain<sup>96</sup>. Like the majority of colorectal cancer cell lines, the HT-29 cell line contains no intact APC protein but two carboxylterminal-truncated APC proteins of approximately 100 kDa and 200 kDa molecular mass instead of a functional APC protein<sup>228</sup>. Furthermore, Wnt signaling, either activated by Wnt ligands or mutations in the *apc* or *beta-catenin* gene, triggers a LEF-1 positive feedback loop to enhance the nuclear chromatin-retained pool of beta-catenin by 100-300%<sup>229</sup>. Therefore, the findings that virus-mediated Klf4 expression led to significant decreases in beta-catenin mRNA and cellular protein levels is proof for the functionality of the expressed transcription factor. It was furthermore observed that promoter-dependent Klf4 expression was directly proportional to detected beta-catenin mRNA and protein levels. Overall, infection of HT-29 cells with GLV-1h291 resulted in highest cytotoxicity and lowest beta-catenin levels.

As described above, the fate of virus-infected cells ultimately is cell death to release the newly formed virus particles<sup>160</sup>. This only leaves a short window of action for virally encoded proteins which act intracellularly, including transcription factors. The finding that the recombinant virus strain GLV-1h68 invades and colonizes HT-29 tumors but fails to inhibit tumor growth, leads to the hypothesis that a membrane-permeable alteration of Klf4 may eventually result in a bystander effect and treatment benefits due to its ability to penetrate the cytoplasmic membrane of neighboring tumor cells. Cell-penetrating peptides have been studied extensively as tools for intracellular delivery of therapeutics<sup>216</sup>. Among the most popular cell-penetrating peptides, the protein transduction domain from the human immunodeficiency virus TAT protein, results in delivery of the biologically active fusion protein to all tissues in mice, opening new possibilities to deliver Klf4 to adjacent, uninfected tumor cells<sup>230</sup>. Therefore, a C-terminally located Tat transduction domain sequence was fused to the original *klf4* gene controlled by the synthetic early/late promoter. The new recombinant vaccinia virus strain encoding *klf4-TAT* in the A56R locus under the control of the synthetic early/late promoter (GLV-1h391) showed identical replication behavior, virus-

## DISCUSSION

mediated marker gene and Klf4 expression compared to GLV-1h291. Western blot detection of HT-29 cell lysates infected with GLV-1h291 and GLV-1h391 showed a higher molecular mass for detected Klf4 in GLV-1h391-infected lysates, which was expected due to the fused TAT sequence. Virus-mediated expression of Klf4-TAT by GLV-1h391 led to a comparable decrease in cellular beta-catenin when compared to untagged Klf4, indicating that the C-terminal fusion of the TAT transduction domain does not interfere with the C-terminally located zinc finger motifs or NLS sequence and the protein retains its functionality<sup>86</sup>. Interestingly, the infection with GLV-1h391 led to an approximately 10-fold decrease in cytotoxicity when compared with the control viruses GLV-1h189 and GLV-1h291. Virus infection of host cells led to the expression of membrane-permeable and functional Klf4-TAT, which is able to enter adjacent uninfected cells and trigger growth arrest and quiescence. While vaccinia virus' mode of cell entry and expression of early genes are independent of the cell proliferative status, replication of thymidine kinase-negative (TK<sup>neg</sup>) vaccinia virus strains like GLV-1h68 and its derivatives is dependent on the host cell expression of thymidine kinase to provide the necessary building blocks for DNA synthesis. Host cell translation of thymidine kinase mRNA is 10-fold higher in S phase than in G1/G0 of the cell cycle and rapidly cleared after cell division, making cellular thymidine kinase expression very transient<sup>231</sup>. Thus, it is not surprising that vaccinia virus strains with a TK<sup>neg</sup> phenotype showed decreased virulence compared to wild-type strains<sup>179</sup>. Even though vaccinia virus growth factor promotes the transition of cells into a proliferative state, expression of membrane-permeable Klf4 could drive uninfected cells towards growth arrest and quiescence, countering the effects of VGF. The observation that Klf4-TAT in sterile conditioned media from virus-infected cells considerably decreased cell proliferation in contrast to conditioned media obtained from control viruses further contributes to this notion. More significantly, a single administration of GLV-1h291 or GLV-1h391 led to significant tumor growth inhibition and significant survival benefits as well as stronger prognosis in HT-29 mouse xenografts compared to the control vaccinia strain GLV-1h68. The strongest tumor inhibition was observed in animals treated with GLV-1h391. However, titrations of tumor tissues showed equally infected primary tumors, ruling out a virus replication-dependent effect on HT-29 tumor growth. Instead, immunohistochemical analysis 21 days post injection clearly demonstrated strong expression of Klf4 in virus patches within the dissected tumors. It has been demonstrated that overexpression of Klf4 in RKO inhibits tumor growth *in vivo*<sup>97</sup>. Therefore, it may be assumed that the observed tumor growth inhibition in HT-29 tumors is triggered by interplay of Klf4-mediated effects and virus replication. While Klf4 expression in HT-29 tumors slows down cell proliferation it may also give the oncolytic vaccinia virus a better chance to catch up with tumor growth and prevent the tumor from outgrowing the virus.

## DISCUSSION

Taken together, arming an already powerful oncolytic vaccinia virus with Klf4 proved to further enhance treatment efficacy in colorectal cancers. Virus-mediated expression of Klf4-TAT significantly inhibits tumor growth in otherwise non-responding HT-29 tumors. This work provided strong indications that the observed therapeutic effects are primarily payload-driven. The expression of Klf4 and Klf4-TAT is safe in athymic nude mice and significantly improved the survival of the animals, strengthening its role as a tumor suppressor in colorectal cancer. It would be of great interest to investigate whether GLV-1h391 can efficiently invade and destroy clinically relevant liver or lung metastases. An intravenously administered oncolytic vaccinia virus, mediating the expression of membrane-permeable transcription factor Klf4 could provide a powerful tool for the future treatment of colorectal cancer in man.

### 5.6 Conclusion

As of lately, oncolytic virotherapy has become one of the most promising and fastest developing fields in cancer research. First reports of oncolytic viral activity lead to the development of various first-, second-, and third-generation oncolytic viruses, of which some are currently being tested in clinical trials. Oncolytic virotherapy offers specific tumor targeting and destruction as well as safe administration with little to no side effects and potential abilities as a cancer imaging tool. Recently, several clinical Phase I trials administering the oncolytic recombinant vaccinia virus GL-ONC1 were started in the UK, the United States and Germany. Vaccinia virus' ability to carry and express a large quantity of foreign genes allowed for the genetic 'arming' of the virus with cytokines, pro-drug converting enzymes as well as immuno-stimulating and anti-angiogenic agents to improve therapeutic efficacy or genes that enable fluorescence or deep tissue imaging. This study describes for the first time the effects of vaccinia virus-mediated expression of (stem cell) transcription factors Nanog, Oct4 and Klf4 on the oncolytic virotherapy of human cancers. Although the expression of Nanog and Oct4 is oftentimes correlated with cancer stem-like subpopulations in cancers, the virus-mediated expression of Nanog led to increased vaccinia virus replication and cytotoxicity in lung adenocarcinoma cells and did not result in impaired treatment efficacy of the virus but made treatment of lung adenocarcinoma tumors more efficient. The virus-mediated expression of Oct4, however, showed no significant differences in tumor therapy. The virus-mediated transient expression of stem cell transcription factors did not shift tumor cells into a more aggressive state and administration was safe in mice. It was also shown for the first time that vaccinia virus GLV-1h68 efficiently infected, replicated in, and lysed a variety of colorectal tumor cells of different progression and administration of a single dose led to significant tumor growth inhibition *in vivo*. Furthermore, the arming of vaccinia virus with the colorectal tumor suppressor transcription factor Klf4 further enhanced

## DISCUSSION

treatment efficacy in colorectal cancer, leading to significant tumor growth inhibition in the otherwise *in vivo* non-responder cell line HT-29. In conclusion, even though transcription factors have a small window of action in vaccinia virus-infected host cells, they may still provide a powerful tool to arm oncolytic viruses for therapeutic purposes or to further research their role in different cancer types or subpopulations in the tumor.

## 6 References

- 1 Society, A. C. Global Cancer Facts & Figures 2nd Edition. (Atlanta, 2011).
- 2 Society, A. C. Cancer Facts & Figures 2012. (2012).
- 3 Krebs in Deutschland 2007/2008. (Berlin, 2012).
- 4 LIVESTRONG, A. C. S. a. The Global Economic Cost of Cancer. (Atlanta, 2010).
- 5 Key, T. J. *et al.* Diet, nutrition and the prevention of cancer. *Public Health Nutr* **7**, 187-200, doi:S1368980004000205 [pii] (2004).
- 6 Dang, C. V. Links between metabolism and cancer. *Genes Dev* **26**, 877-890, doi:26/9/877 [pii]10.1101/gad.189365.112 (2012).
- 7 Hanahan, D. & Weinberg, R. A. The hallmarks of cancer. *Cell* **100**, 57-70, doi:S0092-8674(00)81683-9 [pii] (2000).
- 8 Hanahan, D. & Weinberg, R. A. Hallmarks of cancer: the next generation. *Cell* **144**, 646-674, doi:S0092-8674(11)00127-9 [pii]10.1016/j.cell.2011.02.013 (2011).
- 9 Weinberg, R. A. *The Biology of Cancer*. 1. edn, (Garland Science, 2006).
- 10 Egger, G., Liang, G., Aparicio, A. & Jones, P. A. Epigenetics in human disease and prospects for epigenetic therapy. *Nature* **429**, 457-463, doi:10.1038/nature02625 nature02625 [pii] (2004).
- 11 Amos, C. I. *et al.* A susceptibility locus on chromosome 6q greatly increases lung cancer risk among light and never smokers. *Cancer Res* **70**, 2359-2367, doi:0008-5472.CAN-09-3096 [pii]10.1158/0008-5472.CAN-09-3096 (2010).
- 12 Society, A. C. Lung Cancer (Non-small Cell). (Atlanta, 2012).
- 13 Fong, K. M., Sekido, Y., Gazdar, A. F. & Minna, J. D. Lung cancer. 9: Molecular biology of lung cancer: clinical implications. *Thorax* **58**, 892-900 (2003).
- 14 Rusch, V. *et al.* Differential expression of the epidermal growth factor receptor and its ligands in primary non-small cell lung cancers and adjacent benign lung. *Cancer Res* **53**, 2379-2385 (1993).
- 15 Brader, P. *et al.* Imaging a Genetically Engineered Oncolytic Vaccinia Virus (GLV-1h99) Using a Human Norepinephrine Transporter Reporter Gene. *Clin Cancer Res* **15**, 3791-3801, doi:1078-0432.CCR-08-3236 [pii]10.1158/1078-0432.CCR-08-3236 (2009).
- 16 Zochbauer-Muller, S. *et al.* Aberrant promoter methylation of multiple genes in non-small cell lung cancers. *Cancer Res* **61**, 249-255 (2001).
- 17 Kelloff, G. J. *et al.* Colorectal adenomas: a prototype for the use of surrogate end points in the development of cancer prevention drugs. *Clin Cancer Res* **10**, 3908-3918, doi:10.1158/1078-0432.CCR-03-078910/11/3908 [pii] (2004).

## REFERENCES

- 18 Bond, J. H. Polyp guideline: diagnosis, treatment, and surveillance for patients with colorectal polyps. Practice Parameters Committee of the American College of Gastroenterology. *Am J Gastroenterol* **95**, 3053-3063, doi:S0002927000022279 [pii] 10.1111/j.1572-0241.2000.03434.x (2000).
- 19 Stewart, S. L., Wike, J. M., Kato, I., Lewis, D. R. & Michaud, F. A population-based study of colorectal cancer histology in the United States, 1998-2001. *Cancer* **107**, 1128-1141, doi:10.1002/cncr.22010 (2006).
- 20 Society, A. C. Colorectal Cancer Facts & Figures 2011-2013. (Atlanta, 2011).
- 21 Lynch, H. T. & de la Chapelle, A. Hereditary colorectal cancer. *N Engl J Med* **348**, 919-932, doi:10.1056/NEJMra012242348/10/919 [pii] (2003).
- 22 Lynch, H. T. & de la Chapelle, A. Genetic susceptibility to non-polyposis colorectal cancer. *J Med Genet* **36**, 801-818 (1999).
- 23 Sargent, D. *et al.* Evidence for cure by adjuvant therapy in colon cancer: observations based on individual patient data from 20,898 patients on 18 randomized trials. *J Clin Oncol* **27**, 872-877, doi:JCO.2008.19.5362 [pii]10.1200/JCO.2008.19.5362 (2009).
- 24 Saif, M. W. & Chu, E. Biology of colorectal cancer. *Cancer J* **16**, 196-201, doi:10.1097/PPO.0b013e3181e076af00130404-201005000-00003 [pii] (2010).
- 25 Segditsas, S. & Tomlinson, I. Colorectal cancer and genetic alterations in the Wnt pathway. *Oncogene* **25**, 7531-7537, doi:1210059 [pii]10.1038/sj.onc.1210059 (2006).
- 26 Lynch, H. T. & Lynch, J. F. What the physician needs to know about Lynch syndrome: an update. *Oncology (Williston Park)* **19**, 455-463; discussion 463-454, 466, 469 (2005).
- 27 Smits, R. *et al.* Apc1638T: a mouse model delineating critical domains of the adenomatous polyposis coli protein involved in tumorigenesis and development. *Genes Dev* **13**, 1309-1321 (1999).
- 28 Morin, P. J. *et al.* Activation of beta-catenin-Tcf signaling in colon cancer by mutations in beta-catenin or APC. *Science* **275**, 1787-1790 (1997).
- 29 Johnson, V. *et al.* Exon 3 beta-catenin mutations are specifically associated with colorectal carcinomas in hereditary non-polyposis colorectal cancer syndrome. *Gut* **54**, 264-267, doi:54/2/264 [pii]10.1136/gut.2004.048132 (2005).
- 30 Li, J., Mizukami, Y., Zhang, X., Jo, W. S. & Chung, D. C. Oncogenic K-ras stimulates Wnt signaling in colon cancer through inhibition of GSK-3beta. *Gastroenterology* **128**, 1907-1918, doi:S0016508505006281 [pii] (2005).
- 31 Massague, J., Blain, S. W. & Lo, R. S. TGFbeta signaling in growth control, cancer, and heritable disorders. *Cell* **103**, 295-309, doi:S0092-8674(00)00121-5 [pii] (2000).



## REFERENCES

- 32 Xu, Y. & Pasche, B. TGF-beta signaling alterations and susceptibility to colorectal cancer. *Hum Mol Genet* **16 Spec No 1**, R14-20, doi:16/R1/R14 [pii]10.1093/hmg/ddl486 (2007).
- 33 Biswas, S. *et al.* Transforming growth factor beta receptor type II inactivation promotes the establishment and progression of colon cancer. *Cancer Res* **64**, 4687-4692, doi:10.1158/0008-5472.CAN-03-325564/14/4687 [pii] (2004).
- 34 Vivanco, I. & Sawyers, C. L. The phosphatidylinositol 3-Kinase AKT pathway in human cancer. *Nat Rev Cancer* **2**, 489-501, doi:10.1038/nrc839nrc839 [pii] (2002).
- 35 Katso, R. *et al.* Cellular function of phosphoinositide 3-kinases: implications for development, homeostasis, and cancer. *Annu Rev Cell Dev Biol* **17**, 615-675, doi:10.1146/annurev.cellbio.17.1.61517/1/615 [pii] (2001).
- 36 Arteaga, C. L. The epidermal growth factor receptor: from mutant oncogene in nonhuman cancers to therapeutic target in human neoplasia. *J Clin Oncol* **19**, 32S-40S (2001).
- 37 Lievre, A. *et al.* KRAS mutations as an independent prognostic factor in patients with advanced colorectal cancer treated with cetuximab. *J Clin Oncol* **26**, 374-379, doi:26/3/374 [pii]10.1200/JCO.2007.12.5906 (2008).
- 38 Boiani, M. & Scholer, H. R. Regulatory networks in embryo-derived pluripotent stem cells. *Nat Rev Mol Cell Biol* **6**, 872-884, doi:nrm1744 [pii]10.1038/nrm1744 (2005).
- 39 Thomson, J. A. *et al.* Embryonic stem cell lines derived from human blastocysts. *Science* **282**, 1145-1147 (1998).
- 40 Corsten, M. F. & Shah, K. Therapeutic stem-cells for cancer treatment: hopes and hurdles in tactical warfare. *Lancet Oncol* **9**, 376-384, doi:S1470-2045(08)70099-8 [pii]10.1016/S1470-2045(08)70099-8 (2008).
- 41 Xi, R. & Xie, T. Stem cell self-renewal controlled by chromatin remodeling factors. *Science* **310**, 1487-1489, doi:310/5753/1487 [pii]10.1126/science.1120140 (2005).
- 42 Sherley, J. L. Asymmetric cell kinetics genes: the key to expansion of adult stem cells in culture. *Stem Cells* **20**, 561-572, doi:10.1634/stemcells.20-6-561 (2002).
- 43 Scopelliti, A. *et al.* Therapeutic implications of Cancer Initiating Cells. *Expert Opin Biol Ther* **9**, 1005-1016, doi:10.1517/14712590903066687 (2009).
- 44 Gonzalez, M. A., Tachibana, K. E., Laskey, R. A. & Coleman, N. Control of DNA replication and its potential clinical exploitation. *Nat Rev Cancer* **5**, 135-141, doi:nrc1548 [pii]10.1038/nrc1548 (2005).
- 45 Rho, J. Y. *et al.* Transcriptional profiling of the developmentally important signalling pathways in human embryonic stem cells. *Hum Reprod* **21**, 405-412, doi:dei328 [pii]10.1093/humrep/dei328 (2006).

## REFERENCES

- 46 Tay, Y., Zhang, J., Thomson, A. M., Lim, B. & Rigoutsos, I. MicroRNAs to Nanog, Oct4 and Sox2 coding regions modulate embryonic stem cell differentiation. *Nature* **455**, 1124-1128, doi:nature07299 [pii]10.1038/nature07299 (2008).
- 47 Takahashi, K. & Yamanaka, S. Induction of pluripotent stem cells from mouse embryonic and adult fibroblast cultures by defined factors. *Cell* **126**, 663-676, doi:S0092-8674(06)00976-7 [pii]10.1016/j.cell.2006.07.024 (2006).
- 48 Loh, Y. H., Ng, J. H. & Ng, H. H. Molecular framework underlying pluripotency. *Cell Cycle* **7**, 885-891, doi:5636 [pii] (2008).
- 49 Schulz, W. A. & Hoffmann, M. J. Transcription factor networks in embryonic stem cells and testicular cancer and the definition of epigenetics. *Epigenetics* **2**, 37-42, doi:4067 [pii] (2007).
- 50 Scholer, H. R., Ruppert, S., Suzuki, N., Chowdhury, K. & Gruss, P. New type of POU domain in germ line-specific protein Oct-4. *Nature* **344**, 435-439, doi:10.1038/344435a0 (1990).
- 51 Nichols, J. *et al.* Formation of pluripotent stem cells in the mammalian embryo depends on the POU transcription factor Oct4. *Cell* **95**, 379-391, doi:S0092-8674(00)81769-9 [pii] (1998).
- 52 Klemm, J. D. & Pabo, C. O. Oct-1 POU domain-DNA interactions: cooperative binding of isolated subdomains and effects of covalent linkage. *Genes Dev* **10**, 27-36 (1996).
- 53 Pan, G. J., Chang, Z. Y., Scholer, H. R. & Pei, D. Stem cell pluripotency and transcription factor Oct4. *Cell Res* **12**, 321-329, doi:10.1038/sj.cr.7290134 (2002).
- 54 Niwa, H., Miyazaki, J. & Smith, A. G. Quantitative expression of Oct-3/4 defines differentiation, dedifferentiation or self-renewal of ES cells. *Nat Genet* **24**, 372-376, doi:10.1038/74199 (2000).
- 55 Pardo, M. *et al.* An expanded Oct4 interaction network: implications for stem cell biology, development, and disease. *Cell Stem Cell* **6**, 382-395, doi:S1934-5909(10)00101-3 [pii]10.1016/j.stem.2010.03.004 (2010).
- 56 van den Berg, D. L. *et al.* An Oct4-centered protein interaction network in embryonic stem cells. *Cell Stem Cell* **6**, 369-381, doi:S1934-5909(10)00091-3 [pii]10.1016/j.stem.2010.02.014 (2010).
- 57 Boyer, L. A. *et al.* Core transcriptional regulatory circuitry in human embryonic stem cells. *Cell* **122**, 947-956, doi:S0092-8674(05)00825-1 [pii]10.1016/j.cell.2005.08.020 (2005).
- 58 Abu-Remaileh, M. *et al.* Oct-3/4 regulates stem cell identity and cell fate decisions by modulating Wnt/beta-catenin signalling. *EMBO J*, doi:emboj2010200 [pii]10.1038/emboj.2010.200 (2010).

## REFERENCES

- 59 Kim, J. H. *et al.* Regulation of adipose tissue stromal cells behaviors by endogenic Oct4 expression control. *PLoS One* **4**, e7166, doi:10.1371/journal.pone.0007166 (2009).
- 60 Lengner, C. J. *et al.* Oct4 expression is not required for mouse somatic stem cell self-renewal. *Cell Stem Cell* **1**, 403-415, doi:10.1016/j.stem.2007.07.020 (2007).
- 61 Lengner, C. J., Welstead, G. G. & Jaenisch, R. The pluripotency regulator Oct4: a role in somatic stem cells? *Cell Cycle* **7**, 725-728, doi:5573 [pii] (2008).
- 62 Zangrossi, S. *et al.* Oct-4 expression in adult human differentiated cells challenges its role as a pure stem cell marker. *Stem Cells* **25**, 1675-1680, doi:2006-0611 [pii]10.1634/stemcells.2006-0611 (2007).
- 63 Clark, A. T. The stem cell identity of testicular cancer. *Stem Cell Rev* **3**, 49-59, doi:SCR:3:1:49 [pii] (2007).
- 64 Chang, C. C. *et al.* Oct-3/4 expression reflects tumor progression and regulates motility of bladder cancer cells. *Cancer Res* **68**, 6281-6291, doi:68/15/6281 [pii]10.1158/0008-5472.CAN-08-0094 (2008).
- 65 Chambers, I. *et al.* Functional expression cloning of Nanog, a pluripotency sustaining factor in embryonic stem cells. *Cell* **113**, 643-655, doi:S0092867403003921 [pii] (2003).
- 66 Mitsui, K. *et al.* The homeoprotein Nanog is required for maintenance of pluripotency in mouse epiblast and ES cells. *Cell* **113**, 631-642, doi:S0092867403003933 [pii] (2003).
- 67 Chang, D. F. *et al.* Molecular characterization of the human NANOG protein. *Stem Cells* **27**, 812-821, doi:10.1634/stemcells.2008-0657 (2009).
- 68 Oh, J. H. *et al.* Identification of a putative transactivation domain in human Nanog. *Exp Mol Med* **37**, 250-254, doi:2005063014 [pii] (2005).
- 69 Cavaleri, F. & Scholer, H. R. Nanog: a new recruit to the embryonic stem cell orchestra. *Cell* **113**, 551-552, doi:S0092867403003945 [pii] (2003).
- 70 Lin, T. *et al.* p53 induces differentiation of mouse embryonic stem cells by suppressing Nanog expression. *Nat Cell Biol* **7**, 165-171, doi:ncb1211 [pii]10.1038/ncb1211 (2005).
- 71 Pereira, L., Yi, F. & Merrill, B. J. Repression of Nanog gene transcription by Tcf3 limits embryonic stem cell self-renewal. *Mol Cell Biol* **26**, 7479-7491, doi:MCB.00368-06 [pii]10.1128/MCB.00368-06 (2006).
- 72 Pan, G., Li, J., Zhou, Y., Zheng, H. & Pei, D. A negative feedback loop of transcription factors that controls stem cell pluripotency and self-renewal. *FASEB J* **20**, 1730-1732, doi:fj.05-5543fje [pii]10.1096/fj.05-5543fje (2006).

## REFERENCES

- 73 Xu, R. H. *et al.* NANOG is a direct target of TGFbeta/activin-mediated SMAD signaling in human ESCs. *Cell Stem Cell* **3**, 196-206, doi:S1934-5909(08)00335-4 [pii]10.1016/j.stem.2008.07.001 (2008).
- 74 Zhang, X. *et al.* A role for NANOG in G1 to S transition in human embryonic stem cells through direct binding of CDK6 and CDC25A. *J Cell Biol* **184**, 67-82, doi:jcb.200801009 [pii]10.1083/jcb.200801009 (2009).
- 75 Yu, J. *et al.* Induced pluripotent stem cell lines derived from human somatic cells. *Science* **318**, 1917-1920, doi:1151526 [pii]10.1126/science.1151526 (2007).
- 76 Silva, J. *et al.* Nanog is the gateway to the pluripotent ground state. *Cell* **138**, 722-737, doi:S0092-8674(09)00969-6 [pii]10.1016/j.cell.2009.07.039 (2009).
- 77 Santagata, S., Hornick, J. L. & Ligon, K. L. Comparative analysis of germ cell transcription factors in CNS germinoma reveals diagnostic utility of NANOG. *Am J Surg Pathol* **30**, 1613-1618, doi:10.1097/01.pas.0000213320.04919.1a00000478-200612000-00016 [pii] (2006).
- 78 Chiou, S. H. *et al.* Coexpression of Oct4 and Nanog enhances malignancy in lung adenocarcinoma by inducing cancer stem cell-like properties and epithelial-mesenchymal transdifferentiation. *Cancer Res* **70**, 10433-10444, doi:70/24/10433[pii]10.1158/0008-5472.CAN-10-2638 (2010).
- 79 Nirasawa, S., Kobayashi, D., Tsuji, N., Kuribayashi, K. & Watanabe, N. Diagnostic relevance of overexpressed Nanog gene in early lung cancers. *Oncol Rep* **22**, 587-591 (2009).
- 80 Jeter, C. R. *et al.* NANOG promotes cancer stem cell characteristics and prostate cancer resistance to androgen deprivation. *Oncogene*, doi:onc2011114 [pii]10.1038/onc.2011.114 (2011).
- 81 Meng, H. M. *et al.* Overexpression of nanog predicts tumor progression and poor prognosis in colorectal cancer. *Cancer Biol Ther* **9**, doi:10666 [pii] (2010).
- 82 Ben-Porath, I. *et al.* An embryonic stem cell-like gene expression signature in poorly differentiated aggressive human tumors. *Nat Genet* **40**, 499-507, doi:ng.127 [pii]10.1038/ng.127 (2008).
- 83 Seigel, G. M., Hackam, A. S., Ganguly, A., Mandell, L. M. & Gonzalez-Fernandez, F. Human embryonic and neuronal stem cell markers in retinoblastoma. *Mol Vis* **13**, 823-832, doi:v13/a90 [pii] (2007).
- 84 Zhang, S. *et al.* Identification and characterization of ovarian cancer-initiating cells from primary human tumors. *Cancer Res* **68**, 4311-4320, doi:68/11/4311 [pii]10.1158/0008-5472.CAN-08-0364 (2008).

## REFERENCES

- 85 Saiki, Y. *et al.* Comprehensive analysis of the clinical significance of inducing pluripotent stemness-related gene expression in colorectal cancer cells. *Ann Surg Oncol* **16**, 2638-2644, doi:10.1245/s10434-009-0567-5 (2009).
- 86 Shields, J. M., Christy, R. J. & Yang, V. W. Identification and characterization of a gene encoding a gut-enriched Kruppel-like factor expressed during growth arrest. *J Biol Chem* **271**, 20009-20017 (1996).
- 87 Wei, Z. *et al.* Klf4 interacts directly with Oct4 and Sox2 to promote reprogramming. *Stem Cells* **27**, 2969-2978, doi:10.1002/stem.231 (2009).
- 88 Zhang, P., Andrianakos, R., Yang, Y., Liu, C. & Lu, W. Kruppel-like factor 4 (Klf4) prevents embryonic stem (ES) cell differentiation by regulating Nanog gene expression. *J Biol Chem* **285**, 9180-9189, doi:M109.077958 [pii]10.1074/jbc.M109.077958 (2010).
- 89 Garrett-Sinha, L. A., Eberspaecher, H., Seldin, M. F. & de Crombrughe, B. A gene for a novel zinc-finger protein expressed in differentiated epithelial cells and transiently in certain mesenchymal cells. *J Biol Chem* **271**, 31384-31390 (1996).
- 90 Yet, S. F. *et al.* Human EZF, a Kruppel-like zinc finger protein, is expressed in vascular endothelial cells and contains transcriptional activation and repression domains. *J Biol Chem* **273**, 1026-1031 (1998).
- 91 Zhang, W. *et al.* The gut-enriched Kruppel-like factor (Kruppel-like factor 4) mediates the transactivating effect of p53 on the p21WAF1/Cip1 promoter. *J Biol Chem* **275**, 18391-18398, doi:10.1074/jbc.C000062200C000062200 [pii] (2000).
- 92 Ton-That, H., Kaestner, K. H., Shields, J. M., Mahatanankoon, C. S. & Yang, V. W. Expression of the gut-enriched Kruppel-like factor gene during development and intestinal tumorigenesis. *FEBS Lett* **419**, 239-243, doi:S0014-5793(97)01465-8 [pii] (1997).
- 93 Choi, B. J. *et al.* Altered expression of the KLF4 in colorectal cancers. *Pathol Res Pract* **202**, 585-589, doi:S0344-0338(06)00096-3 [pii]10.1016/j.prp.2006.05.001 (2006).
- 94 Zhao, W. *et al.* Identification of Kruppel-like factor 4 as a potential tumor suppressor gene in colorectal cancer. *Oncogene* **23**, 395-402, doi:10.1038/sj.onc.12070671207067 [pii] (2004).
- 95 Shie, J. L., Chen, Z. Y., Fu, M., Pestell, R. G. & Tseng, C. C. Gut-enriched Kruppel-like factor represses cyclin D1 promoter activity through Sp1 motif. *Nucleic Acids Res* **28**, 2969-2976 (2000).
- 96 Zhang, W. *et al.* Novel cross talk of Kruppel-like factor 4 and beta-catenin regulates normal intestinal homeostasis and tumor repression. *Mol Cell Biol* **26**, 2055-2064, doi:26/6/2055 [pii]10.1128/MCB.26.6.2055-2064.2006 (2006).

## REFERENCES

- 97 Dang, D. T. *et al.* Overexpression of Kruppel-like factor 4 in the human colon cancer cell line RKO leads to reduced tumorigenicity. *Oncogene* **22**, 3424-3430, doi:10.1038/sj.onc.12064131206413 [pii] (2003).
- 98 Shie, J. L. *et al.* Role of gut-enriched Kruppel-like factor in colonic cell growth and differentiation. *Am J Physiol Gastrointest Liver Physiol* **279**, G806-814 (2000).
- 99 Hu, R. *et al.* KLF4 Expression Correlates with the Degree of Differentiation in Colorectal Cancer. *Gut Liver* **5**, 154-159, doi:10.5009/gnl.2011.5.2.154 (2011).
- 100 Foster, K. W. *et al.* Oncogene expression cloning by retroviral transduction of adenovirus E1A-immortalized rat kidney RK3E cells: transformation of a host with epithelial features by c-MYC and the zinc finger protein GKLf. *Cell Growth Differ* **10**, 423-434 (1999).
- 101 Foster, K. W. *et al.* Increase of GKLf messenger RNA and protein expression during progression of breast cancer. *Cancer Res* **60**, 6488-6495 (2000).
- 102 Mackillop, W. J., Ciampi, A., Till, J. E. & Buick, R. N. A stem cell model of human tumor growth: implications for tumor cell clonogenic assays. *J Natl Cancer Inst* **70**, 9-16 (1983).
- 103 Bonnet, D. & Dick, J. E. Human acute myeloid leukemia is organized as a hierarchy that originates from a primitive hematopoietic cell. *Nat Med* **3**, 730-737 (1997).
- 104 Al-Hajj, M., Wicha, M. S., Benito-Hernandez, A., Morrison, S. J. & Clarke, M. F. Prospective identification of tumorigenic breast cancer cells. *Proc Natl Acad Sci U S A* **100**, 3983-3988, doi:10.1073/pnas.05302911000530291100 [pii] (2003).
- 105 Singh, S. K. *et al.* Identification of human brain tumour initiating cells. *Nature* **432**, 396-401, doi:nature03128 [pii]10.1038/nature03128 (2004).
- 106 Fang, D. *et al.* A tumorigenic subpopulation with stem cell properties in melanomas. *Cancer Res* **65**, 9328-9337, doi:65/20/9328 [pii]10.1158/0008-5472.CAN-05-1343 (2005).
- 107 Gibbs, C. P. *et al.* Stem-like cells in bone sarcomas: implications for tumorigenesis. *Neoplasia* **7**, 967-976 (2005).
- 108 Collins, A. T., Berry, P. A., Hyde, C., Stower, M. J. & Maitland, N. J. Prospective identification of tumorigenic prostate cancer stem cells. *Cancer Res* **65**, 10946-10951, doi:65/23/10946 [pii]10.1158/0008-5472.CAN-05-2018 (2005).
- 109 Ricci-Vitiani, L. *et al.* Identification and expansion of human colon-cancer-initiating cells. *Nature* **445**, 111-115, doi:nature05384 [pii]10.1038/nature05384 (2007).
- 110 Visvader, J. E. & Lindeman, G. J. Cancer stem cells in solid tumours: accumulating evidence and unresolved questions. *Nat Rev Cancer* **8**, 755-768, doi:nrc2499 [pii]10.1038/nrc2499 (2008).

## REFERENCES

- 111 Cotsarelis, G., Kaur, P., Dhouailly, D., Hengge, U. & Bickenbach, J. Epithelial stem cells in the skin: definition, markers, localization and functions. *Exp Dermatol* **8**, 80-88 (1999).
- 112 Ward, R. J. & Dirks, P. B. Cancer stem cells: at the headwaters of tumor development. *Annu Rev Pathol* **2**, 175-189, doi:10.1146/annurev.pathol.2.010506.091847 (2007).
- 113 Charafe-Jauffret, E. *et al.* Breast cancer cell lines contain functional cancer stem cells with metastatic capacity and a distinct molecular signature. *Cancer Res* **69**, 1302-1313, doi:0008-5472.CAN-08-2741 [pii]10.1158/0008-5472.CAN-08-2741 (2009).
- 114 Cheung, A. M. *et al.* Aldehyde dehydrogenase activity in leukemic blasts defines a subgroup of acute myeloid leukemia with adverse prognosis and superior NOD/SCID engrafting potential. *Leukemia* **21**, 1423-1430, doi:2404721 [pii]10.1038/sj.leu.2404721 (2007).
- 115 Corti, S. *et al.* Identification of a primitive brain-derived neural stem cell population based on aldehyde dehydrogenase activity. *Stem Cells* **24**, 975-985, doi:2005-0217 [pii]10.1634/stemcells.2005-0217 (2006).
- 116 O'Brien, C. A., Pollett, A., Gallinger, S. & Dick, J. E. A human colon cancer cell capable of initiating tumour growth in immunodeficient mice. *Nature* **445**, 106-110, doi:nature05372 [pii]10.1038/nature05372 (2007).
- 117 Salmaggi, A. *et al.* Glioblastoma-derived tumorspheres identify a population of tumor stem-like cells with angiogenic potential and enhanced multidrug resistance phenotype. *Glia* **54**, 850-860, doi:10.1002/glia.20414 (2006).
- 118 Tang, D. G. *et al.* Prostate cancer stem/progenitor cells: identification, characterization, and implications. *Mol Carcinog* **46**, 1-14, doi:10.1002/mc.20255 (2007).
- 119 Dalerba, P. *et al.* Phenotypic characterization of human colorectal cancer stem cells. *Proc Natl Acad Sci U S A* **104**, 10158-10163, doi:0703478104 [pii]10.1073/pnas.0703478104 (2007).
- 120 Park, S. Y. *et al.* Heterogeneity for stem cell-related markers according to tumor subtype and histologic stage in breast cancer. *Clin Cancer Res* **16**, 876-887, doi:1078-0432.CCR-09-1532 [pii]10.1158/1078-0432.CCR-09-1532 (2010).
- 121 Vaiopoulos, A. G., Kostakis, I. D., Koutsilieris, M. & Papavassiliou, A. G. Colorectal cancer stem cells. *Stem Cells* **30**, 363-371, doi:10.1002/stem.1031 (2012).
- 122 Kelly, P. N., Dakic, A., Adams, J. M., Nutt, S. L. & Strasser, A. Tumor growth need not be driven by rare cancer stem cells. *Science* **317**, 337, doi:317/5836/337 [pii]10.1126/science.1142596 (2007).

## REFERENCES

- 123 Quintana, E. *et al.* Efficient tumour formation by single human melanoma cells. *Nature* **456**, 593-598, doi:nature07567 [pii]10.1038/nature07567 (2008).
- 124 Vaillant, F. *et al.* The mammary progenitor marker CD61/beta3 integrin identifies cancer stem cells in mouse models of mammary tumorigenesis. *Cancer Res* **68**, 7711-7717, doi:68/19/7711 [pii]10.1158/0008-5472.CAN-08-1949 (2008).
- 125 La Porta, C. A. Thoughts about cancer stem cells in solid tumors. *World J Stem Cells* **4**, 17-20, doi:10.4252/wjsc.v4.i3.17 (2012).
- 126 Reya, T., Morrison, S. J., Clarke, M. F. & Weissman, I. L. Stem cells, cancer, and cancer stem cells. *Nature* **414**, 105-111, doi:10.1038/3510216735102167 [pii] (2001).
- 127 Krivtsov, A. V. *et al.* Transformation from committed progenitor to leukaemia stem cell initiated by MLL-AF9. *Nature* **442**, 818-822, doi:nature04980 [pii]10.1038/nature04980 (2006).
- 128 Patrawala, L. *et al.* Side population is enriched in tumorigenic, stem-like cancer cells, whereas ABCG2+ and ABCG2- cancer cells are similarly tumorigenic. *Cancer Res* **65**, 6207-6219, doi:65/14/6207 [pii]10.1158/0008-5472.CAN-05-0592 (2005).
- 129 Wong, D. J. *et al.* Module map of stem cell genes guides creation of epithelial cancer stem cells. *Cell Stem Cell* **2**, 333-344, doi:S1934-5909(08)00073-8 [pii]10.1016/j.stem.2008.02.009 (2008).
- 130 Zhou, S. *et al.* The ABC transporter Bcrp1/ABCG2 is expressed in a wide variety of stem cells and is a molecular determinant of the side-population phenotype. *Nat Med* **7**, 1028-1034, doi:10.1038/nm0901-1028nm0901-1028 [pii] (2001).
- 131 Huss, W. J., Gray, D. R., Greenberg, N. M., Mohler, J. L. & Smith, G. J. Breast cancer resistance protein-mediated efflux of androgen in putative benign and malignant prostate stem cells. *Cancer Res* **65**, 6640-6650, doi:65/15/6640 [pii]10.1158/0008-5472.CAN-04-2548 (2005).
- 132 Ghaffari, S. Cancer, stem cells and cancer stem cells: old ideas, new developments. *F1000 Med Rep* **3**, 23, doi:10.3410/M3-2323 [pii] (2011).
- 133 Tlsty, T. D. & Coussens, L. M. Tumor stroma and regulation of cancer development. *Annu Rev Pathol* **1**, 119-150, doi:10.1146/annurev.pathol.1.110304.100224 (2006).
- 134 Li, Z. & Rich, J. N. Hypoxia and hypoxia inducible factors in cancer stem cell maintenance. *Curr Top Microbiol Immunol* **345**, 21-30, doi:10.1007/82\_2010\_75 (2010).
- 135 Wells, A., Yates, C. & Shepard, C. R. E-cadherin as an indicator of mesenchymal to epithelial reverting transitions during the metastatic seeding of disseminated carcinomas. *Clin Exp Metastasis* **25**, 621-628, doi:10.1007/s10585-008-9167-1 (2008).



## REFERENCES

- 136 Kalani, A. D., Jack, A., Montenegro, G., Degliuomini, J. & Wallack, M. K. Immunotherapy as an adjuvant therapy in the management of advanced, surgically resected, melanoma. *G Ital Dermatol Venereol* **143**, 59-70 (2008).
- 137 Wei, W. Z., Jacob, J., Radkevich-Brown, O., Whittington, P. & Kong, Y. C. The "A, B and C" of Her-2 DNA vaccine development. *Cancer Immunol Immunother* **57**, 1711-1717, doi:10.1007/s00262-008-0464-y (2008).
- 138 Ma, Y. *et al.* Cytokine-induced killer cells in the treatment of patients with solid carcinomas: a systematic review and pooled analysis. *Cytotherapy* **14**, 483-493, doi:10.3109/14653249.2011.649185 (2012).
- 139 Stevenson, C. E. *et al.* Bevacizumab and breast cancer: what does the future hold? *Future Oncol* **8**, 403-414, doi:10.2217/fon.12.22 (2012).
- 140 Bierman, H. R. *et al.* Remissions in leukemia of childhood following acute infectious disease: staphylococcus and streptococcus, varicella, and feline panleukopenia. *Cancer* **6**, 591-605 (1953).
- 141 Csatory, L. K. Viruses in the treatment of cancer. *Lancet* **2**, 825 (1971).
- 142 Pasquinucci, G. Possible effect of measles on leukaemia. *Lancet* **1**, 136 (1971).
- 143 Hansen, R. M. & Libnoch, J. A. Remission of chronic lymphocytic leukemia after smallpox vaccination. *Arch Intern Med* **138**, 1137-1138 (1978).
- 144 Liu, T. C., Galanis, E. & Kirn, D. Clinical trial results with oncolytic virotherapy: a century of promise, a decade of progress. *Nat Clin Pract Oncol* **4**, 101-117, doi:ncponc0736 [pii]10.1038/ncponc0736 (2007).
- 145 Kirn, D., Martuza, R. L. & Zwiebel, J. Replication-selective virotherapy for cancer: Biological principles, risk management and future directions. *Nat Med* **7**, 781-787, doi:10.1038/8990189901 [pii] (2001).
- 146 Southam, C. M. & Moore, A. E. West Nile, Ilheus, and Bunyamwera virus infections in man. *Am J Trop Med Hyg* **31**, 724-741 (1951).
- 147 Huebner, R. J., Rowe, W. P., Schatten, W. E., Smith, R. R. & Thomas, L. B. Studies on the use of viruses in the treatment of carcinoma of the cervix. *Cancer* **9**, 1211-1218 (1956).
- 148 Asada, T. Treatment of human cancer with mumps virus. *Cancer* **34**, 1907-1928 (1974).
- 149 Wheelock, E. F. & Dingle, J. H. Observations on the Repeated Administration of Viruses to a Patient with Acute Leukemia. A Preliminary Report. *N Engl J Med* **271**, 645-651, doi:10.1056/NEJM196409242711302 (1964).
- 150 Milton, G. W. & Brown, M. M. The limited role of attenuated smallpox virus in the management of advanced malignant melanoma. *Aust N Z J Surg* **35**, 286-290 (1966).

## REFERENCES

- 151 Bischoff, J. R. *et al.* An adenovirus mutant that replicates selectively in p53-deficient human tumor cells. *Science* **274**, 373-376 (1996).
- 152 Garber, K. China approves world's first oncolytic virus therapy for cancer treatment. *J Natl Cancer Inst* **98**, 298-300, doi:98/5/298 [pii]10.1093/jnci/djj111 (2006).
- 153 Yu, Y. A. *et al.* Visualization of tumors and metastases in live animals with bacteria and vaccinia virus encoding light-emitting proteins. *Nat Biotechnol* **22**, 313-320, doi:10.1038/nbt937nbt937 [pii] (2004).
- 154 Chen, N. *et al.* A novel recombinant vaccinia virus expressing the human norepinephrine transporter retains oncolytic potential and facilitates deep-tissue imaging. *Mol Med* **15**, 144-151, doi:10.2119/molmed.2009.00014 (2009).
- 155 Haddad, D. *et al.* Insertion of the human sodium iodide symporter to facilitate deep tissue imaging does not alter oncolytic or replication capability of a novel vaccinia virus. *J Transl Med* **9**, 36, doi:1479-5876-9-36 [pii]10.1186/1479-5876-9-36 (2011).
- 156 Frentzen, A. *et al.* Anti-VEGF single-chain antibody GLAF-1 encoded by oncolytic vaccinia virus significantly enhances antitumor therapy. *Proc Natl Acad Sci U S A* **106**, 12915-12920, doi:0900660106 [pii]10.1073/pnas.0900660106 (2009).
- 157 Moss, B. in *Fields Virology Vol. 2* (ed Howley PM Knipe DM) 2905-2946 (Lippincott Williams & Wilkins, 2007).
- 158 Shen, Y. & Nemunaitis, J. Fighting cancer with vaccinia virus: teaching new tricks to an old dog. *Mol Ther* **11**, 180-195, doi:S1525-0016(04)01507-2 [pii]10.1016/j.ymthe.2004.10.015 (2005).
- 159 Smith, G. L., Vanderplasschen, A. & Law, M. The formation and function of extracellular enveloped vaccinia virus. *J Gen Virol* **83**, 2915-2931 (2002).
- 160 Harrison, S. C. *et al.* Discovery of antivirals against smallpox. *Proc Natl Acad Sci U S A* **101**, 11178-11192, doi:10.1073/pnas.04036001010403600101 [pii] (2004).
- 161 Sieczkarski, S. B. & Whittaker, G. R. Viral entry. *Curr Top Microbiol Immunol* **285**, 1-23 (2005).
- 162 Mercer, J. & Helenius, A. Vaccinia virus uses macropinocytosis and apoptotic mimicry to enter host cells. *Science* **320**, 531-535, doi:320/5875/531 [pii]10.1126/science.1155164 (2008).
- 163 Roberts, K. L. & Smith, G. L. Vaccinia virus morphogenesis and dissemination. *Trends Microbiol* **16**, 472-479, doi:S0966-842X(08)00191-1 [pii]10.1016/j.tim.2008.07.009 (2008).
- 164 Tolonen, N., Doglio, L., Schleich, S. & Krijnse Locker, J. Vaccinia virus DNA replication occurs in endoplasmic reticulum-enclosed cytoplasmic mini-nuclei. *Mol Biol Cell* **12**, 2031-2046 (2001).

## REFERENCES

- 165 Schramm, B. & Locker, J. K. Cytoplasmic organization of POXvirus DNA replication. *Traffic* **6**, 839-846, doi:TRA324 [pii]10.1111/j.1600-0854.2005.00324.x (2005).
- 166 Blasco, R. & Moss, B. Role of cell-associated enveloped vaccinia virus in cell-to-cell spread. *J Virol* **66**, 4170-4179 (1992).
- 167 Garber, D. A. *et al.* Expanding the repertoire of Modified Vaccinia Ankara-based vaccine vectors via genetic complementation strategies. *PLoS One* **4**, e5445, doi:10.1371/journal.pone.0005445 (2009).
- 168 Gilbert, S. C. *et al.* Synergistic DNA-MVA prime-boost vaccination regimes for malaria and tuberculosis. *Vaccine* **24**, 4554-4561, doi:S0264-410X(05)00818-2 [pii]10.1016/j.vaccine.2005.08.048 (2006).
- 169 Esteban, M. Attenuated poxvirus vectors MVA and NYVAC as promising vaccine candidates against HIV/AIDS. *Hum Vaccin* **5**, 867-871, doi:9693 [pii] (2009).
- 170 Amato, R. J. & Stepankiw, M. Evaluation of MVA-5T4 as a novel immunotherapeutic vaccine in colorectal, renal and prostate cancer. *Future Oncol* **8**, 231-237, doi:10.2217/fon.12.7 (2012).
- 171 Wein, L. M., Wu, J. T. & Kirn, D. H. Validation and analysis of a mathematical model of a replication-competent oncolytic virus for cancer treatment: implications for virus design and delivery. *Cancer Res* **63**, 1317-1324 (2003).
- 172 Thorne, S. H. *et al.* Rational strain selection and engineering creates a broad-spectrum, systemically effective oncolytic poxvirus, JX-963. *J Clin Invest* **117**, 3350-3358, doi:10.1172/JCI32727 (2007).
- 173 Kim, J. H. *et al.* Systemic armed oncolytic and immunologic therapy for cancer with JX-594, a targeted poxvirus expressing GM-CSF. *Mol Ther* **14**, 361-370, doi:S1525-0016(06)00183-3 [pii]10.1016/j.ymthe.2006.05.008 (2006).
- 174 Hodge, J. W. *et al.* A triad of costimulatory molecules synergize to amplify T-cell activation. *Cancer Res* **59**, 5800-5807 (1999).
- 175 Thorne, S. H., Tam, B. Y., Kirn, D. H., Contag, C. H. & Kuo, C. J. Selective intratumoral amplification of an antiangiogenic vector by an oncolytic virus produces enhanced antivascular and anti-tumor efficacy. *Mol Ther* **13**, 938-946, doi:S1525-0016(06)00004-9 [pii]10.1016/j.ymthe.2005.12.010 (2006).
- 176 Seubert, C. M. *et al.* Enhanced tumor therapy using vaccinia virus strain GLV-1h68 in combination with a beta-galactosidase-activatable prodrug seco-analog of duocarmycin SA. *Cancer Gene Ther* **18**, 42-52, doi:cgt201049 [pii]10.1038/cgt.2010.49 (2011).
- 177 Gross, S. & Piwnica-Worms, D. Spying on cancer: molecular imaging in vivo with genetically encoded reporters. *Cancer Cell* **7**, 5-15, doi:S1535610804003733 [pii]10.1016/j.ccr.2004.12.011 (2005).

## REFERENCES

- 178 Kirn, D. H. & Thorne, S. H. Targeted and armed oncolytic poxviruses: a novel multi-mechanistic therapeutic class for cancer. *Nat Rev Cancer* **9**, 64-71, doi:nrc2545 [pii]10.1038/nrc2545 (2009).
- 179 Buller, R. M., Smith, G. L., Cremer, K., Notkins, A. L. & Moss, B. Decreased virulence of recombinant vaccinia virus expression vectors is associated with a thymidine kinase-negative phenotype. *Nature* **317**, 813-815 (1985).
- 180 Greiner, S. *et al.* The highly attenuated vaccinia virus strain modified virus Ankara induces apoptosis in melanoma cells and allows bystander dendritic cells to generate a potent anti-tumoral immunity. *Clin Exp Immunol* **146**, 344-353, doi:CEI3177 [pii]10.1111/j.1365-2249.2006.03177.x (2006).
- 181 Gentschev, I. *et al.* Regression of human prostate tumors and metastases in nude mice following treatment with the recombinant oncolytic vaccinia virus GLV-1h68. *J Biomed Biotechnol* **2010**, 489759, doi:10.1155/2010/489759 (2010).
- 182 Gholami, S. *et al.* Vaccinia Virus GLV-1h153 Is Effective in Treating and Preventing Metastatic Triple-Negative Breast Cancer. *Ann Surg* **256**, 437-445, doi:10.1097/SLA.0b013e3182654572 (2012).
- 183 Zhang, Q. *et al.* Eradication of solid human breast tumors in nude mice with an intravenously injected light-emitting oncolytic vaccinia virus. *Cancer Res* **67**, 10038-10046, doi:67/20/10038 [pii]10.1158/0008-5472.CAN-07-0146 (2007).
- 184 Gentschev, I. *et al.* Significant Growth Inhibition of Canine Mammary Carcinoma Xenografts following Treatment with Oncolytic Vaccinia Virus GLV-1h68. *J Oncol* **2010**, 736907, doi:10.1155/2010/736907 (2010).
- 185 Gentschev, I. *et al.* Preclinical evaluation of oncolytic vaccinia virus for therapy of canine soft tissue sarcoma. *PLoS One* **7**, e37239, doi:10.1371/journal.pone.0037239PONE-D-11-14526 [pii] (2012).
- 186 Lin, S. F. *et al.* Treatment of anaplastic thyroid carcinoma in vitro with a mutant vaccinia virus. *Surgery* **142**, 976-983; discussion 976-983, doi:S0039-6060(07)00542-9 [pii]10.1016/j.surg.2007.09.017 (2007).
- 187 Lin, S. F. *et al.* Oncolytic vaccinia virotherapy of anaplastic thyroid cancer in vivo. *J Clin Endocrinol Metab* **93**, 4403-4407, doi:jc.2008-0316 [pii]10.1210/jc.2008-0316 (2008).
- 188 Kelly, K. J. *et al.* Novel oncolytic agent GLV-1h68 is effective against malignant pleural mesothelioma. *Hum Gene Ther* **19**, 774-782, doi:10.1089/hum.2008.036 (2008).
- 189 Yu, Y. A. *et al.* Regression of human pancreatic tumor xenografts in mice after a single systemic injection of recombinant vaccinia virus GLV-1h68. *Mol Cancer Ther* **8**, 141-151, doi:8/1/141 [pii]10.1158/1535-7163.MCT-08-0533 (2009).

## REFERENCES

- 190 Yu, Z. *et al.* Oncolytic vaccinia therapy of squamous cell carcinoma. *Mol Cancer* **8**, 45, doi:1476-4598-8-45 [pii]10.1186/1476-4598-8-45 (2009).
- 191 He, S. *et al.* Effective oncolytic vaccinia therapy for human sarcomas. *J Surg Res* **175**, e53-60, doi:S0022-4804(11)01990-1 [pii]10.1016/j.jss.2011.11.1030 (2012).
- 192 Gentschev, I. *et al.* Efficient colonization and therapy of human hepatocellular carcinoma (HCC) using the oncolytic vaccinia virus strain GLV-1h68. *PLoS One* **6**, e22069, doi:10.1371/journal.pone.0022069PONE-D-10-03288 [pii] (2011).
- 193 Kao, S. Y., Calman, A. F., Luciw, P. A. & Peterlin, B. M. Anti-termination of transcription within the long terminal repeat of HIV-1 by tat gene product. *Nature* **330**, 489-493, doi:10.1038/330489a0 (1987).
- 194 Frankel, A. D. & Pabo, C. O. Cellular uptake of the tat protein from human immunodeficiency virus. *Cell* **55**, 1189-1193, doi:0092-8674(88)90263-2 [pii] (1988).
- 195 Ruben, S. *et al.* Structural and functional characterization of human immunodeficiency virus tat protein. *J Virol* **63**, 1-8 (1989).
- 196 Schwarze, S. R., Hruska, K. A. & Dowdy, S. F. Protein transduction: unrestricted delivery into all cells? *Trends Cell Biol* **10**, 290-295, doi:S0962-8924(00)01771-2 [pii] (2000).
- 197 Falkner, F. G. & Moss, B. Transient dominant selection of recombinant vaccinia viruses. *J Virol* **64**, 3108-3111 (1990).
- 198 Schmittgen, T. D. & Livak, K. J. Analyzing real-time PCR data by the comparative C(T) method. *Nat Protoc* **3**, 1101-1108 (2008).
- 199 Shapiro, A. L., Vinuela, E. & Maizel, J. V., Jr. Molecular weight estimation of polypeptide chains by electrophoresis in SDS-polyacrylamide gels. *Biochem Biophys Res Commun* **28**, 815-820 (1967).
- 200 Laemmli, U. K. Cleavage of structural proteins during the assembly of the head of bacteriophage T4. *Nature* **227**, 680-685 (1970).
- 201 Towbin, H., Staehelin, T. & Gordon, J. Electrophoretic transfer of proteins from polyacrylamide gels to nitrocellulose sheets: procedure and some applications. *Proc Natl Acad Sci U S A* **76**, 4350-4354 (1979).
- 202 Worschech, A. *et al.* Systemic treatment of xenografts with vaccinia virus GLV-1h68 reveals the immunologic facet of oncolytic therapy. *BMC Genomics* **10**, 301, doi:1471-2164-10-301 [pii]10.1186/1471-2164-10-301 (2009).
- 203 Ezeh, U. I., Turek, P. J., Reijo, R. A. & Clark, A. T. Human embryonic stem cell genes OCT4, NANOG, STELLAR, and GDF3 are expressed in both seminoma and breast carcinoma. *Cancer* **104**, 2255-2265, doi:10.1002/cncr.21432 (2005).

## REFERENCES

- 204 Takahashi, K. *et al.* Induction of pluripotent stem cells from adult human fibroblasts by defined factors. *Cell* **131**, 861-872, doi:S0092-8674(07)01471-7 [pii]10.1016/j.cell.2007.11.019 (2007).
- 205 Mathieu, J. *et al.* HIF induces human embryonic stem cell markers in cancer cells. *Cancer Res* **71**, 4640-4652, doi:0008-5472.CAN-10-3320 [pii]10.1158/0008-5472.CAN-10-3320 (2011).
- 206 Chen, N. G., Yu, Y. A., Zhang, Q. & Szalay, A. A. Replication efficiency of oncolytic vaccinia virus in cell cultures prognosticates the virulence and antitumor efficacy in mice. *J Transl Med* **9**, 164, doi:1479-5876-9-164 [pii]10.1186/1479-5876-9-164 (2011).
- 207 Chakrabarti, S., Sisler, J. R. & Moss, B. Compact, synthetic, vaccinia virus early/late promoter for protein expression. *Biotechniques* **23**, 1094-1097 (1997).
- 208 Baldick, C. J., Jr. & Moss, B. Characterization and temporal regulation of mRNAs encoded by vaccinia virus intermediate-stage genes. *J Virol* **67**, 3515-3527 (1993).
- 209 Ramakrishna, S. *et al.* PEST motif sequence regulating human NANOG for proteasomal degradation. *Stem Cells Dev* **20**, 1511-1519, doi:10.1089/scd.2010.0410 (2011).
- 210 Moss, B. & Salzman, N. P. Sequential protein synthesis following vaccinia virus infection. *J Virol* **2**, 1016-1027 (1968).
- 211 Wali, A. & Strayer, D. S. Infection with vaccinia virus alters regulation of cell cycle progression. *DNA Cell Biol* **18**, 837-843, doi:10.1089/104454999314836 (1999).
- 212 Worschech, A. *et al.* The immunologic aspects of poxvirus oncolytic therapy. *Cancer Immunol Immunother* **58**, 1355-1362, doi:10.1007/s00262-009-0686-7 (2009).
- 213 Wang, H., Chen, N. G., Minev, B. R. & Szalay, A. A. Oncolytic vaccinia virus GLV-1h68 strain shows enhanced replication in human breast cancer stem-like cells in comparison to breast cancer cells. *J Transl Med* **10**, 167, doi:1479-5876-10-167 [pii]10.1186/1479-5876-10-167 (2012).
- 214 Zhou, H. *et al.* Generation of induced pluripotent stem cells using recombinant proteins. *Cell Stem Cell* **4**, 381-384, doi:S1934-5909(09)00159-3 [pii]10.1016/j.stem.2009.04.005 (2009).
- 215 Warren, L. *et al.* Highly Efficient Reprogramming to Pluripotency and Directed Differentiation of Human Cells with Synthetic Modified mRNA. *Cell Stem Cell*, doi:S1934-5909(10)00434-0 [pii]10.1016/j.stem.2010.08.012 (2010).
- 216 Deshayes, S., Morris, M. C., Divita, G. & Heitz, F. Cell-penetrating peptides: tools for intracellular delivery of therapeutics. *Cell Mol Life Sci* **62**, 1839-1849, doi:10.1007/s00018-005-5109-0 (2005).

## REFERENCES

- 217 Li, Y. *et al.* Carcinoembryonic antigen-producing cell-specific oncolytic adenovirus, OV798, for colorectal cancer therapy. *Mol Cancer Ther* **2**, 1003-1009 (2003).
- 218 Israelsson, S., Jonsson, N., Gullberg, M. & Lindberg, A. M. Cytolytic replication of echoviruses in colon cancer cell lines. *Viol J* **8**, 473, doi:1743-422X-8-473 [pii]10.1186/1743-422X-8-473 (2011).
- 219 Varghese, S. & Rabkin, S. D. Oncolytic herpes simplex virus vectors for cancer virotherapy. *Cancer Gene Ther* **9**, 967-978, doi:10.1038/sj.cgt.77005377700537 [pii] (2002).
- 220 Pecora, A. L. *et al.* Phase I trial of intravenous administration of PV701, an oncolytic virus, in patients with advanced solid cancers. *J Clin Oncol* **20**, 2251-2266 (2002).
- 221 Hirasawa, K. *et al.* Oncolytic reovirus against ovarian and colon cancer. *Cancer Res* **62**, 1696-1701 (2002).
- 222 Kurooka, M. & Kaneda, Y. Inactivated Sendai virus particles eradicate tumors by inducing immune responses through blocking regulatory T cells. *Cancer Res* **67**, 227-236, doi:67/1/227 [pii]10.1158/0008-5472.CAN-06-1615 (2007).
- 223 Diallo, J. S., Vaha-Koskela, M., Le Boeuf, F. & Bell, J. Propagation, purification, and in vivo testing of oncolytic vesicular stomatitis virus strains. *Methods Mol Biol* **797**, 127-140, doi:10.1007/978-1-61779-340-0\_10 (2012).
- 224 Schoenborn, J. R. & Wilson, C. B. Regulation of interferon-gamma during innate and adaptive immune responses. *Adv Immunol* **96**, 41-101, doi:S0065-2776(07)96002-2 [pii]10.1016/S0065-2776(07)96002-2 (2007).
- 225 Karupiah, G., Blanden, R. V. & Ramshaw, I. A. Interferon gamma is involved in the recovery of athymic nude mice from recombinant vaccinia virus/interleukin 2 infection. *J Exp Med* **172**, 1495-1503 (1990).
- 226 Taub, D. D. *et al.* Recombinant human interferon-inducible protein 10 is a chemoattractant for human monocytes and T lymphocytes and promotes T cell adhesion to endothelial cells. *J Exp Med* **177**, 1809-1814 (1993).
- 227 Rahman, M. M. & McFadden, G. Modulation of tumor necrosis factor by microbial pathogens. *PLoS Pathog* **2**, e4, doi:10.1371/journal.ppat.0020004 (2006).
- 228 Morin, P. J., Vogelstein, B. & Kinzler, K. W. Apoptosis and APC in colorectal tumorigenesis. *Proc Natl Acad Sci U S A* **93**, 7950-7954 (1996).
- 229 Jamieson, C., Sharma, M. & Henderson, B. R. Regulation of beta-catenin nuclear dynamics by GSK-3beta involves a LEF-1 positive feedback loop. *Traffic* **12**, 983-999, doi:10.1111/j.1600-0854.2011.01207.x (2011).
- 230 Schwarze, S. R., Ho, A., Vocero-Akbani, A. & Dowdy, S. F. In vivo protein transduction: delivery of a biologically active protein into the mouse. *Science* **285**, 1569-1572, doi:7796 [pii] (1999).

## REFERENCES

- 231 Sherley, J. L. & Kelly, T. J. Regulation of human thymidine kinase during the cell cycle. *J Biol Chem* **263**, 8350-8358 (1988).



## 7 Appendix

### 7.1 Abbreviations

#	number
%	percent
°C	degree Celsius
α	anti
μ	micro
μg	microgram
μL	microliter
μm	micrometer
ANOVA	analysis of variance
BF	bright field
BSA	bovine serum albumine
CCD	charge-coupled device
cDNA	complementary DNA
CEV	cell-associated enveloped virus
cm <sup>2</sup>	centimeter square
CMC	carboxymethylcellulose
CO <sub>2</sub>	carbon dioxide
CPE	cytopathic effect
CRC	colorectal cancer
dH <sub>2</sub> O	double-distilled H <sub>2</sub> O
DMEM	Dulbecco's modified Eagle's medium
DMSO	dimethyl sulfoxid
DNA	deoxyribonucleic acid
dpi	days post injection
ds	double-stranded
EDTA	diaminoethanetetraacetic acid
EEV	extracellular enveloped virus
ELISA	enzyme-linked immunosorbent assay
EMEM	Eagle's minimal essential medium
EMT	epithelial-mesenchymal transition
ER	endoplasmatic reticulum
FACS	fluorescence-activated cell sorting
FAP	familial adenomatous polyposis

## APPENDIX

FBS	fetal bovine serum
Fig.	figure
FTV	fractional tumor volume
fwd	forward
g	grams
GFP	green fluorescent protein
h	hours
H <sub>2</sub> O <sub>2</sub>	hydrogen peroxide
HCl	hydrochloric acid
hpi	hours post infection
hpt	hours post treatment
HRP	horseradish peroxidase
IEV	intracellular enveloped virion
IMV	intracellular mature virus
IV	immature virion
i.v.	intravenous
kb	kilobase
kDa	kilo Dalton
mA	milli ampere
mg	milligram
min	minute
mL	milliliter
mm	millimeter
mM	millimolar
mm <sup>3</sup>	cubic millimeter
mRNA	messenger RNA
MOI	multiplicity of infection
MPA	mycophenolic acid
MRI	magnetic resonance imaging
MVA	modified vaccinia virus Ankara
n	number
N	normal
N <sub>2</sub>	nitrogen
NaOH	sodium hydroxide
n.d.	not detectable
NEAA	non-essential amino acids
neg	negative

## APPENDIX

ng	nanogram
NLS	nuclear localization sequence
NK	natural killer
nm	nanometer
NMWL	nominal molecular weight limit
NSCLC	non-small cell lung cancer
PBS	phosphate buffered saline
PCR	polymerase chain reaction
PDT	photodynamic therapy
PET	positron emission tomography
PFA	paraformaldehyde
pfu	plaque forming units
pg	picogram
pH	potential hydrogenii
PI	propidium iodide
PMSF	phenylmethylsulfonyl fluoride
pos	positive
PVDF	polyvinylidene difluoride
qPCR	quantitative real-time polymerase chain reaction
RNA	ribonucleic acid
r.o.	retro-orbital
rpm	rounds per minute
RPMI	Roswell Park Memorial Institute medium
RT	room temperature
RT-PCR	reverse transcriptase polymerase chain reaction
Ruc	<i>Renilla</i> luciferase
rvs	reverse
SCLC	small cell lung cancer
SDS-PAGE	sodium dodecyl sulfate polyacrylamide gel electrophoresis
sec	second
Tab.	table
TRITC	tetramethylrhodamine isothiocyanat
UC	uninfected control
UV	ultra violet
V	volume
w/v	weight per volume

## 7.2 Acknowledgements

First and foremost, I want to thank Prof. Dr. A.A. Szalay for his trust in me and for giving me the opportunity to work on a very exciting project to earn my PhD degree. Furthermore, I especially would like to thank him and Genelux Corp. for giving me the opportunity to fulfill my life-long dream to live and work in the United States and to explore and experience a different culture and way of life to the full extend. The creative freedom in my research as well as the always constructive criticism and support throughout the three years are very much appreciated. I am convinced that I learned and grew as a scientist and person thanks to the opportunities that were given to me.

I would also like to thank Jochen, Nanhai, Qian, Tony, Rohit, Okyay and Boris for their scientific guidance and support, be it helping with questions about vaccinia virus, laboratory work and techniques or animal work. Without their help this work would not be close to what it is now.

Furthermore, I would like to thank Terry Trevino, Jason Aguilar and Melody Fells for their excellent technical support and their dedication to provide us graduate students with anything we need.

I especially want to thank Lisa for an amazing and long-lasting friendship through years of undergraduate and graduate studies as well as inside and outside of the lab with much help, many advices and definitely some great and unforgettable times.

Thanks to Ricky, Alexa and Jackie for their friendship in and outside of the laboratory and their help and support with my project.

Also, I want to thank Camha for her kind friendship and for always taking care of so many needs, be it housing, traveling, organization or a million other things.

Thank you to all the other members of the Genelux family, whether it is in San Diego, Redlands, Würzburg, Bernried, New York, Washington, or Tübingen.

At the University of Würzburg, I want to thank Prof. Grummt for all the help and support in writing this thesis. I also want to thank Prof. Krohne for being so kind to review my PhD thesis. Also I want to thank Ivo, from whom I learned a lot before I even came to San Diego. I want to thank Ulrike for a lot of guidance and a great trans-atlantic friendship and also Caro, Michael, Barbara, Julia and Johanna for their friendship and help from across the Atlantic.

I want to thank Steven Martin and Scott Cottrell for being two amazing friends and for introducing me to the American way of life.

Last but definitely not least I want to say a special thank you to my parents, my sister and the rest of my family as well as my friends who have always supported me and my decision to follow my dreams – to become a scientist.

### 7.3 Eidstattliche Erklärung

Erklärung gemäß § 4 Absatz 3 der Promotionsordnung der Fakultät für Biologie der Julius-Maximilians-Universität Würzburg:

Hiermit erkläre ich, die vorgelegte Dissertation selbständig angefertigt zu haben und keine anderen als die von mir angegebenen Quellen und Hilfsmittel verwendet zu haben.

Des Weiteren erkläre ich, dass die vorliegende Arbeit weder in gleicher noch in ähnlicher Form bereits in einem anderen Prüfungsverfahren vorgelegen hat.

Zuvor habe ich neben dem akademischen Grad "Diplombiologe, Univ." keine akademischen Grade erworben oder zu erwerben versucht.

---

Würzburg

---

Klaas Ehrig

## 8 Lebenslauf

### Persönliche Daten

Geburtstag: 21. März 1983  
Geburtsort: Braunschweig  
Staatsangehörigkeit: deutsch  
Adresse: Neulandstraße 9  
26835 Brinkum

3922 Jewell Street M307  
San Diego, CA 92109  
USA

### Schulbildung

01-08-1989 – 31-07-1992 Grundschule „Eichenwellschule“ in Leer  
01-08-1992 – 31-07-1993 Grundschule „Grundschule Holtland“ in Holtland  
01-08-1993 – 31-07-1995 Orientierungsstufe „Orientierungsstufe Westergaste“ in  
Brinkum  
01-08-1995 – 31-07-2002 Gymnasium „Ubbo-Emmius Gymnasium“ in Leer

### Wehrersatzdienst

2002 – 2003 Zivildienst im “Friedas Friedenstift” in Oldenburg

### Hochschulausbildung

01-10-2003 – 02-10-2008 Studium der Biologie (Diplom) an der Julius-Maximilians  
Universität in Würzburg  
15-01-2007 – 30-06-2007 ERASMUS Auslandssemester in Umeå, Schweden  
01-12-2008 – 01-09-2009 Diplomarbeit in der Arbeitsgruppe von Prof. Dr. Szalay an der  
Julius-Maximilians-Universität  
01-09-2009 Graduiert als Dipl. Biol. Univ. an der Julius-Maximilians-  
Universität in Würzburg

### Promotionsstudium

seit 01-10-2009 Promotionsstudium in der Arbeitsgruppe von Prof. Dr. Aladar  
Szalay an der Julius-Maximilians-Universität in Würzburg und  
Genelux Corporation, San Diego, USA

## 9 Publikationen

### 9.1 Im Rahmen dieser Arbeit entstandene Publikationen

**Gentschev I\*, Ehrig K\*, Donat U, Hess M, Rudolph S, Chen N, Yu YA, Zhang Q, Bullerdiel J, Nolte I, Stritzker J, Szalay AA.**

Significant Growth Inhibition of Canine Mammary Carcinoma Xenografts following Treatment with Oncolytic Vaccinia Virus GLV-1h68.

J Oncol. 2010;2010:736907. Epub 2010 Jun 23. PMID:20631910

\*authors contributed equally

**Gentschev I, Adelfinger M, Josupeit R, Rudolph S, Ehrig K, Donat U, Weibel S, Chen NG, Yu YA, Zhang Q, Heisig M, Thamm D, Stritzker J, Macneill A, Szalay AA.**

Preclinical evaluation of oncolytic vaccinia virus for therapy of canine soft tissue sarcoma.

PLoS One. 2012;7(5):e37239. Epub 2012 May 15. PMID:22615950

**Ehrig K, Chen NG, Stritzker J, Buckel L, Zhang Q, Szalay AA.**

Growth inhibition of different human colorectal cancer xenografts after a single intravenous injection of oncolytic vaccinia virus GLV-1h68.

J Transl Med (submitted)

**Buckel L, Advani SJ, Frentzen A, Zhang Q, Yu YA, Chen NG, Ehrig K, Stritzker J, Mundt AJ, Szalay AA.**

Vaccinia virus expressed single-chain antibody against VEGF increases response to radiation by targeting the vascular component of the tumor.

Clin Cancer Res (submitted)